

ÉCOLE DOCTORALE ED222 Sciences Chimiques
UMR 7509 CNRS - Université de Strasbourg

THÈSE présentée par :

Liwen FENG

soutenue le : 11 juillet 2017

pour obtenir le grade de : **Docteur de l'université de Strasbourg**

Discipline/ Spécialité : Sciences Chimiques - chimie

**Chemical tools for antimalarial drug
development: synthesis of plasmodione
analogues and ^{13}C -enriched
plasmodione for drug metabolomics
investigations**

Titre français: Outils moléculaires pour le développement de médicaments antipaludiques:
synthèse d'analogues de plasmodione et de $^{13}\text{C}_{18}$ -plasmodione pour des recherches
en métabolomics

THÈSE dirigée par :

Dr. Elisabeth Davioud-Charvet

Directeur de Recherche CNRS, Université de Strasbourg

RAPPORTEURS :

Pr. Philippe Belmont

Professeur, Université Paris Descartes

Dr. Bruno Figadère

Directeur de Recherche CNRS, Université de Paris-Sud

AUTRES MEMBRES DU JURY :

Dr. Stéphanie Blandin

Chargé de Recherche INSERM, Université de Strasbourg

Dr. Cyrille Botté

Chargé de Recherche CNRS, Université Grenoble Alpes

To my family
献给我的家庭

Acknowledgements

First of all, I would like to thank the members of my jury: Dr. Bruno Figadère, Prof. Philippe Belmont, Dr. Stéphanie Blandin and Dr. Cyrille Botté who have accepted to evaluate my PhD thesis work and for the interesting discussions during my thesis defense.

My following thanks go to my thesis supervisor: Dr. Elisabeth Davioud-Charvet. Thanks to her for having welcomed me in her laboratory, for all the confidence and the motivation that she brought me during three years. And also a huge thank to her for the discussions and the patient guidance in science, the expertise in chemistry and biology and also the support for my administrative documents, the help to deal with some paper works, which made my work and my living in Strasbourg easier.

Special great thanks to our collaborator Dr. François Fenaille (LEMM CEA Saclay, Paris) and Dr. Stéphanie Blandin (IBMC, Strasbourg). Without their help, the work presented here would have not been possible.

To all my lab colleagues, Dr. Mourad Elhabiri, Dr. Mouhamad Jida (for interesting discussions in synthesis), Dr. Leandro Cotos-Munoz, Dr. Parastoo Dalvand, Dr. Xavier Martin-Benloch, Dr. Katharina Ehrhardt, Dr. Didier Belorgey, Dr. Max Bielitz, Dr. Don-Antoine Lanfranchi, Dr. Elena Cesar-Rodo, Vrushali Khobragade (for the preparation of the parasite samples), Angeline Cherbonnel, Joan Guillem Mayans Peñarrubia and Enrique Montagud. Thank you for your help, your kindness, as well as the nice atmosphere and happy time of group lunches in the laboratory.

And I also would like to thank the LabEx ParaFrap for the financial support of my PhD salary and all the schools & meetings of the PhD programme.

Thanks to two kindly secretaries of CNRS: Ms. Caroline Ludwig and Mr. Julien Bertrand for preparing the administrative documents and their help for applying to my Titre de séjour.

All my friends who help and support me during the five years in Strasbourg. Wang Yanhui, Xu Chaojie, Wang Shaojun, Hu bowen, Liang Ting, Gu yanan, Zhao Zhuiguang, Yan Yige, Jiang Qian, Ji Qingqing, Zhang Liang, Xu Zhenxin and many more whom I missed to note, thank you for your support, your help, your companion and every happy moment we shared together.

At the end, I also thank my family for your support, your understanding and your encouragement.

Table of Contents

RESUME en français	i
Part 1: Plasmodione as an early lead antimalarial drug	1
1. Introduction	1
2. The 1,4-naphthoquinone series: plasmodione versus atovaquone	4
3. 2-Methyl-1,4-naphthoquinone chemistry	10
3.1. Synthesis of menadione analogues through the naphthol strategy	12
3.2. Synthesis of menadione analogues through Diels-Alder strategy	15
3.3. Synthesis of menadione from β -methylcinnamyl acetate	17
3.4. Synthesis of menadione from formylphenylboronic acid	18
3.5. Synthesis of menadione analogues through demethoxycarbonylative annulation	19
3.6. Synthesis of menadione analogues from bromo veratrum aldehyde	19
4. Putative mode of action of plasmodione	20
5. Antimalarial activity profile of plasmodione	21
6. The objectives of research	21
Chapter I: Synthesis of the multi $^{13}\text{C}_{18}$ - and mono $^{13}\text{C}_1$ -labeled plasmodiones	23
I.1. Synthesis of plasmodione - Completion/optimization of the “express tetralone route”	23
I.1.1. Previous data from the lab	23
I.1.2. Personal work	24
I.2. Synthesis of the enriched- $^{13}\text{C}_{18}$ -plasmodione	30
I.2.1. Synthesis of the ^{13}C -enriched tetralone	30
I.2.2. Synthesis of the $^{13}\text{C}_6$ -enriched trifluoromethylbenzaldehyde	35
I.2.3. Synthesis of ^{13}C -enriched plasmodione	41
I.2.4. Synthesis of the 1- $^{13}\text{C}_1$ -3-[(4-trifluoromethyl)benzyl]-menadione	48
I.2.5. Antimalarial activities	53
Chapter II: Drug metabolism studies on plasmodione-treated parasitized red blood cells	55
II.1. Synthesis of several putative plasmodione metabolites	55
II.1.1. Preliminary Results from the team	55
II.1.2. Personal results	62
II.2. Analysis of plasmodione and its metabolites from pRBC extracts	62
II.2.1. Investigation on the Extraction method	65
II.2.2. Preliminary drug metabolism study	67

II.2.3. Conclusion and perspective.....	70
Chapter III: Synthesis of plasmodione derivatives with increased solubility.....	71
III.1. Synthesis of a plasmodione-based oxetane derivative.....	71
III.1.1. Preliminary Results from the team	72
III.1.2. Personal results	78
III.2. Solubilities and Pharmacokinetic properties.....	83
III.3. Antimalarial activities of 3-benzylmenadiones	85
Chapter IV: exploration of more soluble compounds by introducing of N-alkyl-aryl amines groups	88
IV.1. Preliminary Results from the team	88
IV.2. Personal results	92
IV.2.1. Synthesis of the piperazine-based plasmodione derivative	93
IV. 3. Antimalarial activities of the piperazine-based 3-benzylmenadione.....	95
Part 2: Synthesis a gold(I)-phosphole-thiosugar complex as a thioredoxin reductase inhibitor.....	97
I. Introduction	97
II. Preliminary Results from the team.....	99
III. Personal results	102
III.1. The synthesis of GoPi-sugar	102
IV. Inhibition of parasitic TrxRs and GR/TR by GoPi-sugar	103
V. Anti-parasitic activity of GoPi-sugar	105
V.1. Anti-Schistosoma mansoni worms activity of gold complexes	105
V.2. Anti-Brugia pahangi worms activity of gold complexes	107
V.3. Anti-Trypanosoma brucei gambiense activity of gold complexes.....	108
V.4. Anti-Leishmania donovani activity of gold complexes	109
V.5. Anti-Acanthamoeba castellanii activity of gold complexes	110
Part 3: General conclusion and perspectives	112
Part 4: Materials and methods.....	115
1. General information for organic synthesis.....	115
2. Synthesis of the multi ¹³ C ₁₈ - and mono ¹³ C ₁ -labeled plasmodiones.....	117
3. Synthesis of putative drug metabolites	131
4 Synthesis of 3'-(oxetane-3-yloxy)plasmodione	136
5. Synthesis of a 3-benzylmenadione derivative with potential antimalarial properties	143
6. Synthesis of GoPi-sugar.....	150
7. General information for drug metabolism study.....	153
8. Extraction yields of putative drug metabolites investigation.....	155

9. Preliminary drug metabolism study with fully ¹³ C-enriched plasmodione treated pRBCs preparation	161
--	-----

Abbreviation

Å	Ångström
ACN	acetonitrile
ACT	artemisinin-based combination
aq.	aqueous
ART	artemisinin
calcd.	calculated
CAN	cerium ammonium nitrate
CN	cyano
<i>conc.</i>	concentrated
CoQ ₁₀	Coenzyme Q ₁₀ or ubiquinol
CQ	chloroquine
CytP ₄₅₀	cytochrome P450
DCM	dichloromethane
DDQ	2,3-dichloro-5,6-dicyano-1,4-benzoquinone
DHODH	dihydroorotate dehydrogenase
DIPEA	<i>N,N</i> -diisopropylethylamine
DMF	dimethylformamide
DMS	dimethyl succinate
DMSO	dimethyl sulfoxide
DNA	deoxyribonucleic acid
DTNB	Ellman's reagent (5,5'-dithiobis-(2-nitrobenzoic acid))
EI	electron impact
equiv.	equivalent
ESI	electrospray ionization
EtOAc	ethyl acetate
G6PD	glucose-6-phosphate dehydrogenase
GR	glutathione reductase
GSSG	glutathione disulfide
h	hour
HIV	human immunodeficiency virus
HRMS	high resolution mass spectrometry
hTrxR	human thioredoxin reductase
Hz	Hertz
IC ₅₀	50 % inhibitory concentration
ICP	inductively coupled plasma
ITN	insecticide-treated bednets
<i>J</i>	coupling constant
LC	liquid chromatography
m.p.	melting point
MB	methylene blue
MD	menadione
MDFA	methyl 2,2-difluoro-2-(fluorosulfonyl)acetate
mETC	mitochondrial electron transport chain

MHz	megahertz
MOM	methoxymethyl
MRM	multiple reaction monitoring
MS	mass spectrometry
NADPH	reduced nicotinamide adenine dinucleotide phosphate
NBS	<i>N</i> -bromosuccinimide
<i>n</i> -BuLi	<i>n</i> -butyllithium
NMP	<i>N</i> -Methyl-2-pyrrolidine
NMR	nuclear magnetic resonance
PCC	pyridinium chlorochrome
PDC	pyridinium dichromate
PFIX	protoporphyrin IX
Ph	phenyl
PIDA	phenyliodonium (III) diacetate
pKa	acidity constant
pRBC	parasized red blood cell
PTSA	<i>p</i> -toluenesulfonic acid
Py	pyridine
QTOF-MS	quadrupole time-of-flight mass spectrometry
RA	rheumatoid arthritis
RBC	red blood cell
Rf	retention value
ROS	reactive oxygen species
rt	room temperature
SAR	structure activity relationships
S _N Ar	aromatic nucleophilic substitution
SPE	solid phase extraction
TBAF	<i>n</i> -butylammonium tetrafluoride
TFA	trifluoroacetic acid
TGR	thioredoxin-glutathione reductase
THF	tetrahydrofuran
TLC	thin layer chromatography
TMS	trimethylsilyl
TMSCF ₃	trimethyl-(trifluoromethyl)silane
TR	trypanothione reductase
Trx	thioredoxin
TrxR	thioredoxin reductase
TS ₂	trypanothione disulfide
UHPLC	ultra-high performance liquid chromatography
UV	ultraviolet
WHO	world health organization
yDHODH	yeast dihydroorotate dehydrogenase

RESUME en français

1) Introduction

Le paludisme (ou malaria) est une maladie parasitaire tropicale responsable de 214 million de cas cliniques dans le monde en 2015 donnant lieu à 438,000 morts par an, touchant en majorité des enfants de moins de 5 ans en Afrique. Les agents responsables de l'infection appartiennent à 5 espèces de parasites protozoaires du genre *Plasmodium*, dont l'espèce la plus dangereuse est *P. falciparum*, qui entraîne les formes les plus sévères de la maladie comme le neuropaludisme, anémie hémolytique et détresse respiratoire. Plusieurs médicaments antipaludiques comme les quinolines, quinine ou chloroquine, sont connus pour soigner les infections palustres au moment des symptômes déclarés de l'infection. Cependant, la résistance à ces médicaments est apparue et s'est propagée dans le monde depuis les 50 dernières années. L'artémisinine d'origine naturelle a été découverte comme agent antipaludique dans les années 1970s par Youyou Tu, qui a reçu le Prix Nobel de physiologie ou médecine en 2015. Les combinaisons médicamenteuses basées sur l'artémisinine (ACT) ont été largement utilisées avec succès pour soigner le paludisme.¹ Mais, le coût des ACT est relativement élevé et la résistance à ce traitement a commencé à apparaître en Asie du Sud-Est, s'est propagée dans les autres continents, mettant à risque les traitements ACT pour soigner le paludisme.² Aussi, de nouveaux médicaments sont nécessaires et réclamés.

Le dérivé tête de série 3-[4-(trifluorométhyl)benzyl]-menadione, appelé plasmodione, a été identifié comme candidat-médicament antipaludique dans mon laboratoire d'accueil.³ De récentes investigations sur le mode d'action ont montré que la plasmodione agissait comme un agent redox avec des IC_{50} dans le bas nM (≈ 50 nM) dans des essais avec les parasites en culture *in vitro* et une toxicité modérée contre les lignées cellulaires humaines ($IC_{50} \approx 50$ μ M).⁴ Une bioactivation^{3,5} a été proposée pour expliquer l'activité antipaludique de la plasmodione (Figure 1), faisant intervenir : i) une oxydation benzylique (pas encore prouvée), ii) la réduction démontrée de la benzoylmenadione générée par la glutathion réductase (GRs) du globule rouge parasité (*p*RBC) tout en consommant le NADPH dans un cycle futile redox qui perturbe le milieu reducteur, iii) la formation d'espèces oxygénées réactives (ROS) à l'origine d'une hausse de stress oxydant intracellulaire,⁵ iv) la transformation du métabolite benzoylmenadione, réduit à $1e^-$, par un couplage oxydatif phénolique

en benzoxanthone. Ce dernier métabolite inhibe la formation d'hemozine.⁵ Au cours du cycle redox, la benzoylmenadione réduite transfère un électron au Fe^{III} de la méthémoglobine, le nutriment majoritaire du parasite, régénérant l'oxyhemoglobine (Fe^{II}) en un flux continu consommant le NADPH. La conversion continue d'oxyhemoglobine, qui n'est pas digérée par les protéases parasitaires, conduit à la mort plasmodiale mais pas à celle des globules rouges non parasités.⁵

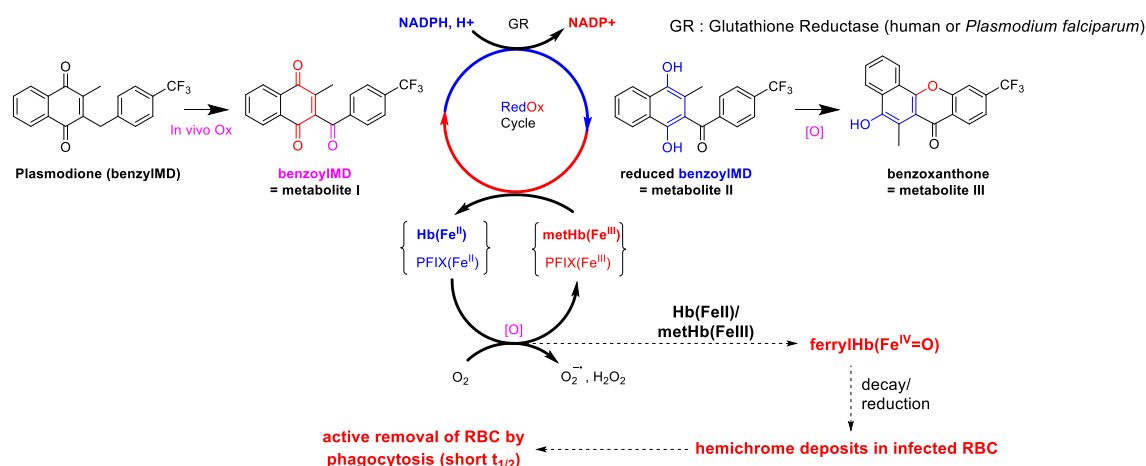


Figure 1. Voie métabolique hypothétique de la plasmodione.

Finalement, le déséquilibre redox induit par la plasmodione mime les effets d'un déficit acquis en glucose-6-phosphate déshydrogénase (G6PD) qui est à l'origine de la protection observée chez les porteurs de mutations génétiques en G6PD vis-à-vis des accès palustres sévères et du neuropaludisme.⁶ La plasmodione redox-active exerce des effets additifs spécifiques qui résultent en l'arrêt du développement du parasite, sans nocivité pour les globules rouges non parasités, porteurs ou non du déficit en G6PD. En effet, la réponse au stress oxydant induite par le déficit en G6PD ou par la plasmodione spécifiquement dans le pRBC entraîne l'enrichissement des membranes en hémichrome, le biomarqueur de sénescence des globules rouges.⁵ Il en résulte l'élimination des RBC par phagocytose par les macrophages, et les porteurs du déficit en G6PD ont des globules rouges caractérisés par un temps de ½ vie plus court à l'origine d'un milieu défavorable au développement parasitaire.

L'optimisation de la plasmodione et la compréhension de son métabolisme *in vivo* sont essentiels à son développement comme candidat-médicament. La voie de bioactivation est difficile à prouver *in situ* dans les parasites : la plasmodione est rapidement métabolisée *in vitro* et seulement quelques données structurales et de réactivité sur la formation des métabolites ont été collectées, rendant l'étude du métabolisme insuffisant. Visualiser *in situ* dans les parasites la distribution de la

molécule non marquée et de ses métabolites sans affecter sa structure est difficile. Aussi, dans le projet de thèse, la synthèse de la plasmodione enrichie par 18 isotopes du carbone ($^{13}\text{C}_{18}$ -plasmodione) a été envisagée pour des études de son métabolisme puisque la molécule lourde garde les mêmes propriétés que la molécule non enrichie.

Dans la première partie de la thèse, des outils chimiques ont été conçus pour investiguer le métabolisme et l'interactome de la plasmodione, afin de tracer, identifier et visualiser les métabolites responsables de l'activité antipaludique dans les parasites. L'optimisation de deux étapes limitantes dans la synthèse totale de la plasmodione partant d'un benzaldéhyde 4-substitué et d'une tétralone comme produits de départ a été finalisée. Puis, à partir des cinq synthons enrichis en ^{13}C de départ, les moins chers, la synthèse totale de la $^{13}\text{C}_{18}$ -plasmodione a été réalisée et optimisée.

Dans la seconde partie de la thèse, la préparation d'un analogue *N*-alkyle et d'un dérivé oxétane de la plasmodione avec l'objectif d'augmenter sa solubilité a été étudiée à travers l'utilisation de la réaction de couplage de type Buchwald-Hartwig pallado-catalysée. Dans la troisième partie de la thèse, cinq métabolites postulés ont été fraîchement préparés et utilisés dans une étude du profil métabolique de la plasmodione après incubation de pRBC avec la plasmodione non enrichie en ^{13}C et la $^{13}\text{C}_{18}$ -plasmodione.

2) Résultats et discussion

La plasmodione est facilement synthétisée en une étape à partir des produits de départ commerciaux, la menadione et l'acide 4-trifluorométhyl-phénylacétique par la réaction de Kochi-Anderson (Schéma 1. A), rendant une préparation à large échelle facile, peu coûteuse et accessible. Cependant, à cause du choix limité et du coût élevé des synthons de départ commercial, enrichis en ^{13}C , la synthèse de la $^{13}\text{C}_{18}$ -plasmodione a été conçue à travers une voie synthétique convergente en 10 étapes, passant par les deux intermédiaires-clefs, une tétralone et le 4-trifluorométhyl-benzaldéhyde,⁷ à partir des 5 éléments de base enrichis en ^{13}C : les $^{13}\text{C}_6$ *p*-dibromobenzène et $^{13}\text{C}_6$ -benzène, l'anhydride $^{13}\text{C}_4$ -succinique et l'acide $^{13}\text{C}_2$ -acétique, et le $^{13}\text{C}_1$ -diméthylformamide (Schéma 1. B). Chaque étape de la synthèse totale a été élaborée et améliorée en utilisant au préalable les composés non marqués.

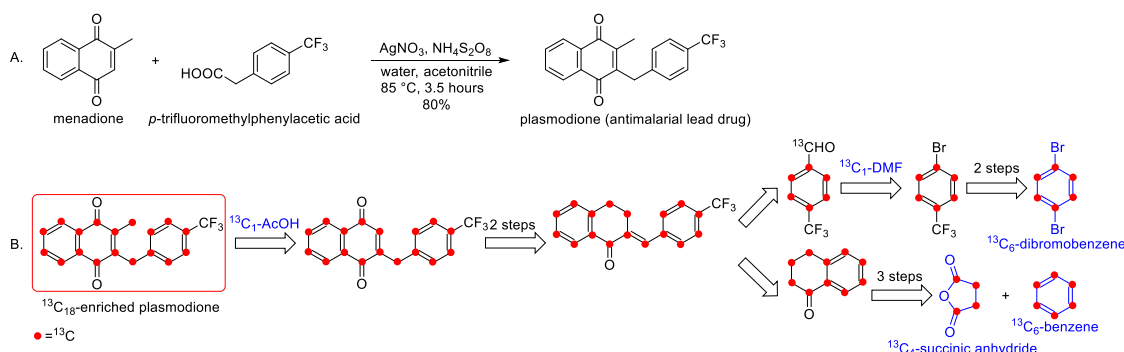


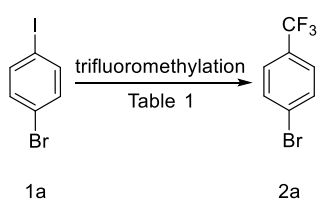
Schéma 1. A) Synthèse de la plasmodione non marquée. B) Schéma rétrosynthétique de la $^{13}\text{C}_{18}$ -plasmodione.

Synthèse du $^{13}\text{C}_7$ -4-trifluorométhylbenzaldéhyde

Le $^{13}\text{C}_7$ -*p*-trifluorométhylbenzaldéhyde **3b** a été synthétisé en 3 étapes (rendement total de 23%, Schéma 2): le $^{13}\text{C}_6$ -*p*-bromoiodobenzène **1b** a été préparé par une réaction d'iodation avec I_2 et *n*-BuLi sous conditions classiques (rendement 75%). Le rendement limité est dû à la génération de son régioisomère en *ortho*, *e.g.* l'*o*-bromoiodobenzène formé par effet de résonance. Quelles que soient les conditions de température (de $-78\text{ }^\circ\text{C}$ à $25\text{ }^\circ\text{C}$), l'*o*-bromoiodobenzène formé à hauteur de 20% de conversion du matériel de départ a toujours accompagné le régioisomère en *para*. Une étape de séparation par chromatographie sur gel de silice a été essentielle pour purifier le *p*-bromoiodobenzène (**1a/1b**) désiré.

La substitution de l'atome d'iode par un groupe trifluorométhyle a été explorée en utilisant le réactif de trifluorométhylation $[\text{CuCF}_3]$ utilisé comme catalyseur. La génération de CuCF_3 *in situ* a été développée en utilisant différents réactifs, *e.g.* NaCO_2CF_3 et MeCO_2CF_3 , qui demandent une température d'activation élevée ($\sim 150\text{-}160\text{ }^\circ\text{C}$). Cependant, le trifluorométhylbenzène **2a** désiré est volatil ($T_{\text{éb.}}\ 160\text{ }^\circ\text{C}$), rendant les réactifs trifluorométhyles mentionnés peu appropriés. Le réactif de Ruppert, le triméthyl-(trifluorométhyl)silane (TMSCF_3) et le méthyl-2,2-difluoro-2-(fluorosulfonyl)acetate (MDFA) ont été sélectionnés dans la route étudiée. Le MDFA a été étudié par Chen *et al.*⁸ Le TMSCF_3 est un réactif largement utilisé pour la trifluorométhylation sous conditions douces pour former CF_3^- .⁹ En premier, le groupe méthyle du réactif MDFA a été substitué par CuI et les réactions de décarboxylation et désulfonylation consécutives produisent le carbène $:\text{CF}_2$ par chauffage (environ $80\text{-}100\text{ }^\circ\text{C}$). Ensuite, le carbène $:\text{CF}_2$ réagit avec l'anion F^- pour former CF_3^- en

équilibre et se coordine avec le cuivre pour former CuCF_3 *in situ*. La trifluoromethylation se produit avec des rendements similaires en utilisant le MDFA or le TMSCF_3 (Tableau 1). A cause de la volatilité du produit désiré, et de la difficulté à purifier le produit de réaction en petite quantité (moins de 2 mL) par distillation, le produit brut doit être utilisé dans la prochaine étape sans purification. Dans ce cas, il a été nécessaire de s'assurer que tout le matériel de départ (*p*-bromoiodobenzene 1a et 1b) a été consommé. La trifluorométhylation s'est révélée très sensible à la qualité de CuI (stocké sous argon).



Conditions	Rendement*
CuI (1.5 equiv.), MDFA (5 equiv.), NMP, 16h, 100 °C	95%
CuI (2 equiv.), TMSCF_3 (2 equiv.), NMP, 16h, 100 °C	90%

Tableau 1: Conditions de la réaction trifluorométhylation. NMP=N-Méthyl-2-pyrrolidone. * Les rendements ont été déterminés par ^1H NMR en utilisant le trifluorométhoxytoluène comme étalon interne.

Dans la prochaine étape de la synthèse, la réaction d'hydroformylation¹⁰ avec le réactif de Grignard a produit le *p*-trifluorométhylbenzaldéhyde **3** avec un rendement global de 50% (**3a**) / 30% (**3b**) après 2 étapes. En utilisant le réactif $i\text{PrMgBr}$, le groupe bromoaryle a été transformé en réactif de Grignard $[\text{phen}]_3\text{-Mg}$ formé *in situ*, une réaction qui est accélérée en présence de $n\text{-BuLi}$. Puis, le réactif de Grignard généré réalise une attaque nucléophile du $^{13}\text{C}_1\text{-DMF}$ pour former le benzaldéhyde désiré. A cause de la sensibilité élevée envers toute trace d'eau et la volatilité du matériel de départ, l'utilisation du Na_2SO_4 a été requise pour enlever le maximum d'eau *in situ*.

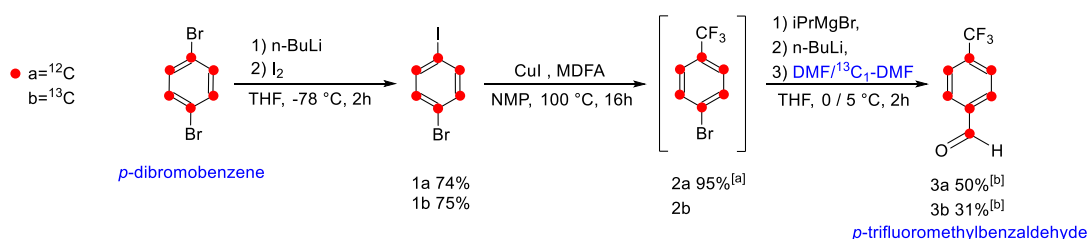


Schéma 2: La synthèse du 4-trifluorométhyl-benzaldéhyde **3a/3b**. [a] Le rendement de la réaction de trifluorométhylation a été estimé par ^1H NMR en utilisant le trifluorométhoxytoluène comme étalon interne. [b] Rendement global sur 2 étapes à partir du *p*-bromoiodobenzene (1a/1b) comme matériel de départ.

Synthèse de la $^{13}\text{C}_{10}$ -tétralone

La tétralone $^{13}\text{C}_{10}$ -marquée uniformément a été synthétisée selon une procédure connue.¹¹ La $^{13}\text{C}_{10}$ -tétralone **6b** a été produite par la réaction de Friedel-Crafts (rendement 96%), la réduction de Wolff-Kishner (rendement 95%) et une réaction de cycloaddition (rendement 95%) à partir de l'anhydride $^{13}\text{C}_4$ -succinique et le $^{13}\text{C}_6$ -benzène avec d'excellents rendements (rendement total de 87%, Schéma 3).

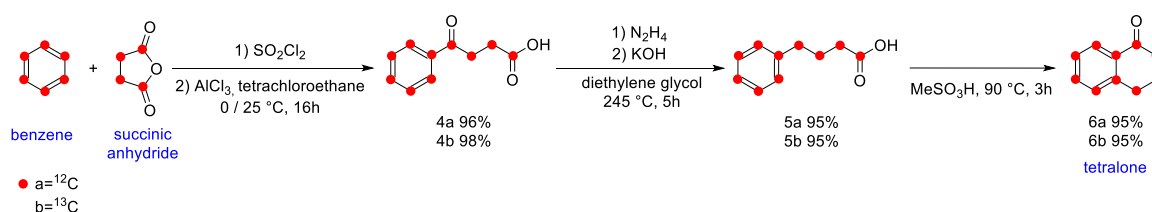


Schéma 3. Route synthétique de la tétralone **6a/6b**.

Synthèse de la $^{13}\text{C}_{18}$ -plasmodione à travers la route dite « tétralone express »

Les deux derniers intermédiaires, $^{13}\text{C}_{10}$ -tétralone (**6a/6b**) et $^{13}\text{C}_7$ -*p*-trifluorométhylbenzaldéhyde (**3a/3b**), ont été combinés via la route dite « tétralone express », qui avait été précédemment développée dans notre laboratoire,¹² pour produire la plasmodione et analogues en 4 étapes. En premier lieu, j'ai contribué à l'optimisation de cette route au niveau des 2 étapes peu effectives – aromatisation et méthylation – avant de l'appliquer aux matériels enrichis en ^{13}C . La méthodologie finale avec les matériels non enrichis a été publiée dans un article⁷ auquel j'ai participé comme second auteur.

Mes études initiales sur la décarboxylation radicalaire d'acides carboxyliques (acide acétique versus acide phénylacétique) utilisant la réaction de Kochi-Anderson ont montré que la stabilité du radical méthyle versus le radical benzyle est plus faible, et que le radical méthyle plus réactif devait détruire le produit désiré. Afin de suivre la cinétique de réaction et les produits de réaction par spectroscopie ^1H NMR (Figure 2), nous avons utilisé la 2-(4-(trifluorométhyl)benzyl)-naphthalène-1,4-dione **9a** non enrichie comme matériel de départ dans la réaction modèle. Après 15 min d'agitation, la conversion de **9a** atteignait quasiment 50% et nous avons observé que le produit désiré

était rapidement généré. Après 60 min, la majorité du matériel de départ était consommée mais pas complètement. Avec une bonne agitation, nous avons observé que la meilleure conversion avait lieu après 75 min. Cependant, après 90 min, la génération de produits secondaires a été observée et le rendement de la réaction diminuait. La préparation de la $^{13}\text{C}_{18}$ -plasmodione **10b** tient compte de la route synthétique optimisée avec 50% de rendement après 2 étapes de purification (chromatographie suivie d'une précipitation).

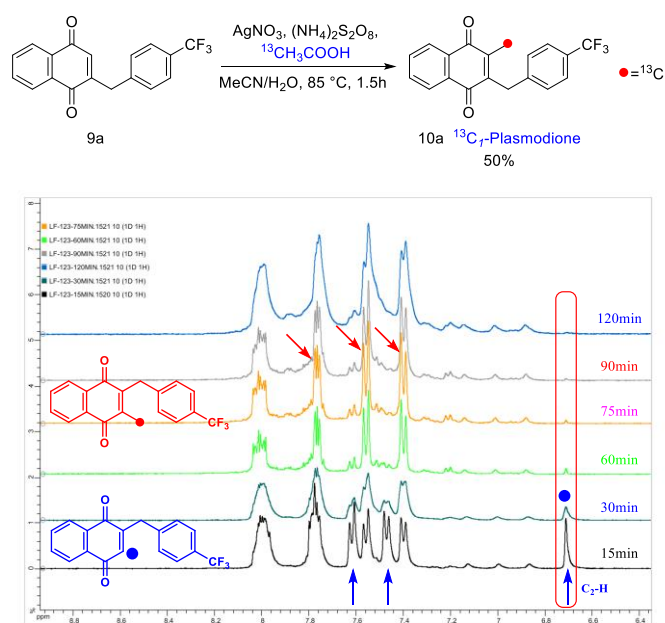


Figure 2: Etudes cinétiques de spectroscopie ^1H NMR de la réaction Kochi-Anderson entre **9a** et l'acide $2\text{-}^{13}\text{C}_1$ -acétique. La flèche bleue pointe les pics correspondants aux protons de **9a**, la flèche rouge pointe les pics correspondants aux protons de **10a**, le point bleu représente le proton sur la position C-2 de **9a**. L'étude ^1H NMR a été réalisée dans un mélange de $\text{CD}_3\text{CN}/\text{D}_2\text{O}$.

En appliquant la méthodologie aux molécules enrichies en ^{13}C , la $^{13}\text{C}_{18}$ -plasmodione **10b** a été obtenue par synthèse totale (Schéma 4) via i) une réaction de condensation (rendement 75%) des deux intermédiaires, *p*-trifluorométhylbenzaldéhyde (**3a/3b**) et tétralone (**6a/6b**), sous conditions basiques (KOH), puis ii) une réaction d'isomérisation utilisant le RhCl_3 (rendement 80%), suivie iii) d'une oxydation avec le phenyliodonium diacétate (PIDA) (rendement 75%), et finalement la réaction d'alkylation de Kochi-Anderson (rendement 50%) avec l'acide $^{13}\text{C}_1$ -acétique en présence de $\text{AgNO}_3/(\text{NH}_4)_2\text{S}_2\text{O}_8$.

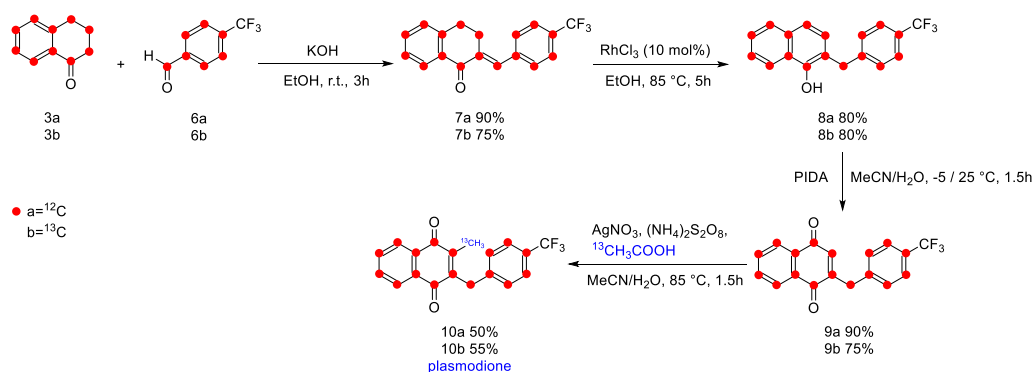


Schéma 4: La synthèse de plasmodione **10a/10b** à partir de tétralone **3a/3b** et de *p*-trifluorométhylbenzaldéhyde **6a/6b**.

Etude du profil métabolique: analyse de la plasmodione et de ses métabolites dans les extraits de globules rouges parasités (pRBC).

Le mécanisme d'action de la plasmodione a été récemment proposé.³ Cependant, la voie métabolique putative est difficile à prouver. Basée sur une étude préliminaire, la bioactivation de la plasmodione a été proposée pour passer par une cascade de réactions redox commençant avec l'oxydation benzylique. La benzoylmenadione générée est très oxydante et est bioreduite *in situ* dans les parasites. Puis, cette forme réduite à un électron a été suggérée d'être transformée en benzoxanthone par une réaction de couplage phenolique.⁵ Ainsi, le premier objectif de l'étude du profil métabolique a été de traquer la benzoxanthone dans les pRBC. La technique analytique basée sur la chromatographie liquide couplée à la spectrométrie de masse en tandem (HPLC/MS-MS) est une technique puissante et générale qui possède une grande sensibilité et sélectivité dans les études métaboliques de médicaments. Avec cette méthodologie, l'étude du profil métabolique de la plasmodione a été analysé au Laboratoire d'Etudes du Métabolisme des Médicaments (Dr Junot, CEA Saclay, Paris).

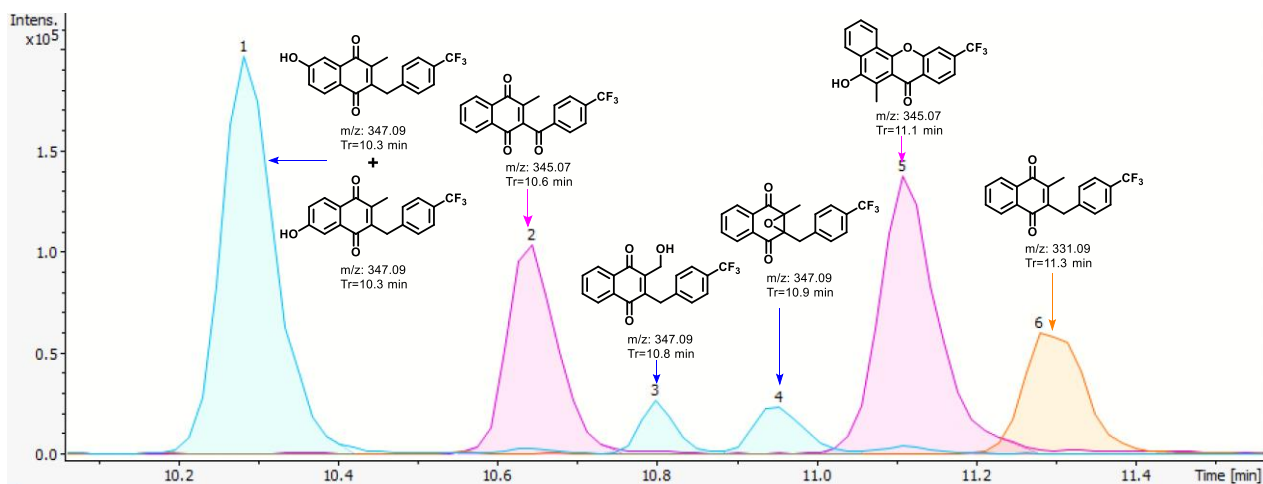


Figure 3. Profils chromatographiques de la plasmodione et de ses 6 métabolites putatifs à 50 μ M.

Afin d'analyser les métabolites générés à partir de la plasmodione, cinq métabolites potentiels précédemment synthétisés¹² ont été fraîchement préparés et analysés par la technique LC-MS/MS (mQTOF). En premier, l'identification du potentiel de collision approprié et le gradient de l'éluant ont été explorés afin d'établir la méthode analytique finale. En regardant le résultat ci-dessous, la plasmodione et ses métabolites putatifs ont été bien séparés en utilisant une colonne C18-Hypersil GOLD, excepté pour les deux dérivés 6- et 7-hydroxyl-benzylmenadiones qui ont montré une polarité très similaire (Figure 3). Heureusement, ces deux régioisomères hydroxyl-benzylmenadiones ont montré des profils de fragmentation distincts qui leur ont permis d'être différenciés sans ambiguïté.

La détermination des rendements d'extraction a été accomplie avec les milieux de culture et les lysats de pRBC. Deux méthodes différentes d'extraction ont été employées en utilisant à la fois le MeOH ou le système de solvants $\text{CHCl}_3/\text{MeOH}/\text{H}_2\text{O}$ (v/v/v = 1/3/1), permettant de comparer les rendements. Une étape supplémentaire d'extraction en phase solide (SPE) a été ajoutée après l'extraction pour éliminer les biométabolites non désirés comme les sucres, les sels, ... L'interprétation de la multitude des données obtenues en LC-MS/MS pour analyser le profil métabolique complet de la plasmodione est encore en cours d'analyse au CEA et à l'ECPM. Les conclusions finales seront dessinées et discutées dans le mémoire de thèse et la présentation orale lors de la soutenance de thèse.

Synthèse d'un dérivé oxétane de plasmodione (3'-(oxetan-3-yloxy)plasmodione)

L'oxétane est l'un des cycles non-planaires à 4 sommets contenant une fonction éther, populaires et récemment introduits en chimie médicinale dans le développement et l'optimisation des médicaments afin d'améliorer les propriétés pharmacocinétiques des molécules parentes.¹³ Ce motif est connu pour être un bon accepteur de liaison(s) H et d'acide de Lewis, avec une polarité et une solubilité aqueuse augmentées, une lipophilicité diminuée, et des biostabilité et biodisponibilité améliorées pour les molécules finales. De plus, l'oxétane est relativement stable même dans des conditions alcalines fortes. La synthèse de la 3'-(oxetane-3-yloxy)plasmodione **15** a été réalisée selon une route à 4-étapes avec un rendement global de 48,6 % (Schéma 5). La réaction de Kochi-Anderson a été appliquée à la ménadione et l'acide 2-(3-fluoro-4-(trifluorométhyl)phényl)acétique commercial comme matériels de départ. Puis, la réduction et la méthylation de la naphthoquinone en 1,4-diméthoxy-naphtalène ont été réalisées en *one pot* en utilisant le chlorure d'étain/HCl, puis le dimethylsulfate/KOH.³ Enfin, la substitution nucléophile aromatique est produite dans le DMSO en utilisant l'anion 3-hydroxyoxétane, généré par l'hydrure de sodium.¹⁴ Finalement, l'intermédiaire précédent a été oxydé par le cérium ammonium nitrate (CAN) pour donner la 3'-(oxetane-3-yloxy)plasmodione **15**.

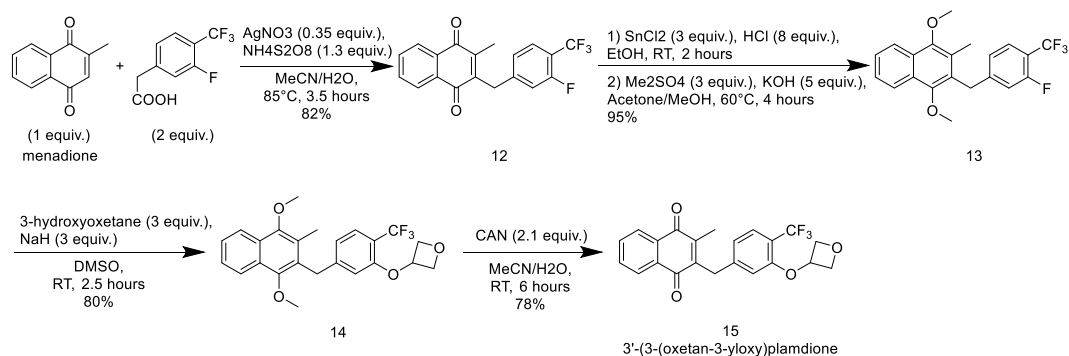


Schéma 5. Route synthétique de la 3'-(oxetan-3-yloxy)plasmodione **15**.

Synthèse d'un dérivé pipérazine de plasmodione

Au-delà du développement de la plasmodione, d'autres dérivés benzyl-ménadione fonctionnalisés par des groupes amino-alkyles en C-4 du cycle phényle de la chaîne benzylique ont été conçus et synthétisés comme des analogues de plasmodione potentiellement améliorés au

niveau de leur solubilité. En particulier, un dérivé pipérazinyl-benzylménadione **20** a été préparé comme agent antipaludique potentiel.

En premier, la réaction radicalaire de Kochi-Anderson a été réalisée entre la ménadione et l'acide 2-(4-chlorophenyl)acétique en présence de nitrate d'argent et le persulfate d'ammonium pour donner la 2-(4-chlorobenzyl)-3-méthyl-naphtalène-1,4-dione **16** avec 85% de rendement. Puis, la réduction/protection du dérivé benzylménadione **16** en dérivé 1,4-diméthoxy-naphtalène **17** ont été appliquées avec les mêmes conditions que précédemment. Ensuite, en s'appuyant sur la réaction de Buchwald-Hartwig, le 4-chlorobenzyl-1,4-diméthoxy-naphtalène **17** a été couplé avec la *t*-butylbenzylpiperazine pour donner le produit **18** avec 95% de rendement. Après une étape déméthylation avec BBr_3 puis de re-oxidation à l'air la pipérazinyl-benzylménadione désirée **19** est obtenue avec 55% de rendement. La préparation du chlorhydrate de *t*-butylbenzylpiperazine benzylménadione a été réalisée en utilisant TMSCl dans le méthanol qui permet de générer HCl *in situ* pour une préparation du sel à échelle modérée (Schéma 6).

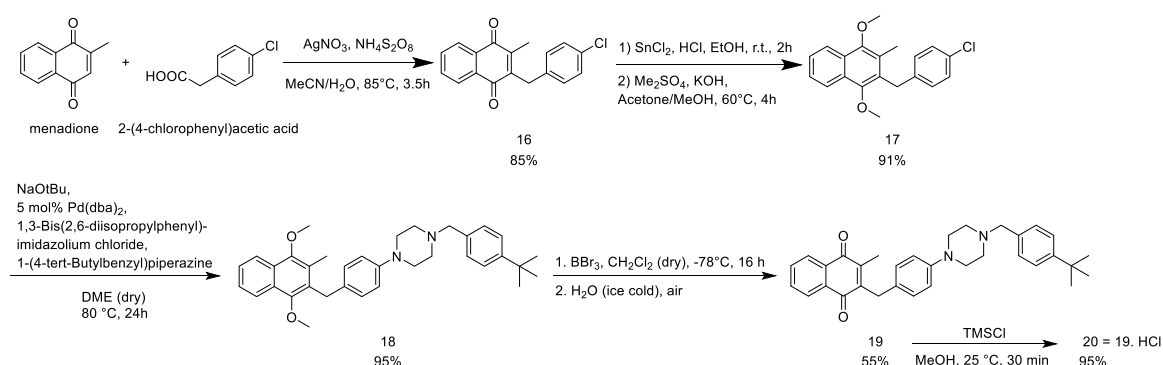


Schéma 6. Route synthétique d'un dérivé pipérazinyl-benzylménadione **20**.

3) Conclusion générale

Le projet de thèse a permis d'élaborer de nouveaux outils moléculaires pour appréhender le développement de nouvelles approches en métabolomics et en chimie médicinale antipaludique. Mes travaux de thèse ont permis d'obtenir la $^{13}\text{C}_{18}$ -plasmodione par synthèse totale, en 10 étapes, à l'échelle de 50 mg, avec un enrichissement en ^{13}C très élevé (>90%) et un rendement global de 4.5%. Chaque étape de la synthèse a été étudiée préalablement avec les réactifs non enrichis. La $^{13}\text{C}_{18}$ -plasmodione est en cours d'utilisation pour son étude de profil métabolique dans les pRBC afin de

confirmer/infirmier l'hypothèse de bioactivation, la découverte de nouveaux métabolites, et permettre de nouvelles stratégies d'optimisation de la tête de série antipaludique sans affecter ses propriétés biologiques. En-deçà de la synthèse de la ¹³C₁₈-plasmodione, deux nouveaux analogues de plasmodione dans le but d'améliorer les propriétés pharmacocinétiques ont été préparés et étudiés pour leur action antipaludique. L'introduction d'un groupe oxétane a augmenté la solubilité et la biodisponibilité de l'analogue de plasmodione final alors que l'introduction du groupe piperazinyl au squelette benzylménadione a augmenté sa solubilité aqueuse, ouvrant de nouvelles perspectives d'utiliser ces agents après administration orale dans les tests *in vivo*.

4) References

- ¹ Tu Y.Y., The discovery of artemisinin (qinghaosu) and gifts from Chinese medicine, *Nat. Med.*, **2011**, *17*, 1217–20
- ² Fairhurst R.M., Nayyar G.M., Breman J.G., Hallett R., Vennerstrom J.L., Duong S., Ringwald P., Wellems T.E., Plowe C.V., Dondorp A.M., Artemisinin-Resistant Malaria: Research Challenges, Opportunities, and Public Health Implications, *Am. J. Trop. Med. Hyg.*, **2012**, *87*, 231-241
- ³ Müller, T., Johann, L., Jannack, B., Bruckner, M., Lanfranchi, D. A., Bauer, H., Sanchez, C., Yardley, V., Deregnacourt, C., Schrevel, J., Lanzer M., Schirmer R.H., Davioud-Charvet E., Glutathione reductase-catalyzed cascade of redox reactions to bioactivate potent antimalarial 1,4-naphthoquinones – a new strategy to combat malarial parasites. *J. Am. Chem. Soc.*, **2011**, *133*, 11557-71.
- ⁴ Ehrhardt K., Davioud-Charvet E., Ke H., Vaidya A.B., Lanzer M., Deponte M., The antimalarial activities of methylene blue and the 1,4-naphthoquinone 3-[4-(trifluoromethyl)benzyl]-menadione are not due to inhibition of the mitochondrial electron transport chain, *Antimicrob. Agents. Chemother.*, **2013**, *57*, 2114-20.
- ⁵ Bielitz M., Belorgey D., Ehrhardt K., Johann L., Lanfranchi D.A., Gallo V., Schwarzer E., Mohring F., Jortzik E., Williams D.L., Becker K., Arese P., Elhabiri M., Davioud-Charvet E., Antimalarial NADPH-Consuming Redox-Cyclers As Superior Glucose-6-Phosphate Dehydrogenase Deficiency Copycats, *Antioxid. Redox. Signal.*, **2015**, *22*, 1337-51
- ⁶ Ehrhardt K., Deregnacourt C, Goetz AA, Tzanova T, Gallo V, Arese P, Pradines B, Adjalley SH, Bagrel D, Blandin S, Lanzer M, Davioud-Charvet E. The Redox Cyclers Plasmodione Is a Fast-Acting Antimalarial Lead Compound with Pronounced Activity against Sexual and Early Asexual Blood-Stage Parasites. *Antimicrob. Agents. Chemother.*, **2016**, *60*, 5146-58.
- ⁷ Cesar Rodo E., Feng L., Jida M, Ehrhardt K., Bielitz M., Boilevin J., Lanzer M., Williams D.L., Lanfranchi D.A., Davioud-Charvet E. A platform of regioselective methodologies to access polysubstituted 2-methyl-1,4-naphthoquinone derivatives: scope et limitations. *Eur. J. Org. Chem.*, **2016**, 1982–93.
- ⁸ Chen Q.Y., Wu S.W., Methyl Fluorosulphonyldifluoroacetate; a New Trifluoromethylating Agent, *Chem. Commun.*, **1989**, 705-706
- ⁹ Oishi M., Kondo H., Amii H., Aromatic trifluoromethylation catalytic in copper, *Chem. Commun.* **2009**, *14*, 1909-1911
- ¹⁰ Gallou F., Haenggi R., Hirt H., Marterer W., Schaefer F., Seeger-Weibel M., A practical non-cryogenic process for the selective functionalization of bromoaryls, *Tetrahedron Lett.*, **2008**, *49*, 5024-5027
- ¹¹ Zhang Z., Sangaiah R., Gold A., Ball L.M., Synthesis of uniformly ¹³C-labeled polycyclic aromatic hydrocarbons, *Org. Biomol. Chem.*, **2011**, *9*, 5431-5435
- ¹² Cesar Rodo Elena. Thèse PhD, Université de Strasbourg, “Synthèse totale de (aza)naphthoquinones polysubstituées à visée antiparasitaire.” Soutenance le 5 octobre 2015.
- ¹³ Wuitschik G., Carreira E.M., Wagner B., Fischer H., Parrilla I., Schuler F., Rogers-Evans M., Müller K., Oxetanes in drug discovery: structural and synthetic insights, *J. Med. Chem.*, **2010**, *53*(8), 3227-3246
- ¹⁴ Bizier N.P., Wackerly J.W., Braunstein E.D., Zhang M., Nodder S.T., Carlin S.M., Katz J.L., An alternative role for acetylenes: activation of fluorobenzenes toward nucleophilic aromatic substitution, *J. Org. Chem.* **2013**, *78*(12), 5987-5998.

Part 1: Plasmodione as an early lead antimalarial drug

1. Introduction

Malaria is a parasitic disease, threatening 3.2 billion people who are living in the tropical and sub-tropical regions.¹ According to the world health organization (WHO), 214 million cases of malaria occurred giving rise, to 438,000 deaths per year in 2015, 70% malaria decedents are young children¹. *Plasmodium* is a protozoan parasite that infects humans via *anopheles* mosquito. Five plasmodial species are responsible for malaria in Humans.^{2,3} *Plasmodium falciparum* is the most dangerous parasite species and causes severe disease such as cerebral malaria, hemolytic anemia and respiratory distress; 99% malaria deaths are due to *Plasmodium falciparum*.^{1,4,5} These number represent a 48% decline in mortality since 2000. In 2015, whereas malaria is still the fourth highest cause of death, accounting for 10% of child deaths in sub-Saharan Africa, an equally impressive drop in malaria-related morbidity has been observed. These spectacular statistics are partly due to the massive use of insecticide-treated bednets (ITN) and artemisinin-based combination therapies (ACT). In sub-Saharan Africa, of the million cases averted due to malaria control interventions it is estimated that 69% were accounted for the use of ITN, 21% for ACT and 10% for indoor residual spraying.

Following the bite of female *anopheles* mosquitoes, *plasmodium* parasites are transmitted to human through an infective form, named sporozoite.^{6,7} The sporozoites of *Plasmodium* parasites reach the blood vessels and invade the liver where they generate merozoites. Subsequently, the *Plasmodium* merozoites can invade human red blood cells to start the intraerythrocytic cycle. After invasion of the red blood cells, the parasites develop through different stages: rings, trophozoites, schizonts and then

¹ World Malaria Report 2015, World Health Organization. December 2015. ISBN 978-92-4-156515-8

² Mueller I., Zimmerman P.A., Reeder J.C., *Plasmodium malariae* and *Plasmodium ovale* – the ‘bashful’ malaria parasites, *Trends Parasitol.*, **2007**, 23, 278-283

³ Collins W.E., *Plasmodium knowlesi*: A malaria parasite of monkeys and humans, *Annu Rev Entomol*, **2012**, 57, 107-121

⁴ Bartoloni A., Zammarchi L., Clinical Aspects of Uncomplicated and Severe Malaria, *Mediterr J Hematol Infect Dis*, **2012**, 4, e2012026.

⁵ Snow R.W., Guerra C.A., Noor A.M., Myint H.Y., Hay S.I., The global distribution of clinical episodes of *Plasmodium falciparum* malaria. *Nature*, **2005**, 434, 214-217

⁶ Cowman A.F., Berry D., Baum J., The cellular and molecular basis for malaria parasite invasion of the human red blood cell, *J Cell Biol*, **2012**, 198, 961-971

⁷ Schlagenhauf-Lawlor P., Travelers' Malaria, *BC Decker Inc*, **2008**, 70-71

merozoites ready to re-invade red blood cells. This cycle lasts 48 h in the human pathogen, *P. falciparum*, and 24 h in the murine pathogen, *P. berghei*. The trophozoites digest a large quantity of its host cell's hemoglobin as a source of essential nutrients and reproduce asexually. Finally, a part of rings form the sexual stages called gametocytes. After maturation, from stage I to V, gametocytes become infectious to the insect vector *Anopheles* and can be transmitted in a blood meal through a bite of the mosquito. (Scheme 1)

Several antimalarial drugs like quinine, chloroquine and mefloquine are known to cure malarial infections.⁸ These quinoline-containing antimalarial drugs are considered as inhibitors of the heme detoxification by interfering with the digestion of hemoglobin in the blood stages of the malaria life cycle. It is well reported that the host hemoglobin digestion takes place in an acidic compartment, called digestive or food vacuole, and provides the essential nutrients (amino-acids) for the parasite growth. Also, this process liberates a large amount of toxic heme that the parasite detoxifies by biocrystallization under the form of an insoluble pigment, called hemozoin (or malaria pigment) (Figure 1a). Inhibiting this detoxification process leads to the death of parasites because of an elevation of the toxic and lipophilic heme in membranes and other compartments. However, drug resistances appeared and spread all over the world in the last 50 years. The naturally occurring artemisinin was discovered in 1970s by Tu *et al.* With its peroxy bridge the natural compound has a very different mode of action compared to that of quinoline-containing antimalarial drugs, making the ACT extremely useful in treatment of multi-drug resistant infection (Figure 1b). The ACT has been recommended by WHO as the first-line therapy to treat *Plasmodium falciparum* infected patients, and is widely and successfully used to cure malaria.^{1,9,10,11} The mechanism of action of artemisinin is not exactly clear until nowadays. Based on previous study, artemisinin was proposed to be bioactivated by ferrous iron species and to react with heme inside *Plasmodium falciparum*-parasitized red blood cell (pRBC). This event that leads to heme alkylation was also shown to generate reactive oxygen species

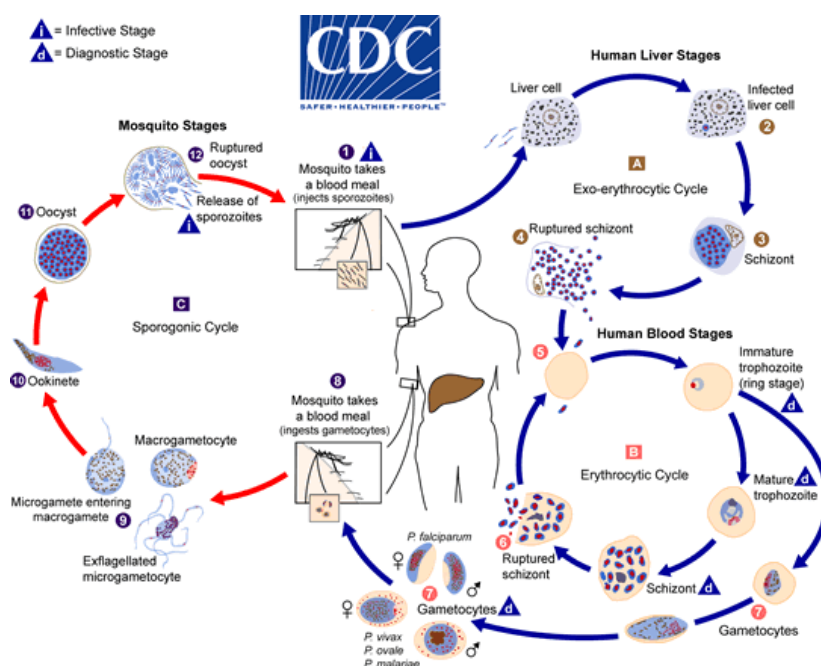
⁸ Foley M., Tilley L., Quinoline antimalarials: mechanisms of action and resistance and prospects for new agents., *Pharmacol Ther.* **1998**, 79, 55-87.

⁹ Collaboration Research Group for Qinghaosu. A novel kind of sesquiterpene lactone artemisinin. *Chinese Science Bulletin*, **1977**, 22, 142.

¹⁰ Rao Y., Li R.H., Zhang D.Q., A monumental landmark of scientific research in traditional Chinese medicine, *Science and Culture Review*, **2011**, 8, 27-44.

¹¹ Tu Y.Y., The discovery of artemisinin (qinghaosu) and gifts from Chinese medicine, *Nature Medicine*, **2011**, 17, 1217–1220.

(ROS) by Fenton reaction, leading to iron-dependent cell death (ferroptosis)^{12,13}. Also, artemisinin and its endoperoxides derivatives were observed to interfere with iron transport/utilization in hemozoin-producing and iron-dependent parasites, such as *Plasmodium* and *Schistosoma*.¹⁴ Wang *et al.* had been identified that artemisinin acts with several and promiscuous targets in 2016.¹⁵ Because artemisinin has a relatively intricate chemical structure, industrial synthetic preparation of the endoperoxide drug is difficult, making its price very high. On the other hand, drug resistance has started to emerge in Southeast Asia, putting ACT at risk to cure malaria.^{16,17} Therefore, developing an alternative drug with novel mechanisms of action is urgently required.



¹² Ooko E, Saeed ME, Kadioglu O, Sarvi S, Colak M, Elmasaoudi K, Janah R, Greten HJ, Efferth T. Artemisinin derivatives induce iron-dependent cell death (ferroptosis) in tumor cells. *Phytomedicine*. **2015**, 22, 1045-54.

¹³ Portela J., Boissier J., Gourbal B., Pradines V., Collière V., Coslédan F., Meunier B., Robert A., Antischistosomal activity of trioxaquinones: in vivo efficacy and mechanism of action on *Schistosoma mansoni*, *PLoS Negl Trop Dis*, **2012**, 6, e1474.

¹⁴ Sun J, Li C, Wang S. Organism-like formation of *Schistosoma* hemozoin and its function suggest a mechanism for anti-malarial action of artemisinin. *Sci Rep*. **2016**, 6, 34463.

¹⁵ Wang J.G., Zhang C.J., Chia W.N., Loh C.C., Li Z.J., Lee Y.M., He Y.K., Yuan L.X., Lim T.K., Liu M., Liew C.X., Lee Y.Q., Zhang J.B., Lu N.C., Lim C.T., Hua Z.C., Liu B., Shen H.M., Tan K.S., Lin Q.S., Haem-activated promiscuous targeting of artemisinin in *Plasmodium falciparum*, *Nat Commun*, **2015**, 6, 10111

¹⁶ O'Brien C., Henrich P.P., Passi N., Fidock D.A., Recent clinical and molecular insights into emerging artemisinin resistance in *Plasmodium falciparum*, *Current Opinion in Infectious Disease*, **2011**, 6, 570-577

¹⁷ Fairhurst R.M., Nayyar G.M., Breman J.G., Hallett R., Vennerstrom J.L., Duong S., Ringwald P., Wellems T.E., Plowe C.V., Dondorp A.M., Artemisinin-Resistant Malaria: Research Challenges, Opportunities, and Public Health Implications, *Am J Trop Med Hyg*, **2012**, 87, 231-241

Scheme 1. Life cycle of *Plasmodium*. (copy the scheme from from Ref.18)

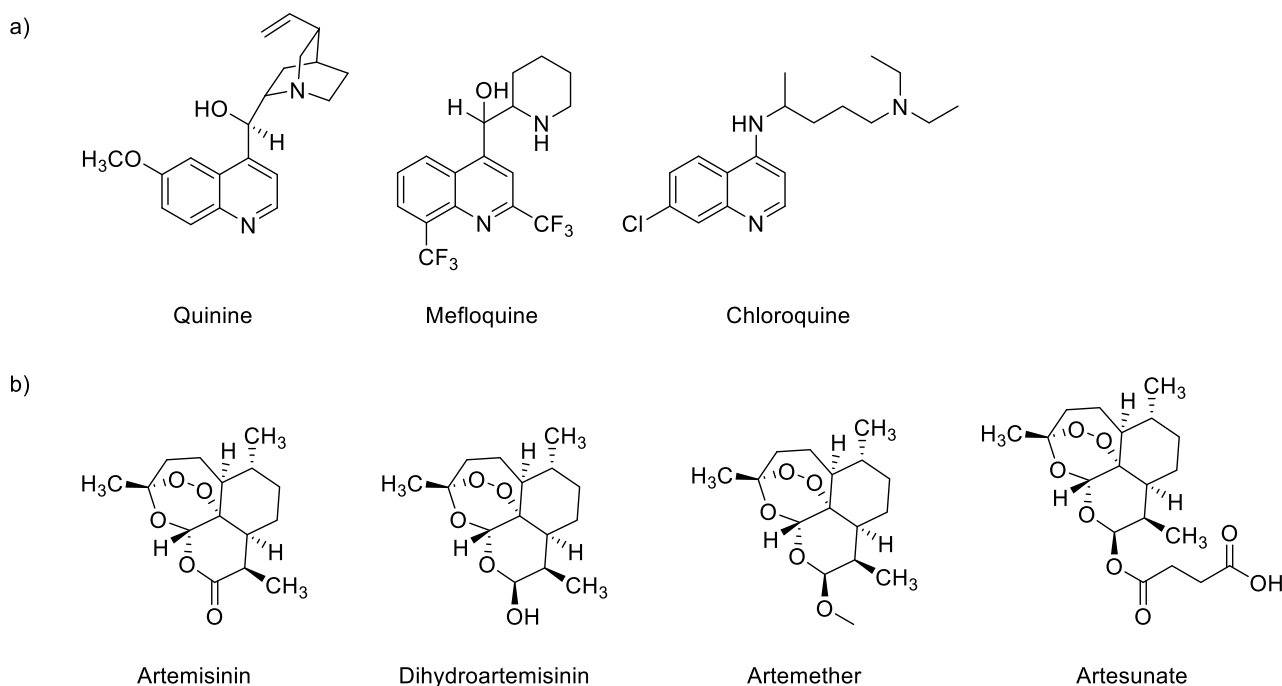


Figure 1. a) the structure of quinoline-containing antimalarial drugs. b) the structure of artemisinin and its antimalarial derivatives.

2. The 1,4-naphthoquinone series: plasmodione *versus* atovaquone

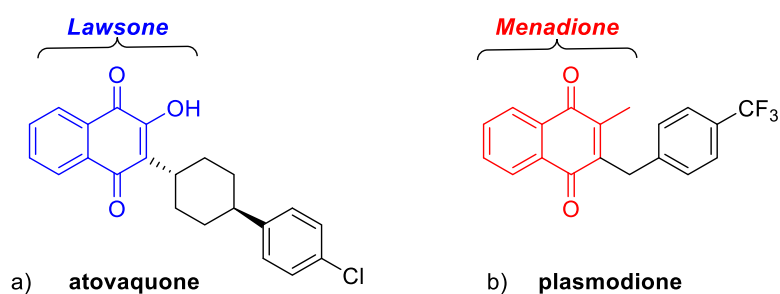


Figure 2. a). Structure of atovaquone. b). Structure of plasmodione.

The first investigation on 1,4-naphthoquinones as antimalarial drugs was over than 70 years, the outbreak of World War II caused severe undersupplying of quinine and the alternative antimalarial

¹⁸ US Centers for Disease Control and Prevention. March 1, 2016.

drugs were urgently required.¹⁹ More than 300 quinone derivatives were explored and demonstrated for antimalarial activity in *Plasmodium lophurae*-infected ducks assay, some of them were shown to have better activity than quinine.²⁰ However, these series of compounds were not successful in the clinical trials.^{21,22} Due to the insufficiency of bio-absorptivity and bio-stability, all of these compounds were devoid of activity while they were evaluated in malarial patients by oral administration. In order to solve these problems, several 2-cyclohexyl-3-hydroxy-1,4-naphthoquinone analogues were designed and evaluated for their cytotoxicity to the *Plasmodium falciparum in vitro*, but only atovaquone (also named 566C80, Figure 2a) was found that retains antimalarial activity after liver passage.^{23,24,25}

Atovaquone is a *trans*-4-(4-chlorophenyl)cyclohexane substituted 3-hydroxy-1,4-naphthoquinone. The atovaquone/proguanil combination drug (named Malarone® or Malanil®) is used in prophylaxis of malaria, and in treatments to cure chloroquine-resistant infections.²⁶ Atovaquone was shown to selectively inhibit the parasite mitochondrial electron transport chain (mETC) without interference with the host mETC.^{27,28,29} It can bind to the ubiquinol (CoQ₁₀) oxidation site of cytochrome bc₁, inhibit the regeneration of ubiquinone and disturb the mitochondrial

¹⁹ Fieser L.F., Richardson A.P., Naphthoquinone Antimalarials. II. Correlation of Structure and Activity Against *P. lophurae* in Ducks, *J. Am. Chem. Soc.*, **1948**, *70*, 3156–3165.

²⁰ Hudson A.T., Atovaquone - a novel broad-spectrum anti-infective drug, *Parasitol Today*, **1993**, *9*, 66-68

²¹ Fieser L.F., Heymann H., Seligman A.M., Naphthoquinone antimalarials. XX. Metabolic degradation. *J Pharmacol Exp Ther*, **1948**, *94*, 112–124.

²² Fieser L.F., Chang F.C., Dauben W.G., Heidelberger C., Heymann H., Seligman A.M., Naphthoquinone antimalarials. XVIII. Metabolic oxidation products. *J Pharmacol Exp Ther*, **1948**, *94*, 85–96.

²³ Hudson A.T., Randall A.W., Fry M., Ginger C.D., Hill B., Latter V.S., McHardy N., Williams R.B., Novel anti-malarial hydroxynaphthoquinones with potent broad-spectrum anti-protozoal activity. *Parasitology*, **1985**, *90*, 45–55.

²⁴ Hudson A.T., Pether M.J., Randall A.W., Fry M., Latter V.S., McHardy N., In vitro activity of 2-cycloalkyl-3-hydroxy-1,4-naphthoquinones against *Theileria*, *Eimeria* and *Plasmodia* species, *Eur J Med Chem*, **1986**, *21*, 271–275.

²⁵ Hudson A.T., Dickins M., Ginger C.D., Gutteridge W.E., Holdich T., Hutchinson D.B., Pudney M., Randall A.W., Latter V.S., 566C80: a potent broad spectrum anti-infective agent with activity against malaria and opportunistic infections in AIDS patients, *Drugs Exp Clin Res*. **1991**, *17*, 427-435.

²⁶ Nakato H., Vivancos R., Hunter P.R., A systematic review and meta-analysis of the effectiveness and safety of atovaquone–proguanil (Malarone) for chemoprophylaxis against malaria, *J. Antimicrob. Chemother.*, **2007**, *60*, 929-936

²⁷ Srivastava I.K., Morrissey J.M., Darrouzet E., Daldal F., Vaidya A.B., Resistance mutations reveal the atovaquone-binding domain of cytochrome b in malaria parasites, *Mol Microbiol*. **1999**, *33*, 704-711

²⁸ Fry M., Pudney M., Site of action of the antimalarial hydroxynaphthoquinone, 2-[*trans*-4-(4'-chlorophenyl) cyclohexyl]-3-hydroxy-1,4-naphthoquinone (566C80), *Biochem Pharmacol.*, **1992**, *43*, 1545-1553.

²⁹ Srivastava I.K., Rottenberg H., Vaidya A.B., Atovaquone, a broad spectrum antiparasitic drug, collapses mitochondrial membrane potential in a malarial parasite, *J Biol Chem.*, **1997**, *272*, 3961-3966.

membrane electronic potential.^{30,31,32} In addition, at the asexual erythrocyte stage of *P. falciparum*, the mETC plays an irreplaceable role for the nucleic acid biosynthesis, specifically different to the mammal cells. It can regenerate ubiquinone as electron acceptor for dihydroorotate dehydrogenase (DHODH), which is the 4th enzyme in the pyrimidine biosynthesis pathway (Scheme 2).^{33,34} As a result, the parasites have not the capacity to salvage exogenous pyrimidine, and therefore completely rely on their own endogenous pyrimidine biosynthesis. Inhibition of the pyrimidine biosynthesis can arrest the growth of the parasites.³⁵ This mode of mechanism of atovaquone had been proved in the presence of yeast dihydroorotate dehydrogenase (γ DHODH) encoded by transgenic *P. falciparum* strains.³⁶ In the meanwhile, the resulting mutant parasite strains provide an effective means to screen potential inhibitors of the mETC.

³⁰ Kessl J.J., Ha K.H., Merritt A.K., Lange B.B., Hill P., Meunier B., Meshnick S.R., Trumppower B.L., Cytochrome b mutations that modify the ubiquinol-binding pocket of the cytochrome bc1 complex and confer anti-malarial drug resistance in *Saccharomyces cerevisiae*, *J. Biol. Chem.*, **2005**, *280*, 17142-17148

³¹ Kessl J.J., Moskalev N.V., Gribble G.W., Nasr M., Meshnick S.R., Trumppower B.L., Parameters determining the relative efficacy of hydroxy-naphthoquinone inhibitors of the cytochrome bc1 complex, *Biochim. Biophys. Acta.*, **2007**, *1767*, 319-326

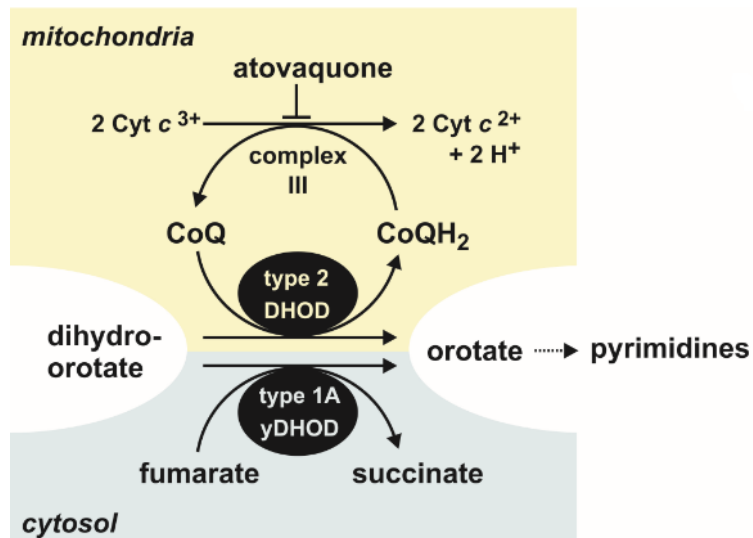
³² Biagini G.A., Fisher N., Shone A.E., Mubarak M.A., Srivastava A., Hill A., Antoine T., Warman A.J., Davies J., Pidathala C., Amewu R.K., Leung S.C., Sharma R., Gibbons P., Hong D.W., Pacorel B., Lawrenson A.S., Charoensutthivarakul S., Taylor L., Berger O., Mbekeani A., Stocks P.A., Nixon G.L., Chadwick J., Hemingway J., Delves M.J., Sinden R.E., Zeeman A.M., Kocken C.H., Berry N.G., O'Neill P.M., Ward S.A., Generation of quinolone antimalarials targeting the *Plasmodium falciparum* mitochondrial respiratory chain for the treatment and prophylaxis of malaria, *Proc Natl Acad Sci U S A.* **2012**, *109*, 8298-8303

³³ Vaidya A.B., Mather M.W., Mitochondrial evolution and functions in malaria parasites, *Annu Rev Microbiol.* **2009**, *63*, 249-267.

³⁴ Painter H.J., Morrissey J.M., Mather M.W., Vaidya A.B., Specific role of mitochondrial electron transport in blood-stage *Plasmodium falciparum*, *Nature*, **2007**, *446*, 88-91.

³⁵ Gutteridge W.E., Dave D., Richards W.H., Conversion of dihydroorotate to orotate in parasitic protozoa, *Biochim. Biophys. Acta.*, **1979**, *582*, 390-401.

³⁶ Ke H., Morrissey J.M., Ganesan S.M., Painter H.J., Mather M.W., Vaidya A.B., Variation among *Plasmodium falciparum* strains in their reliance on mitochondrial electron transport chain function, *Eukaryot Cell.*, **2011**, *10*, 1053-1061.



Scheme 2. Scheme of the targeted mitochondrial electron transport in atovaquone-sensitive *P. falciparum* parasites. Expression of a gene encoding yDHOD provides a cytosolic bypass in transgenic *P. falciparum* strains. Such strains become independent of the mETC and are therefore not only resistant to atovaquone but also to other antimalarials targeting the mETC. (copy the scheme from ref. 37)

³⁷ Ehrhardt K, Davioud-Charvet E, Ke H, Vaidya AB, Lanzer M, Deponce M., The antimalarial activities of methylene blue and the 1,4-naphthoquinone 3-[4-(trifluoromethyl)benzyl]-menadione are not due to inhibition of the mitochondrial electron transport chain. *Antimicrob Agents Chemother.*, **2013**, 57, 2114-2120.

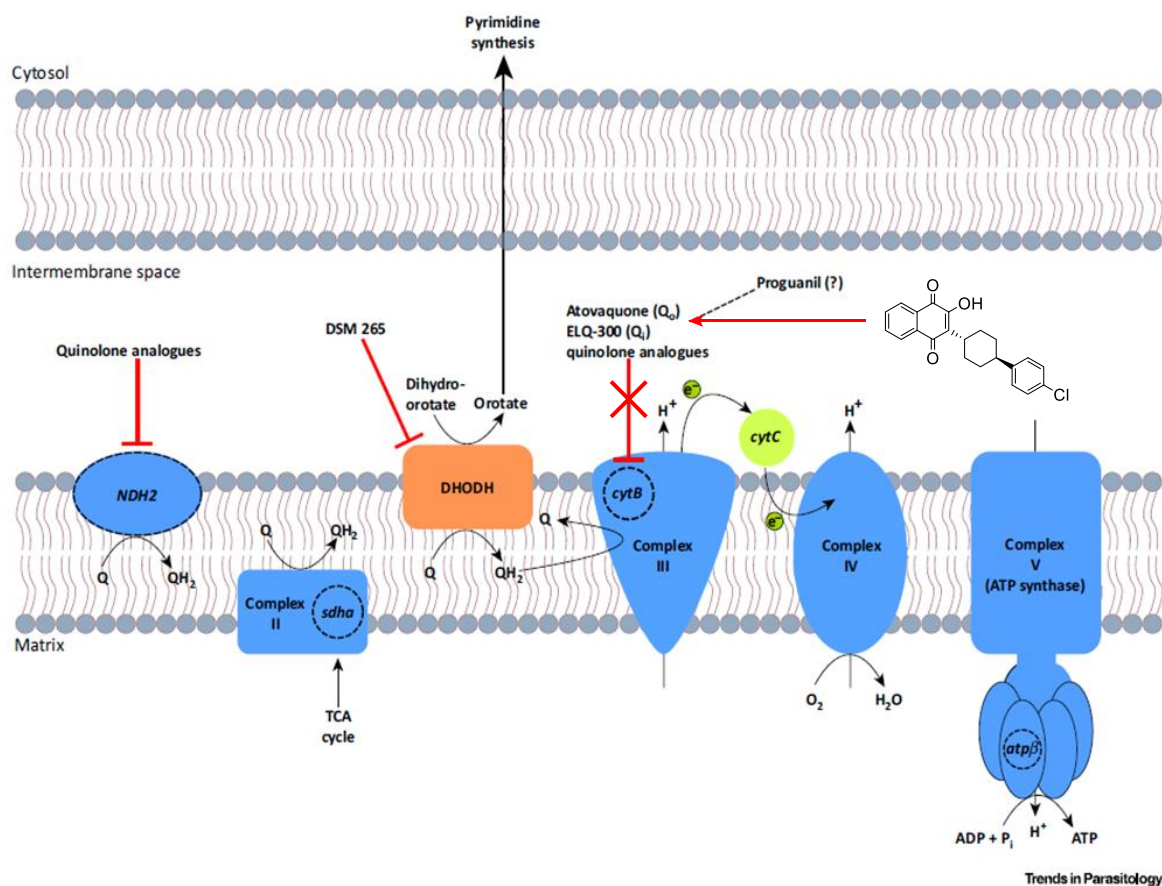


Figure 3. Inhibitors of the *Plasmodium* Mitochondrial Electron Transport Chain (copied the figure from Ref.38).

The research of my host team is focused on exploitation and development of antimalarial agents, which affect the redox equilibrium of *P. falciparum*-pRBCs. Among the chemical series we investigated, the team discovered the 3-[4-(trifluoromethyl)-benzyl]-menadione (henceforth named plasmodione, or benzylmenadione 1c, structure see Figure 2b) and its derivatives with potent antimalarial activity in cell culture with nanomolar scale IC₅₀ values. The lead compound has no chiral center making the drug more accessible than atovaquone. Thanks to the 2-methyl-1,4-naphthoquinone in the core part of plasmodione, this promising lead drug has oxidant and electron transfer properties. Recent research has shown that plasmodione via its benzylmenadione metabolite can act as electrons acceptor with the flavoprotein glutathione reductase (GR) and, under its reduced form, converts methemoglobin(Fe^{III}) to oxyhemoglobin(Fe^{II}). The NADPH-dependent futile cycle interplays with the

³⁸ Goodman CD, Buchanan HD, McFadden GI. Is the Mitochondrion a Good Malaria Drug Target? *Trends Parasitol.* **2017**, *33*, 185-193.

hemoglobin catabolites, methemoglobin and Fe(III)-protoporphyrin IX. However, although both atovaquone and plasmodione have redox properties and structural similarities, they do not share the same mechanism pathway to inhibit the growth of the parasites. Apart from obvious antimalarial differences, an important property seems to be the redox potential values.³⁷ The low redox potential of atovaquone (-0.51 V) indicates that, under physiological conditions, atovaquone and lawsone reduction is considerably less favored compared to menadione reduction (-0.14 V)³⁹. Even under highly reducing intracellular conditions with an estimated half-cell redox potential for NADPH around -0.34 V⁴⁰, the redox potential for atovaquone will be too low for efficient reduction by two-electron reduced GRs, which have redox potentials around -0.24 V at pH 7.⁴¹ Furthermore, the ability of human and *P. falciparum* GR to reduce either atovaquone or lawsone (2-hydroxy-1,4-naphthoquinone, Figure 2a) was studied at substrate concentrations of up to 25 μ M or 100 μ M, respectively, but no NADPH consumption was observed,^{42,43} attesting for distinct mechanisms of action displayed by atovaquone and plasmodione.

Previous studies in the laboratory³⁷ have shown that atovaquone lost its antimalarial activity when tested in the transgenic *P. falciparum* strain 3D7attB-yDHODH (Table 1), expressing the yDHODH. In contrast, plasmodione maintained its antiplasmodial activity against the strain 3D7attB-yDHODH, proving that plasmodione and atovaquone do not share similar effect on mETC, in agreement with distinct targets for plasmodione to exert its antiparasitic activity.

³⁹ Lopez-Shirley, K., F. Zhang, D. Gosser, M. Scott, and S. R. Meshnick.. Antimalarial quinones: redox potential dependence of methemoglobin formation and heme release in erythrocytes. *J. Lab. Clin. Med.*, **1994**, *123*, 126-130.

⁴⁰ Deponte, M. Glutathione catalysis and the reaction mechanisms of glutathione-dependent enzymes. *Biochim. Biophys. Acta.*, **2013**, *1830*, 3217-66.

⁴¹ Veine, D. M., L. D. Arscott, and C. H. Williams, Jr. Redox potentials for yeast, *Escherichia coli* and human glutathione reductase relative to the NAD⁺/NADH redox couple: enzyme forms active in catalysis. *Biochemistry*, **1998**, *37*, 15575-15582.

⁴² Davioud-Charvet, E., and D. A. Lanfranchi. Subversive substrates of glutathione reductases from *Plasmodium falciparum*-infected red blood cells as antimalarial agents, p 375-396. In Selzer P (ed) *Drug Discovery in Infectious Diseases*, **2011**, vol 2, Wiley-VCH, Weinheim.

⁴³ Lanfranchi, D. A., D. Belorgey, T. Muller, H. Vezin, M. Lanzer, and E. Davioud-Charvet. Exploring the trifluoromenadione core as a template to design antimalarial redox-active agents interacting with glutathione reductase. *Org. Biomol. Chem.*, **2012**, *10*, 4795-4806.

Agent	Mean IC ₅₀ (nM) for Strain		
	3D7	3D7attB	3D7attB-yDHODH
Atovaquone	0.24 ± 0.03	0.54 ± 0.03	2230 ± 419
Plasmodione	46.3 ± 2.04	47.6 ± 4.79	55.1 ± 5.6

Table 1. Averaged IC₅₀ values (nM) determined from growth inhibition assays with strains 3D7, 3D7attB, and 3D7attB-yDHODH^a). All values are means ± standard error of the mean from three independent growth inhibition assays. (from ref. 37)

3. 2-Methyl-1,4-naphthoquinone chemistry

1,4-Naphthoquinones are ubiquitously present in all kinds of cellular, well-known examples, 2-methyl-1,4-naphthoquinone (also called menadione or vitamin K3) and plumbagin (2-methyl-5-hydroxy-1,4-naphthoquinone) derivatives. Owing to its redox properties, numbers of 1,4-naphthoquinone compounds are well known to act as electron acceptors in the respiration electron transfer chain. In contrast, versatile methodologies for the preparation of synthetic unsymmetrical 2-methyl-1,4-naphthoquinone derivatives are rare. In order to discover and prepare our lead antimalarial lead plasmodione and its large number of diverse analogues and potential metabolites, a synthetic platform toward polysubstituted benzylmenadiones has been previously established in our laboratory.^{44,45,46}

First, the lead compound plasmodione can be synthesized by only one step through the Kochi-Anderson reaction (under Jacobsen–Torssell condition) making the large-scale preparation of our lead plasmodione and its analogues⁴⁷ easy, low cost and available (Scheme 3). Many phenylacetic acids can proceed decarboxylation and generate the benzyl radical in the presence of silver nitrate and ammonium peroxydisulfate under moderate heating. Then, the resulting benzyl radical can react with

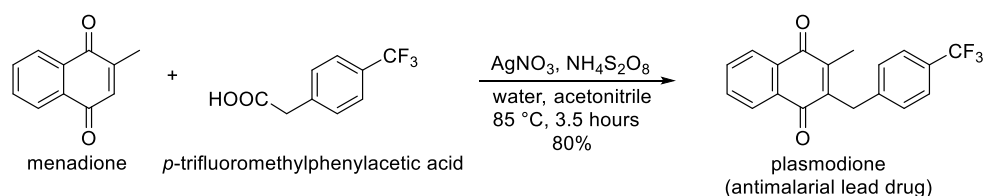
⁴⁴ Lanfranchi, D. A., Cesar-Rodo, E., Bertrand, B., Huang, H.-H., Day, L., Johann, L., Elhabiri, M., Becker, K., Williams, D. L., Davioud-Charvet, E. Synthesis and biological evaluation of 1,4-naphthoquinones and quinoline-5,8-diones as antimalarial and schistosomicidal agents. *Org. Biomol. Chem.* **2012**, *10*, 6375-6387.

⁴⁵ Cesar Rodo Elena, PhD thesis, University of Strasbourg, “Synthèse totale de (aza)naphthoquinones polysubstituées à visée antiparasitaire”, October 5, **2015**.

⁴⁶ Cesar Rodo E., Feng L., Jida, M., Ehrhardt K., Bielitz M., Boilevin J., Lanzer M., Williams D. L., Lanfranchi D. A., Davioud-Charvet E., A platform of regioselective methodologies to access to polysubstituted 2-methyl-1,4-naphthoquinones derivatives: scope and limitations, *Eur. J. Org. Chem.*, **2016**, *11*, 1982–1993.

⁴⁷ Müller T., Johann L., Jannack B., Brückner M., Lanfranchi D. A., Bauer H., Sanchez C., Yardley V., Deregnacourt C., Schrével J., Lanzer M., Schirmer R. H., Davioud-Charvet E., Glutathione reductase-catalyzed cascade of redox reactions to bioactivate potent antimalarial 1,4-naphthoquinones – A new strategy to combat malarial parasites. *J. Am. Chem. Soc.* **2011**, *133*, 11557-71.

the menadione core to yield the desired benzylmenadione. Thanks to this decarboxylation radical coupling reaction providing a powerful method, the retrosynthesis of polysubstituted benzylmenadione can be directed to “western” part (menadione part) functionalization *versus* “eastern” part (phenylacetic acid part) functionalization (Scheme 4).



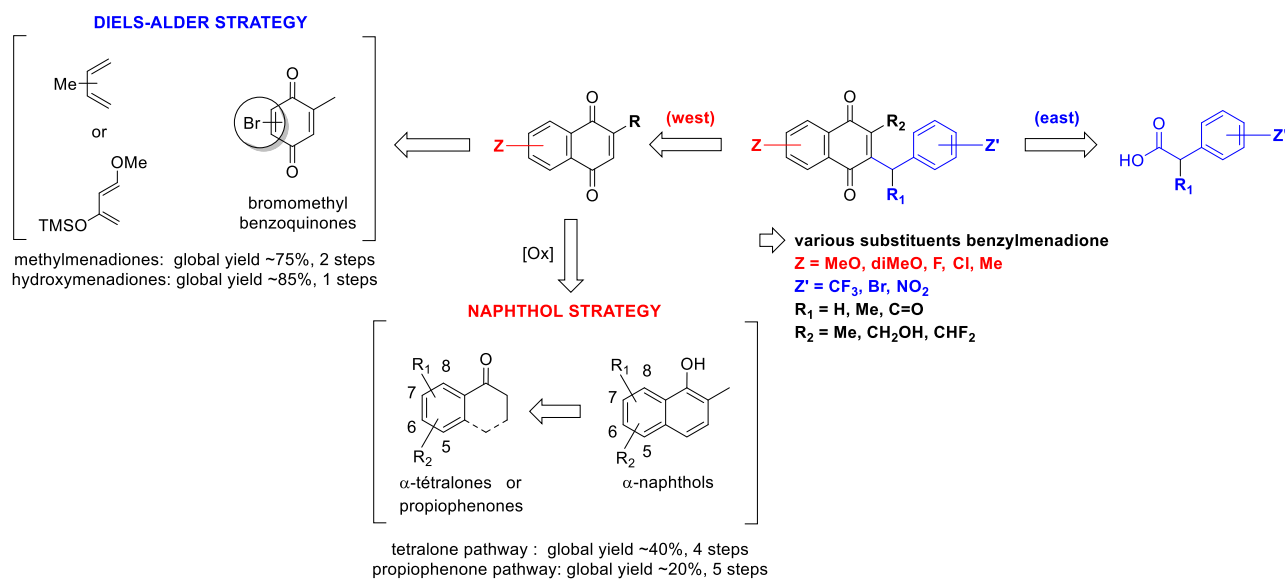
Scheme 3. The synthesis of plasmodione by Kochi-Anderson reaction.

The functionalization of the “eastern” part of benzylmenadiones has been first developed in the team. The nucleophilic/electrophilic aromatic substitution provides a versatile method to approach diversified east part of benzylmenadiones. In addition, numbers of commercially available mono/polysubstituted phenylacetic acids support this approach feasible.^{47,48,49}

In general, many synthetic routes of 1,4-naphthoquinones have been reported in the literature, which employed a naphthol as an intermediate. Following the oxidation, these intermediates produced the related 1,4-naphthoquinone. Besides, the Diels-Alder cyclization provided a more direct and regioselective approach to 1,4-naphthoquinone. However, owing to the 2-methyl group of menadione, there was no general synthetic route to prepare polysubstituted menadione analogues. Therefore, through both naphthol and Diels-Alder strategies, a small library of polysubstituted menadione analogues^{44,46,48} was built as templates for synthesis of polysubstituted 3-benzylmenadione analogues and their putative drug metabolites for further drug development.

⁴⁸ Bielitz M., Belorgey D., Ehrhardt K., Johann L., Lanfranchi D. A., Gallo V., Schwarzer E., Mohring F., Jortzik E., Williams D. L., Becker K., Arese P., Elhabiri M., Davioud-Charvet E., Antimalarial NADPH-consuming redox-cyclers as superior G6PD deficiency copycats, *Antioxid. Redox Signal.* **2015**, *22*, 1337-51.

⁴⁹ Sidorov P., Desta I., Chessé M., Horvath D., Marcou G., Varnek A., Davioud-Charvet E., Elhabiri M. Redox polypharmacology is an emerging strategy to combat malarial parasites. *ChemMedChem.*, **2016**, *11*, 1339–51.



Scheme 4. Platform of synthetic methodologies to prepare a large number of diverse polysubstituted menadiones and analogues of the redox-active antimalarial lead plasmodione.⁴⁶

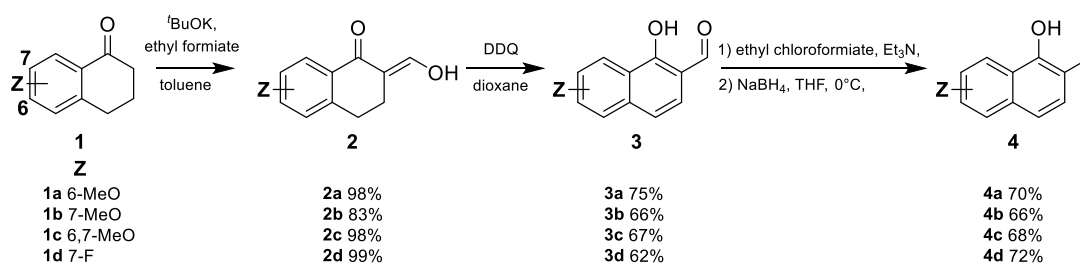
3.1. Synthesis of menadione analogues through the naphthol strategy

For the naphthol strategy, upon to the starting material, commercially available tetralones or propiophenones, two synthetic routes were utilized to produce α -naphthol intermediates. First, a synthetic route starting from tetralone analogues was established to offer corresponding naphthol intermediates. The commercially available 1-tetralone **1** was combined with ethyl formate by a condensation reaction in the presence of *t*BuOK.⁵⁰ Then, the aromatization with DDQ was followed by the reduction of intermediate with NaBH₄.^{51,52} This three steps-long route has led to the corresponding naphthol intermediates **4** in good yields (36%-51% total yields) (Scheme 5).

⁵⁰ Pearce B. C., Parker R. A., Deason M. E., Dischino D. D., Gillespie E., Qureshi A. A., Volk K., Wright J. J., Hypocholesterolemic and antioxidant activities of benzopyran and tetrahydronaphthalene analogues of the tocotrienols, *J. Med. Chem.*, **1994**, *37*, 526–541.

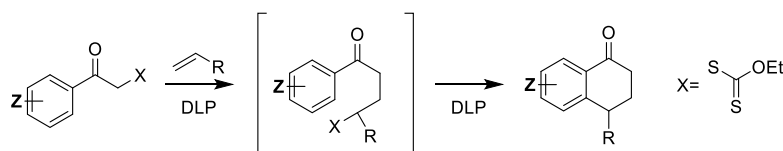
⁵¹ Kim S. H., Gunther J. R., Katzenellenbogen J. A., Nonclassical SNAPFL Analogue as a Cy5 Resonance Energy Transfer Partner, *Org. Lett.*, **2008**, *10*, 4931–4934.

⁵² Minanmi N., Kikima S., Reduction of *o*-Acylphenols through Ethyl *o*-Acylphenylcarbonates to *o*-Alkylphenols with Sodium Borohydride, *Chem. Pharm. Bull.*, **1979**, *6*, 1490–1494.



Scheme 5. Synthesis of 2-methylnaphthol intermediates **4** from 1-tetralone **1** analogues.

Secondary, the synthesis of naphthols was developed through the xanthate-mediated, radical addition-cyclization developed by Zard *et al.*⁵³, but here from propiophenones (Scheme 6). Based on this degenerative radical reaction, the desired tetralone analogues could be easily approached from propiophenone-based xanthate-substituted derivatives.

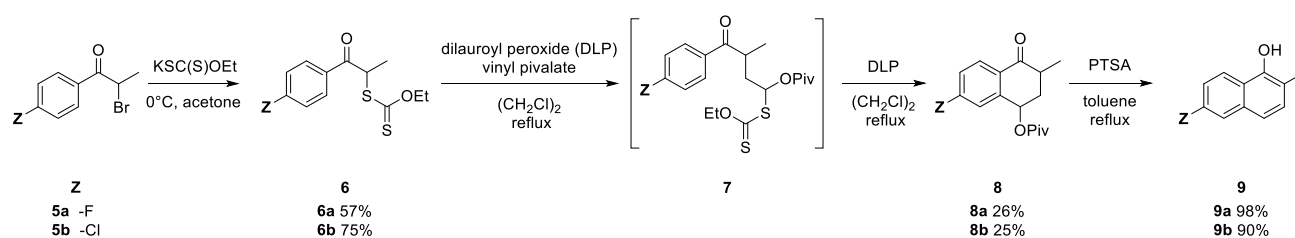


Scheme 6. Synthesis of tetralone analogues by a xanthate radical cyclisation sequence.

The chemistry of Zard and co-workers was aimed at synthesizing naphthols from tetralone, lacking the α -methyl group. Thus, the research of our laboratory has completed the synthesis of α -methylnaphthols analogues from commercial available propiophenones derivatives. The bromopropiophenones were easily obtained from commercial propiophenones analogues **5** by bromination with Br_2 . Then, the resulting bromopropiophenones were treated with potassium ethyl xanthate in acetone to produce desired xanthates precursors **6**. Subsequently, via a xanthate intermediate **7**, the radical addition of the resulting xanthate **6** was started with dilauroyl peroxide (DLP) as initiator and then reacted with vinyl pivalate to give the xanthate-mediated **7**. Following the resulting intermediate **7** was added an additional 1.2 equiv. DLP to push the reaction yielding the relative tetralones **8**. Finally, resulting from the OPiv group acting as a leaving group the previous

⁵³ a) Cordero-Vargas A., Quiclet-Sire B., Zard S. Z., Total Synthesis of 10-Norparvulenone and of O-Methylasparvenone Using a Xanthate-Mediated Free Radical Addition–Cyclization Sequence, *Org. Lett.*, **2003**, 5, 3717–3719; b) Cordero-Vargas A., Pérez-Martín I., Quiclet-Sire B., Zard S. Z., Synthesis of substituted naphthalenes from α -tetralones generated by a xanthate radical addition–cyclisation sequence, *Org. Biomol. Chem.*, **2004**, 2, 3018–3025.

tetralones **8** were aromatized with *p*-toluenesulfonic acid (PTSA) in toluene to produce the corresponding naphthols **9** in excellent yields (Scheme 7).



Scheme 7. Synthesis of 2-methylnaphthol intermediates **9** from propiophenone.

Several oxidizing agents have been proposed to oxidize the naphthols to provide the menadiones, such as copper(II) chloride (CuCl_2), phenyliodonium diacetate (PIDA), Fremy's salt, manganese dioxide (MnO_2), chromium trioxide (CrO_3) and cerium(IV) ammonium nitrate (CAN).^{54,55,56,57,58,59} A previous study⁴⁶ in our laboratory conducted a series of trials with 6-methoxynaphthol **4a** to screen the reactivity of these oxidants, in addition to Ag_2O and *N*-bromosuccinimide (NBS) (Scheme 8a).^{60,61} However, most of these oxidants were not satisfactory to perform this oxidation reaction. Only the reaction with Fremy's salt led to excellent yield (99%). Owing to the instability and expensiveness of Fremy's salt, PIDA was alternatively selected because it provided better yields than the others in this

⁵⁴ Bringmann G., Zhang G., Hager A., Moos M., Irmer A., Bargou R., Chatterjee M., Chatterjee M., Anti-Tumoral Activities of Dioncoquinones B and C and Related Naphthoquinones Gained from Total Synthesis or Isolation from Plants, *Eur. J. Med. Chem.*, **2011**, *46*, 5778–5789.

⁵⁵ Pelter A., Elgendy S. M. A., Phenolic oxidations with phenyliodonium diacetate, *J. Chem. Soc. Perkin Trans. 1*, **1993**, *16*, 1891–1896.

⁵⁶ Teuber H.-J., Rau W., Reaktionen mit Nitrosodisulfonat, II. Mitteil.: Über die Bildung von Chinonen aus einwertigen Phenolen, *Chem. Ber.* **1953**, *86*, 1036–1047.

⁵⁷ Krishna Kumari L., Pardhasaradhi M., A facile oxidation of 1-naphthols to 1,4-naphthoquinones using active manganese dioxide, *Indian J. Chem., Sect. B*, **1982**, *21*, 1067–1070.

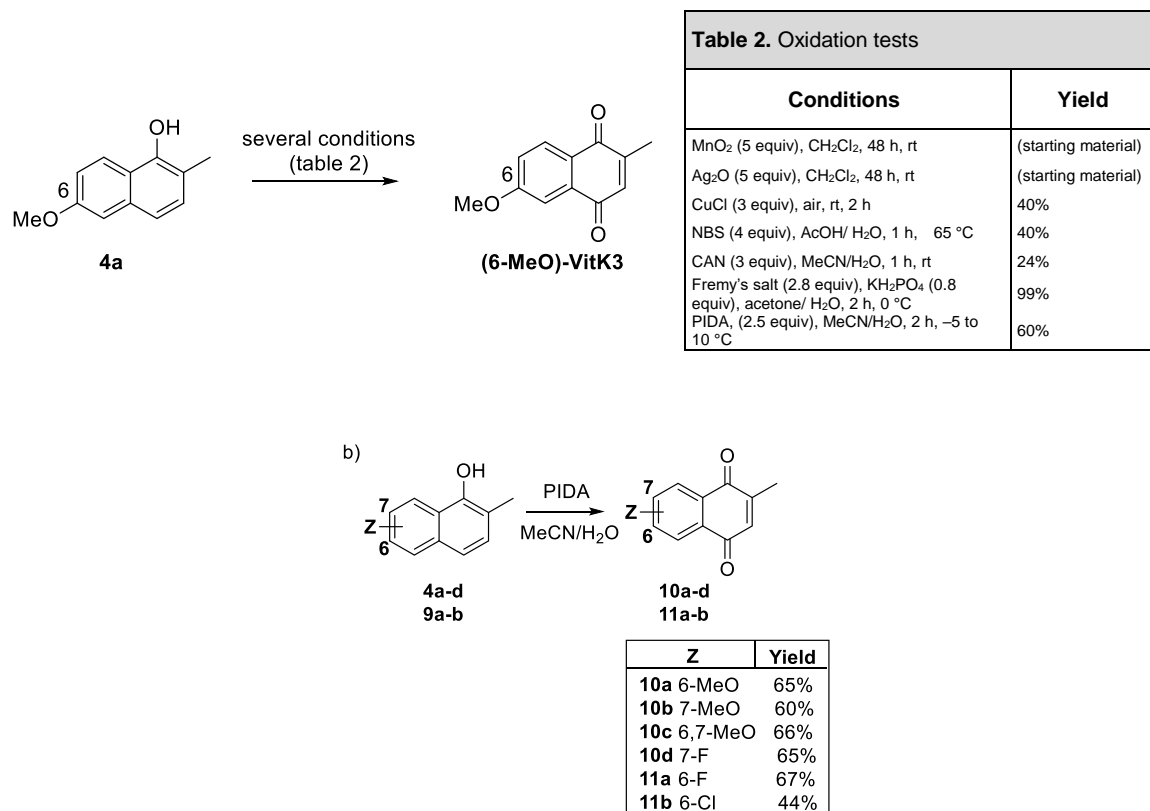
⁵⁸ Fawaz G., Fieser L. F., Naphthoquinone Antimalarials. XXIV. A New Synthesis of Lapinone, *J. Am. Chem. Soc.*, **1950**, *72*, 996–1000.

⁵⁹ Nair V., Deepthi A., Cerium(IV) Ammonium Nitrate — A Versatile Single-Electron Oxidant, *Chem. Rev.*, **2007**, *107*, 1862–1891.

⁶⁰ Tanoue Y., Sakata K., Hashimoto M., Morishita S., Hamada M., Kai N., Nagai T., A facile synthesis of naturally occurring binaphthoquinones: efficient oxidative dimerization of 4-alkoxy-1-naphthols using silver(II) oxide–40% nitric acid, *Tetrahedron*, **2002**, *58*, 99–104.

⁶¹ Grunwell J. R., Karipides A., Wigal C. T., Heinzman S. W., Parlow J., Surso J. A., Clayton L., Fleitz F. J., Daffner M., Stevens J. E., The formal oxidative addition of electron-rich transoid dienes to bromonaphthoquinones, *J. Org. Chem.*, **1991**, *56*, 91–95.

reaction. The oxidation reactions of naphthols **4** and **9** were proceeded with PIDA and produced menadione analogues **10** and **11** with satisfactory to moderate yields (Scheme 8b).



Scheme 8. a) Screening oxidants for oxidation of 6-methoxynaphthol **4a**. b) Oxidation of the corresponding 2-methylnaphthols **4 a-d** and **9 a-b** to menadione analogues **10 a-d** and **11 a-b**.

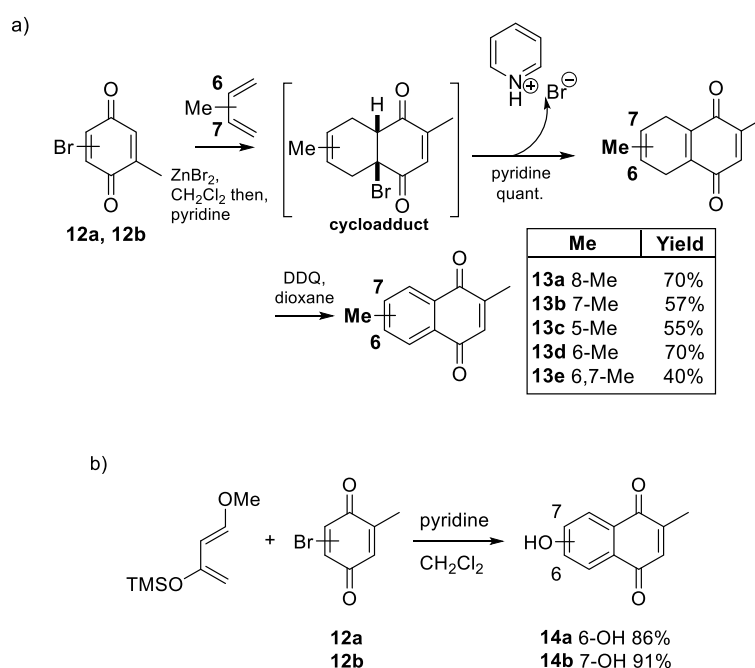
3.2. Synthesis of menadione analogues through Diels-Alder strategy

Recently, our group has reported a synthetic strategy of series of menadiones derivatives **13a-e** through regioselective annulations of quinones by Diels–Alder reactions. Firstly, two kinds of haloquinones (2-bromo-5-methylbenzoquinone **12a** or 2-bromo-6-methylbenzoquinone **12b**) react with piperylene, isoprene or 2,3-dimethylbuta-1,3-diene, in presence of ZnBr₂ as catalytic reagent to produce the cycloadduct intermediate. The treatment of the latter by one equivalent of pyridine to eliminate HBr effectively and oxidation with DDQ in the solution of dioxane allowed to prepare the corresponding methylmenadiones **13a-e** in yields 40%-70%.⁶² It is worth noting that the cycloadduct intermediate of Diels–Alder reaction was sensitive under basic conditions. In particular, the presence of some bases as Et₃N or *i*Pr₂NEt cause the complete degradation of the cycloadduct. Thus, the use of

⁶² Venuti M. C., Loe B. E., Jones G. H., Young J. M., Topical nonsteroidal antipsoriatic agents. 2. 2,3-(Alkylidenedioxy)naphthalene analogs of Ionapalene, *J. Med. Chem.*, **1988**, *31*, 2132–2136.

pyridine for elimination of hydrobromic acid is the sole satisfactory method discovered to prepare the Diels-Alder product quantitatively (Scheme 9a).

In addition, two other hydroxymenadiones have been synthesized by combining bromo-1,4-benzoquinones **12a-b** and Danishefsky's diene⁶³ via Diels-Alder reaction. The cycloadduct intermediate was formed in dichloromethane by the cyclization of 1,3-dioxybutadiene and bromoquinones, then aromatization with loss of one equivalent of methanol and eliminated hydrobromic acid by pyridine to give the corresponding products **14a-b** in yields of 86%-91%. (Scheme 9b)⁴⁶

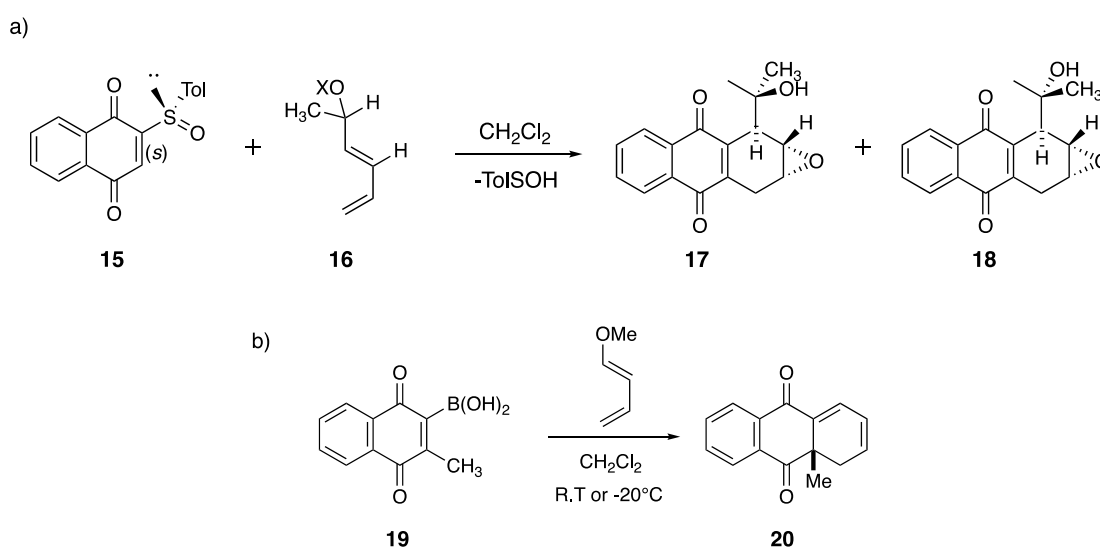


Scheme 9. a) Synthesis of methylated menadiones **13a-e** via Diels-Alder reaction. b) Synthesis of hydroxymenadiones with Danishefsky's diene **14a-b**.

Besides, using bromine as a leaving group to perform the Diels-Alder reaction, M. C. Carreno's group has reported that synthesis of 1,4-naphthoquinone derivatives by introduction of two other additional units as leaving groups in Diels-Alder reaction. However, the reported syntheses were not aimed at preparing substituted 2-methyl-1,4-naphthoquinones. A series of 1,4-dihydro-9,10-anthraquinones (**17** and **18**) resulted from regioselective Diels-Alder reactions between quinone (+)-**5** and 2 equivalent of racemic dienes **16** in solution of CH_2Cl_2 . In this reaction, the group of sulfoxide

⁶³ Danishefsky S., Kitahara T., Useful diene for the Diels-Alder reaction, *J. Am. Chem. Soc.*, **1974**, *96*, 7807–7808.

can be eliminated spontaneously. (Scheme 10a)⁶⁴ The second type of leaving group focused on boron substituent. The derivatives of quinonyl boronic acids **19** as initial materials reacted with diene derivatives in CH₂Cl₂ at r.t. or -20°C. Variety of adducts have been isolated following a photodeboronation or dehydroboronation process in satisfactory yields. (Scheme 10b) It is interesting to note that the boron substituent on the quinones backbone can not only increase the dienophilic reactivity of quinones to achieve the Diels-Alder reactions under mild conditions with a very short reaction times, and also be used as a regiocontrol factor to form regioisomeric products in Diels-Alder reaction. Therefore, the application of two leaving groups such as sulfoxide or boron substituent in Diels-Alder reaction might offer a new synthetic strategy of formation of menadiones derivatives.



Scheme 10. a) synthesis of optically active 1,4-dihydro-9,10-anthraquinones (**17** and **18**). b) one example of Diels-Alder reaction of **19** with 1-methoxy-1,3-butadiene.

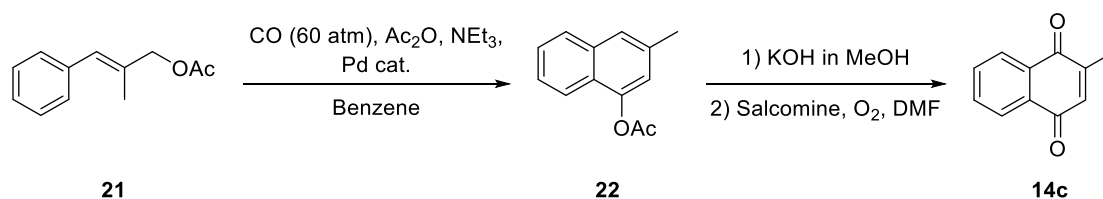
3.3. Synthesis of menadione from β -methylcinnamyl acetate

However, menadione derivatives have been also prepared by other synthetic methods. In 1988, M. Hidai and co-workers proposed a Palladium catalyzed cyclocarbonylation reaction with initial material β -methylcinnamyl acetate leading to the formation of 3-methyl-1-naphthylacetate.⁶⁵ Interestingly, the authors have found that enhancement of equivalents of Ac₂O reagent can increase

⁶⁴ Carreno M. C., Garcia-Cerrada S., Urbano A., Vitta C. D., Studies of Diastereoselectivity in Diels-Alder Reactions of Enantiopure (SS)-2-(p-Tolylsulfinyl)-1,4-naphthoquinone and Chiral Racemic Acyclic Dienes., *J. Org. Chem.*, **2000**, *65*, 4355-4363.

⁶⁵ Matsuzaka H., Hiroe Y., Iwasaki M., Ishii Y., Koyasu Y., Hidai M., A Novel Palladium or Platinum Catalyzed Cyclocarbonylation Reaction of Cinnamyl Compounds for Synthesis of 1-Naphthol Derivatives, *J. Org. Chem.*, **1988**, *53*, 3832-3838.

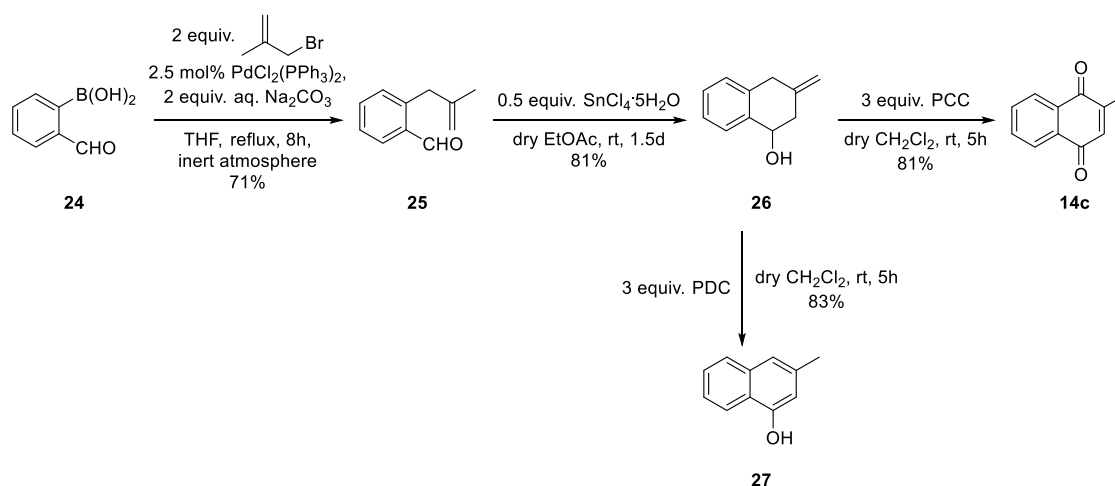
effectively the rate of the reaction. Menadione **14c** has been prepared by saponification and oxidation with oxygen and bis(salicylidene)ethylenediiminocobalt(II) in 59% yields. (Scheme 11)



Scheme 11. Strategy of formation of menadione **14c** with β -methylcinnamyl acetate.

3.4. Synthesis of menadione from formylphenylboronic acid

A strategy pathway of synthesis of menadione has been studied by S. Basak and D. Mal.⁶⁶ Compound **25** was obtained by Suzuki coupling between the boronic acid **24** and methylallyl bromide. The yield of this coupling can be improved to 71% by increasing the amount of starting materials. The reaction of methylidene tetrahydronaphthol **26** has been employed with **25** and 0.5 equivalent of $\text{SnCl}_4 \cdot 5\text{H}_2\text{O}$ in dry ethyl acetate solution in 81% yields. In dry dichloromethane, treatment of **26** with 3 equivalents of pyridinium dichromate (PDC) afforded the product α -naphthol **27**. When compound **26** reacted with 3 equiv. of pyridinium chlorochromate (PCC) the reaction led to the formation of menadione **14c**. (Scheme 12).⁶⁷



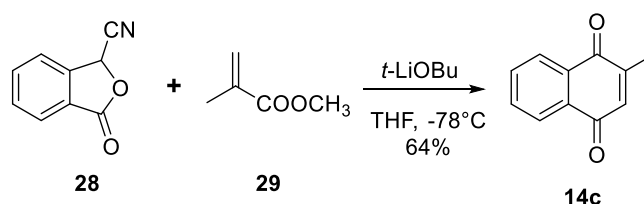
Scheme 12. Synthetic method of menadione **14c** based on boronic acid.

⁶⁶ Basak S., Mal D., Intramolecular carbonyl-ene reactions in the synthesis of peri-oxygenated hydroaromatics, *Tetrahedron*, **2016**, 72, 1758-1772.

⁶⁷ Ren J., Lu L., Xu J., Yu T., Zeng B. B., Selective Oxidation of 1-Tetralones to 1,2-Naphthoquinones with IBX and to 1,4-Naphthoquinones with Oxone® and 2-Iodobenzoic Acid, *Synthesis*, **2015**, 47, 2270-2280.

3.5. Synthesis of menadione analogues through demethoxycarbonylative annulation

Another strategy of synthesis of menadione **14c** has been also reported in the same group.⁶⁸ In this case, cycloaddition reactions with 3-methoxyphthalide derivatives **28** and methyl methacrylate **29** have been completed in the presence of *t*-LiO*Bu* in THF solution at -78°C producing the corresponding menadiones in yields of 20%-64% (Scheme 13).



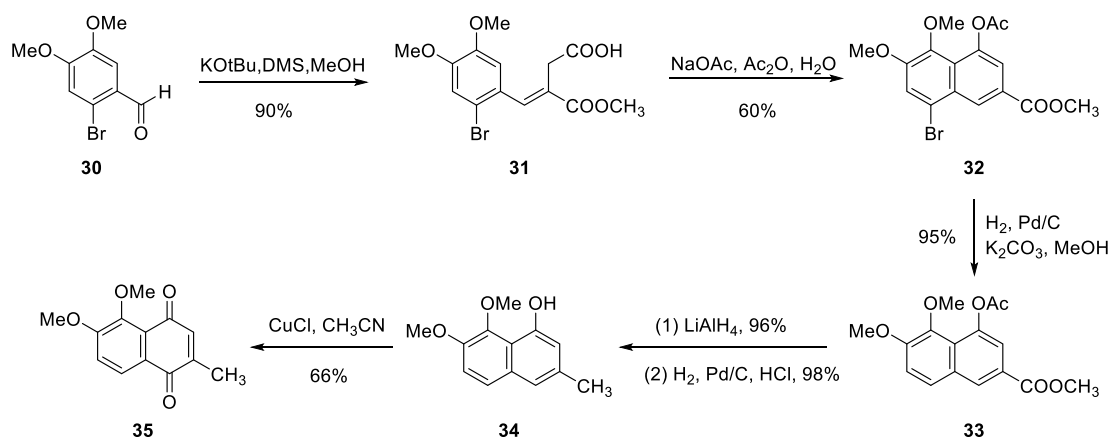
Scheme 13. one of example of synthesis of menadione **14c**.

3.6. Synthesis of menadione analogues from bromo veratrum aldehyde

A selected example of synthesis of menadione derivatives was reported by G. Bringmann *et al.*⁶⁹ (Scheme 14). The synthetic pathway started by a Stobbe condensation reaction between bromo veratrum aldehyde **30** and dimethyl succinate (DMS) giving *E*-configured acid **31**, which was determined by NMR spectrum. The cyclisation of compound **31** in acetic anhydride provided the naphthalene **32** by using sodium acetate in 60% yield. In the presence of Pd/C and K₂CO₃, the bromine and the acetate groups on the compound **32** backbone were removed in methanol to produce the protected naphthol **33** almost quantitatively. Following two steps of reduction reactions with use of LiAlH₄ and Pd/C, methylnaphthalene **34** was obtained in 94% yield, which was oxidized with CuCl in air to afford the para-naphthoquinone **35** in 66% yield.

⁶⁸ Mal D., Ghosh K., Jana S., Synthesis of Vitamin K and Related Naphthoquinones via Demethoxycarbonylative Annulations and a Retro-Wittig Rearrangement, *Org. Lett.*, **2015**, *17*, 5800–5803.

⁶⁹ Bringmann G., Zhang Gl., Hager A., Moos M., Irmer A., Bargou R., Chatterjee Manik., Anti-tumoral activities of dioncoquinones B and C and related naphthoquinones gained from total synthesis or isolation from plants, *Eur. J. Med. Chem.*, **2011**, *46*, 5778-5789.



Scheme 14. An example of synthesis of menadione derivative **35**.

4. Putative mode of action of plasmodione

The lead benzylmenadione derivative, named plasmodione, has been identified as a potent antimalarial early lead drug. Recent investigations on the mode of action revealed that plasmodione acts as a redox-active agent with potent antimalarial activity expressed by low IC_{50} (≈ 50 nM) in cultures of malarial parasites *in vitro* and displayed moderate toxicity against human cells (≈ 50 μ M). A bioactivation pathway through a cascade of redox reactions was hypothesized to explain the antimalarial activity of plasmodione, starting from a benzylic oxidation (Figure 4).^{42,47,48} Then, the generated benzoylmenadione metabolite was shown to be reduced by the glutathione reductases (GRs) of parasitized red blood cell (pRBC) and to consume NADPH into a redox cycle, leading to inhibition of glutathione regeneration. During this redox cycle the reduced benzoylmenadione was shown to transfer one electron to Fe^{III} of methemoglobin and to continuously convert it to oxyhemoglobin (Fe^{II}) in a redox-cycle at the expense of NADPH. The regeneration of oxyhemoglobin, which is not digested by the parasitic proteases, leads to the death of the parasites in pRBCs. This process also accelerated the formation of reactive oxygen species (ROS), which enhanced intracellular oxidative stress and caused cellular damage. Following the generation of ROS, the reduced benzoylmenadione metabolite was proposed to be transformed to benzoxanthone, which was shown to prevent the formation of hemozoin.⁴⁸ Besides, the ROS induced the generation of membrane-associated hemichrome, which is a biomarker of senescence of RBC, rendering the half-life of pRBC shorter than normal RBC.

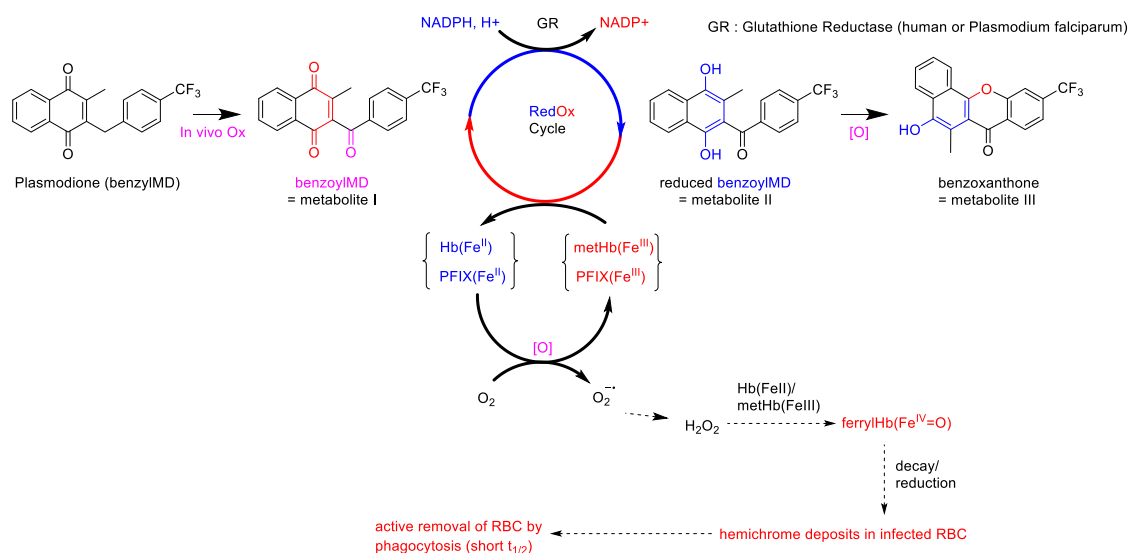


Figure 4. Hypothesized drug metabolism pathway of plasmodione.

5. Antimalarial activity profile of plasmodione

The potent antimalarial activity of the previously identified early lead compound 3-[4-(trifluoromethyl)benzyl]-menadione (henceforth called plasmodione), has been investigated in *P. falciparum* blood stages.³⁷ A detailed parasitological characterization⁷⁰ of plasmodione's activity profile *in vitro* revealed (i) a potent antiplasmodial activity against asexual stages of *P. falciparum* in strains with varying degrees of drug resistance and in sexual stages (early gametocytes), (ii) a safe toxicological profile for possible human use, (iii) a high intra-erythrocytic ring-specific activity, (iv) a killing speed as fast as artemisinin, (v) a low potential to induce drug resistance and (vi) synergistic effects with licensed antimalarial drugs or physiological nicotinamide involved in NADPH biosynthesis in malarial parasites. Based on detailed physicochemical studies we proposed that the antimalarial selectivity of plasmodione comes largely from its specific bioactivation within pRBCs, involving a cascade of redox reactions starting from the benzylic oxidation (Figure 4, metabolite I).

6. The objectives of research

In the first part of the PhD thesis, chemical tools were designed for a drug metabolism and future proteomics investigation. The heavy isotopically-labeled ¹³C₁₈-enriched plasmodione, keeping the same molecular property as unlabeled lead drug, might be used as a chemical tool to track, identify

⁷⁰ Ehrhardt K., Deregnaucourt C., Goetz A.-A., Tzanova T., Pradines B., Adjalley S. H., Blandin S., Bagrel D., Lanzer M., Davioud-Charvet E., The redox-cycler plasmodione is a fast acting antimalarial lead compound with pronounced activity against sexual and early asexual blood-stage parasites., *Antimicrob. Agents Chemother.* **2016**, *60*, 5146-58.

and visualize the drug metabolites, which are responsible for antimalarial activity. Optimization of two steps in the total synthesis of plasmodione derivatives was completed from 4-substituted benzaldehyde and a tetralone as synthetic intermediates. Then, from five cheapest ^{13}C -enriched starting-blocks a direct synthesis of the $^{13}\text{C}_{18}$ -enriched plasmodione was designed and optimized.

In the second part of the PhD thesis, the putative drug metabolites were freshly re-prepared, the extraction method for drug metabolism study was established and the preliminary drug metabolism study with $^{13}\text{C}_{18}$ -enriched plasmodione treated pRBCs was performed.

In the third and fourth parts of the PhD work, the preparation of oxetane and *N*-alkyl-aryl derivatives of plasmodione with potential improved solubility was also investigated through aromatic nucleophilic substitution ($\text{S}_{\text{N}}\text{Ar}$) and palladium-catalyzed Buchwald-Hartwig coupling reaction, respectively.

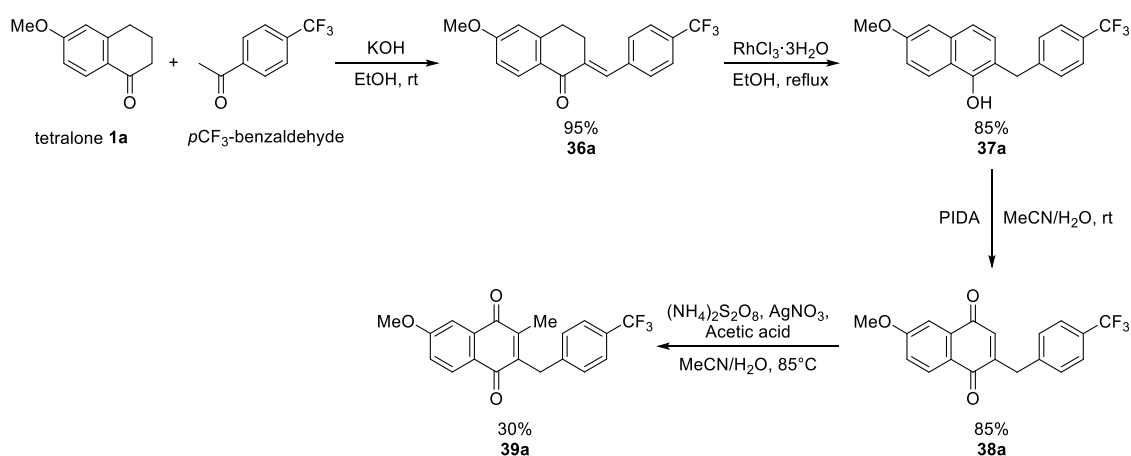
The fifth chapter was dedicated to the synthesis of a known gold(I) phosphole complex, which had been described as an irreversible and potent inhibitor of the human seleno-dependent thioredoxin reductase. The broad antiparasitic profile of GoPi-sugar was evaluated via external collaborations.

Chapter I: Synthesis of the multi $^{13}\text{C}_{18}$ - and mono $^{13}\text{C}_1$ -labeled plasmodiones

I.1. Synthesis of plasmodione - Completion/optimization of the “express tetralone route”

I.1.1. Previous data from the lab

The Kochi-Anderson reaction combining menadione and various substituted phenylacetic acids can provide plasmodione derivatives in a very efficient way. Apart from this strategy, an alternative plasmodione synthesis pathway has been explored in our laboratory. This synthesis pathway named “tetralone express route” was designed to combine various tetralones and benzaldehydes as starting materials and to give the desired plasmodione derivatives, such as the 7-methoxy representative **39a** (Scheme 15).⁴⁶



Scheme 15. Synthesis of 7-methoxy-plasmodione derivative **39a** through the “tetralone express route”.

Compared to the former strategy based on the Kochi-Anderson reaction, the “tetralone express route” redefined the “eastern part” and “western part” functionalization of plasmodione in the synthetic scheme. This new synthetic strategy raises up the diversity of starting materials for polysubstituted plasmodione synthesis. Starting from the required tetralone and benzaldehyde the condensation reaction allowed us to form the α -methylene ketone **36a** with an exo double bond by using potassium hydroxide under classical conditions. Subsequently, the rhodium catalyzed isomerization reaction with rhodium chloride led to the naphthol **37a**, followed by the oxidation reaction with PIDA to produce

the corresponding desmethyl-plasmodione **38a**. Finally, the radical methylation reaction under Kochi-Anderson conditions afforded the desired plasmodione derivative **39a**.

This strategy of “tetralone express route” has been designed by the former PhD student Elena Cesar Rodo and Don Antoine Lanfranchi in the team.⁴⁵ However, this synthetic route was not satisfactory due to the low reproducibility of the rhodium catalyzed isomerization and the low yield of the Kochi-Anderson methylation in the last step.

The resulting isomerization was a key step of “tetralone express route”. Several conditions of this aromatization have been screened in our laboratory, including various oxidation reactant, to treat the starting α -methylene ketone **36a**. These conditions were including PIDA, TFA, *t*-BuOK, RuCl₃, DDQ, trimethylphenol/TFA, MnO₂, Ag₂O, CrO₃, CuCl₃ and RhCl₃. Therefore, only RhCl₃ can efficiently lead to the aromatization of α -methylene ketone **36a** to give the desired naphthol **37a** with satisfying yield (85%). Nevertheless, a low reproducibility of this rhodium catalyzed isomerization was observed when the reaction was done by different experimentators, and still represented a difficulty before my contribution to the optimization process.

I.1.2. Personal work

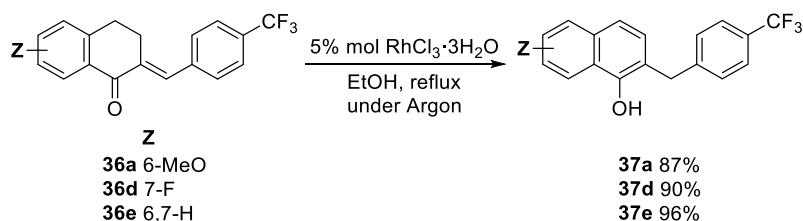
Before starting the total synthesis of a fully ¹³C enriched plasmodione governing my PhD research project it has been essential to re-consider two steps in the “tetralone express route” allowing to prepare plasmodione with high yield.

My first contribution started with the investigations on the rhodium catalyzed isomerization. Based on the mechanism study proposed by Paiaro *et al.*⁷¹, Rh^{III}Cl₃ is first reduced by ethanol to form HRh^ICl₂ and then coordinates to the olefin portion of α -methylene ketone **36a** (Scheme 17). Subsequently, oxidative addition and β -elimination leads to the shift of the double bond from the exo- position to the endo- position resulting in formation of the methylene ketone (Scheme 17), and finally aromatizing to the most thermodynamically stable naphthol **37a** (the calculated free energies were estimated by *ChemBioOffice 2012*⁷²). It is worth to note that the reactivity of the rhodium catalyst was highly depending on the stability of the Rh^I intermediate during the catalytic process. Indeed, we found that the active Rh^I intermediate was sensitive to oxygen in open air and lost its efficiency. Consequently, as long as the solvent was well-degassed and the reaction proceeded under strict

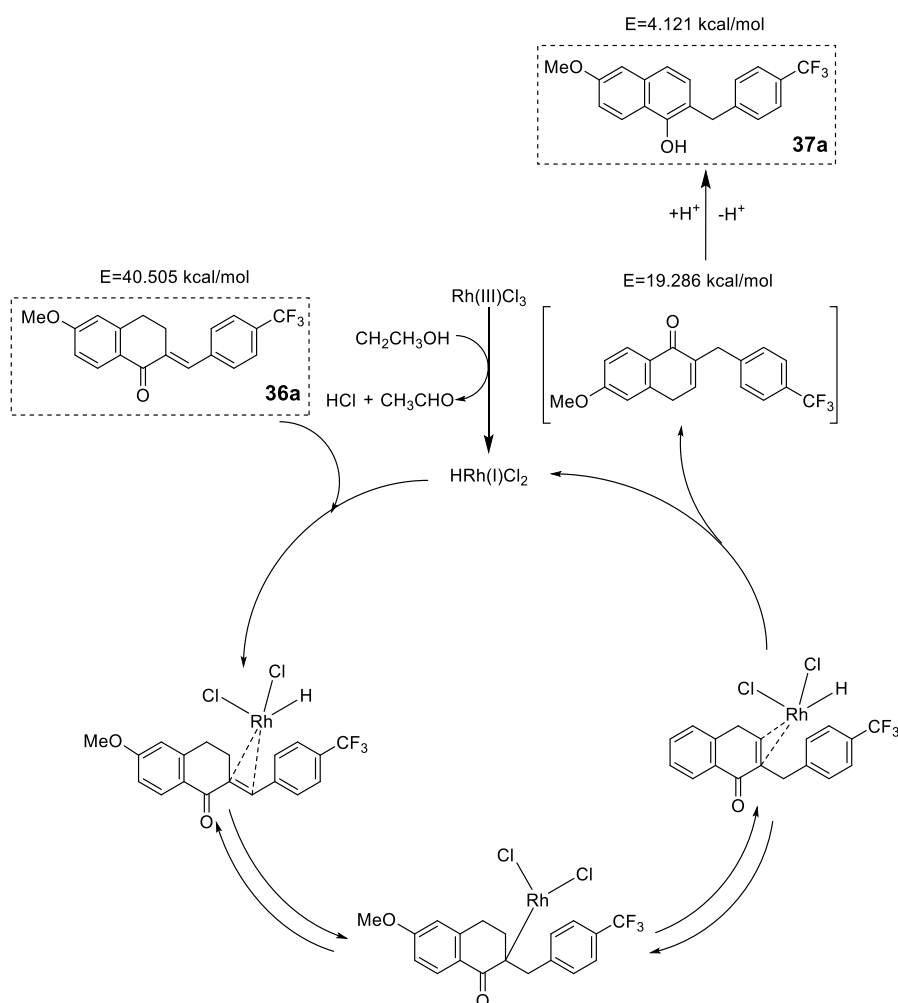
⁷¹Paiaro G., Musco A., Diana G., Chemical and structural characterization of some π -allylic derivatives of rhodium(III), *J. Organomet. Chem.*, **1965**, *4*, 466–474.

⁷² *ChemBioOffice 2012*, PerkinElmer, Inc., **2012**.

anaerobic condition, both the yield and reproducibility of this series of reaction were highly improved (Scheme 16).



Scheme 16. Optimized rhodium chloride catalyzed isomerization reaction.



Scheme 17. Proposed mechanism of the Rhodium-catalyzed olefin isomerization.⁴⁶

The methylation with acetic acid under Kochi-Anderson conditions was possible. But, the preliminary trial of the resulting reaction was not adequate. As described in the introduction part of my thesis, the yields of the Kochi-Anderson reaction using a phenylacetic acid as partner in the coupling reaction with menadiones were ranged from 50% to 87%, depending on the substitution pattern (yields were not always optimized). However, when the reaction partners switch to acetic acid

and desmethylmenadione derivatives, the radical alkylation reaction was limited to 30%. In order to increase the yield of this reaction, we independently varied the ratio of acetic acid, silver nitrate and ammonium persulfate (data not shown). But, these changes did not improve the outcome of the reaction. Further, we postulated that the stability of the methyl radical is much lower than that of the benzyl radical; in the meanwhile, in the reaction mixture, the active methyl radical would possibly destroy the desired product. Therefore, that is why we have launched an investigation about the reaction kinetics by NMR spectroscopy.

We have devised this experiment by using 2-[4-(trifluoromethyl)benzyl]naphthalene-1,4-dione **38e** as the starting material in a mixture of CD₃CN/D₂O for the reaction model. According to the results below (Figure 5), after 15 min, we observed that reaction conversion reached over than 50% in parallel to rapid generation of the desired plasmodione. At 1 hour, the conversion of the starting material was almost complete, and generation of the plasmodione **39e** almost exclusive, as correlated by the disappearance of the proton at C-2 of the starting material (Figure 5a). After 1,5 hour, we observed the formation of side-products and the decrease of the yield of the reaction (Figure 5b). Based on the kinetic profile of this radical methylation determined by ¹⁹F NMR analysis, the optimized protocol afforded plasmodione **39e** after two purification steps (chromatography of silica gel column followed by recrystallization) with an isolated yield of 50%.

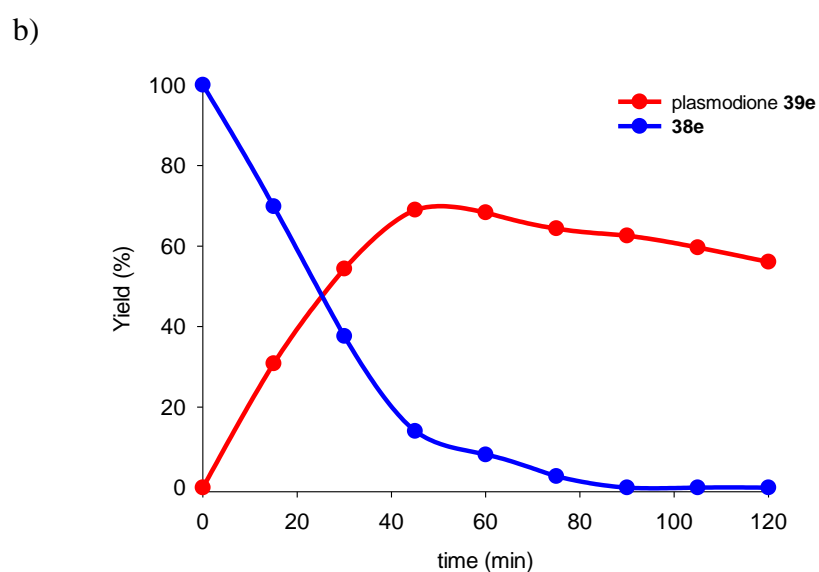
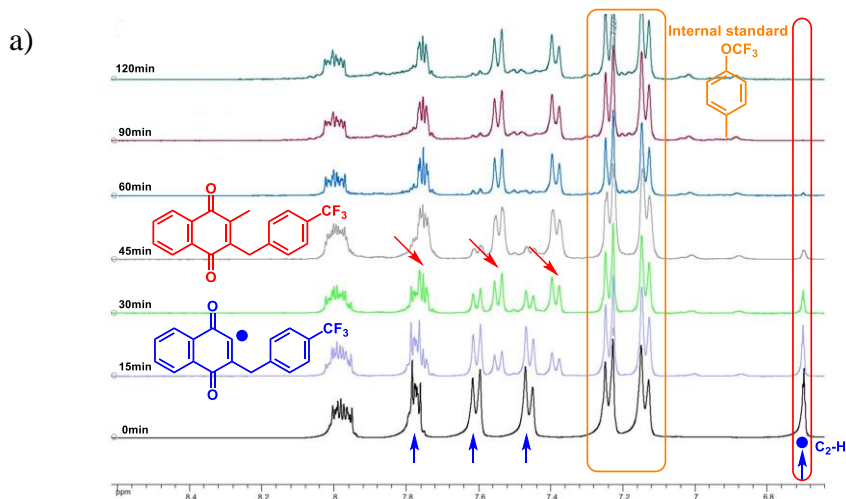
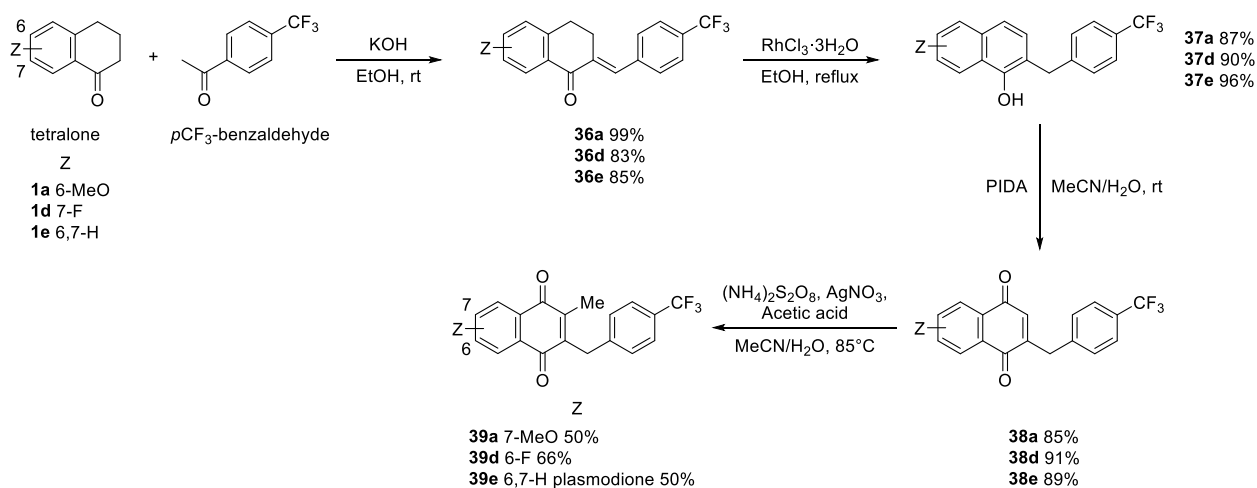


Figure 5. a) Kinetic ^1H NMR spectroscopy studies of the Kochi-Anderson reaction between desmethylmenadione **38e** and acetic acid. b) Kinetic profile of Kochi-Anderson reaction of **38e** (blue line) leading to plasmodione **39e** (red line), determined by ^{19}F NMR analysis experiments. Both 2 NMR studies were performed in a mixture of $\text{CD}_3\text{CN}/\text{D}_2\text{O}$, using 1-methyl-4-(trifluoromethoxy)benzene (orange box) as an internal standard.



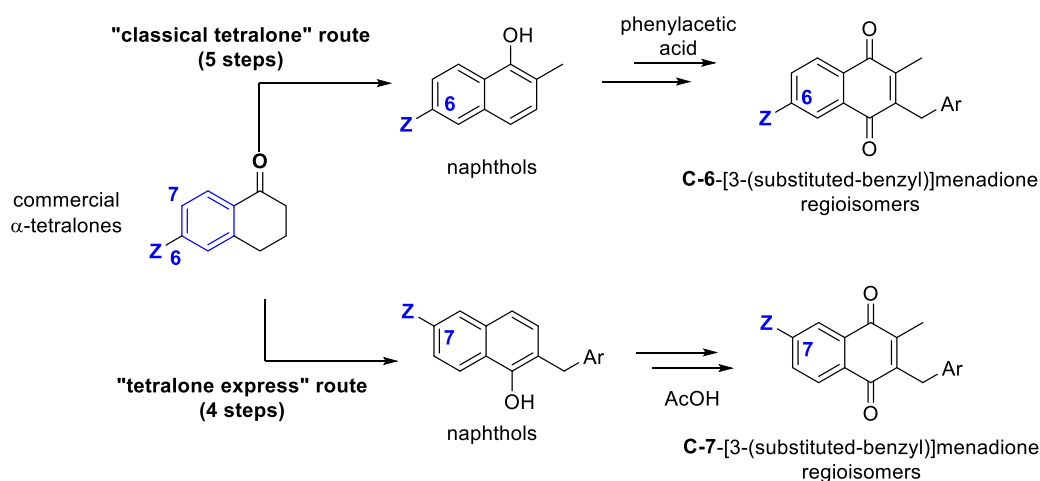
Scheme 18. Synthesis of plasmodione and its derivatives **39a**, **39d** and **39e** through the optimized “tetralone express route”.

After these 2 steps improvement, the “tetralone express route” can provide desired plasmodione derivatives (**39a**, **39d** and **39e**) in 4 satisfying yielding steps (Table 3). This route was exemplified with 3 compounds, *i.e.* plasmodione, and two C-6-, or C-7- [3-(substituted-benzyl)]menadione regioisomers with an overall yield of 37% (**39a**, 7-MeO), 45% (**39d**, 6-F), and 36% (**39e**, 6,7-H), respectively. The traditional synthetic strategy, via Kochi-Anderson radical coupling reaction, combining the *p*-trifluoromethyl phenylacetic acid and menadione, allows to prepare plasmodione in multigram scale with an overall yield of 80%. For comparison, when using the naphthol strategy combined with the Kochi-Anderson reaction using a phenylacetic acid in the last step, both C-6-, or C-7- [3-(substituted-benzyl)]menadione regioisomers were prepared in five steps with an overall yield of 23 % (**39a**, 7-MeO), and 16 % (**39d**, 6-F), respectively. Hence, the “optimized tetralone express route” not only reduced one step in the synthetic pathway (Scheme 18), but also improved the overall yield of the synthesis whatever the substituent on the menadione core.

compound	naphthol route ¹ (based on sequence from tetralones 1a,1d via → 2a,2d → 3a,3d → 4a,4d → 10a,10d → to 17a,17d) total yield, % (n steps)	“tetralone express route” ¹ (based on sequence from tetralones 1a,1d via → 22a,22d → 23a,23d → 24a,24d → to 17a,17d) total yield, % (n steps)
39a , 7-OMe (= 17b in ref.46)	23 % (5)	37 % (4)
39d , 6-F (= 17e in ref.46)	16 % (5)	45 % (4)
39e , 6,7-H (= plasmodione)	na	36 % (4)
39e , 6,7-H (= plasmodione)	≈ 80% (1) via Kochi-Anderson reaction	

Table 3. Comparison overyields from different strategies of plasmodione derivatives synthesis. Data from ref.46, na means the synthesis does not apply.

Also, we found very convenient to prepare two distinct regioisomers at C-6 or C-7 from the same commercial tetralone depending on the selected synthetic scheme (Scheme 19).



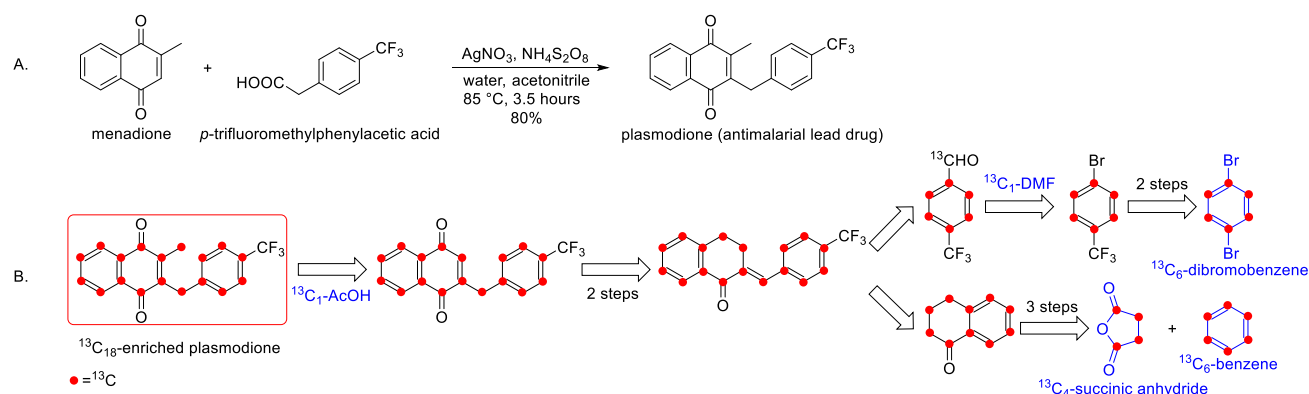
Scheme 19. Access to two distinct Z-substituted plasmodione regioisomers at C-6 or C-7 from a same commercial Z-substituted tetralone.

In addition, this latter strategy provided a new way to design a synthetic route for the preparation of the $^{13}\text{C}_{18}$ -enriched-plasmodione, which was limited by the rare and expensive commercial starting materials.

I.2. Synthesis of the enriched- $^{13}\text{C}_{18}$ -plasmodione

In order to identify the drug metabolites in *Plasmodium falciparum*-parasitized red blood cells our first objective was aimed at preparing an enriched- $^{13}\text{C}_{18}$ -plasmodione.

The original plasmodione can be synthesized in one step from commercial starting materials, menadione and the corresponding phenyl acetic acid by Kochi-Anderson reaction, rendering the large-scale preparation easy, cheap and available (Scheme 20a). However, because of the limited choice and the high cost of commercially available ^{13}C -enriched starting materials, the synthetic route of the (almost) fully ^{13}C -labeled plasmodione had to be changed. Noteworthy is to mention that only one carbon (from the CF_3 group) is not enriched in the target molecule. Based on the cheapest commercial available starting materials, $^{13}\text{C}_6$ *p*-dibromobenzene, $^{13}\text{C}_6$ -benzene, $^{13}\text{C}_4$ -succinic anhydride, $^{13}\text{C}_1$ -dimethylformamide and $^{13}\text{C}_1$ -acetic acid, the synthesis of fully $^{13}\text{C}_{18}$ -enriched plasmodione was designed through a convergent synthetic route via two key intermediates, the tetralone and the 4-trifluoromethyl benzaldehyde, by using a 10 steps sequence (Scheme 20b). Each step of this total synthesis was elaborated and improved by using unenriched compounds.



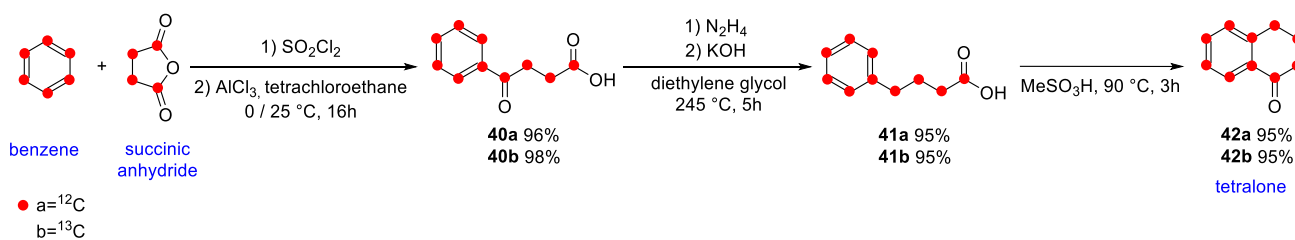
Scheme 20 a) The synthesis of unlabeled plasmodione. b) The retrosynthesis of the fully $^{13}\text{C}_{18}$ labeled plasmodione.

I.2.1. Synthesis of the ^{13}C -enriched tetralone

The uniformly $^{13}\text{C}_{10}$ -labeled tetralone was synthesized according to the reported procedure (Ball *et al.*).⁷³ The $^{13}\text{C}_{10}$ -tetralone **42b** was produced by a 3 steps-long route. First, a Friedel-Crafts reaction was performed with sulfonyl chloride and aluminum chloride, combining the $^{13}\text{C}_6$ -benzene and $^{13}\text{C}_4$ -

⁷³ Zhang Z., Sangaiah R., Gold A., Ball L.M., Synthesis of uniformly ^{13}C -labeled polycyclic aromatic hydrocarbons, *Org. Biomol. Chem.*, **2011**, 9, 5431-5435

succinic anhydride, to afford the keto acid **40 a-b** (yield 96% and 98%). Subsequently, a Woff-Kishner reduction was initiated with hydrazine and potassium hydroxide, leading the phenylbutanoic acid **41a-b** (yield 95%). Finally, the cyclization (yield 95%) from resulting phenylbutanoic acid **41a-b** under acid conditions allowed to give the desired $^{13}\text{C}_{10}$ -tetralone **42b** (total yield 87%, Scheme 21). Because these three reactions proceeded with excellent yields, and their side product in trace amount did not influence to the next step of the reaction, these compounds were not purified by chromatography before next step.



Scheme 21. Synthesis of the tetralone **42a-b**.

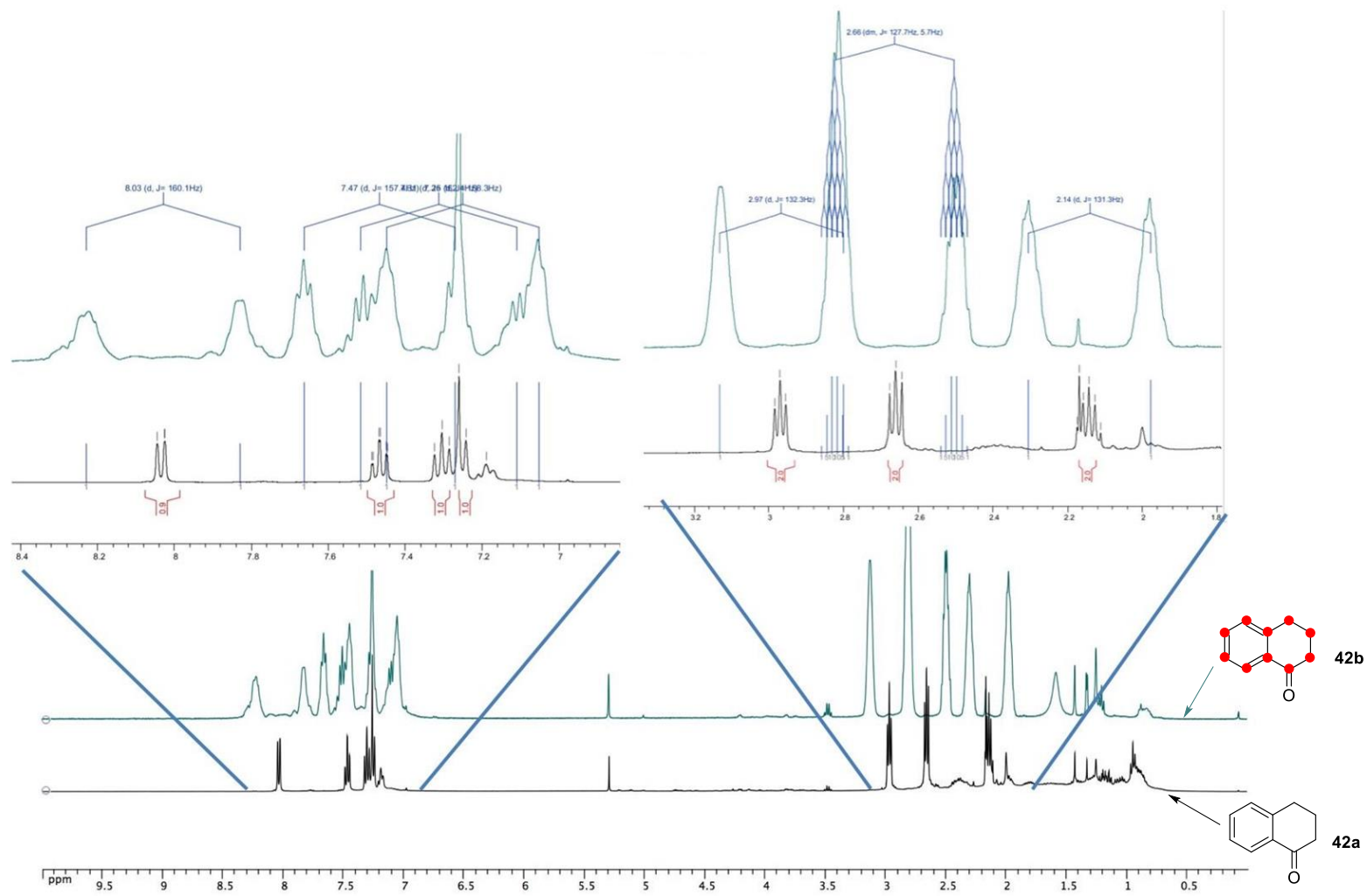


Figure 6. ^1H NMR (400 MHz, CDCl_3) of tetralone **42a** and $^{13}\text{C}_{10}$ -enriched tetralone **42b**. The black line represents **42a** and the green line represents **42b**.

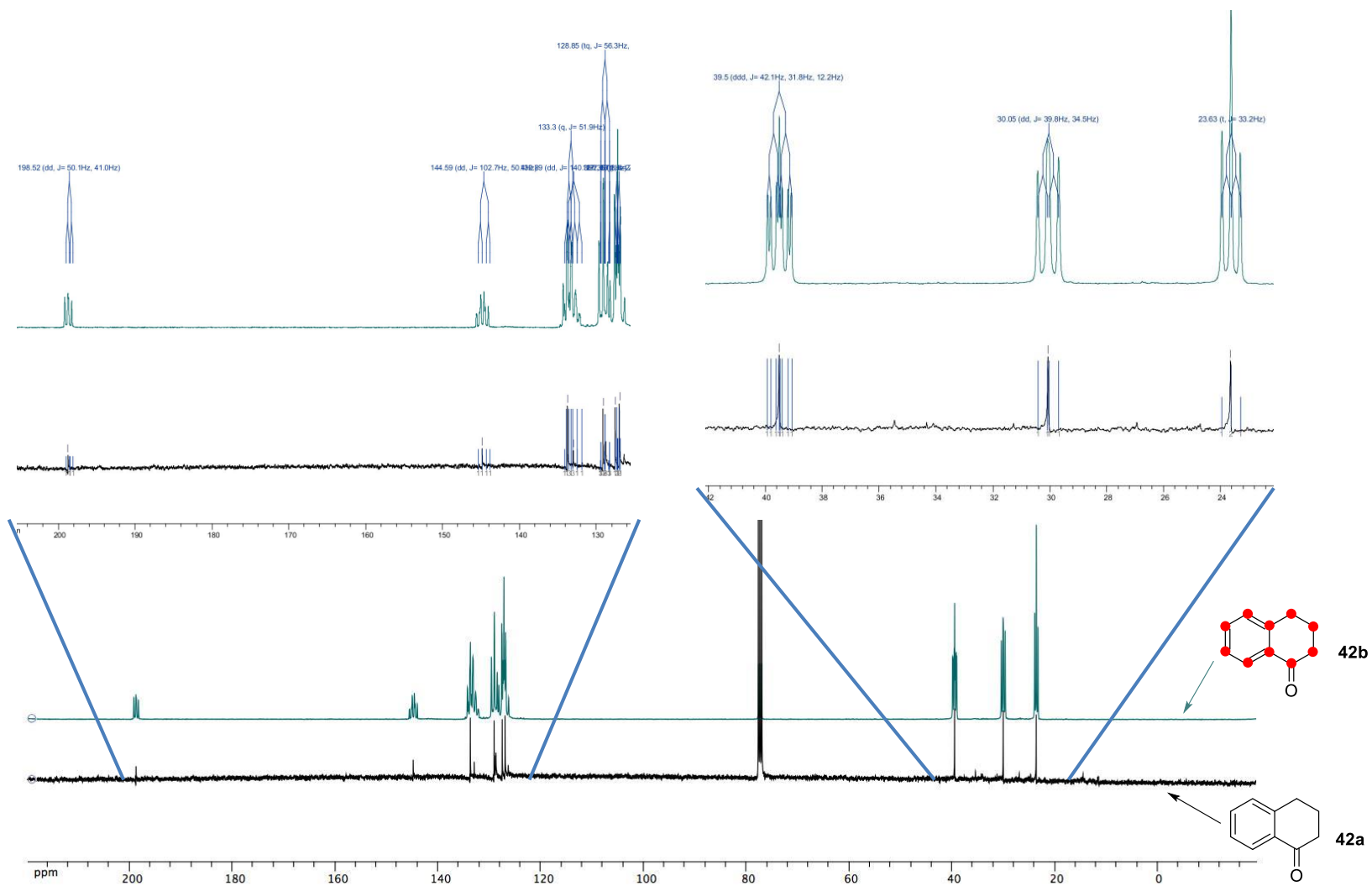


Figure 7. ^{13}C NMR (100 MHz, CDCl_3) of tetralone **42a** and $^{13}\text{C}_{10}$ -enriched tetralone **42b**. The black line represents **42a** and the green line represents **42b**.

The relative abundances of the different isotopes of a chemical element are constant in natural materials. However, there are different situations where samples of an element show different relative abundances from those which are normally in nature: they can be fossils showing natural radioactive decay, materials isolated from isotopic separation processes, or man-made isotopically-enriched materials. Relative natural isotopic abundances of carbon are about 99% for carbon-12 as the major isotope, 1% for the minor carbon-13, and tiny amounts for the radioactive carbon-14 isotope. Carbon isotopes and mainly C-13 are used extensively in many different applications, including the nuclear magnetic resonance (NMR) spectroscopy to carbon (most commonly known as carbon-13 nuclear magnetic resonance, carbon-13 NMR or ^{13}C NMR). This latter application is used in organic chemistry research to identify carbon atoms in an organic molecule, just as proton NMR identifies hydrogen atoms. For instance, ^{13}C NMR is very useful in chemical structure elucidation in organic chemistry, studies into molecular structures, climate changes and air pollution,⁷⁴ cellular metabolism, food labeling, or microorganism detection. As only elements that have a nuclear spin quantum number other than zero are NMR active, ^{13}C NMR detects only the ^{13}C isotope of carbon, whose nuclear spin value is 1/2, because the main carbon isotope, ^{12}C , is not detectable by NMR since it has zero net spin.

As such ^{13}C -enriched compounds represent an important tool in drug metabolism studies. They have huge different profile both in ^1H NMR and ^{13}C NMR spectra, especially in the case of multi- ^{13}C -enriched compounds. Owing to the ^{13}C atom is spin 1/2, they can generate J -coupling with each other and with the other atoms such as ^1H and ^{19}F . Normally, because of the low isotopic abundance of ^{13}C atom, isotopically-unlabeled products do not reveal a significant signal of J -coupling between ^{13}C and ^1H in the NMR spectra. However, when the fully ^{13}C -enriched compounds are characterized by NMR spectra, this influence cannot be ignored.

To illustrate the purpose, we can obviously observe that the peaks of the ^{13}C -enriched tetralone **42a** from ^1H NMR spectrum shown in Figure 6, were conspicuously different than the natural tetralone **42b**. Because of $^2J_{^{13}\text{C}-^1\text{H}}$, the spin of both ^{13}C atom and ^1H are 1/2, all the peaks of the proton which is bonding to the ^{13}C atom are split in two signals. Besides, owe to more J -coupling such as $^3J^4J$ between proton and ^{13}C , the shape of the peaks is wide and the signals have low sensitivity, making difficult to identify the structure of ^{13}C -enriched compounds by NMR spectra. Nevertheless, ^{13}C -enriched and unenriched compounds with same molecular structure keep the same chemical properties, expressed

⁷⁴ Subbalakshmi Y., Patti A.F., Lee G.S., Hooper M.A., Structural characterisation of macromolecular organic material in air particulate matter using Py-GC-MS and solid state ^{13}C -NMR, *J. Environ. Monit.*, **2000**, 2, 561-565.

by invariable chemical shifts in NMR spectra. Thus, we can confirm the structure of ^{13}C -enriched compounds from ^1H NMR spectra profile by comparing the NMR spectra.

Similarly to the ^1H NMR spectrum, the ^{13}C NMR of $^{13}\text{C}_{10}$ -tetralone **42b** has also more complexity (Figure 7). Because the fully ^{13}C -enriched compounds have numbers of adjacent and magnetically nonequivalent ^{13}C atom, the signal of each ^{13}C is multiplied by several peaks. As presented in ^1H NMR spectrum, the chemical shifts of both fully ^{13}C -enriched and natural compounds are unchanged, and comparing both ^{13}C NMR spectra can also profile the molecular structure of the fully ^{13}C -enriched product. Because the synthesis of $^{13}\text{C}_{10}$ -tetralone **42b** has been reported by Ball *et al.*,⁷³ both ^1H and ^{13}C NMR spectra of the newly prepared $^{13}\text{C}_{10}$ -tetralone **42b** were compared to the published data and analyzed carefully. Our detailed analyses were confirmed with accuracy and allowed to conclude on the purity of $^{13}\text{C}_{10}$ -tetralone **42b**.

I.2.2. Synthesis of the $^{13}\text{C}_6$ -enriched trifluoromethylbenzaldehyde

The $^{13}\text{C}_6$ -*p*-trifluoromethylbenzaldehyde **45b** was synthesized in 3 steps (total yield 23%, Scheme 23). First, the $^{13}\text{C}_6$ -*p*-bromoiodobenzene **43b** was prepared according to an iodination reaction with I_2 and *n*-BuLi under classical conditions (yield 75%).⁷⁵ The limitation of the yield was due to the generation of the side product, *i.e.* the *o*-bromoiodobenzene due to the resonance effect. No matter how varying the reaction temperature (from $-78\text{ }^\circ\text{C}$ to $25\text{ }^\circ\text{C}$), this *o*-bromoiodobenzene was accompanied to the extent of 20% of conversion from the starting material.

Second, the trifluoromethyl-substitution was extensively explored in drug development due to the fluorine properties that increase the bio-availability and metabolic resistance of the drugs.⁷⁶ The $[\text{CuCF}_3]$ was usually used in trifluoromethylation as catalyst.⁷⁷ However, this catalyst was not stable in open air, it was not convenient to prepare the trifluoromethylation without glove box.⁷⁸ Generation of CuCF_3 *in situ* was developed by using different generators, e.g. NaCO_2CF_3 and MeCO_2CF_3 , which

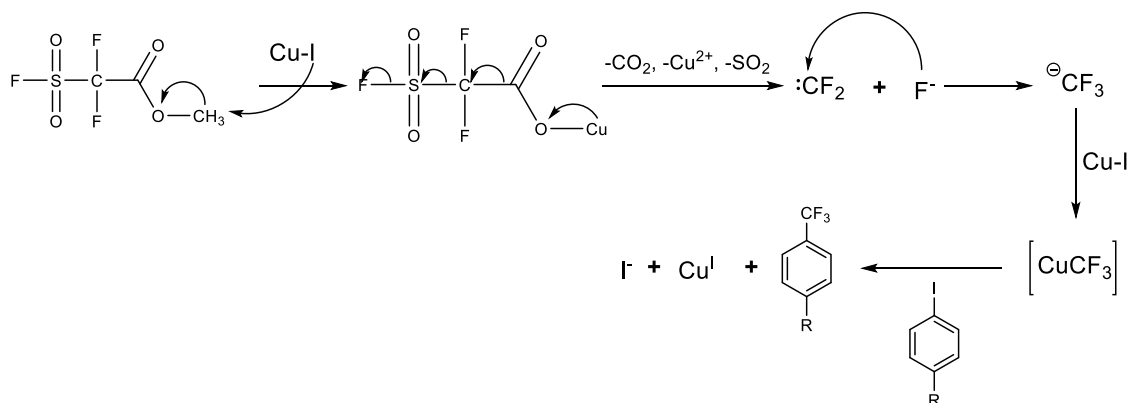
⁷⁵ Aakeröy C.B., Chopade P.D., Desper J., Establishing a Hierarchy of Halogen Bonding by Engineering Crystals without Disorder, *Cryst. Growth Des.*, **2013**, *13*, 4145–4150

⁷⁶ Purser S., Moore P.R., Swallow S., Gouverneur V., Fluorine in medicinal chemistry, *Chem. Soc. Rev.*, **2008**, *37*, 320-330.

⁷⁷ Morimoto H., Tsubogo T., Litvinas N.D., Hartwig J.F., A broadly applicable copper reagent for trifluoromethylations and perfluoroalkylations of aryl iodides and bromides, *Angew. Chem. Int. Ed.*, **2011**, *50*, 3793-3798.

⁷⁸ Lishchynskyi A., Novikov M.A., Martin E., Escudero-Adán E.C., Novák P., Grushin V.V., Trifluoromethylation of Aryl and Heteroaryl Halides with Fluoroform-Derived CuCF_3 : Scope, Limitations, and Mechanistic Features, *J. Org. Chem.*, **2013**, *78*, 11126–11146.

needed high temperature (about 150~160 °C) for their activation.⁷⁹ However, the desired *p*-bromo-trifluoromethylbenzene **44** is volatile (bp. 160 °C), rendering both trifluoromethyl reagents (cited above) not convenient. The trifluoromethyl generator Trimethyl-(trifluoromethyl)silane (TMSCF₃) and Methyl 2,2-difluoro-2-(fluorosulfonyl)acetate (MDFA) were chosen in our case. The TMSCF₃ was broadly used in trifluoromethylation with fluoride compounds under gentle conditions to form CF₃⁻.^{80,81} The *N*-Methyl-2-pyrrolidone (NMP) was chosen as solvent for the reaction because of its b.p. 202 °C.



Scheme 22. Proposed mechanism of CF₃ unit generation from MDFA.

The MDFA was originally studied by Chen *et al.* and a proposed mechanism was reported (Scheme 22).^{82, 83} First, the methyl group of MDFA is substituted by CuI. Subsequently, decarboxylation and desulfonylation take place to produce a carbene :CF₂ by heating (about 80~100 °C), and then the :CF₂ carbene was reacted with F⁻ anions to form CF₃⁻ in equilibrium and coordinate with copper to form CuCF₃ *in situ*. With TMSCF₃, the trifluoromethylation proceeded with similar yields when compared to MDFA or (Figure 8). Due to the volatility of the desired product, making the crude product very hard to purify by distillation in a small quantity scale (less than 2 mL), the resulting crude product had to be used in the next reaction without purification. In this case, it was

⁷⁹ Schareina T., Wu X.-F., Zapf A., Cotté A., Gotta M., Beller M., Towards a Practical and Efficient Copper-Catalyzed Trifluoromethylation of Aryl Halides, *Top. Catal.*, **2012**, 55, 426–431.

⁸⁰ Oishi M., Kondo H., Amii H., Aromatic trifluoromethylation catalytic in copper, *Chem. Commun.*, **2009**, 14, 1909-1911.

⁸¹ Urata H., Fuchikami T., A novel and convenient method for trifluoromethylation of organic halides using CF₃SiR₃/KF/Cu(I) system, *Tetrahedron Lett.*, **1991**, 32, 91-94.

⁸² Chen Q.Y., Wu S.W., Methyl fluorosulphonyldifluoroacetate; a new trifluoromethylating agent, *J. Chem. Soc., Chem. Commun.*, **1989**, 705-706.

⁸³ Chen Q.Y., Trifluoromethylation of organic halides with difluorocarbene precursors, *J. Fluor. Chem.*, **1995**, 72, 241-246.

necessary to ensure that all starting material (*p*-bromoiodobenzene **43a** and **43b**) was consumed. The trifluoromethylation was also found very sensitive to the quality of CuI (to store under argon).

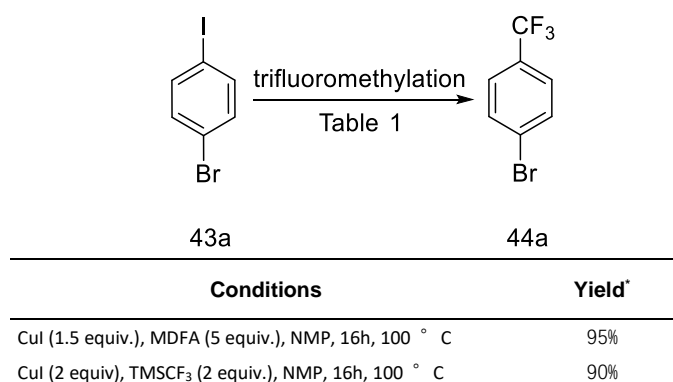
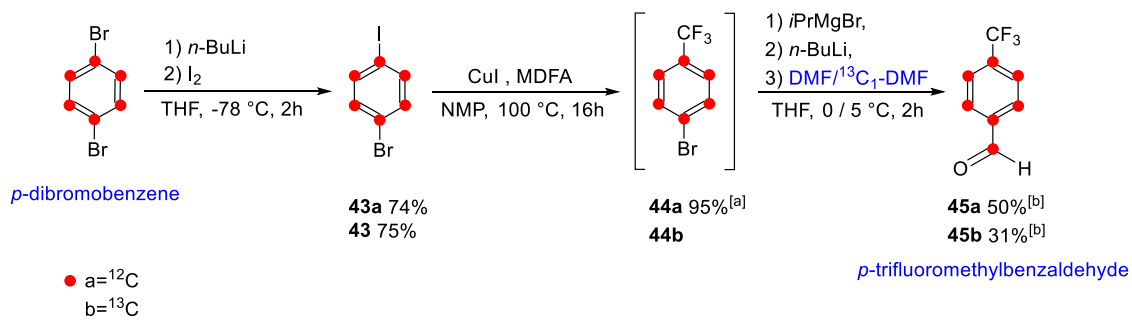


Figure 8. The conditions of trifluoromethylation reaction were shown in the table. NMP=N-Methyl-2-pyrrolidone. *The yields were estimated by ¹⁹F NMR with using trifluoromethoxytoluene as internal standard.

In the next step of preparation, the hydroformylation with the Grignard reagent produced the *p*-trifluoromethylbenzaldehyde **45b** (in two steps with an overall yield of 30%). This methodology for benzaldehyde formation in relatively high temperature (0 °C to 5 °C) was developed by Gallou *et al.*⁸⁴ By using *i*PrMgBr, the bromoaryl group was transformed to [phen]₃-Mg Grignard reagent *in situ*, a reaction that was accelerated by using *n*-BuLi. Subsequently, the resulting Grignard reagent nucleophilic attacked to ¹³C₁-DMF to form desired benzaldehyde product. Because of the highly water sensitivity of this reaction and the volatility of starting material, it required to use Na₂SO₄ *in situ* in order to remove the maximum of water.

⁸⁴ Gallou F., Haengi R., Hirt H., Marterer W., Schaefer F., Seeger-Weibel M., A practical non-cryogenic process for the selective functionalization of bromoaryls, *Tetrahedron Lett*, **2008**, 49, 5024-5027.



Scheme 23. The synthesis of the 4-trifluoromethyl benzaldehyde **45a-b**. [a] The yield of trifluoromethylation reaction was estimated by ¹H NMR with using trifluoromethoxytoluene as internal standard. [b] The yields of 2 steps reactions, accounting *p*-bromoiodobenzene **43a/43b** as starting material.

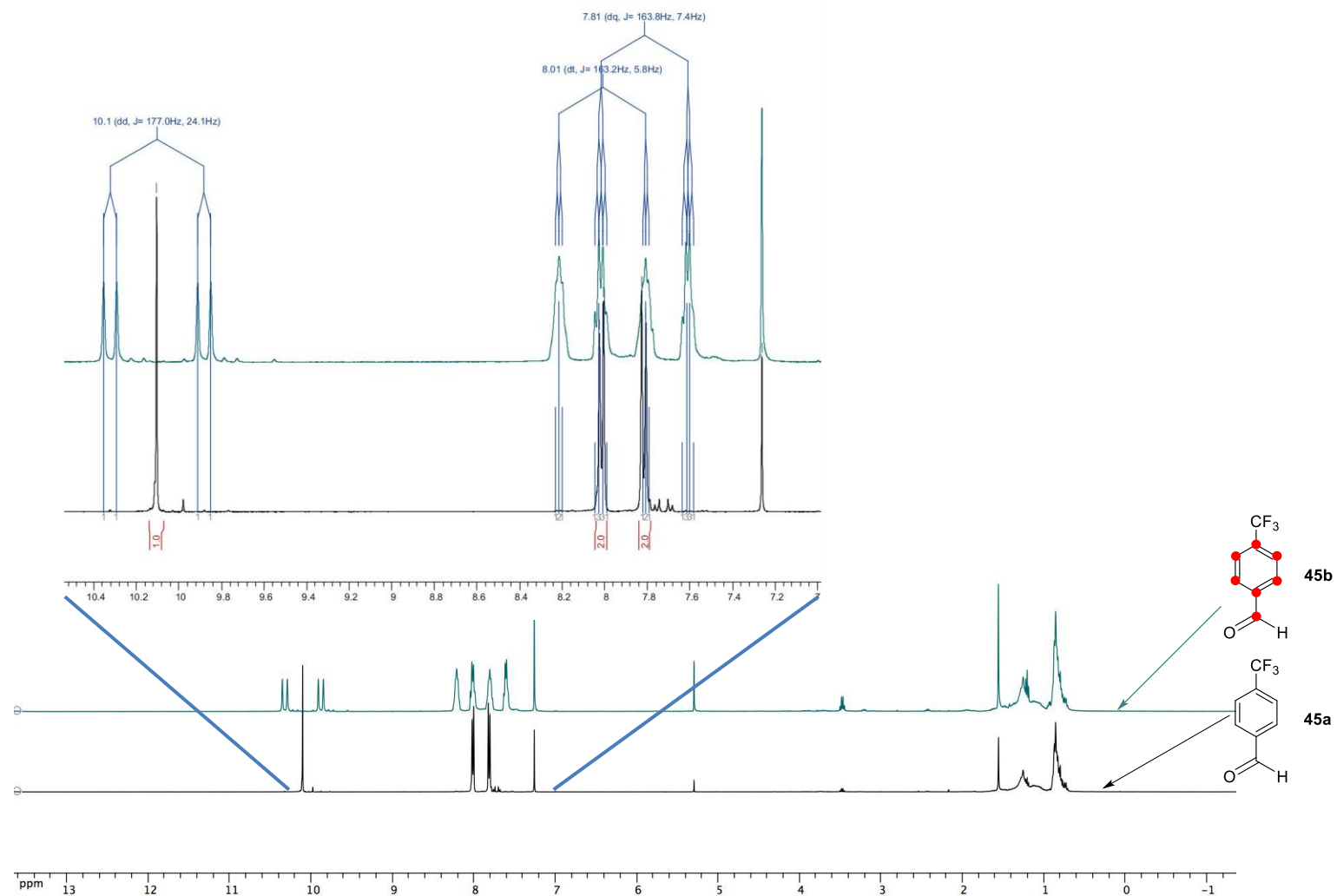


Figure 9. ^1H NMR (400 MHz, CDCl_3) of *p*-trifluoromethylbenzaldehyde **45a** and $^{13}\text{C}_7$ -*p*-trifluoromethylbenzaldehyde **45b**. The black line represents **45a** and the green line represents **45b**.

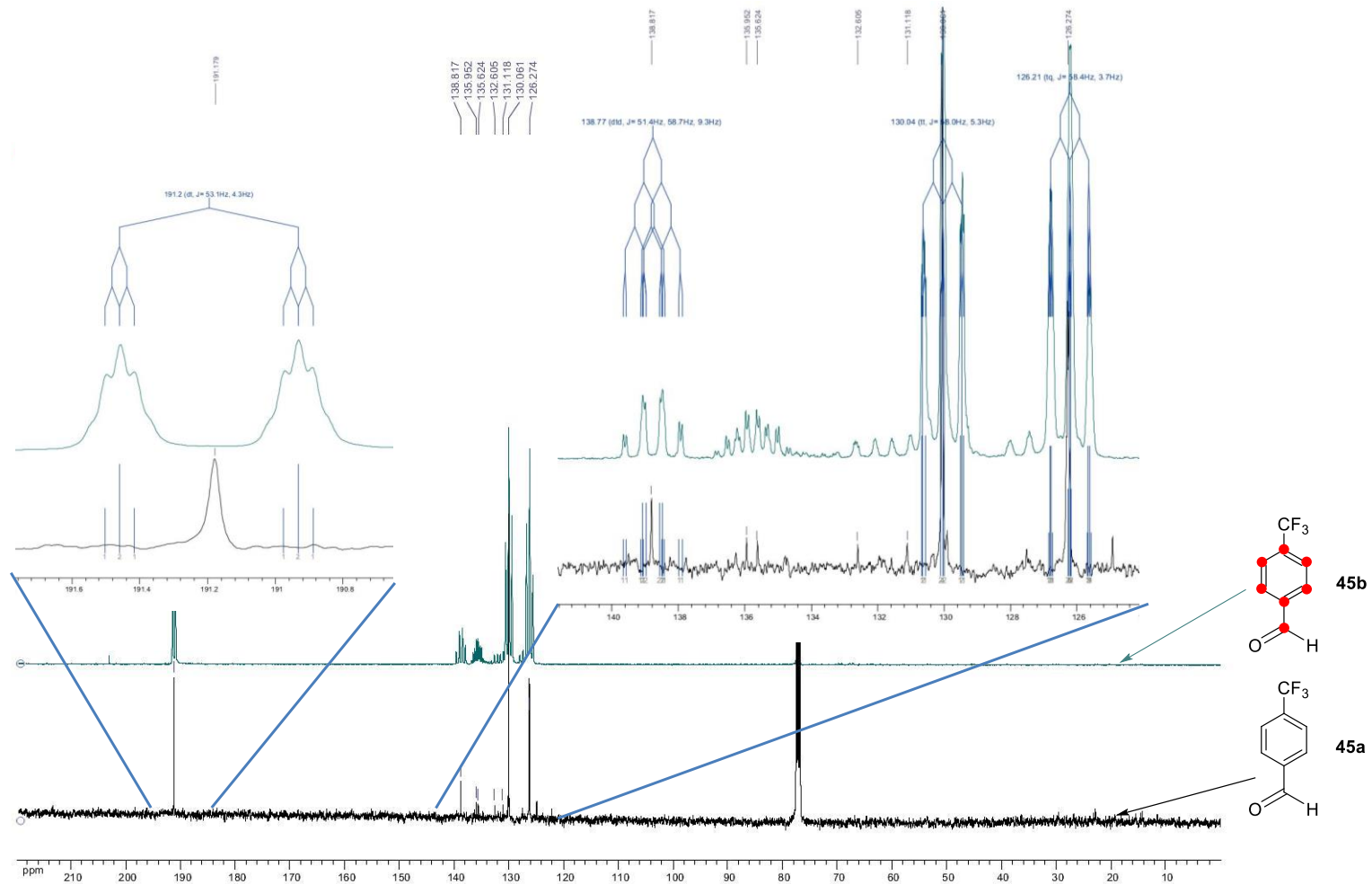
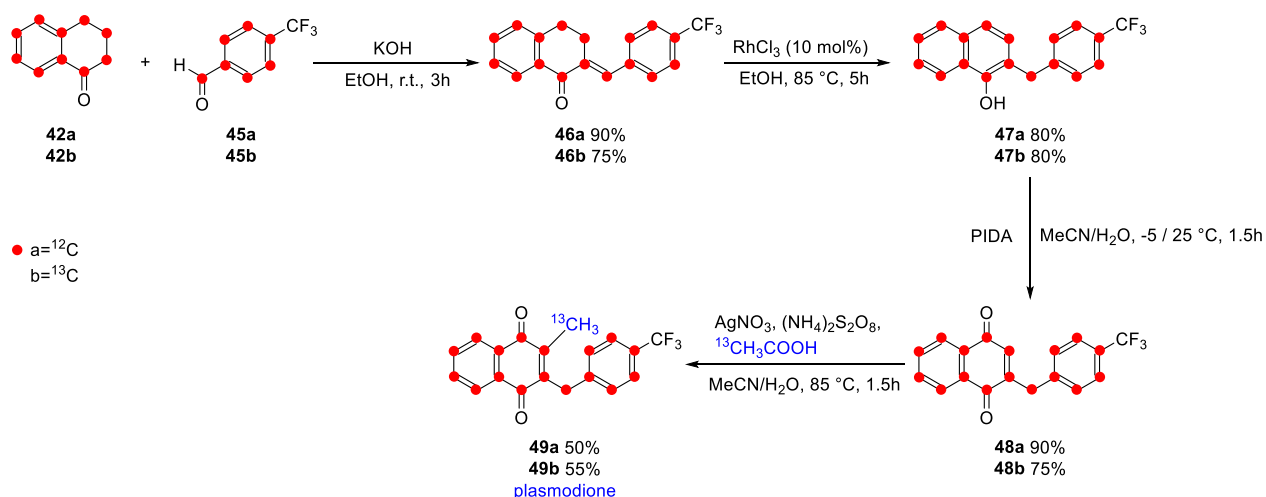


Figure 10. ^{13}C NMR (100 MHz, CDCl_3) of *p*-trifluoromethylbenzaldehyde **45a** and $^{13}\text{C}_7$ -*p*-trifluoromethylbenzaldehyde **45b**. The black line represents **45a** and the green line represents **45b**.

Based on the ^1H and ^{13}C NMR, we could verify the structure of $^{13}\text{C}_7$ -*p*-trifluoromethylbenzaldehyde **45b**. In the ^1H NMR spectrum of **45b**, the peak of the proton at the aldehyde position at 10.1 ppm was split to a doublet-doublet signal with a $^2J_{13\text{C}-1\text{H}}$ constant of 177.0 Hz (Figure 9). And the peaks of the protons in the phenyl ring were multiplied to doublet-triplet and doublet-quadruplet peaks at 8.01 ppm and 7.81 ppm, with $^2J_{13\text{C}-1\text{H}}$ constant 163.2 Hz and 163.8 Hz. Respectively, in the ^{13}C NMR spectrum of **45b**, the peak of carbon at the aldehyde position at 191.2 ppm was divided to doublet-multiplet (Figure 10). By comparing both ^1H and ^{13}C NMR spectra, we found that all the peaks of $^{13}\text{C}_7$ -*p*-trifluoromethylbenzaldehyde **45b** retained the same chemical shifts as in the spectra of unlabeled trifluoromethylbenzaldehyde **45a**. These NMR data unambiguously assigned the molecular structure of the expected fully ^{13}C -enriched key-intermediate.

1.2.3. Synthesis of ^{13}C -enriched plasmodione.

The two resulting intermediates $^{13}\text{C}_{10}$ -tetralone **42b** and $^{13}\text{C}_7$ -*p*-trifluoromethylbenzaldehyde **45b** were combined through an optimized “express tetralone route” which were described in our previous studies, to produce the $^{13}\text{C}_{18}$ -plasmodione **49b** in 4 steps (Scheme 24).⁴⁶ First, a condensation reaction from both previously described *p*-trifluoromethylbenzaldehyde (**45a** and **45b**) and tetralone (**42a** and **42b**), under classical conditions (KOH as a base), led to the tetralone with an *exo* double bond (**46a** and **46b**) with 90 and 75% yield, respectively. Then, isomerization reaction with RhCl_3 catalysis under the conditions described in details, proceeded with similar yields (80%) to obtain the α -benzyl naphthols **47a** and **47b**. These naphthols were submitted to the oxidation reaction with Phenyliodonium Diacetate (PIDA), which generated the benzyl-*1,4*-naphthoquinones **48a** and **48b** with 90% and 75% yield, respectively. Finally, the Kochi-Anderson alkylation reaction was applied in the presence of $^{13}\text{C}_1$ -acetic acid with $\text{AgNO}_3/(\text{NH}_4)_2\text{S}_2\text{O}_8$, to produce $^{13}\text{C}_1$ -enriched plasmodione **49a** and the fully $^{13}\text{C}_{18}$ -enriched lead plasmodione **49b** with 50 and 55% yield, respectively.



Scheme 24. The synthesis of plasmidione **49a-b** from tetralone **42a-b** and *p*-trifluoromethylbenzaldehyde **45a-b**.

According to the previous studies of the radical methylation based on the Kochi-Anderson reaction, the stability of methyl radical was much lower, and the more reactive methyl radical has been thought to destroy the desired product.⁴⁶ In order to follow the reaction kinetics and to track the reaction products by ¹H NMR spectroscopy (Figure 11), we used unlabeled 2-(4-(trifluoromethyl)benzyl)-naphthalene-1,4-dione **48a** as the starting material for the model reaction. Similarly to the previous study, after 15 min stirring, the reaction conversion reached almost 50% and we observed that the desired product was quickly generated. After 60 min, the starting material was almost consumed but not completely. With the reaction stirring, we observed the best conversion when the reaction was stopped at 75 min, a longer time with respect to the 60 min applied to prepare the unlabeled acetic acid as reaction partner. After 90 min, the generation of side products was observed and the yield of the reaction decreased. The preparation of the fully ¹³C₁₈-enriched-plasmidione **49b** from **48b** account for the optimized process with 55% yield after 2 purification steps (chromatography followed by precipitation).

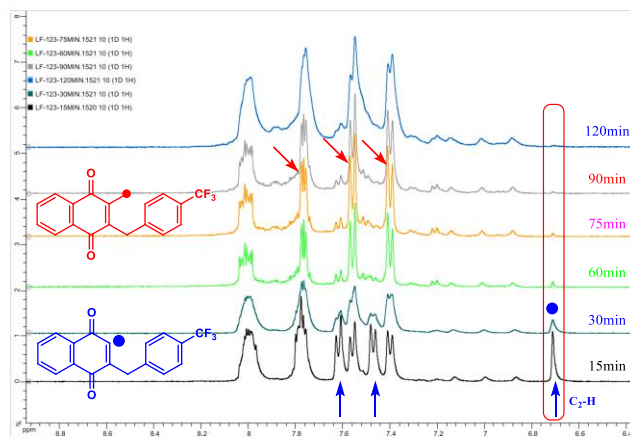
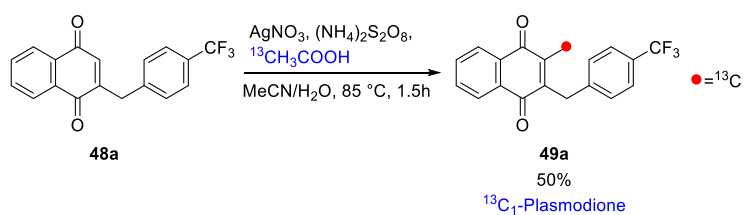


Figure 11. Kinetic ¹H NMR spectroscopy studies of the Kochi-Anderson reaction between **48a** and 2-¹³C₁-acetic acid, the blue arrow directs the peak of the proton of **48a**, the red arrow directs the peak of the proton of **49a**, the blue spot represents the proton at C-2 position of **48a**. The ¹H NMR study was performed in a mixture of CD₃CN/D₂O.

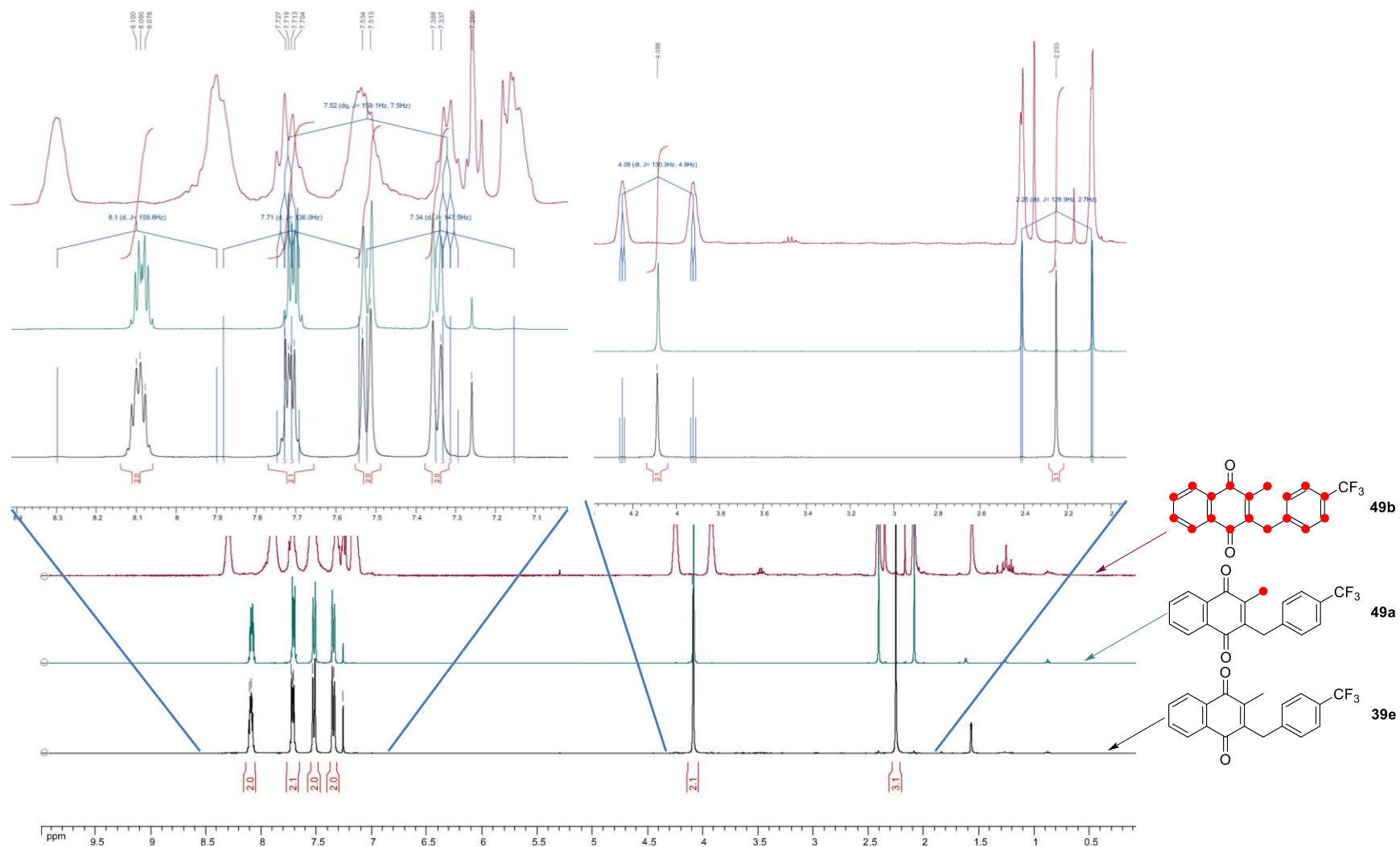


Figure 12. ^1H NMR (400 MHz, CDCl_3) of plasmodione **39e** and $^{13}\text{C}_{18}$ -plasmodione **49b** and $^{13}\text{C}_1$ -plasmodione **49a**. The black line represents **39e**, the red line represents **49b** and the green line represents **49a**.

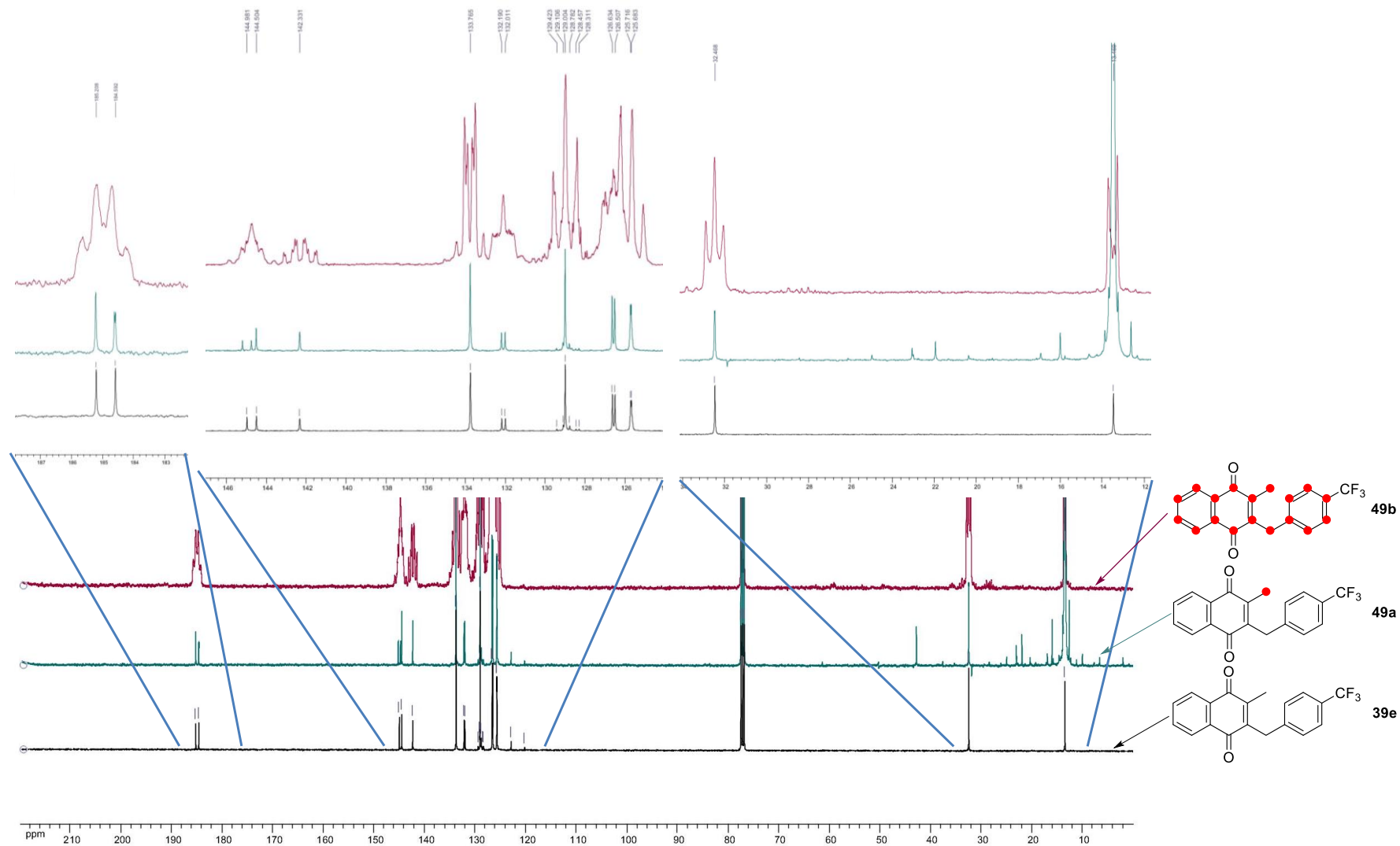
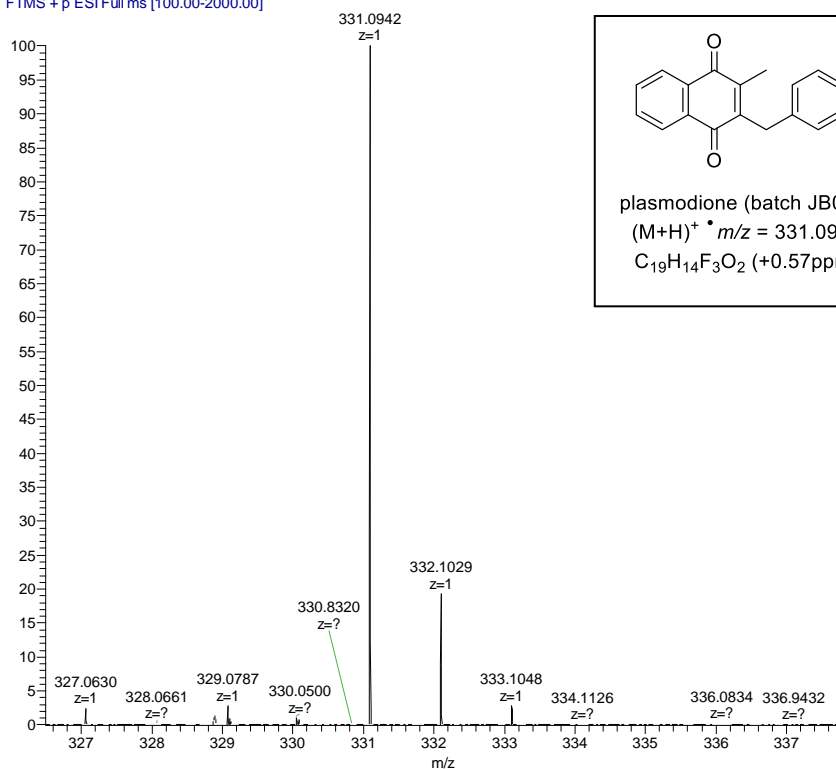


Figure 13. ^{13}C NMR (100 MHz, CDCl_3) of plasmidione **39e** and $^{13}\text{C}_{18}$ -plasmidione **49b** and $^{13}\text{C}_1$ -plasmidione **49a**. The black line represents **39e**, the red line represents **49b** and the green line represents **49a**.

According to the ^1H and ^{13}C NMR spectra, the structure of $^{13}\text{C}_{18}$ -plasmodione **49b** has been confirmed. In the ^1H NMR spectra of **49b**, the peaks of the proton at the naphthoquinone part were divided by two, at 8.10 ppm and 7.71 ppm with $^2J_{13\text{C}-1\text{H}}$ constants 159.8 Hz and 136.0 Hz (Figure 12). The peaks of the proton at the part of phenyl group were split at 7.52 ppm and 7.32 ppm with $^2J_{13\text{C}-1\text{H}}$ constants of 159.1 Hz and 147.5 Hz. The two protons at the benzyl chain were revealed as a doublet at 4.08 ppm with $^2J_{13\text{C}-1\text{H}}$ constant 130.3 Hz. The protons of methyl group showed signals at 2.25 ppm with $^2J_{13\text{C}-1\text{H}}$ constant 128.9 Hz. As observed in ^1H NMR, by comparing these three ^{13}C NMR spectra, all the peaks of $^{13}\text{C}_{18}$ -plasmodione **49b** can be recovered in the same chemical shift as unlabeled plasmodione **39e** and mono-labeled **49a** (Figure 13). It was worth to note that the peak of the carbon CF_3 was covered by the intense signals of the other carbon because its signal was too weak comparing to the ^{13}C -labeled part. All these NMR data corroborated the exact assignment to the molecular structure of desired ^{13}C -enriched plasmodione **49b** and **49a**.

Due to the high cost starting material, only 50 mg fully $^{13}\text{C}_{18}$ -enriched-plasmodione **49b** was obtained though the 10 steps-long synthesis (overall yield of 5 %).

JB047 #12-269 RT: 1.05-2.32 AV: 148 NL: 8.71E5
T: FTMS + p ESI Full ms [100.00-2000.00]



LF129-2 #77-85 RT: 0.96-1.05 AV: 9 NL: 1.37E5
T: FTMS + p ESI Full ms [95.00-1000.00]

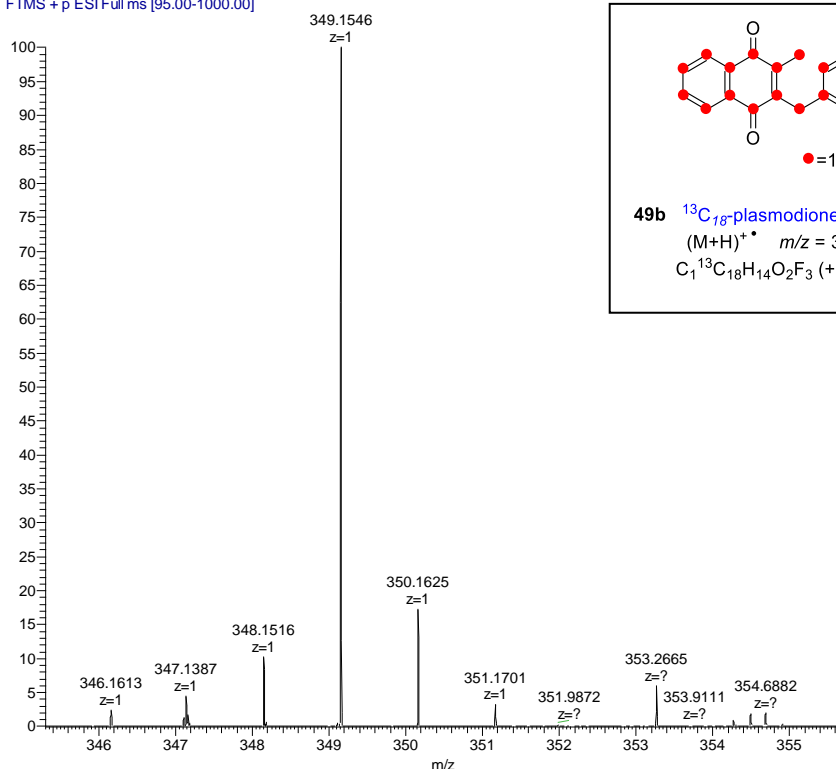
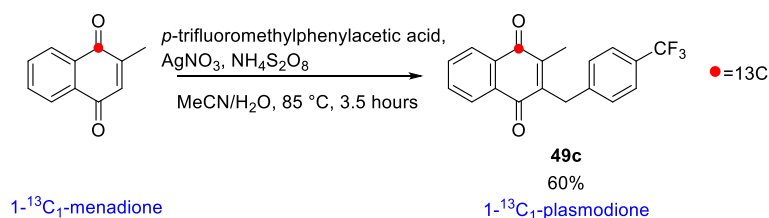


Figure 14. ESI-MS mass spectra of ¹³C₁₈-plasmodione **49b**. Data from Laboratoire d'Etudes du Métabolisme des Médicaments, CEA, Saclay. Condition of MS analysis, both compounds were resuspended in 1mL of MeOH, thus yielding 1.95 mg/mL and 1.08 mg/mL solutions for JB047 (**39e**) and LF129 (**49b**), respectively. The two mixtures were then diluted in a 50% MeOH solution to give

~20µg/mL solutions. Analyses were performed by infusing these solutions at 5µl/min on an LTQ-Orbitrap Discovery instrument (R=30,000 at m/z 400) at CEA Saclay.

I.2.4. Synthesis of the 1-¹³C₁-3-[(4-trifluoromethyl)benzyl]-menadione

In order to spare the expensive product **49b** in the drug metabolism study, we also prepared another ¹³C-labeled plasmidione **49c** for the preliminary metabolism study in order to establish the analytical conditions. The synthesis was performed by one step Kochi-Anderson reaction, starting from *p*-trifluoromethylphenylacetic acid and 50 mg of ¹³C₁-menadione^{85,86}, which has been provided as a gift from Dr. H. Zimmermann (Max Planck Institute, Heidelberg) (Scheme 25).



Scheme 25. The synthesis of 1-¹³C₁-plasmodione.

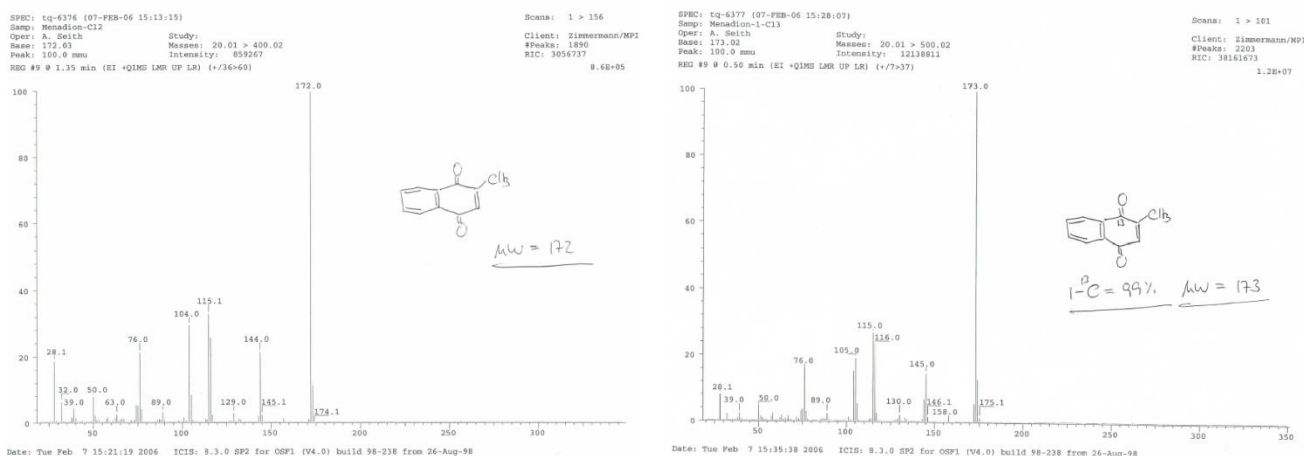


Figure 15. Mass spectra of menadione and 1-¹³C₁-menadione.

⁸⁵ Pushkar Y.N., Golbeck J.H., Stehlik D., Asymmetric Hydrogen-Bonding of the Quinone Cofactor in Photosystem I Probed by ¹³C-Labeled Naphthoquinones, *J. Phys. Chem. B*, **2004**, *108*, 9439–9448

⁸⁶ Karyagina I., Golbeck J. H., Srinivasan N., Stehlik D., Zimmermann H., *Appl. Magn. Reson.*, **2006**, *30*, 287-310

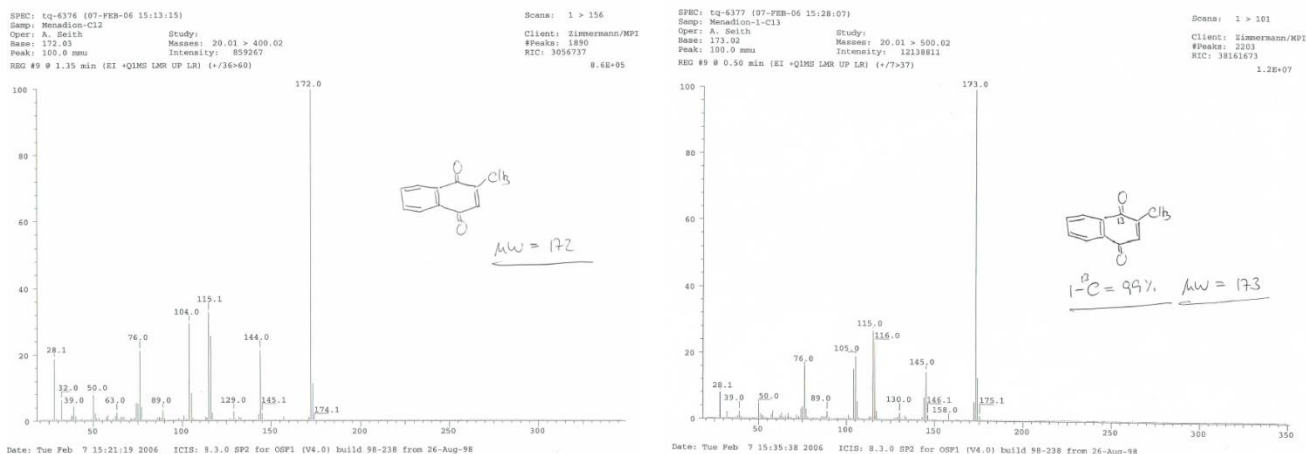


Figure 16. Mass spectra of menadione and $1\text{-}^{13}\text{C}_1$ -menadione.

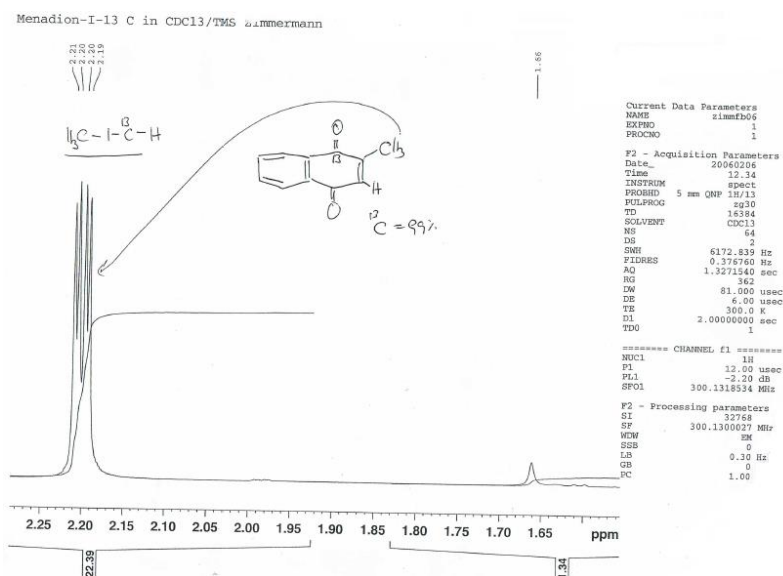
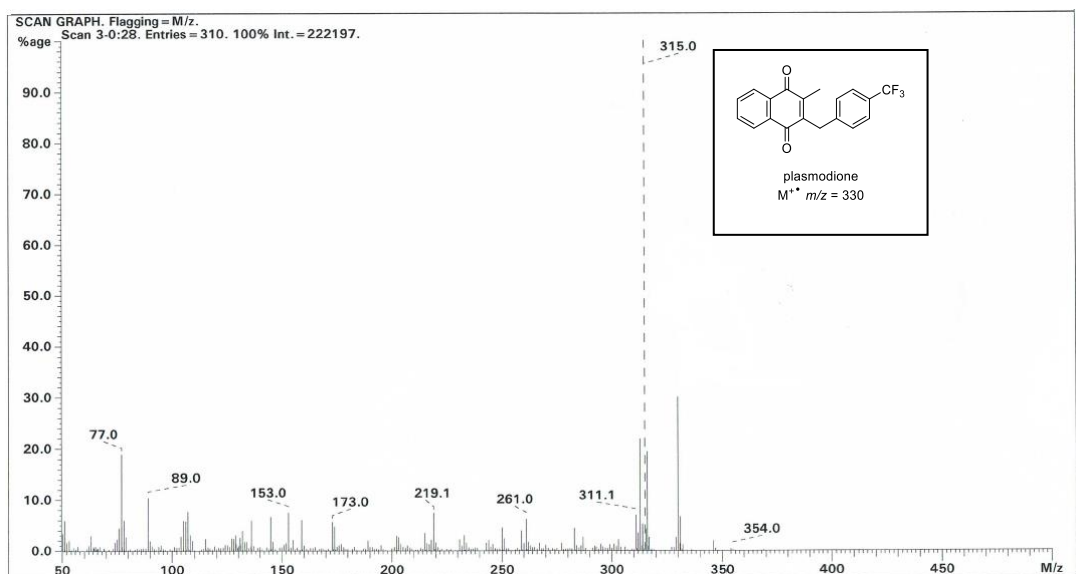


Figure 17. ^1H NMR spectra of $1\text{-}^{13}\text{C}_1$ -menadione.



Inlet : Direct Ion Mode : EI+
Spectrum Type : Normal Ion (MF-Linear)
RT : 1.28 min Scan# : (17,19)+(27,28)
BP : m/z 316.0687 Int. : 258.88
Output m/z range : 225.9941 to 382.2255 Cut Level : 0.00 %

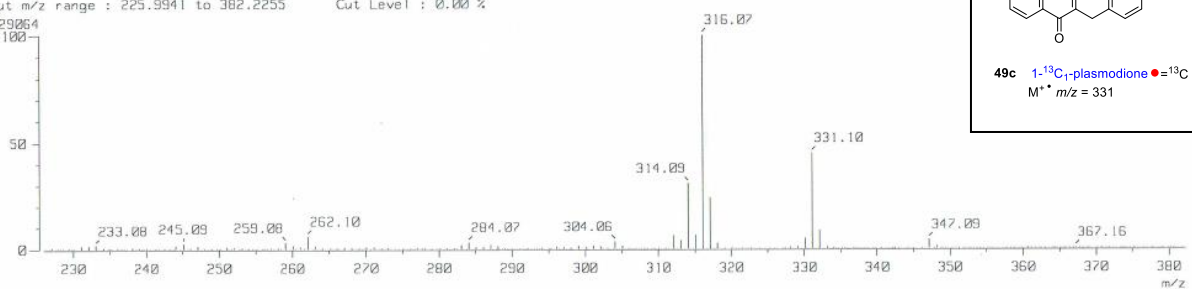


Figure 18. EI-MS mass spectra of 1-¹³C₁-plasmodione **49c**.

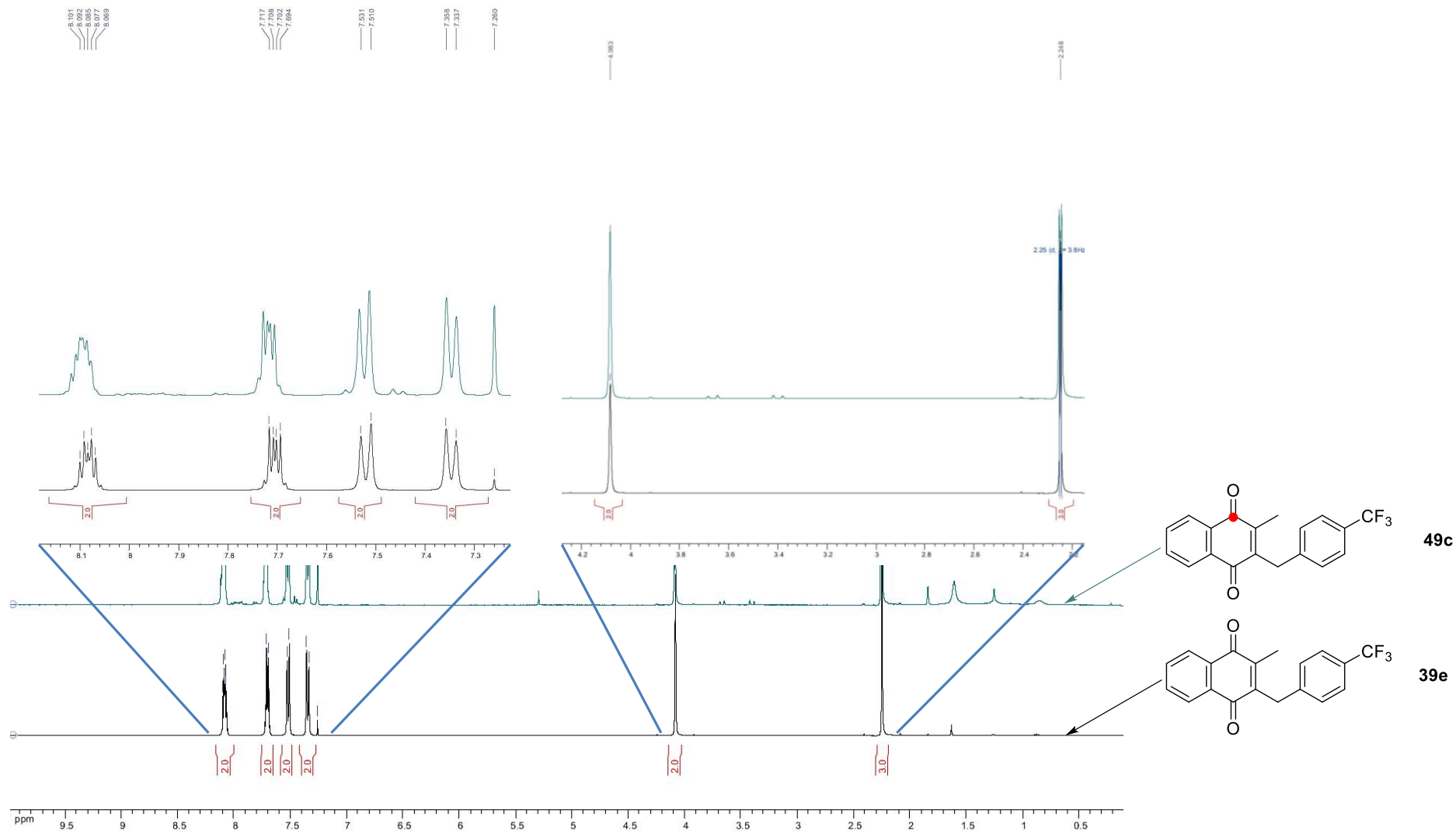


Figure 19. ¹H NMR (400 MHz, CDCl₃) of plasmidione **39e** and 1-¹³C₁-plasmidione **49c**. The black line represents **39e** and the green line represents **49c**.

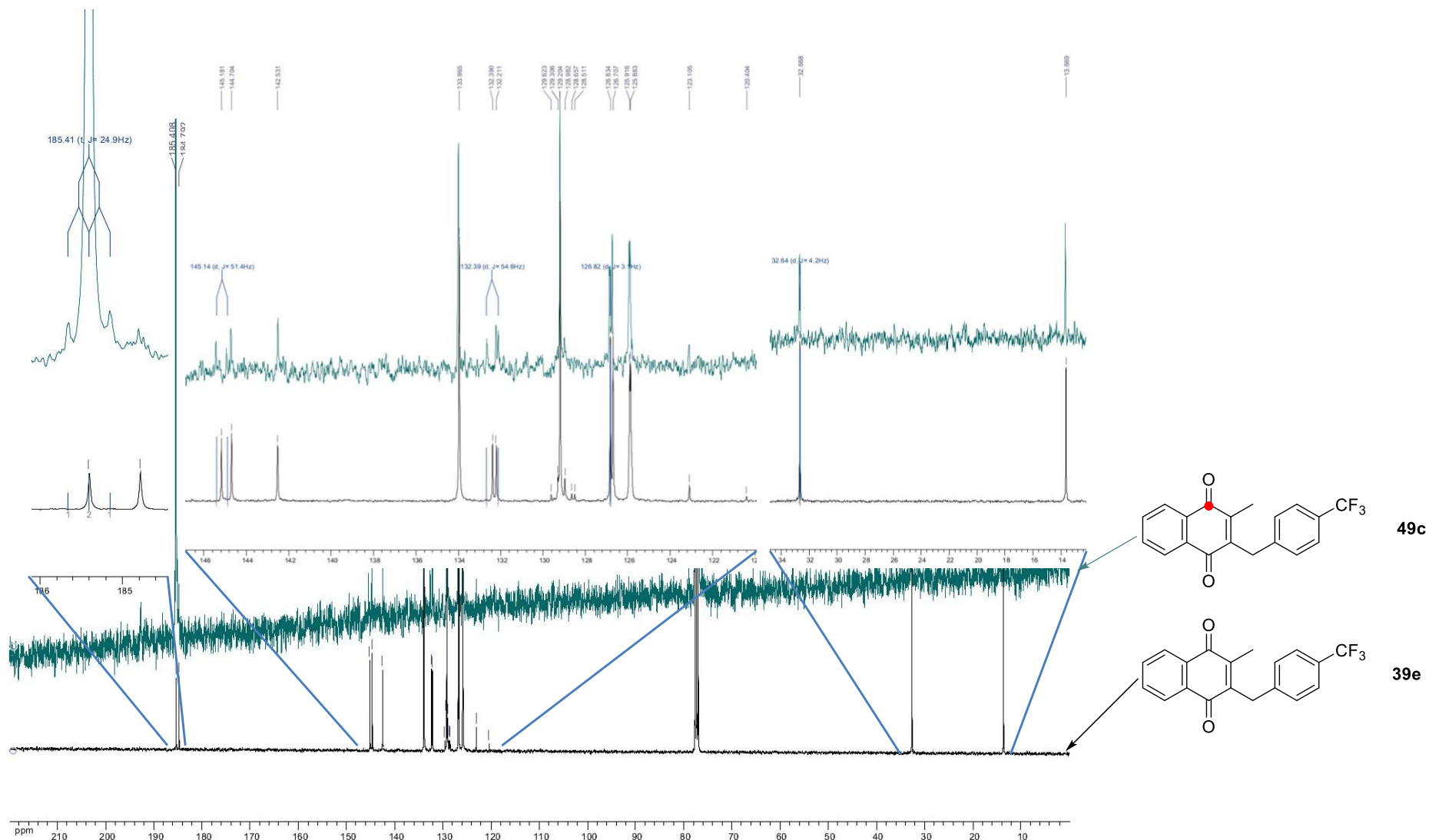


Figure 20. ^{13}C NMR (100 MHz, CDCl_3) of plasmidione **39e** and $1-^{13}\text{C}_1$ -plasmidione **49c**. The black line represents **39e** and the green line represents **49c**.

To conclude this chapter, the $^{13}\text{C}_{18}$ -plasmodione was synthesized by a 10 steps-long sequence via an optimized “tetralone express route” with an overall yield of 5 % for **49b** versus 10.4 % for **49a**. Besides, 2 mono- ^{13}C -labeled plasmodione **49a** and **49c** were produced.

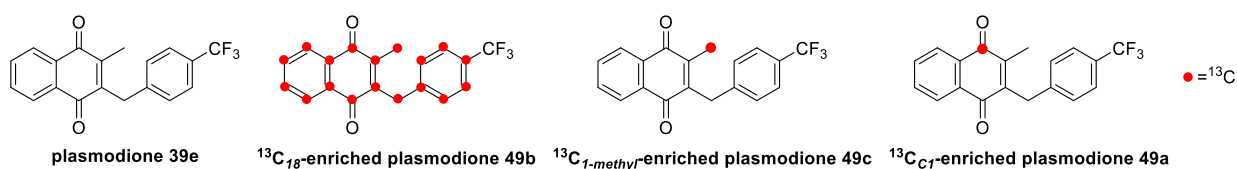
In the course of this work, we could observe that some reactions to produce the ^{13}C -enriched compounds and unlabeled compounds have different yields. Essentially, ^{13}C atoms have the same number of electrons as ^{12}C but different number of neutrons. The ^{13}C -labeled compounds keep the same chemical properties as unenriched compounds. However, higher number of neutrons means increasing the weight of the molecule and decreasing the kinetic energy. Consequently, we cannot predict if this can have an impact on the reactivity of the ^{13}C -enriched compounds compared to that of unlabeled compounds. Therefore, it was difficult to predict the kinetics of the ^{13}C -enriched reaction versus the same reaction with unlabeled starting materials. For example, some reactions like the rhodium-catalyzed isomerization reaction showed the same yields. But, for the oxidation reaction, the yields are different, *i.e.* for **48a** (90 %) versus **48b** (75 %).

Besides, the presence of 90 % abundance of ^{13}C atom causes huge differences of signal patterns in ^1H and ^{13}C NMR spectra of ^{13}C -labeled versus unlabeled compounds. The most significant effect is generating $^2J_{13\text{C}-1\text{H}}$ coupling constants of the ^1H NMR signals, which are ranged from 120 Hz to 170 Hz.⁸⁷ By analyzing the NMR chemical shifts, the ^{13}C -labeled compounds can be correctly profiled by NMR spectra.

I.2.5. Antimalarial activities

In order to compare the chemical quality of the various plasmodiones **39e** and the impact of ^{13}C atoms on the antimalarial activity of the different ^{13}C -enriched & non- ^{13}C -enriched plasmodione derivatives (**49a-c**), whatever the synthetic route, IC_{50} values were determined with rodent *P. berghei* parasites in *ex vivo* assays (Table 4). Noteworthy is the fact that both batches of plasmodione **39e** (**P_TM29**, **JB047**) used in the biological study did not contain a residual amount of silver salts (coming from the Kochi-Anderson reaction) that could poison the drug even at trace level. The evaluation was assessed by ICP-MS at ECPM by Anne Boos. The Ag content was determined as < 1 mg/kg.

⁸⁷ Yadav L. D. S., *Organic Spectroscopy*, Springer Netherlands, 2005, chapter 6.3, 197-199. DOI: 10.1007/978-1-4020-2575-4



Compound	Synthetic route (n steps)	IC ₅₀ ± SD (nM) ^a <i>P. berghei</i>
JB047 (plasmodione 39e)	Kochi-Anderson (1)	181.4 ± 14.7
LF132 (plasmodione 39e)	« tetralone express » (4)	201.9 ± 50.1
LF129 ($^{13}\text{C}_{18}$ -plasmodione 49b)	« tetralone express » (10)	186.1 ± 2.6
BJ721 ($^{13}\text{C}_{\text{C}1}$ -plasmodione 49c)	Kochi-Anderson (1)	181.3 ± 3.2
LF128 ($^{13}\text{C}_{1\text{-methyl}}$ -plasmodione 49a)	« tetralone express » (4)	180.6 ± 5.2

Table 4. IC₅₀ values of plasmodione (**39e**, **49a-c**) as antimalarial agents against *P. berghei* parasites determined in *ex vivo* cultures and chemical tools for metabolism studies. Conditions: *P. berghei* GFPLuc strain, 24h incubation, standard protocol. The protocols used to determine the activity of antimalarial compounds against *P. berghei* blood stage parasites under *ex vivo* conditions were detailed in the materials and methods from A.-A. Goetz PhD dissertation, Strasbourg University, 2016. All antimalarial activities were measured in Dr. Stéphanie Blandin, Anopheles Group, U963 INSERM / UPR9022 CNRS, Institut de Biologie Moléculaire et Cellulaire (IBMC), Strasbourg University. The IC₅₀ values in *P. berghei* assays were measured by Dr. Katharina Ehrhardt, IBMC.

Chapter II: Drug metabolism studies on plasmodione-treated parasitized red blood cells

II.1. Synthesis of several putative plasmodione metabolites

In the previous study, we have successfully synthesized the fully ^{13}C labeled plasmodione **49b** and two mono- $^{13}\text{C}_1$ -labeled plasmodione **49a** and **49c**. In addition, in order to study the drug metabolism of our lead drug, we have also synthesized a series of putative plasmodione metabolites.

Although there are not cytochromes P450 (cytP₄₅₀) in the pRBC cultures *in vitro*, the *plasmodium falciparum* parasites digest a large amount of methemoglobin and release free heme iron III (FPIX Fe^{III}), both which can catalyze oxidation reactions to oxidize/metabolize our lead drug.⁸⁸ These drug metabolites might impact on the life cycle of the living parasites, leading to the death of parasites. According to the mechanism of oxidation reactions catalyzed by cytP₄₅₀ enzymes, the expected primary drug metabolites are expected to be oxidized at different loci of the benzylmenadione core, i. e. the naphthoquinone ring, methyl group or benzyl chain of plasmodione, generating the corresponding hydroxyl-, epoxy-, benzhydrol, or benzoyl derivatives.⁸⁹ Thus, we have synthesized these putative drug metabolites for the drug metabolism study. With these synthetic drug metabolites, firstly, we can analyze by LC/MS-MS whether they could be formed upon incubation of the lead drug in pRBC samples; second, the structure of unknown drug metabolites might also be anticipated from structure/fragmentation information of these synthetic metabolites; finally, we can find out the optimized conditions to extract the desired drug metabolites from pRBCs samples.

II.1.1. Preliminary Results from the team

In the previous study, presented in the introduction chapter, our laboratory has established a versatile strategy to synthesize a series of plasmodione derivatives. From the previous studies developed in the team a bioactivation of plasmodione has been postulated to take place *in vitro* and/or *in vivo* to explain the antimalarial activity of plasmodione. This biotransformation might occur via a

⁸⁸ Spolitak T., Hollenberg P.F., Ballou D.P., Oxidative hemoglobin reactions: Applications to drug metabolism. *Arch Biochem Biophys.* **2016**, *600*, 33-46.

⁸⁹ Meunier B., de Visser S.P., Shaik S., Mechanism of Oxidation Reactions Catalyzed by Cytochrome P450 Enzymes, *Chem. Rev.*, **2004**, *104*, 3947–3980

cascade of redox reactions that is thought to generate a large array of metabolites. While some of them might be inactive and prone to elimination from the cells (unproductive metabolism) some others might play an essential role in killing the parasites, or in adapting the host cell response to limit the infection (fitness).

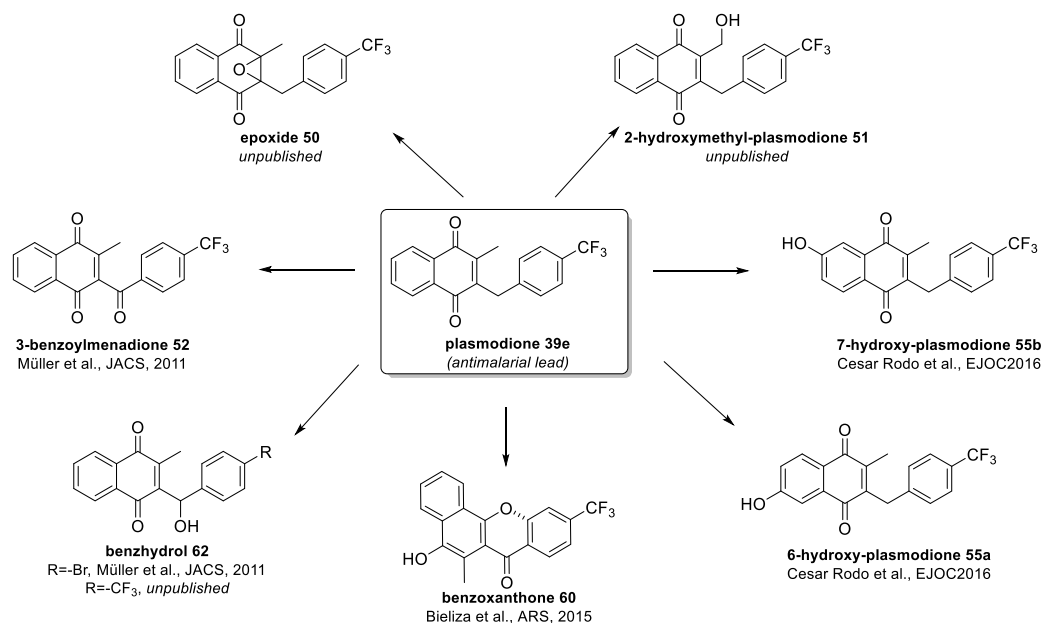
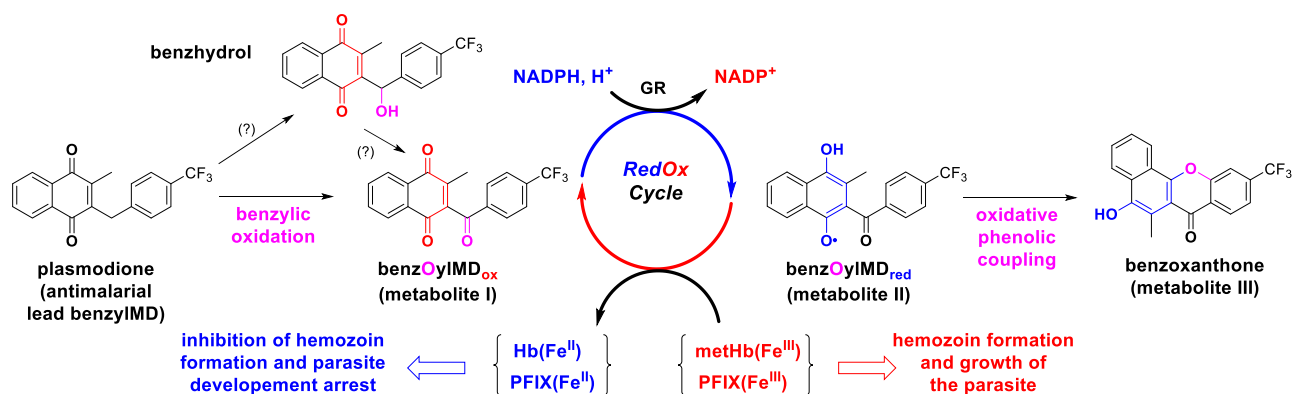


Figure 21. Structures of plasmodione and its potential metabolites.

The studies of the team have already proposed that some metabolites (Figure 21) could be key in the drug bioactivation process, but linking observations from models in solutions to observations *in situ* in parasites is one of the hardest steps in confirming the mode of action of any drug, especially of any antimalarial agent. The particular difficulties are associated to: i) the complexity of the malarial parasites, which exist in different stages in two distinct hosts, *i.e.* the human and the insect vector, the mosquito; ii) the redox chemistry, which involve very rapid reactions due to electron transfers, in oxidation and reduction reactions, in a complex biological milieu (with metals, sugars, proteins, ..., catalyzing/modifying the rate of these redox reactions). Consequently, it is becoming increasingly accepted that a step forward is needed from the traditional target-based approach of drug development in MedChem programs towards an integrated perspective of drug action in biochemical complex systems. To make progress in understanding the mechanisms of plasmodione action, it will be essential to decipher the drug interaction networks connecting drug and/or drug metabolites targets to all components of the biological systems (parasite, host cell, insect) in the future. Therefore, it is essential that the bioorganic chemists can synthesize key chemical tools for the chemical biologists.



Scheme 26. Putative redox cascade reactions accounting for the observed antimalarial activity of plasmodione.

Several plasmodione metabolites (Figure 21, Scheme 26) were previously synthesized and/or investigated with potential isolated targets (hemoglobin, heme, both recombinant NADPH-dependent glutathione reductases from pRBC) in solution or in parasites:

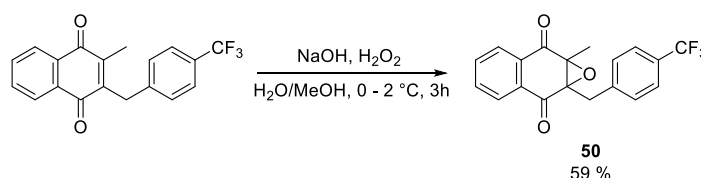
- the *p*-CF₃-benzoylmenadione **52**,⁴⁷ by oxidation of plasmodione in the presence of chromium trioxide and periodic acid,
- the *p*-bromo-benzhydrol analogue of compound **62**, via a 5-steps-long route³
- the 6- and 7-hydroxy-plasmodione derivatives **55a/55b**,⁴⁶ via a Diels-Alder reaction using Danifshesfsky diene and 2-bromo-(5- or 6-)methyl-1,4-benzoquinones
- the oxidative phenolic coupling product, called benzoxanthone **60**, via a 6 steps synthetic scheme,⁴⁸ and an optimized route.

Besides, two additional potential metabolites were prepared (unpublished results):

- the 1,7-epoxide **50** via epoxidation by H₂O₂.
- the hydroxymethyl-plasmodione **51**, in the presence of methanol under Kochi-Anderson conditions.

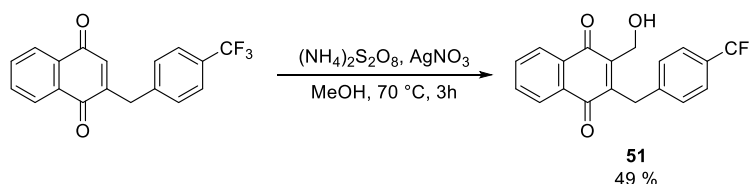
In total, seven putative drug metabolites (Figure 21) were produced.

Epoxy-plasmodione derivative **50** has been formed by epoxidation reaction of plasmodione (Scheme 27).⁹⁰ The similar reaction has been reported in the literature.⁹¹ In the mixture of H₂O/MeOH (4/1), initial compound plasmodione was oxidized by hydrogen peroxide in the presence of NaOH at 0 °C leading to the formation of product **50** in yields of 59 %.



Scheme 27. Synthesis of 1a-methyl-7a-(4-(trifluoromethyl)benzyl)-1a,7a-dihydronaphtho[2,3-b]oxirene-2,7-dione **50**.

Under the Kochi-Anderson conditions, methanol was converted to $\cdot\text{CH}_2=\text{O}$ radical reagent by using Ag (II) as catalyst obtained by oxydation of silver nitrate by ammonium persulfate.^{90,92} Reaction between desmethylplasmodione and radical reagent was allowed to generate hydroxymethylplasmodione **51** (Scheme 28).⁴⁶ The product was purified by column chromatography (SiO₂, Toluene) and isolated with 49% yield.



Scheme 28. Synthetic method of preparation of 2-hydroxymethyl-plasmodione derivative **51**.

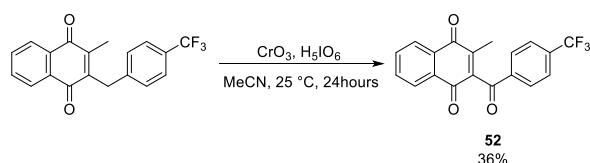
The benzoylmenadione derivative **52** was prepared by oxidation reaction of corresponding benzylic compound in presence of chromium (VI) oxide and periodic acid.⁴⁷ The reaction was

⁹⁰ Cesar Rodo E., Lanfranchi D. A., Boilevin J. *et al.*, preliminary results or unpublished results.

⁹¹ Fioroni G., Fringuelli F., Pizzo F., Vaccaro L., Epoxidation of α,β -unsaturated ketones in water. An environmentally benign protocol, *Green Chem.*, **2003**, 5, 425-428

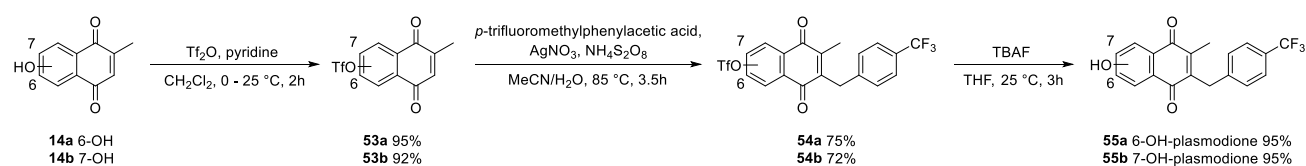
⁹² Nam T.G., Rector C.L., Kim H.Y., Sonnen A.F., Meyer R., Nau W.M., Atkinson J., Rintoul J., Pratt D.A., Porter N.A., Tetrahydro-1,8-naphthyridinol analogues of alpha-tocopherol as antioxidants in lipid membranes and low-density lipoproteins, *J. Am. Chem. Soc.*, **2007**, 129, 10211–10219.

performed in acetonitrile at room temperature for 24 hours affording the product **3** in 36 % yield (Scheme 29).



Scheme 29. Synthesis of the 3-benzoylmenadione derivative **52**.

After deprotonation of the hydroxy group of 6- or 7-hydroxymenadiones derivatives **14a/14b** with pyridine, reaction was treated by triflic anhydride in the dichloromethane giving the desired products **53a/53b** with 95 % yields. Kochi-Anderson reaction has been proceeded in presence of *p*-trifluoromethylphenylacetic acid to yield the plasmodione derivatives **54a/54b**. The final products **55a/55b** were obtained by deprotection of the triflate group on the plasmodione backbone **54a/54b** by using TBAF reagent in the solution of THF at room temperature in excellent yield (Scheme 30).⁴⁶

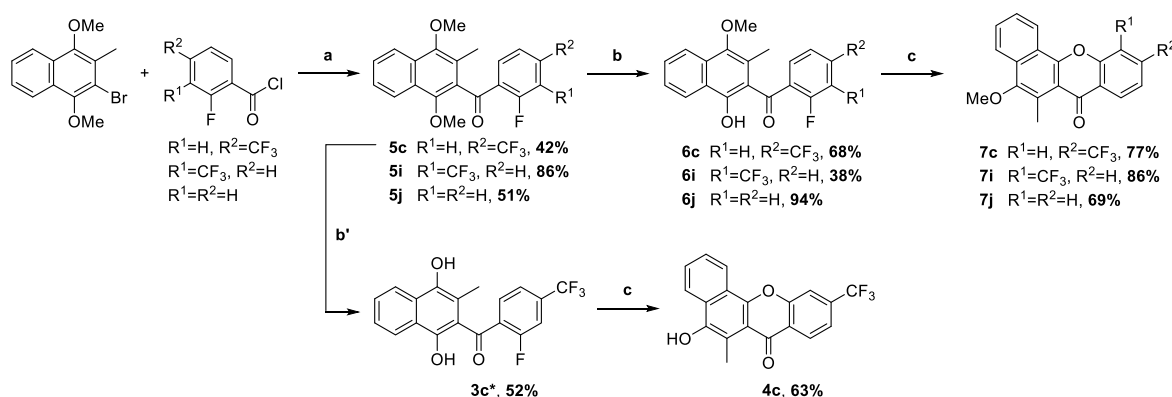


Scheme 30. Synthesis of the 6-/7-hydroxy-plasmodione derivatives **55a/55b**.

A first 3 steps-long synthesis of the benzoxanthone **60** (called benzoxanthone 4c in the ref.48, Bielitzka *et al.*, 2015) and several analogues had been designed (Scheme 31) and published. However, the phenolic compounds revealed to be air-sensitive, unstable over time and the overall yield (13.8%) of the synthetic route to prepare the benzoxanthone **60** was rather low. As we needed a significant amount for both physico(bio)chemical⁹³ and drug metabolism studies a new synthesis has been designed in 6 steps allowing to prepare the benzoxanthone **60** with an overall yield of 41% (unpublished).⁹⁰

⁹³ Johann L., Lanfranchi D. A., Davioud-Charvet E., Elhabiri M., A physicochemical study with redox-cyclers as drugs against blood feeding-parasites, *Curr. Pharm. Des.*, **2012**, *18*, 3539-3566.

The first synthesis of the benzoxanthone **60** was established via the benzophenone intermediate (dihydrobenzoylmenadione) through S_NAr reaction (Scheme 31).⁴⁸ The benzoxanthones **60** (4c) and analogues (7c-j) were obtained in three steps starting from 2-bromo-3-methyl-1,4-dimethoxynaphthalene. Benzoylation with *o*-fluorobenzoyl chloride derivatives following Br/Li exchange in the presence of 1.1 equiv. of BuLi at -78 °C led to the 2-benzoyl-3-methyl-1,4-dimethoxynaphthalene (5c-j). Selective mono-demethylation in the presence of 1.0 equiv. of BBr₃ (1 M in DCM) afforded compounds (6c-j). A final aromatic nucleophilic substitution under basic conditions allowed cyclization of compounds (6c-j) into the targeted benzoxanthones (7c-j) with yields ranging from 69 to 86% (Scheme 31). When both methoxy groups of the 1,4-dimethoxynaphthalene (5c) were deprotected by dropwise addition of 1.0 equiv. of pure BBr₃, the nucleophilic substitution directly led to the phenolic benzoxanthone **60** (4c), which is postulated to be a cyclized metabolite of plasmodione (Scheme 31).



Reagents and conditions:

a) 1.0 equiv. bromonaphthalene, 1.1 equiv. 2-fluoro-benzoyl chloride, 1.1 equiv. BuLi, dry THF, -78 °C, 30 min;

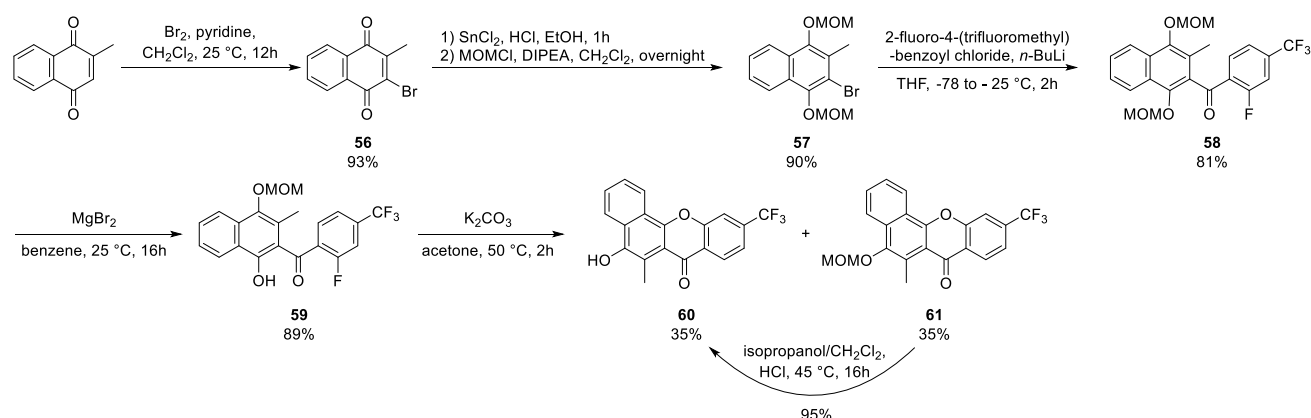
b) 1.0 equiv. BBr₃ (1 M in DCM), 0 °C, 2 h;

c) 2.0 equiv. K₂CO₃, dry acetone, 50 °C, 2h; b') 1.0 equiv. pure BBr₃, 0 °C, 1 h.

Scheme 31. Three-step synthetic route to the benzoxanthones **60** (called 4c in ref.48) and analogues (called 7c,7i-7j in ref.48).

In the optimized route (Scheme 32), bromomenadione **56** was first prepared by bromination of menadione with bromine and pyridine in 93% yield. Subsequently, the quinone core of compound **56** was reduced by tin chloride/HCl as reduction reagent, and then protected by MOM-protection reaction with methoxymethyl chloride (MOM chloride) in the presence of a mild base such as *N,N*-diisopropylethylamine (DIPEA) in dichloromethane at room temperature. During the work-up it was essential to isolate under argon and azeotropically dry the 2-bromo-3-methyl-dihydro-naphthoquinone with desoxygenated toluene because this intermediate is highly sensitive to air oxidation. Then, the bromo-lithium exchange reaction was performed with naphthol **57** and *n*-BuLi, leading to the

carbanion acting as a nucleophilic reagent in the next step. Following, the resulting lithium intermediate was reacted with 2-fluoro-4-(trifluoromethyl)benzoyl chloride affording benzoylmenadione derivative **58**. The next step of the preparation, selective mono-deprotection reaction of MOM group of benzoylmenadione has been allowed to produce compound **59**. It is worth noting that only the *O*-MOM group in α -position to the C=O of the benzoyl chain can be deprotected by MgBr_2 because of the chelating effect⁹⁴. This deprotection of α -ketophenols had been successfully set-up in flavones chemistry in the team. As in the first synthesis of the benzoxanthone **60**, the aromatic nucleophilic substitution/cycloaddition from benzoylmenadione derivative **59** allowed to produce the *O*-MOM-benzoxanthone derivative **61** with K_2CO_3 in acetone. Noteworthy is to mention that partial deprotection of the *O*-MOM-benzoxanthone **61** took place because the *O*-MOM group could be deprotected by HF generated during the reaction. Finally, *O*-MOM-benzoxanthone **61** was deprotected to give benzoxanthone **60** in the mixture of isopropanol/dichloromethane under acidic conditions with 95% yield.

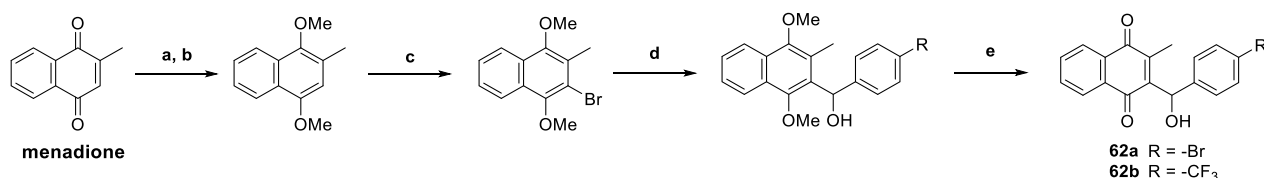


Scheme 32. Optimized synthesis of the benzoxanthone derivative **60**.

The (\pm)-2-((4-bromophenyl)(hydroxy)methyl)-menadione (shorten as benzhydrol) was also prepared as a putative metabolite of plasmodione (Scheme 33). Its synthesis followed lithiation of the 2-methyl-3-bromo-1,4-dimethoxy-naphthalene and *p*-bromobenzaldehyde addition to give the benzhydrol intermediate. Oxidation with cerium ammonium nitrate (CAN) afforded the benzhydrol **62a** (R = -Br). The yields are those obtained for the *p*-bromo analogue. The *p*-trifluoromethyl analogue **62b** (R = -CF₃) has recently been synthesized (unpublished data).⁹⁵

⁹⁴ Martin-Benlloch X., Elhabiri M., Lanfranchi D. A., Davioud-Charvet E., A practical and economical high-yielding six steps-sequence synthesis of a flavone: Application to the multigram scale synthesis of ladanein, *Org. Process Res. Dev.*, **2014**, *18*, 613–617.

⁹⁵ Cotos-Munoz L. *et al.*, unpublished results.



Reaction conditions:

(a) 2.5 equiv. SnCl₂, HCl, EtOH, rt, 0.5 h;

(b) 5.0 equiv. KOH, 3.0 equiv. Me₂SO₄, acetone, 60 °C, 2 h, (73 %);

(c) 1.0 equiv. Br₂, CH₂Cl₂, 0 °C, 1 h, then rt, 2 h, (73 %);

(d) 1.05 equiv. nBuLi, THF, -78 °C, 0.5 h, then 1.0 equiv. p-trifluoromethylbenzaldehyde, THF, -78 °C, 10 min, then rt, 1 h, (73 %);

(e) 3.0 equiv. CAN, CH₃CN, H₂O, rt, 1 h (86 %).

Scheme 33. Synthesis of the (±)-3-[4-substituted-(phenyl)-hydroxy-methyl]menadione **62a** and **62b**.⁴⁷

II.1.2. Personal results

Some of the synthetic metabolites were out of stock for the drug metabolism study, or were found quite unstable (epoxide **50**, 2-hydroxymethyl-plasmodione **51**, benzoxanthone **60**). Consequently, several of them were freshly prepared for developing the reference analysis by LC/MS-MS before the identification in pRBC samples in my PhD thesis.

Upon deprotonation and oxidation, the phenolic benzoxanthone might expose a favorable Michael acceptor site, making susceptible to polymerization under moisture conditions. The compound was found not conducive to storage, even kept at -78°C, for long time (months). The benzoxanthone **60** has to be re-prepared before the experiment of drug metabolism study. In addition, owing to the sensitivity of the experiment, requiring high purity of the putative metabolites as standard, I have re-synthesized epoxy-plasmodione derivative **50** and hydroxyl-plasmodiones derivatives **55a**.

II.2. Analysis of plasmodione and its metabolites from pRBC extracts

The mechanism of action of plasmodione had been recently proposed (Scheme 26), however, this putative drug metabolism pathway was difficult to be confirmed. Based on a former study, the promising antimalarial lead drug was proposed to affect the redox homeostasis of pRBC indirectly through its metabolites. Under its oxidized form, the benzoylmenadione was found more oxidant than the parent benzyolmenadione in agreement with the redox potential values ($E^{1/2} = -0.61\text{V}$ and $E^{2/2} = -1.35\text{V}$ for plasmodione **39e** versus $E^{1/2} = -0.43\text{V}$ and $E^{2/2} = -1.12\text{V}$ for benzyolmenadione **52**).⁴⁸ Under its reduced form, the reduced benzoylmenadione can transfer one electron to methemoglobin in a continuous cycle, consuming NADPH and regenerating both oxyhemoglobin and the oxidized benzoylmenadione. Hence, plasmodione metabolites might interplay with haemoglobin catabolites

and impact the endogenous redox potential of pRBC, ending with the formation and enrichment of membrane-bound hemichromes.⁴⁸ These latter hemoglobin species are biomarkers of senescence of red blood cells and trigger on active elimination of old red blood cells by macrophages.

By redox-cycling NADPH and hemoglobin, it was postulated that the increased oxidative stress leads to the death of the parasite. Several metabolites, in particular the benzoxanthone **60**, that could account for the direct killing of the malarial parasites are also postulated (Scheme 26). In particular, the benzoxanthone **60** was unambiguously shown to alkylate heme and to prevent the β -hematin crystallisation, at a similar extent as chloroquine.⁴⁸

However, this drug metabolite is very active and labile in solution (30% degradation in buffer pH 5.2 or 7.0 after 24h) *in vitro*. Thus, the primary objective of the drug metabolism study is to identify this benzoxanthone confirming whether it is generated from the pRBC or not.

In order to analyze the drug metabolites, Ultra-high performance liquid chromatography (UHPLC) coupled to MS/MS (QTOF) was employed. UHPLC/MS-MS is a powerful and versatile analytical technique that has very high sensitivity and selectivity in drug metabolism studies. With this method, the drug metabolism was investigated at the Laboratoire d'Etudes du Métabolisme des Médicaments (CEA Saclay, LEMM, Drs. François Fenaille and Christophe Junot). First, appropriate collision potential and the fixed program of chromatographic eluent gradient required to establish analytical methods. Based on the result below, the plasmodione and its synthetic drug metabolites were well characterized and fragmented by mass spectrometry (Figure 23). In the same time, the lead drug and its putative metabolites were well separated by using Hypersil GOLD C18-column, expected both 6- and 7-hydroxyl-benzylmenadione derivatives **55a/55b** which showed very similar polarity (Figure 22). Respectively, these two hydroxyl-benzylmenadiones **55a/55b** have different fragmentation pathways so that they can be distinguishably identified (Figure 23 a. and b.). In another side, the acquisitions of ionization intensity of these compounds were not satisfactory, the intensity of all the compounds range from 5×10^4 to 2×10^5 at 50 μ M. However, the drug concentration used to treat pRBC was limited to 5 μ M. Due to the hydrophobicity of the lead drug and some of the putative metabolites, their ionization levels were insufficient while the compounds were spraying at the electrode. This would limit their detection in pRBC samples while they are in low concentration, unless good extraction yields of the lead drug and its metabolites are found.

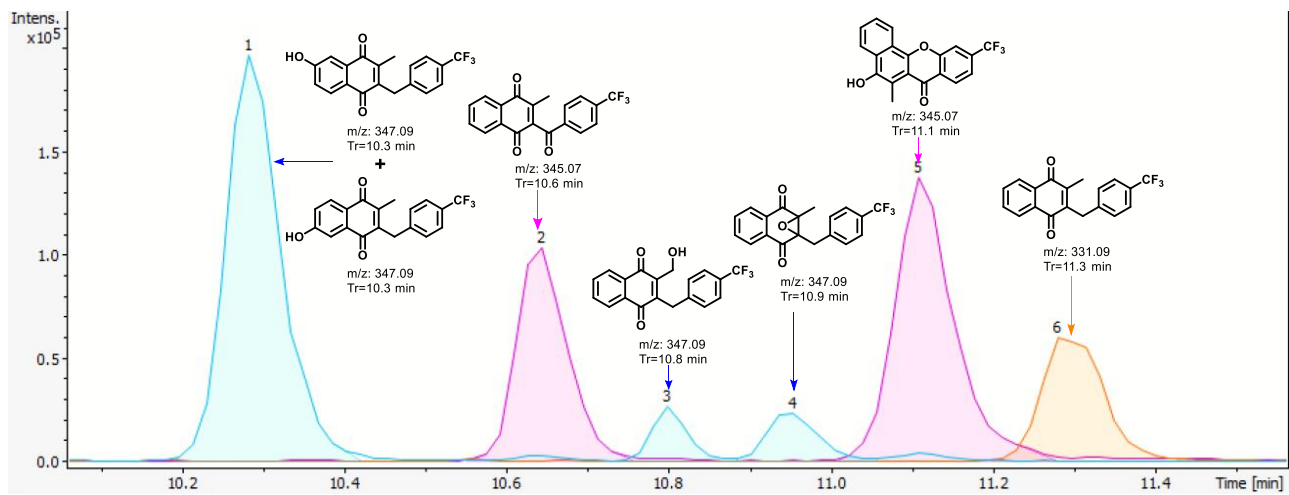


Figure 22. Chromatography spectra of the lead drug and 6 putative drug metabolites at 50 μM.

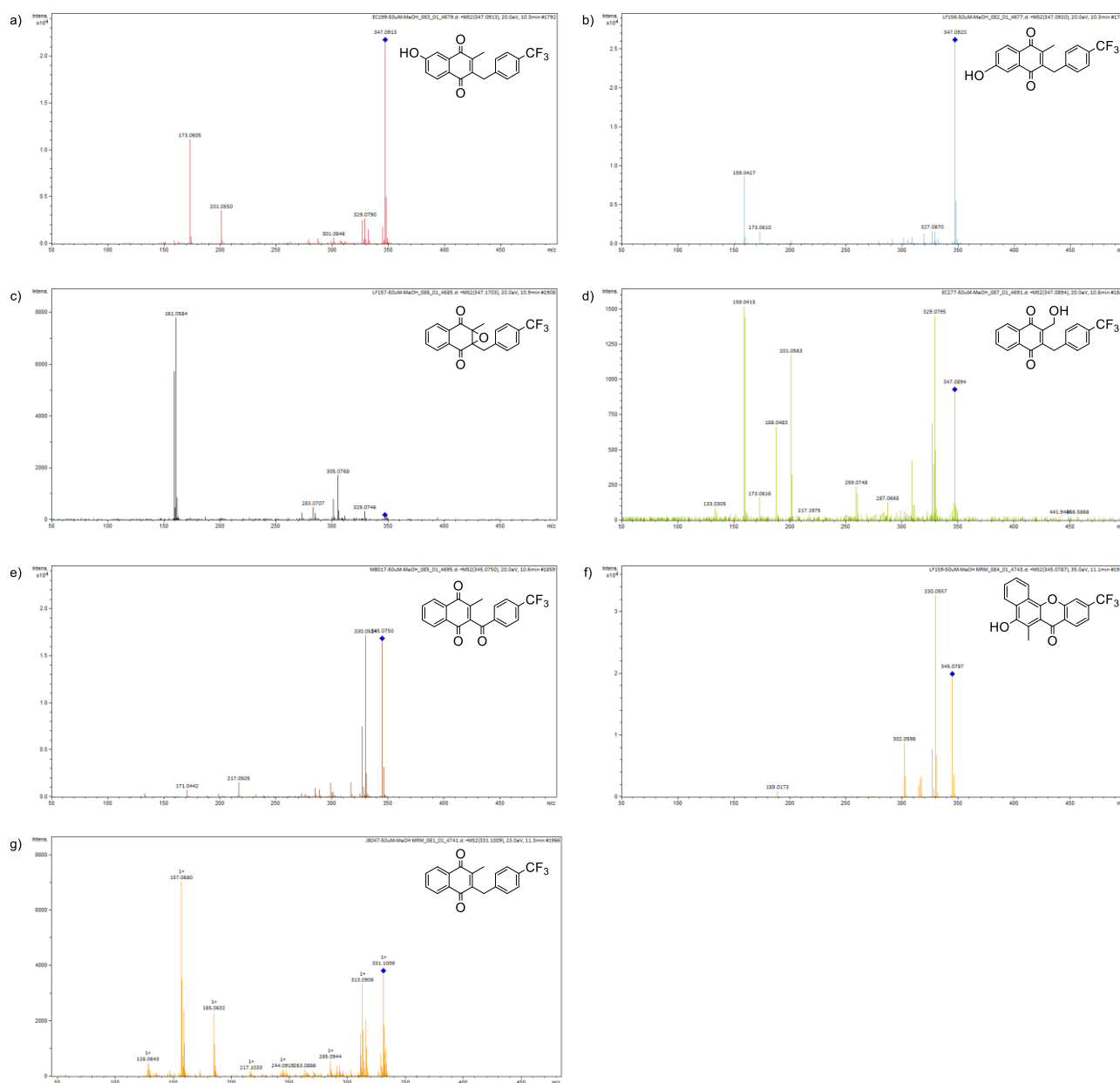


Figure 23. Mass spectrometry of plasmodione and its synthetic drug metabolites. a) 7-hydroxy-plasmodione derivatives **55b**. b) 6-hydroxy-plasmodione derivatives **55a**. c) epoxy-plasmodione derivative **50**. d) hydroxymethyl-plasmodione derivative **51**. e) 3-benzoylmenadione derivative **52**. f) benzoxanthone derivative **60**. g) lead drug plasmodione **39e**.

II.2.1. Investigation on the Extraction method

The investigation of extraction yields was performed with both culture medium and pRBC lysates. The extraction assay was first applied to the culture medium (Table 5 a.). Two different methods were employed to the drug metabolite extraction, by using MeOH and CHCl₃/MeOH/H₂O (v/v/v = 1/3/1)

solvent system. Comparing to these two methods, the extraction with using MeOH as solvent had less Matrix effect and better extraction yields than the chloroform solvent system. Nevertheless, some highly lipophilic/reactive putative drug metabolites such as hydroxymethyl-plasmodione derivative **51** and benzoxanthone derivative **60** were not observed after the extraction. As a result of the hydrophobic properties and reactivities, the lead drug and its putative metabolites were captured by the proteins or the membranes of pRBC. Besides, ionic effect or Matrix effect might affect the desired compounds ionization. Thus, moderate acidification would help these compounds to acquire better ionic intensity from the mass spectrometry. Consequently, after acidifying the culture medium samples with formic acid (5% by volume) before MeOH addition, all the putative drug metabolites were recovered by the mass spectrometry and had better acquisition rate.

Depending on these previous data, the extraction assay was applied to the 5 mM plasmodione-treated pRBC lysates (*Plasmodium falciparum* 3D7 strain, parasitemia 5%, haematocrit 4%, 2.8×10^7 of pRBC). Extraction was performed by MeOH (800 μ L), with and without acidification (Table 5 b.). In addition, owing to the higher complexity of the endogenous metabolite content of pRBC lysate *versus* culture medium, the solid phase extraction (SPE) was considered in the extraction method. Three hydrophobic like SPE columns were selected, two of them were C18-E but with different capacity, one of them was Strata-X, which contained *p*-benzylpiperidin-2-one unit polymer sorbent to establish π - π interactions, hydrophobic interactions and hydrogen-bonding dipole-dipole interaction with the metabolites. The results are shown below (Table 5 b.). Both acidification or no-acidification treatment distinctly influenced compound recovery. For example, the no-acidification condition showed a better extraction yield with the more hydrophilic compounds, such as 6-hydroxy- and 7-hydroxy-plasmodiones derivatives **55a** and **55b**, respectively. On the other hand, the acidification condition displayed a better extraction yield with the more hydrophobic compounds, such as the 3-benzoylmenadione **52** and the epoxy-plasmodione **50**. Unfortunately, the benzoxanthone derivative **60**, which is the most important putative metabolite, was not detected in the spectrum after extraction. Even in the acidification condition, the extraction yield of benzoxanthone derivative **60** was very low. One hypothesis was proposed that benzoxanthone derivative **60** might be bound via a covalent bond to some endogenous metabolites very quickly so that we could not see any free benzoxanthone derivative **60** after extraction.

a)

	39e	60	50	51	52	55a + 55b
MeOH	8.37%	48.10%	46.48%	0.00%	0.00%	58.02%
CHCl ₃ +MeOH+H ₂ O	3.78%	13.78%	15.89%	0.00%	0.00%	4.86%
MeOH + 5% HCOOH	19.99%	68.25%	50.67%	15.19%	43.88%	52.34%

b)

	39e	60	50	51	52	55a + 55b
MeOH	24.88%	0.00%	18.99%	0.00%	39.13%	37.84%
MeOH + 5% HCOOH	26.70%	6.03%	62.29%	0.00%	32.66%	35.88%
MeOH + SPE 1	41.49%	0.00%	51.88%	0.00%	29.30%	58.49%
MeOH + SPE 1 + 5% HCOOH	39.98%	7.28%	68.54%	0.00%	61.33%	27.06%
MeOH + SPE 2	26.95%	0.00%	83.37%	0.00%	37.98%	66.54%
MeOH + SPE 2 + 5% HCOOH	41.34%	0.00%	98.05%	0.00%	43.11%	29.18%
MeOH + SPE 3	0.00%	0.00%	29.58%	0.00%	31.24%	47.01%

Table 5. a) Acquisition rate of each compound extracted from culture medium. b) Acquisition rate of each compound extracted from drug treated pRBC lysates. Acquisition rate = $[C_{obs.}]/[C_{int.}]$, $C_{obs.}$ = the concentration detected after extraction, $C_{int.}$ = initial incubation concentration. SPE 1: C18-E (55 μ m, 70Å, 50 mg/ 1 mL), Phenomenex; SPE 2: C18-E (55 μ m, 70Å, 100 mg/ 3 mL), Phenomenex; SPE 3: Strata-X (33 μ m polymeric Reversed Phase, 60 mg/ 3 mL), Phenomenex.

II.2.2. Preliminary drug metabolism study

The preliminary drug metabolism experiment was performed with four extraction conditions below (Table 6). Based on the previous pRBC extraction results, the drug metabolites might bind to endogenous metabolites, membrane components, prosthetic groups, sugars or proteins, the extraction condition of SPE 2 with 5% HCOOH which had the best acquisition rate was selected. Another SPE (Vac tC18, Waters Sep-Pak, SPE 4), which has similar hydrophobicity to C18-E column and has better properties to extract large molecules was employed in the drug metabolism experiment. In parallel, no SPE conditions were also required for comparison in this experiment in order to recover as much as unknown drug metabolites that might be generated in pRBCs, and gain to more mass data.

To identify the drug metabolism pathway and explore unknown drug metabolites, the fully ¹³C labeled plasmodione **49b** was used to treat the pRBCs. The mass spectrometer can theoretically

recognize ^{13}C -labeled compounds because they show different isotopic distribution of molecular peaks, compared to the natural compounds. However, from complex mixtures, it could not isolate the signal of ^{13}C -labeled compounds easily. Therefore, treatment of pRBCs with 50% fully ^{13}C -labeled lead drug **49b** and 50% unlabeled lead drug **39e** (50%/50% in concentration) can make visible molecular peaks of all drug metabolites with pairs of m/z peaks with a difference of 18 units. This method leads to more convenient detection of fully ^{13}C labeled compounds for the machine.

Based on the previous study, with 5 μM drug concentration, the lead drug plasmodione **39e** can inhibit the growth of synchronized *Plasmodium falciparum* parasites (ring stage) 90% after 5 hours, suggesting that the drug metabolism takes place very quickly. If the drug concentration is higher, the lead drug would kill the parasites more quickly and one can expect less drug metabolites to be formed. Thus, the total drug concentration was limited to 5 μM . However, with the 50%/50% fully ^{13}C -labeled/unlabeled drug (**49b/39e**) treatment of pRBCs the signal seen as a pair of two peaks would decrease in intensity in the mass spectra while keeping the same total concentration in the LC/MS profile. Therefore, more material, meaning higher numbers of pRBCs and higher percentage of parasitemia, was necessary for our experiment.

No SPE without acid ^a		No SPE with 5%HCOOH ^b		SPE 4 without acid ^c		SPE 2 with 5% HCOOH ^d	
+18		+18		+18		+18	
429.3723	447.3443	425.2145	443.3338	425.2145	443.3338	380.2554	398.3265
738.5073	756.5532	876.2474	894.2568	429.3723	447.3443	425.2145	443.3338
1036.6428	1072.7064			556.3948	574.4816	429.3723	447.3443
				613.4282	631.4760	447.2008	465.2534
				615.1802	633.1806	477.3177	495.4885
				617.5224	635.4341	556.3948	574.4816
				783.5778	804.5561	722.2790	758.4194
				1230.3606	1266.3614	1006.7054	1024.6480
				1420.9720	1438.8566	1036.6428	1072.7064

Table 6. The preliminary result of a drug metabolism study by UHPLC coupled to / mass spectrometry MS-MS under four extraction conditions. a) extracted by MeOH alone. b) after acidification with 5% HCOOH, extracted by MeOH. c) extracted by MeOH and then concentrated by SPE 4. d) after acidification with 5% HCOOH, extracted by MeOH and then concentrated by SPE 2. SPE 2: C18-E (55 μm , 70 \AA , 100 mg/ 3 mL), Phenomenex; SPE 4: Vac tC18 (37-55 μm , 125 \AA , 100 mg/ 1 mL), Waters Sep-Pak.

The experiment of drug metabolism was designed depending on the previous viewpoint. The culture medium of synchronized *Plasmodium falciparum* (4% hematocrit, 9% parasitemia, ring stage) was treated with 2.5 μM fully ^{13}C labeled plasmodione **49b** and 2.5 μM unlabeled plasmodione **39e** for 5 hours. Then, the pRBCs lysate (1.2×10^8), which contained 4.2 times more pRBCs approximately than in the previous experiment, was extracted with 8000 μL of MeOH under four conditions described below. To the mass spectrometry study, all the samples have been analyzed by two methods. One of them was keeping the same acquisition method as before, based on a Multiple Reaction Monitoring (MRM) approach to target the synthetic putative drug metabolites. The MRM was set up to record 331.0942 ± 0.02 , 345.0767 ± 0.02 and 347.0907 ± 0.02 , which correspond to the masses of the parent drug and the 6 putative drug metabolites. Another acquisition method was set up to record full MS acquisition and to automatically switch to MS/MS acquisition when mass differences of 18 mass units between two peaks were observed within the same mass spectra.

As the result of the preliminary drug metabolism study through the MRM approach, unfortunately, neither any of the 6 putative drug metabolites, nor the parent plasmodione were recovered from the mass data. By comparison, from the other approach, the mass data gave a huge quantity of information. Because extraction has still taken such many compounds from pRBC lysate, there are many events that can hit the conditions, which were set up to the machine. Thus, it required to compare the MS/MS spectra of different compounds with a difference of 18 mass units to analyze whether the m/z peaks have a relevant mass difference of 18 units or correspond to the molecular mass, which has lost a fragment with 18 unit difference. In addition, it also needed to confirm this mass existence in the spectra of unlabeled plasmodione-treated samples, which should not show the pair of m/z peaks with a difference of 18 m/z units. After analyzing all mass data, several relevant mass data were extracted (Table 6). According to these data, all the masses were higher than the masses of parent drug or putative metabolites, confirming that our lead drug was metabolized or processed in the metabolic pathways of pRBCs before/after coupling to some other endogenous metabolites (sugars, prosthetic groups, terpenic chains, ...). In the meanwhile, the lead drug was not detected from the pRBC lysate, suggesting that our lead drug was completely metabolized very quickly. It will be necessary to decrease the incubation time of the drug in the presence of pRBC to capture the free drug and metabolites before they are completely biotransformed in the metabolic pathways. However, owing to the later acquisition method leading to lower sensitivity of the detection by the LC/MS-MS system, the acquisition time of the mass spectrometry was longer than that in the MRM approach. Furthermore, the reproducibility of the results above was not satisfactory. All these informations were difficult to recover in each of the

repeated experiments. Thus, more duplicate experiments and established statistics are necessary in the following experiments.

II.2.3. Conclusion and perspective

First, 6 out of 7 putative drug metabolites were freshly re-prepared and employed in the drug metabolism investigation. The extraction method had been well established with different conditions and used in experiments to track the drug metabolites. With the help of SPE, better acquisition of the LC/MS-MS system was obtained from pRBC lysate. However, I could not complete all the experiment before my PhD defense. The perspective of this investigation is to repeat the experiments at various time (0 to 1 hour) of drug incubation under the same conditions. Subsequently, the objectives will be aimed at fully characterizing the fragmentation of all drug metabolites-adducts by varying the collision energy of the mass spectrometry and anticipating the structure of the adducts. Finally, depending on the mass and fragmentation of the drug metabolites-adducts, the synthesis of these adducts would allow to confirm the hypothesis and identification the mode of action of plasmodione metabolism.

Chapter III: Synthesis of plasmodione derivatives with increased solubility

III.1. Synthesis of a plasmodione-based oxetane derivative

In medicinal chemistry, it is common to introduce a small structural unit to parent lead drugs in order to prevent metabolic attack at an exposed site, reduce their susceptibility to enzymatic modification and increase bio-availability, such as *gem*-dimethyl unit, carbonyl unit and oxetane (or named trimethylene oxide unit).^{96, 97} However, the substitution of *gem*-dimethyl makes the lipophilicity of the parent drug increasing, and the electrophilic properties of carbonyl unit leads to decreasing the bio-stability, while the oxetane unit becomes a very powerful chemical tool in the drug development.^{96,97,98}

The oxetane is a non-planar 4-membered ring containing inner ether. This moiety is known to be a pronounced H-bond and Lewis acid acceptor, increasing the molecular polarity and aqueous solubility, decreasing the lipophilicity, and even improving metabolic stability and bio-availability of the parent drug.^{99,100,101,102} Furthermore, the oxetane is relatively stable even if suffering strong alkaline conditions.¹⁰³ Based on these attractive properties in drug optimization, the replacement of a

⁹⁶ Wuitschik G., Rogers-Evans M., Müller K., Fischer H., Wagner B., Schuler F., Polonchuk L., Carreira E. M., Oxetanes as promising modules in drug discovery. *Angew. Chem., Int. Ed.* **2006**, *118*, 7900-7903.

⁹⁷ Wuitschik G., Rogers-Evans M., Buckl A., Bernasconi M., Märki M., Godel T., Fischer H., Wagner B., Parrilla I., Schuler F., Schneider J., Alker A., Schweizer W. B., Müller K., Carreira E. M., Spirocyclic oxetanes: synthesis and properties. *Angew. Chem., Int. Ed.* **2008**, *47*, 4512–4515.

⁹⁸ Wuitschik G., Carreira E.M., Wagner B., Fischer H., Parrilla I., Schuler F., Rogers-Evans M., Müller K., Oxetanes in drug discovery: structural and synthetic insights, *J. Med. Chem.*, **2010**, *5*, 3227-3246

⁹⁹ Bennett, G. M., Philip, W. G., The influence of structure on the solubilities of ethers. Part II. Some cyclic ethers. *J. Chem. Soc.* **1928**, 1937–1942.

¹⁰⁰ Berthelot, M., Besseau, F., Laurence, C., The hydrogen-bond basicity pKHB scale of peroxides and ethers. *Eur. J. Org. Chem.* **1998**, *5*, 925–931.

¹⁰¹ Brandon, M., Tamres, M., Searles, S., The iodine complexes of some saturated cyclic ethers. I. The visible region. *J. Am. Chem. Soc.* **1960**, *82*, 2129–2134.

¹⁰² Sisler, H. H., Perkins, P. E., Molecular addition compounds of dinitrogen tetroxide. VI. Binary systems with trimethylene oxide, 2,5-dimethyl tetrahydrofuran and 1,3-dioxolane. *J. Am. Chem. Soc.* **1956**, *78*, 1135–1136.

¹⁰³ Searles, S., The reaction of trimethylene oxide with Grignard reagents and organolithium compounds. *J. Am. Chem. Soc.* **1951**, *73*, 124–125.

hydrogen atom by an oxetane unit provides the chemical approach to introduce a steric bulk while decreasing the lipophilicity, without impacting intrinsic pharmacological properties to a large extent.

III.1.1. Preliminary Results from the team

Several short-term attempts to introduce various oxetane groups in the plasmodione core were undertaken in the team by Max Bielitz (postdoc, ca. 2 months in 2015), and by Enrique Jose Montagut Cañete (Master 2 student, ca. 2 months in 2016). Three strategies of the synthesis of oxetane-plasmodione derivatives are shown in Figure 24.

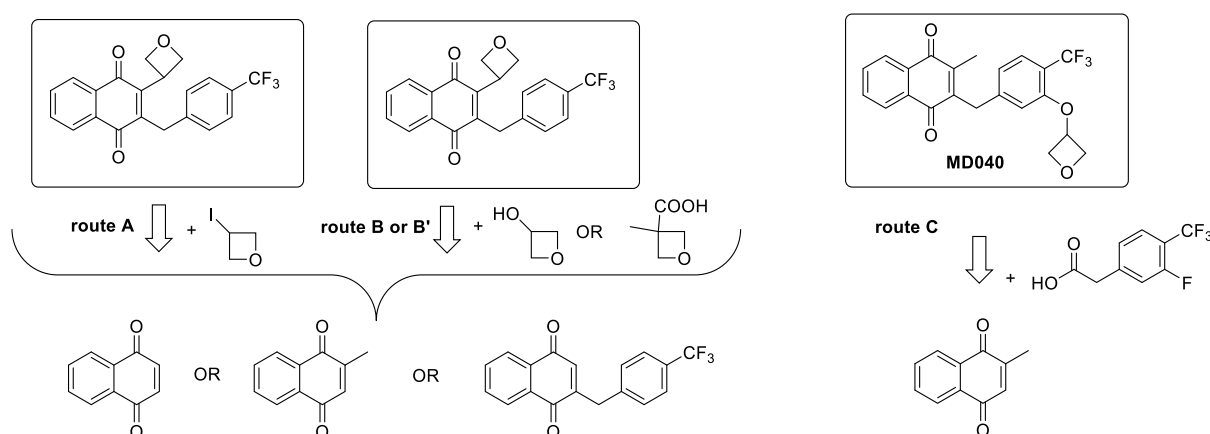


Figure 24. The strategy of introducing oxetane unit to lead drug plasmodione.

This project was first investigated with the synthesis of 3-oxetane menadione/plasmodione derivatives. Introducing the oxetane unit at C-3 position of menadione core might increase the steric hindrance with a minimal space, decrease the susceptibility to oxidative enzymatic modification and prevent the formation of epoxidated metabolites. Furthermore, the oxetane unit would improve the hydrophilicity of the parent drug.

At the beginning, the synthesis of 3-oxetane naphthoquinone was performed via route A. (Scheme 34). Following with this strategy, the starting material menadione **14c** was reacted with 3-iodooxetane under Minisci conditions.^{104,105,106} However, this strategy was not satisfactory. According to TLC

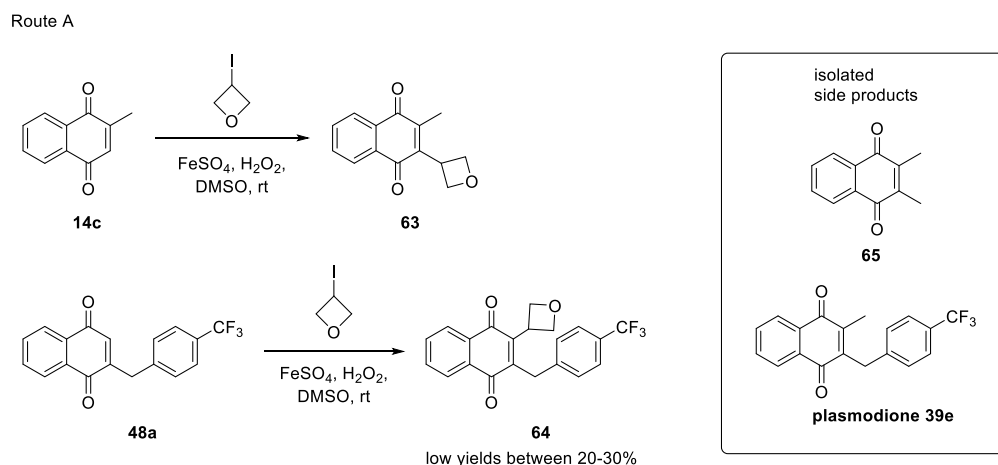
¹⁰⁴ Coppa F., Fontana F., Minisci F., Nogueira Barbosa M.C., Vismara E., Homolytic alkylation of naphthoquinone and methyl-naphthoquinone. Enthalpic steric and polar effects, *Tetrahedron*, **1991**, 47, 7343-7352

¹⁰⁵ Duncton M.A.J., Minisci reactions: Versatile CH-functionalizations for medicinal chemists, *Med. Chem. Commun.*, **2011**, 2, 1135-1161.

¹⁰⁶ Duncton M.A.J., Estiarte M.A., Johnson R.J., Cox M., O'Mahony D.J.R., Edwards W.T., Kelly M.G., Preparation of Heteroaryloxetanes and Heteroarylazetidines by Use of a Minisci Reaction, *J. Org. Chem.*, **2009**, 74, 6354-6357.

plate, we found that the conversion of the reaction was not completed even when more FeSO₄/H₂O₂ reagent was added. With the help of NMR spectra, it was shown that the starting material converted to the side-product dimethyl-naphthoquinone **65** quickly, which had the same R_f value as menadione by TLC. This undesired methylation reaction had been reported by Minisci *et al.*¹⁰⁴ A methyl radical was generated from the solvent dimethylsulfoxide (DMSO) under Minisci conditions, leading to the undesired compound **65** formation. Nevertheless, the desired 3-oxetane menadione **63** was formed but revealed to be highly unstable in the solution, it decomposed so quickly even only a short time after NMR analysis.

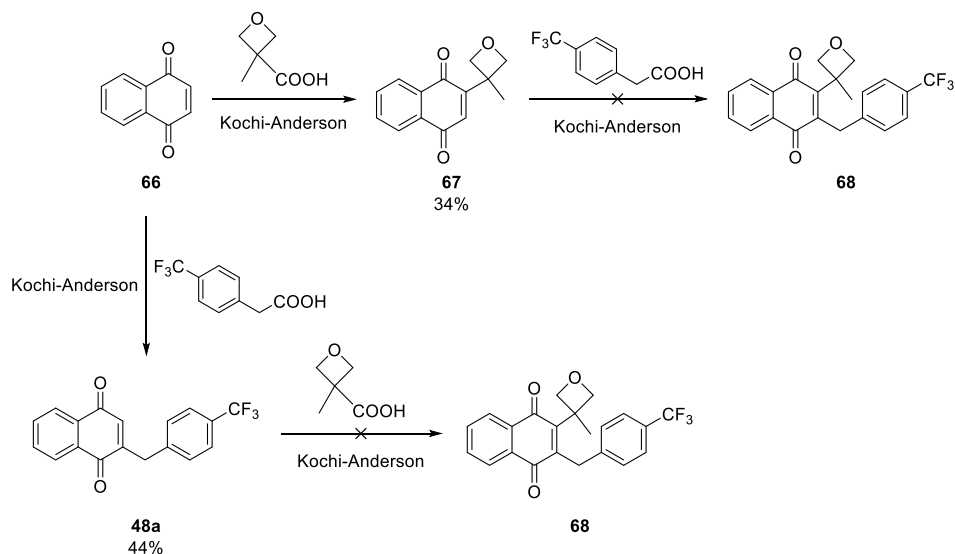
In parallel, the synthesis of the 3-oxetane-based plasmodione analogue **64** from desmethylplasmodione **48a** was also unfavorable. The 3-oxetane derivative **64** was not only obtained in low yield between 20-30%, but also accompanied by a side-product or a rotamer. Even if the crude product was purified by several columns and a preparative TLC, these purification steps did not help to obtain the pure product. It might be that the desired product decomposed into many side-products during the purification. Similarly, as described above, the undesired methylation reaction took also place in this reaction, producing the known plasmodione **39e**.



Scheme 34. Synthetic pathway via Minisci reaction used to obtain oxetane menadione/plasmodione derivatives.

Secondarily, we also attempted to synthesize oxetane-based plasmodione analogues via route B, by using the Kochi-Anderson reaction, which has been previously reported in the introduction part of my thesis (Scheme 35). This radical reaction allowed us to functionalize the 1,4-naphthoquinone **66** at positions C-2 and C-3. In the presence of AgNO₃ and (NH₄)₂S₂O₈, via a radical decarboxylation of the corresponding carboxylic acid, this reaction can provide the desired alkylated naphthoquinone product.

Route B



Scheme 35. Synthetic pathways via two Kochi-Anderson reactions used to obtain the bis-substituted naphthoquinones.

Two approaches in route B, through a different order of two consecutive Kochi-Anderson reactions, were followed to introduce the methyloxetane moiety at C-2 to access the desired oxetane-based plasmodione analogue **68**. First, starting from the unsubstituted 1,4-naphthoquinone **66**, the yield of the decarboxylation reaction with 3-methyloxetane-3-carboxylic acid, decreased to 34%. This drop might be explained by the generation of a tertiary radical, which had higher steric hindrance rendering more difficult to approach the naphthoquinone core and resulting in less reactivity. Noteworthy is to mention that in this reaction the starting material was never totally consumed and it has been always obtained several side products in small quantity, which were difficult to isolate. In the next step of this approach, the Kochi-Anderson reaction, with the 4-(trifluoromethyl) phenylacetic acid and the 3-methyloxetane-3-naphthoquinone **67** as partners, nevertheless, did not produce the desired oxetane-based plasmodione analogue **68**.

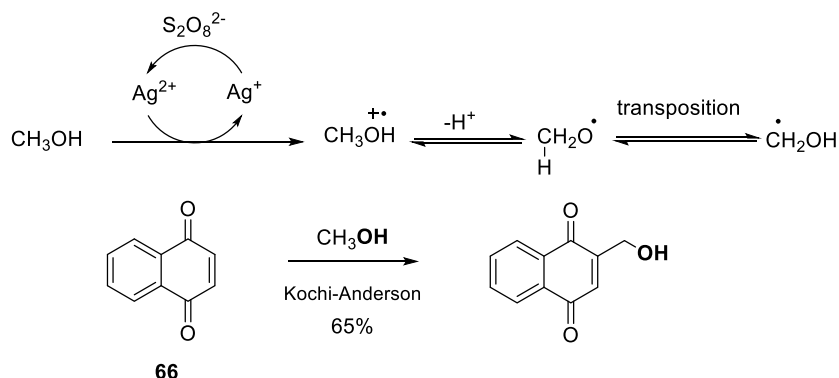
The second approach of route B was also evaluated by applying inverse order of Kochi-Anderson reactions. The desmethyl-plasmodione **48a** was synthesized through the optimized “tetralone express route” from tetralone **42a**, but, when there are no substituents on the menadione core, it turned out to be more straightforward and effective (44% yield) to prepare it by a Kochi-Anderson reaction from 1,4-naphthoquinone **66** and the respective phenylacetic acid. However, in the next step, the Kochi-Anderson reaction did not combine the oxetane unit and instead, afforded a large array of minor side-products, which were difficult to be isolated.

In order to explore the conditions of the synthesis of various 3-oxetane-based plasmodione derivatives, different coupling partners of the Kochi-Anderson reaction were used and investigated here. Instead of carboxylic acids, corresponding alcohols (Table 7) were employed under these conditions with the 1,4-naphthoquinone **66**.¹⁰⁷ As the classical Kochi-Anderson reaction, the key intermediate hydroxymethyl radical was generated from MeOH in the presence of AgNO₃ and (NH₄)₂S₂O₈, as mentioned in chapter II (Scheme 36).⁹² First, MeOH was oxidized by Ag²⁺, which was reoxidized from Ag¹⁺ by (NH₄)₂S₂O₈, to produce MeOH radical cation. After deprotonation, the radical of the resulting intermediate, which is theoretically more stable (the lone pair electrons of oxygen can stabilize the π -orbital radical of carbon), is easy to transfer from oxygen to carbon and react with the 1,4-naphthoquinone **66**.

As negative reference, the EtOH was employed as coupling partner, and as expected, the reaction did not lead to the desired product. Instead, this reaction produced the ethyloxyl product **70** because the central radical intermediate is less reactive than the terminal radical, the resulting radical rearrangement between oxygen and carbon was not revealed. Further, two oxetane-based alcohols were used in this investigation. In the first case, the reaction with oxetane-3-ol did not produce the expected oxetanyl-naphthoquinone, any desired product, the radical of this oxetane derivative might be too unstable. In the second case, when the (3-methyloxetan-3-yl)methanol was used as coupling partner, an unpredicted oxetane-based naphthoquinone **67** was generated because of the deformylation of the starting alcohol. The radical was transferred to the tert-butyl position, which was more stable and reacted to the naphthoquinone core. However, the yield of this reaction was not satisfactory (16%) precluding any application in the synthesis of oxetane-based plasmodione analogues without future improvement of the synthetic methodologies.

¹⁰⁷ Elena Cesar Rodo, PhD thesis, Strasbourg University, October 5, 2015.

Route B'



Scheme 36. Mechanism of the hydroxymethyl radical formation from methanol with AgNO_3 and $(\text{NH}_4)_2\text{S}_2\text{O}_8$.⁹²

Reactant	Product	Yield
MeOH*		65%*
EtOH		39%
	---	---
		16%

*Elena Cesar Rodo, unpublished results, PhD thesis.

Table 7. Different alcohols used under Kochi-Anderson condition in the reaction with the 1,4-naphthoquinone **66**.

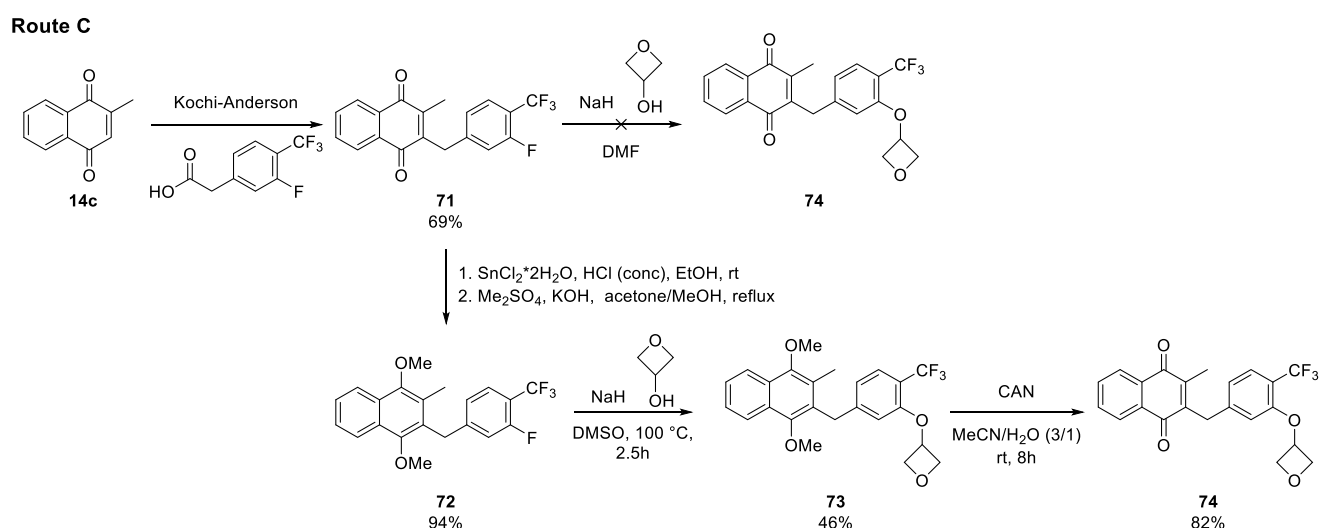
Finally, the third approach, via route C, has been developed to study the introduction of an oxetane unit at the phenyl ring of plasmodione (Scheme 37).¹⁰⁸ In order to inhibit the metabolism of unproductive plasmodione *in vivo* which would lead to plasmodione elimination, the oxetane-

¹⁰⁸ A preliminary study was developed by Max Bielitz but the final compound **15** was produced in 30 mg scale.

plasmidione derivative **74** containing an oxetan-3-*O*-ether unit at *ortho* position of the CF₃ unit was designed.

This synthetic pathway involves [3-fluoro-4-(trifluoromethyl)phenyl]acetic acid as substrate of the Kochi-Anderson reaction. Then, an aromatic nucleophilic substitution (S_NAr) reaction was envisioned to substitute the fluorine atom by the hydroxylate of the oxetan-3-ol.

The first attempt of this strategy was not successful, because the methyl of the menadione core can be easily deprotonated in basic conditions, opening a reactive Michael acceptor site in this plasmidione derivative **71**. Hence, working with menadione chemistry under basic conditions makes easy decomposition of these reactive menadione derivatives. Therefore, from the beginning, the protection of menadione core had been considered to design the synthesis of oxetane-based plasmidione analogues.



Scheme 37. Synthetic route of 3'-(oxetan-3-yloxy)plasmidione **74**.

Starting from menadione **14c** and the corresponding phenylacetic acid, the benzylmenadione **71** was prepared under Kochi-Anderson conditions as previously reported with 69% yield. Then, plasmidione derivative **71** was reduced to the dihydronaphthoquinone in the presence of tin(II)chloride and concentrated HCl in ethanol. After neutralization by water, the resulting dihydronaphthoquinone intermediate was redissolved in acetone under argon and allowed to react with dimethylsulfate and KOH.¹⁰⁹ The 1,4-dimethoxynaphthalene **72** was isolated in 94% yield. In the next

¹⁰⁹ Bauer H., Fritz-Wolf K., Winzer A., Kühner S., Little S., Yardley V., Vezin H., Palfey B., Schirmer R.H., Davioud-Charvet E., A fluoro analogue of the menadione derivative 6-[2'-(3'-methyl)-1',4'-naphthoquinolyl]hexanoic acid is a suicide substrate of glutathione reductase. Crystal structure of the alkylated human enzyme, *J. Am. Chem. Soc.*, **2006**, *128*, 10784-10794

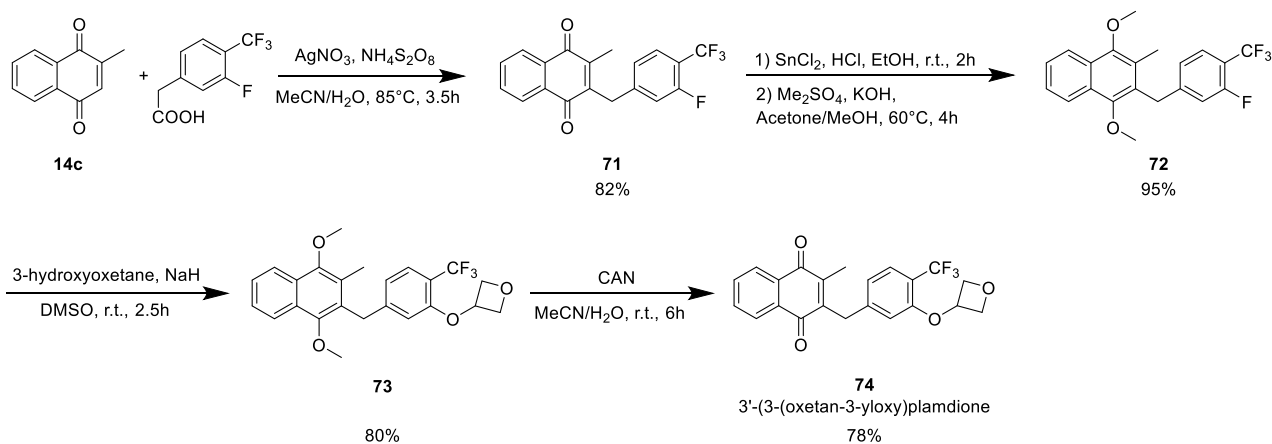
step, oxetanol was deprotonated by NaH in DMSO and the S_NAr reaction between 1,4-dimethoxynaphthalene **72** and oxetanolate provided the oxetanyl-based 1,4-dimethoxynaphthalene **73** with 46% yield.¹¹⁰ Finally, the resulting intermediate **73** was deprotected/oxidized by using CAN, giving the final compound 3'-(oxetane-3-yloxy)plasmodione **74** with 82% yield.

One part of my PhD work has been to improve the synthesis of this 3'-(oxetane-3-yloxy) plasmodione **74**, in particular by finding better conditions of the S_NAr to allow the production of the compound in bulk, for a detailed chemical pharmacokinetic and biological characterization.

III.1.2. Personal results

The objective of this chapter is to identify the synthetic methodology to prepare the 3'-(oxetane-3-yloxy)plasmodione **74** in a gramme scale by a high yielding 4-steps route (Scheme 38). First, the Kochi-Anderson reaction using two starting materials, menadione **14c** and 2-(3-fluoro-4-(trifluoromethyl)phenyl)acetic acid, afforded the corresponding benzylmenadione **71** in 82% yield. Subsequently, the reduction and methylation protection were successively performed with an overall yield of 95% by using tin chloride/HCl and dimethylsulfate/KOH according known standard protocols. Then, the aromatic nucleophilic substitution reaction was proceeded in DMSO by using 3-hydroxyoxetane and NaH, generated by sodium hydride. With studying the reaction in detail, I observed that this reaction was sensitive to the temperature, even by using fresh reagents. When the reaction was performed at 80 °C, the yield of the reaction was 9%. When temperature of the reaction reduced to 60°C, the reaction isolated yield increased to 55%. At the end of this experiment, the reaction was stirred at room temperature, the isolated yield increased to 80%. Finally, the resulting intermediate was oxidized by ceric ammonium nitrate to give the 3'-(oxetane-3-yloxy)plasmodione **74**. The overall yield of the 4 steps sequence is 48.6% *versus* 24.5 %.

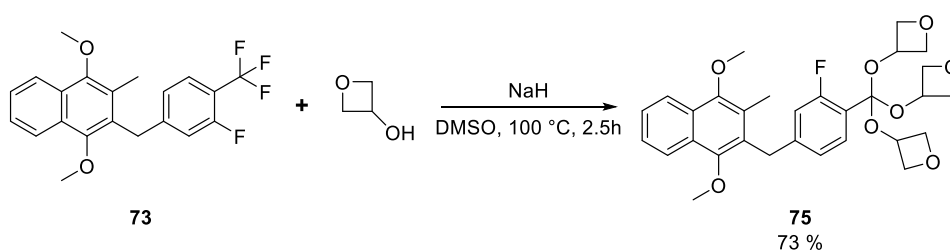
¹¹⁰ Bizier N.P., Wackerly J.W., Braunstein E.D., Zhang M.F., Nodder S.T., Carlin S.M., Katz J.L., An Alternative Role for Acetylenes: Activation of Fluorobenzenes toward Nucleophilic Aromatic Substitution, *J. Org. Chem.*, **2013**, 78, 5987–5998



Scheme 38. Optimized synthetic route of 3'-(oxetan-3-yloxy)plasmidione **74**.

During the investigation of the aromatic nucleophilic substitution reaction to produce the 3'-(oxetane-3-yloxy)-[4'-trifluoromethyl-benzyl]1,4-dimethoxynaphthalene derivative **73**, an unexpected and interesting compound was produced while I was studying the influence of the temperature. When the reaction proceeded at 100 °C for 2.5 hours, the original nucleophilic aromatic substitution was switched to nucleophilic substitution (Scheme 39). This reaction did not produce the desired 3'-(oxetane-3-yloxy)-[4'-trifluoromethyl-benzyl]derivative **73** but, a 3'-fluoro-[4'-(tri-oxetane-3-yloxy)-methyl-benzyl]derivative **75**. Based on the ^1H NMR spectrum, the integration of the protons at the oxetane unit confirmed that the molecule has 3 oxetane units (Figure 26, 3 protons at red point position and 12 protons at blue point position). The ^{19}F NMR spectrum also showed that the signal of CF_3 (around -62 ppm) has totally disappeared and the signal of F at the phenyl ring still remained (around -112 ppm) (Figure 25). In addition, the HRMS spectrum revealed the presumable signal (540.2105 m/z). According to these ^1H NMR, ^{19}F NMR and HRMS spectra, the structure of 3'-fluoro-[4'-(tri-oxetane-3-yloxy)-methyl-benzyl] derivative **75** was successfully characterized. Nevertheless, the mechanism of this reaction is difficult to understand. One can explain the possible mechanism of this reaction by suggesting that the nucleophilic aromatic substitution reaction proceeded when the temperature was rather low; the pre-formed hydroxylate anion attacks the C-F bond at the phenyl ring instead of CF_3 at low temperature. In other hand, the nucleophilic substitution at CF_3 unit having steric hindrance needs high energy to pass the access barrier. At high temperature allowing to cross the energy barrier, the nucleophilic attack would take place at the CF_3 unit to form the more thermodynamic stable product. This theory might explain the regioselectivity of nucleophilic substitution.

To conclude chapter III, we have investigated 3 strategies to synthesize oxetane-based plasmodione derivatives. The first strategy employed Minisci conditions. The second strategy was developed through 3 different approaches under Kochi-Anderson conditions. And the third strategy was built on a 4 high yielding steps synthetic route to produce 3'-(oxetane-3-yloxy)plasmodione **74**. After optimization of this synthetic route, we have obtained 1 g of the desired 3'-(oxetane-3-yloxy)plasmodione **74** for a detailed chemical pharmacokinetic and biological characterization. Furthermore, during the optimization, a new a 3'-fluoro-[4'-(tri-oxetane-3-yloxy)-methyl-benzyl] derivative **75** was discovered. More work will be necessary to investigate the scope of this reaction or if the formation of compound **75** was substrate-specific. The perspectives of this project will focus on the investigation of synthetic methodologies for the synthesis of new oxetane derivatives of plasmodione for drug development. In addition, a specific attention will be concentrated on the 3'-fluoro-[4'-(tri-oxetane-3-yloxy)-benzyl]-1,4-dimethoxy-3-methylnaphthalene **75** after a new batch has been re-synthesized - for characterizing its antiparasitic properties.



Scheme 39. Synthesis of 3'-fluoro-[4'-(tri-oxetane-3-yloxy)-benzyl]-1,4-dimethoxy-3-methylnaphthalene **75**.

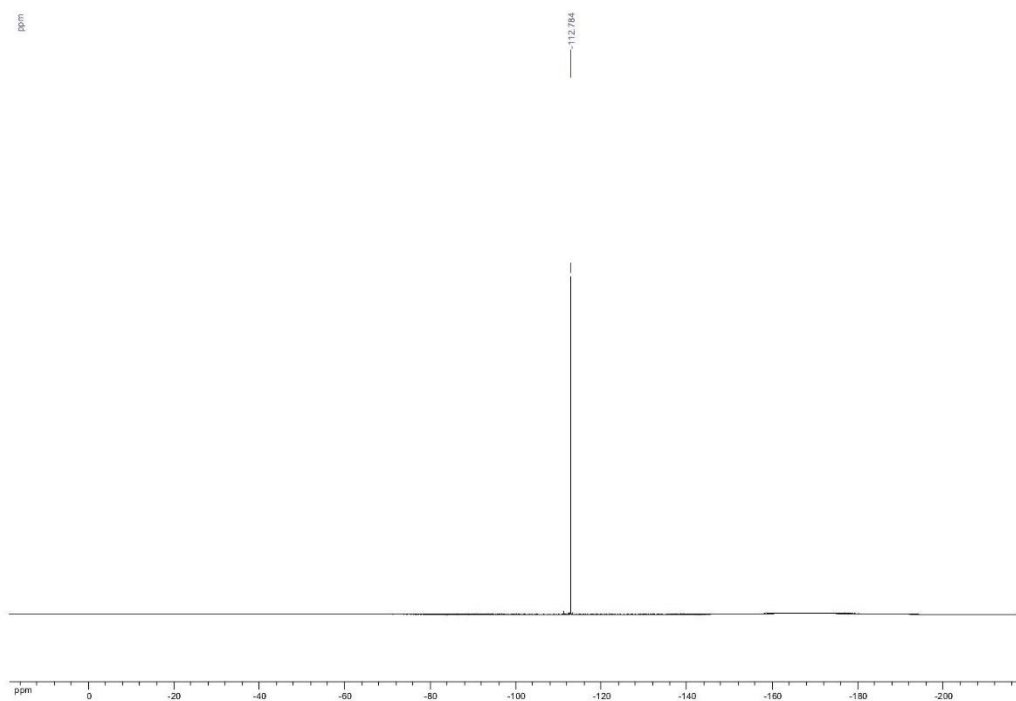


Figure 25. ^{19}F NMR (376 MHz, CDCl_3) of 3'-fluoro-[4'-(tri-oxetane-3-yloxy)-benzyl]-1,4-dimethoxy-3-methylnaphthalene **75**.

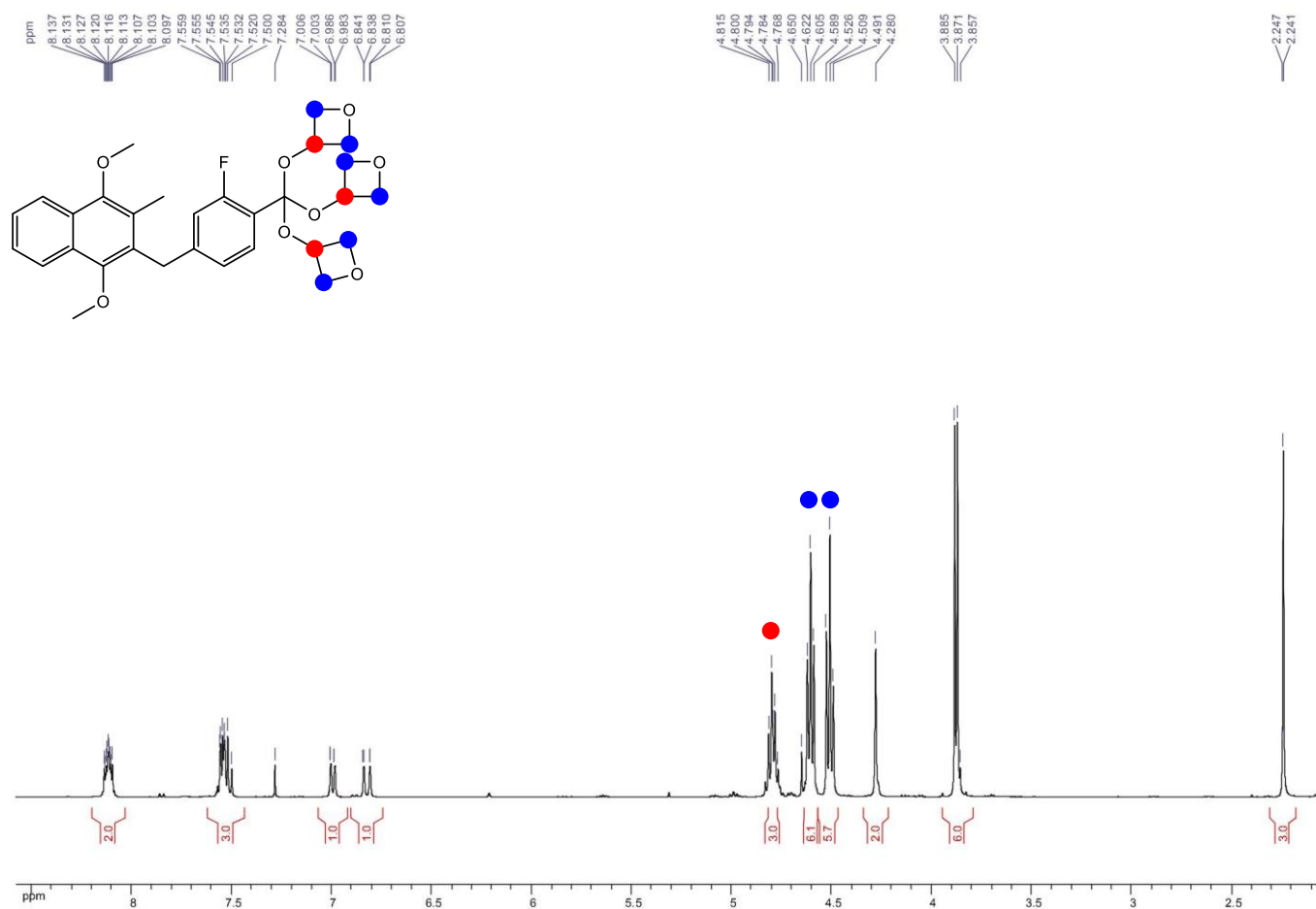
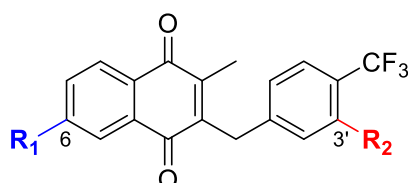


Figure 26. ¹H NMR (400 MHz, CDCl₃) of 3'-fluoro-[4'-(tri-oxetane-3-yloxy)-benzyl]-1,4-dimethoxy-3-methylnaphthalene **75**. The red points represent the protons in α - *para* position to the oxygen of the oxetane ring. The blue points represent the protons in β - position to the oxygen of the oxetane ring.

III.2. Solubilities and Pharmacokinetic properties

Two analogues of plasmodione were introduced in the biological study on the antimalarial activity profile:

- the 6-fluoro-plasmodione **39d** (MD30)
- the 3'-(oxetan-3-yloxy)plasmodione **74** (MD40).



R₁=H, R₂=H, plasmodione **39e** (MD1c)

R₁=F, R₂=H, 6-fluoroplasmodione **39d** (MD30)

R₁=H, R₂=oxetan-3-yloxy, 3'-(oxetan-3-yloxy)plasmodione **74** (MD40)

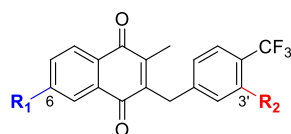
Figure 27. Structure of plasmodione derivatives MD1c **39e**, MD30 **39d** and MD40 **74**.

First, plasmodione **39e** and MD30 **39d** were compared in *P. falciparum* strain NF54 assays using either 50 % human serum or 0.5% AlbuMAX® (Lipid - Rich Bovine Serum Albumin) in culture media (Table 8). In the presence of human serum *versus* AlbuMAX, a significant increase of the IC₅₀ value of plasmodione **39e** (270 nM versus 57 nM) was observed, indicating an important binding of plasmodione to the serum proteins. In contrast, with AlbuMAX, the IC₅₀ values of MD30 **39d** remained similar in both media tested, suggesting that MD30 **39d** did not strongly bind to serum proteins. The serum shift effect, at least 5 times lower for MD30 **39d** than for plasmodione, might attest for improved pharmacokinetic properties of MD30 **39d** compared to plasmodione **39e**. Finally, in preliminary experiments *in vivo*, MD30 **39d** was observed to be more effective than plasmodione **39e** with 48 % efficacy in terms of parasite reduction compared to untreated controls, following *per os* administration at 50 mg/kg for 4 days (data not shown).

Compounds	<i>P. falciparum</i> strain NF54 IC ₅₀ (nM)		Serum shift effect
	0.5% AlbuMAX	50% human serum	
P_TM29 (plasmodione 39e)	57	270	4.7
DAL54 (MD30 39d)	93	80	0.9

Table 8. Serum shift effect deduced from the IC₅₀ values of 3-benzylmenadione derivatives determined in the presence of human serum or 0.5% AlbuMAX® in *P. falciparum* strain NF54 cultures *in vitro* (data from Basel, Dr. Matthias Rottmann, Swiss Tropical and Public Health Institute).

Introduction of a fluorine atom at C-6 did not increase the solubility of the final plasmodione analogue **39d** in the aqueous buffer, even containing 10% DMSO (Table 9). Under the same conditions, the 3'-(oxetan-3-yloxy)plasmodione **74** revealed to be calculated 8-fold more soluble in PBS – 10% DMSO than plasmodione.



R₁=H, R₂=H, plasmodione **39e**
R₁=F, R₂=H, 6-fluoroplasmodione **39d**
R₁=H, R₂=oxetan-3-yloxy, 3'-(oxetan-3-yloxy)plasmodione **74**

Compound	Solubility (μM) ^a
P_TM 29 (plasmodione, MD1c, 39e)	0.44 ± 0.05
DAL54 (MD30, 39d)	0.06 ± 0.01
LF148 (MD40, 74)	3.7 ± 0.7

Table 9. Solubilities of plasmodione and of its derivatives MD30 & MD40 (**74**).^aConditions : in PBS – 10% DMSO (measured by TechMed^{ILL}, Strasbourg)

Finally, the bioavailability of plasmodione **39e** was evaluated in mice and found to be 57% (Table 10)

Clairance	Drug half-life	Distribution volume	Area under the curve upon intraveinuous administration ASC (min.ng/mL)	Area under the curve upon oral administration ASC (min.ng/mL)
Cl (mL/min/kg)	t _{1/2} (min)	V _d (mL/kg)	IV ASC (min.ng/mL)	PO ASC (min.ng/mL)
91	5.7	1993	10947	6249
bioavailibility MD1c (P_TM29)		ASC (PO) / ASC (IV) = 57%		

Table 10. Pharmacokinetic parameters of plasmodione **39e** in mice.

III.3. Antimalarial activities of 3-benzylmenadiones

Plasmodione **39e** (MD1c) and methylene blue (MB) displayed similar IC₅₀ values against *P. berghei ex vivo* (Figure 28). However, *in vivo* in *P. berghei*-infected mice, plasmodione **39e** is less effective than MB to kill parasites in cultures. This loss of efficacy in reducing parasitemia from *ex vivo* cell cultures to an *in vivo* mouse model might be due to a weak bioavailability of plasmodione **39e**. Therefore, an optimization of the pharmacokinetic properties of plasmodione is essential to increase its bioavailability in order to cure animals.

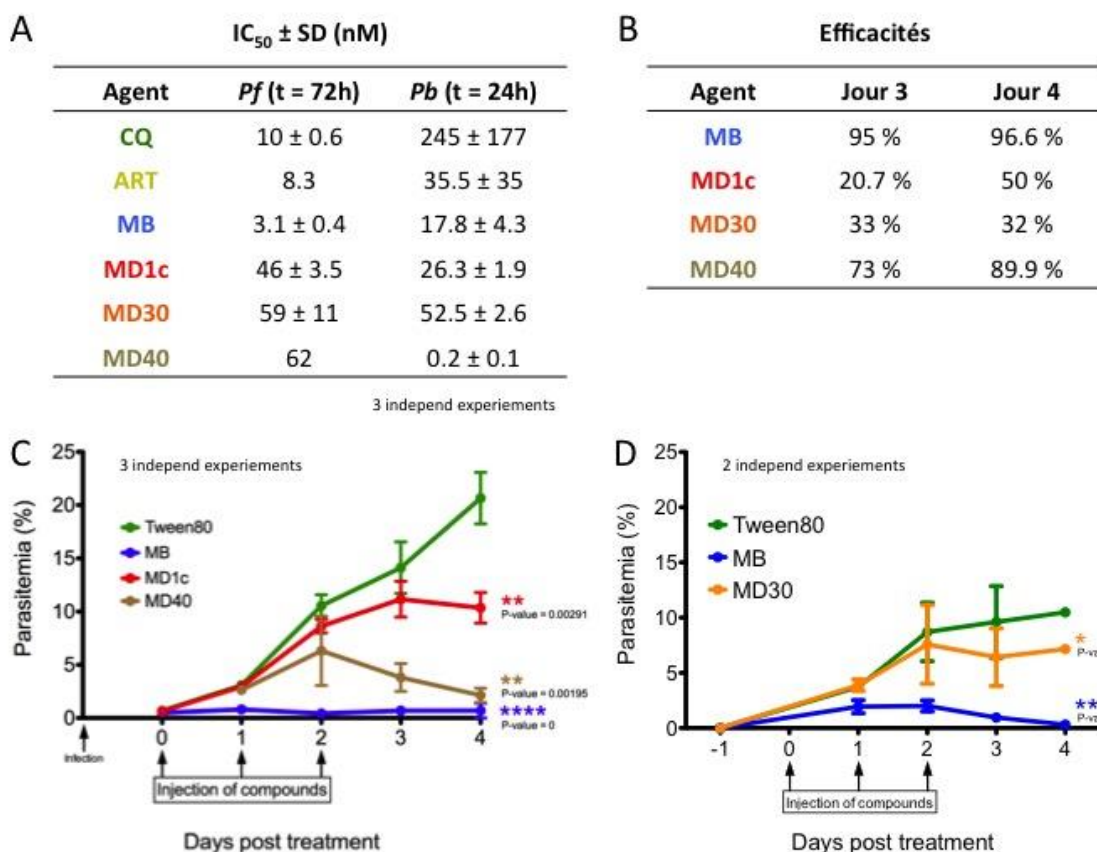
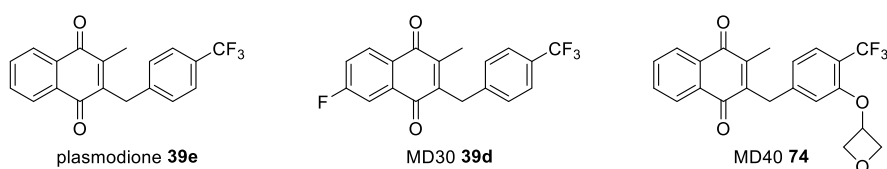


Figure 28. *In vitro* and *in vivo* antimalarial activities of plasmodione **39e** (MD1c) and of its 6-fluoro-**39d** (MD30) and 3'-(oxetan-3-yloxy)plasmodione **74** (MD40) against *P. falciparum* and *P. berghei* parasites (Figure from A.-A. Goetz PhD dissertation, confidential). All antimalarial activities were measured in Dr. Stéphanie Blandin, Anopheles Group, U963 INSERM / UPR9022 CNRS, Institut de Biologie Moléculaire et Cellulaire (IBMC), Strasbourg University.

Panels: (A) The IC₅₀ values of benzylmenadiones against the asexual stages of *P. berghei ex vivo* were compared to the values obtained with *P. falciparum* in cultures, in parallel to other antimalarial drugs used as references (MB, ART and CQ). The IC₅₀ values against *P. berghei* parasites determined in *ex vivo* cultures were measured by PhD student, Alice-Anne Goetz (A.-A. Goetz PhD dissertation, 2016, confidential). The IC₅₀ values in *P. falciparum* assays were measured by Dr. Katharina Ehrhardt (Ehrhardt *et al.*, 2016). (B) The *in vivo* efficacy of benzylmenadiones was evaluated by Dr. Alice-Anne Goetz. (C) et (D) Mice were treated *in vivo* by intraperitoneal administration of daily plasmodione **39e** (30 mg/kg), MD30 **39d** (30 mg/kg), MD40 **74** (30 mg/kg), or methylene blue (15 mg/kg) for 3

consecutive days, 24h post-infection. The parasitemia in mice was measured every day before drug treatment. Tween80 was used as vehicle for compounds (70% tween 80, 30% EtOH, 1/10 in H₂O) and as negative control, while methylene blue was used as positive control. Abbreviations: CQ: chloroquine; ART: artemisinin; MB: methylene blue; MD1c: plasmodione **39e**; MD30: 6-fluoro-benzylmenadione **39d**; MD40: 3'-(oxetan-3-yloxy)plasmodione **74**.

The 3-benzylmenadiones are known to be effective to kill the asexual *P. falciparum* stages in cultures after 72h incubation in the 50 nM nanomolaire range *in vitro*.⁷⁰ In order to determine their activity against *P. berghei* ANKA-infected mice, it was essential first, to test them against the luciferase-expressing *P. berghei* PbGFP-luc strain *in vitro* in the drug assay with an incubation time of 24h. Some antimalarial drugs known as references in clinics were used as controls: chloroquine (CQ), artemisinin (ART), methylene blue (MB). The IC₅₀ values measured are shown in Figure 28 Panel A. By comparing the IC₅₀ values of plasmodione (*P. falciparum*: IC₅₀ = 46 nM *versus* *P. berghei*: 26 nM), we could confirm that the early lead drug is still active against *P. berghei*; it is also the case for ART, MB, and CQ. Both 6-fluoro- (MD30 **39d**) and 3'-(oxetan-3-yloxy)- plasmodione (MD40 **74**) behaved as plasmodione **39e** in the *P. falciparum* assays. In the *P. berghei* assays the 6-fluoro analogue MD30 **39d** was about ca. 2-fold less active than plasmodione **39e** but, the 3'-(oxetan-3-yloxy)- plasmodione **74** (MD40) surprisingly showed a 200-fold higher activity than plasmodione one. Before we can conclude about these *P. berghei* *versus* *P. falciparum* assays it will be important to check if stage populations of *P. berghei* and *P. falciparum* in these experiments were the same (*i.e.* rings *versus* trophozoites). Repeats of these last experiments will need to be performed with synchronized parasitic stages at the same point in the cycle.

Compared to plasmodione both compounds (MD30 **39d** and MD40 **74**) decreased the parasitemia *in vivo*, with significant efficacy differences appearing from Day 3: 33 % (MD30 **39d**) *versus* 73 % (MD40 **74**), and then still increasing for the optimized MD40 **74** from Day 4: 32 % (MD30 **39d**) *versus* 89.9 % (MD40 **74**). The very last experiments *in vivo* used the batch LF148 for repeats of experiments using MD40 **74**. The introduction of fluorine at C-6 of plasmodione did not optimize the solubility, or the efficacy of the compound *in vivo* while the introduction of an oxetane increased both the solubility of the compound by a factor 8.4 and the efficacy *in vivo* in mice. Furthermore, the requirement of other models will be essential to obtain relevant data and cross-check both the *Plasmodium* species and host models in the future program.

Chapter IV: exploration of more soluble compounds by introducing of *N*-alkyl-aryl amines groups

The bioavailability and activity/solubility of the early lead plasmodione is poor, yielding risks for further drug development. Hence, previous investigations on pharmaco-modulation of plasmodione were developed to answer whether the 4-trifluoromethyl group could be replaced or whether the substituent could be moved on the aryl ring without sacrificing the antimalarial activity.

IV.1. Preliminary Results from the team

It is quite known from the data of the literature on the activity of numerous 4- or 8-aminoquinolines or phenothiazines that numerous antimalarial drugs used in clinical medicine possess chemical structures characterized by *N*-dialkyl substituents, which contribute to their bioavailability and good solubility in aqueous media. Some examples are given in Figure 29.

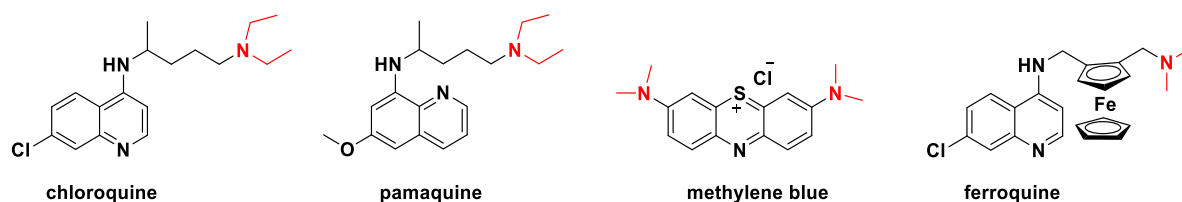


Figure 29. The most important clinically used antimalarial drugs presenting a terminal $-N(\text{Me})_2$ or $-N(\text{Et})_2$ group in their side chains.

The broadly used chloroquine (CQ) is a diprotic weak base ($\text{pK}_a = 8.4$ and 10.6), which accumulates in the food vacuole and binds to Fe^{III} -heme leading to a stable 1:1 π - π complex ($K_D \sim 2$ - $15 \mu\text{M}$ at $\text{pH } 7.5$), which prevents the biocrystallisation of the toxic heme in an insoluble pigment called hemozoin.¹¹¹ In contrast, upon reduction and different protonation states, methylene blue (MB) has

¹¹¹ Johann L., Lanfranchi D.A., Davioud-Charvet E., Elhabiri M. A, physico-biochemical study on potential redox-cyclers as antimalarial and anti-schistosomal drugs., *Curr. Pharm. Des.*, **2012**, *18*, 3539-3566.

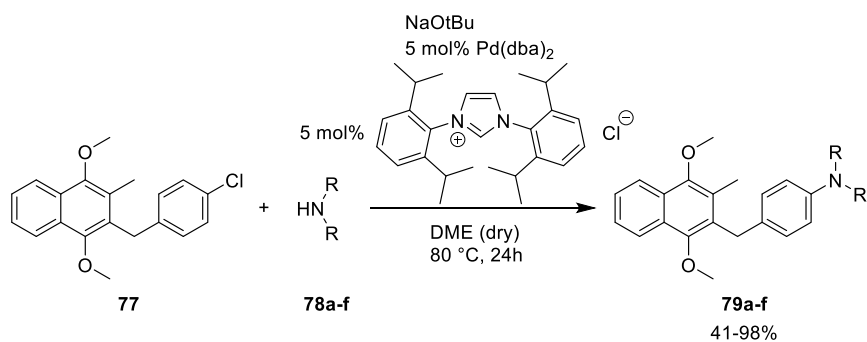
the ability to change its structure and display different lipophilicities.¹¹² Due to its very low pK_a ($pK_a = 0$), MB does not accumulate in acidic vesicles but may shuttle in and out the cell compartments depending on its redox state. The final result of MB-catalyzed redox-cycling is an arrest of parasite development.³⁷

As a part of our medicinal chemistry program on 1,4-naphthoquinone scaffolds, the structure-activity relationship (SAR) study was guided by the evaluation of the antimalarial activity of several plasmodione derivatives in which the 4'-CF₃ group was replaced either by an amino group or by a *N,N*-dialkyl amino group. *N,N*-dimethyl- or *N,N*-diethyl-aryl analogues of plasmodione were synthesized via a reductive amination reaction and their antimalarial potential was investigated in comparison to plasmodione to learn the structural requirements for antimalarial activity of optimized plasmodione derivatives.¹¹³

In continuation of the SAR studies on the plasmodione series, the substitution at the benzylic chain of plasmodione was explored in the present study, in particular by using the Pd-catalyzed reaction, named the Buchwald-Hartwig reaction, to prepare *N,N*-dialkylaryl homologues, because this versatile reaction allows to introduce a large structural diversity in medicinal chemistry. Among the prepared derivatives, a piperazine-based benzylmenadione derivative **80c** was selected as a potent antimalarial compound. However, the availability of the final compound isolated in a small scale (<100 mg-to check) was limited by the last step of the synthetic route, as we will discuss it later.

¹¹² Blank O., Davioud-Charvet E., Elhabiri M., Interactions of the antimalarial drug methylene blue with methemoglobin and heme targets in *Plasmodium falciparum*: a physico-biochemical study. *Antioxid. Redox Signal.* **2012**, *17*, 544–554.

¹¹³ Urgan K., Jida M., Ehrhardt K., Müller T., Lanzer M., Maes L., Elhabiri M., Davioud-Charvet E., Pharmacomodulation of the antimalarial plasmodione: synthesis of biaryl- and *N*-arylalkylamine analogues, antimalarial activities and physicochemical properties. *Molecules.* **2017**, *22*, E161.



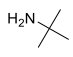
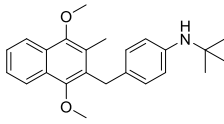
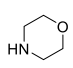
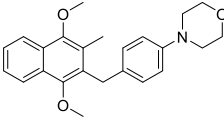
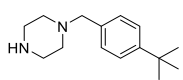
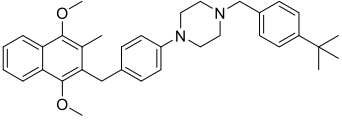
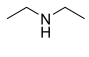
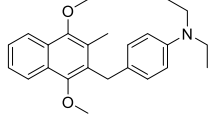
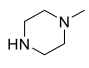
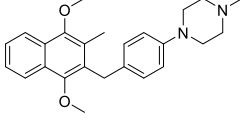
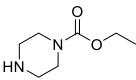
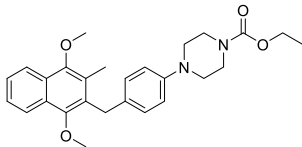
Entry	Amine	Product	Yield
1	 78a	 79a	82 %
2	 78b	 79b	98 %
3	 78c	 79c	95 %
4	 78d	 79d	41 %
5	 78e	 79e	59 %
6	 78f	 79f	60 %

Table 11. Scope of the Buchwald-Hartwig reaction applied to the synthesis of *N*-alkylarylamines in the benzylmenadone series.¹¹⁴

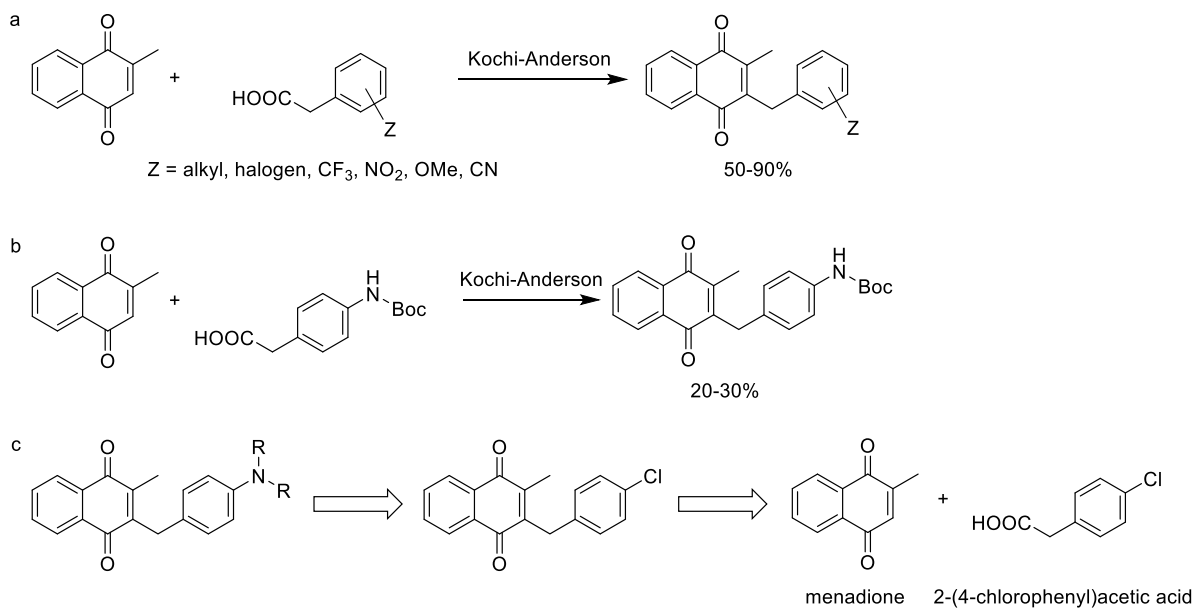
¹¹⁴ Müller T. PhD thesis dissertation, 2008, Heidelberg university.

As previously discussed in the introduction part, the Kochi-Anderson reaction offers a versatile strategy to synthesize a broad array of various benzylmenadione derivatives. Based on the previous study, this silver-catalyzed decarboxylation is an efficient radical reaction to prepare new benzylmenadione derivative combining commercially available carboxylic acids and menadione with 50-90% yields (Scheme 40a).^{46,47} However, the amine group acts as an electron donor in this reaction, which interferes with silver-catalyzed electron transfer, causing the arrest of the reaction. Through *N*-protection (NHBoc) the yields of *N,N*-amino-benzylmenadione derivatives are rather moderate (Scheme 40b). Therefore, the synthesis of *N*-alkylarylamine of benzylmenadione derivatives was designed by using a 3 steps route. Starting from the Kochi-Anderson coupling reaction combining two starting materials, menadione and halide phenylacetic acid. Then, the Buchwald-Hartwig amination coupling reaction could give the desired product in rather satisfying yields (Table 11, Scheme 40c).

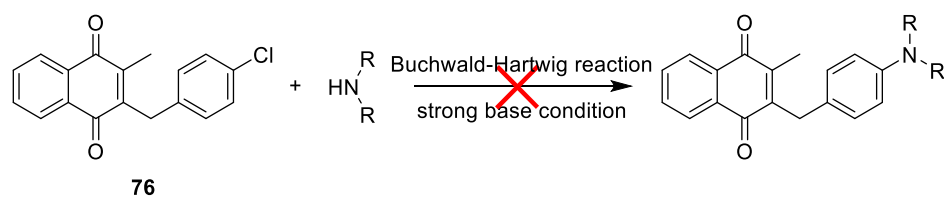
The first attempts of the Buchwald-Hartwig reaction were performed with the 4-chloro-benzylmenadione derivative as starting material (Scheme 41).^{115, 116} The starting material was prepared from menadione in good yield (85%) by the described silver-catalyzed decarboxylation reaction between menadione **14c** and the corresponding chlorophenylacetic acid derivative. However, benzylmenadione was unstable under the strong base conditions, for example NaOtBu, which was an essential reagent of Buchwald-Hartwig reaction. Due to the acidic protons of CH₃ or CH₂ of peripheral substituents linked to the quinone moiety as previously described, the enone generated with strong base led to undesired side products. Therefore, the protection of the quinone as 1,4-dimethoxynaphthalene is necessary.

¹¹⁵ Wolfe J. P., Wagaw S., Buchwald S. L., An Improved Catalyst System for Aromatic Carbon-Nitrogen Bond Formation: The Possible Involvement of Bis(Phosphine) Palladium Complexes as Key Intermediates, *J. Am. Chem. Soc.*, **1996**, *118*, 7215-7216.

¹¹⁶ Driver M.S., Hartwig J.F., A Second-Generation Catalyst for Aryl Halide Amination: Mixed Secondary Amines from Aryl Halides and Primary Amines Catalyzed by (DPPF)PdCl₂, *J. Am. Chem. Soc.*, **1996**, *118*, 7217-7218



Scheme 40. a). General Kochi-Anderson reaction. b) Kochi-Anderson reaction with aminated phenylacetic acid. c). Retrosynthesis of aminated benzylmenadione derivative.



Scheme 41. First attempt of Buchwald-Hartwig reaction.

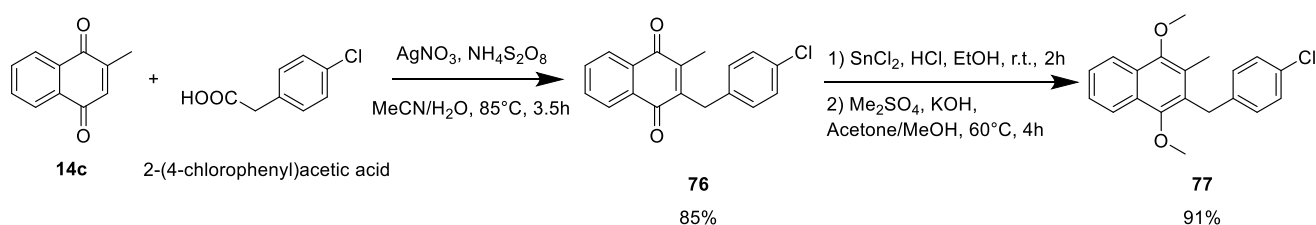
One part of my PhD work was to improve this synthesis and to prepare the compound in bulk, for a detailed chemical, pharmacokinetic and biological characterization of piperazine-based benzylmenadione derivative **80c**.

IV.2. Personal results

During my thesis, for 10 months, I co-supervised at the bench the Erasmus student (from Barcelona University), Jose Antonio Navarro Huerta, who re-synthesized the compound, as base (JN034) and chlorhydrate (JN043) forms, in bulk for both in vitro and in vivo studies.

IV.2.1. Synthesis of the piperazine-based plasmodione derivative

First, the Kochi-Anderson reaction was performed between menadione and 2-(4-chlorophenyl)acetic acid to give 2-(4-chlorobenzyl)-3-methylnaphthalene-1,4-dione **76**. This efficient radical reaction with silver nitrate and ammonium persulfate was obtained with 85% yield. Secondly, reduction of the resulting 4'-chlorobenzylmenadione derivative **76** was performed with tin(II) chloride and HCl conc., followed by methylation with dimethylsulfate in the presence of KOH to give the 2-(4-chlorobenzyl)-1,4-dimethoxy-3-methylnaphthalene **77** in 91% yield (previously presented in chapter III).¹⁰⁹ Due to the highly air-sensitive dihydronaphthalene intermediate, the use of tin(II) chloride/HCl conc. forming a relatively stable complex was found the most effective reductant to protect the intermediate during neutralization with water (Scheme 42).



Scheme 42. Synthesis of methylated benzylmenadione **77**.

Based on reported studies, the organometallic palladium complexes have become the main tool to develop C-N bond formation in versatile cross-coupling reactions in general.^{117,118} A series of aminated benzylmenadione synthesis was developed by using Buchwald-Hartwig palladium coupling reaction.^{110,116} These reactions were high yielding (41%-98%) and efficient, especially for the piperazine derivative **20c** (Table 11). In the meanwhile, this reaction was sensitive to water, the quality of the solvent would be highly affecting the reaction yield.

¹¹⁷ Wolfe J.P., Wagaw S., Marcoux J.F., Buchwald S.L., Rational Development of Practical Catalysts for Aromatic Carbon–Nitrogen Bond Formation, *Acc. Chem. Res.*, **1998**, *31*, 805–818

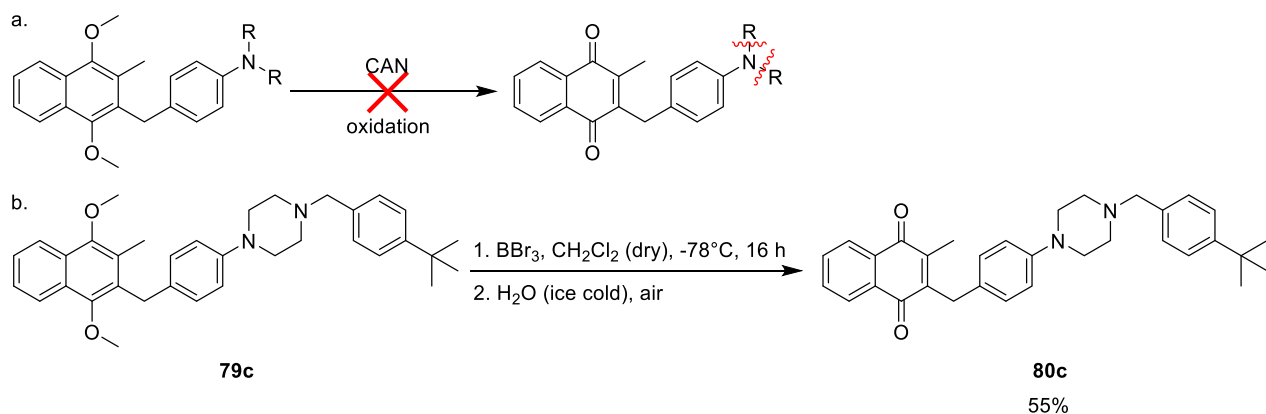
¹¹⁸ Hartwig J.F., Evolution of a fourth generation catalyst for the amination and thioetherification of aryl halides, *Acc Chem Res.* **2008**, *41*, 1534-1544

The CAN oxidation reaction was first used to perform the demethylation reaction. However, the amine group had more nucleophilic property, the cesium took the electron easier from the amine group than from the dimethoxynaphthalene moiety, resulting in no re-oxidation of the starting material to the desired naphthoquinone (Scheme 43a). Therefore, BBr₃ reagent has been employed as alternative reagent to regenerate the quinone **80c** with 55% yield. (Scheme 43b).¹¹⁹

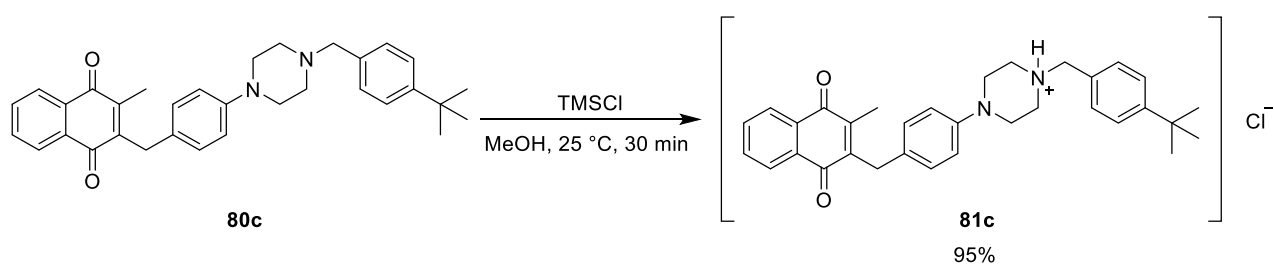
Based on the biology assay, the hydrophilicity of the *tert*-butyl-benzylpiperazine benzylmenadione **80c** was not satisfactory. Salinization was used to increase the water solubility in saline phosphate buffer for *in vivo* tests in mice. Thus, we decided to salinize the *tert*-butylbenzylpiperazine benzylmenadione **80c** by using TMSCl in methanol, which can form exact quantity of HCl in situ in small quantity scale (Scheme 44).

To conclude chapter IV, an optimized synthetic route of piperazine-based benzylmenadione derivative **80c** was investigated and developed in gramme scale. With this 4 steps synthesis, the piperazine-based benzylmenadione derivative **80c** was re-prepared in 1 g with 42% overyield, for a detailed chemical, pharmacokinetic and biological characterization. Furthermore, a half of piperazine-based benzylmenadione derivative **80c** was salinized by HCl to produce piperazine-based benzylmenadione derivative salt **81c**, which might have better hydrophilicity and better pharmacokinetic properties.

¹¹⁹ Chai C.L., Elix J.A., Moore F.K., Concise formal total synthesis of hybocarpone and related naturally occurring naphthazarins, *J. Org. Chem.* **2006**, *71*, 992-1001



Scheme 43. a) CAN oxidation reaction did not work due to the present of amine group. b) Demethylation and reoxidation reaction by using BBr_3 reagent.



Scheme 44. Salinization with HCl generated *in situ* by using TMSCl in methanol.

IV. 3. Antimalarial activities of the piperazine-based 3-benzylmenadione

The antimalarial activity of the piperazine derivative **80c** (**P_TM87**) was initially evaluated as 10-fold less active than the early lead plasmodione (Table 12). However, in various screening assays, the compound revealed to be more active against another protozoan, *Trypanosoma cruzi*. This recently obtained data was too preliminary to be developed in the frame of my PhD thesis.

Compound	IC ₅₀ ± SD (nM) ^a	IC ₅₀ ± SD (nM) ^b	IC ₅₀ (μM)
	Dd2	Dd2	hMRC-5
P_TM87 (base 81c)	697.5 ± 128,9 (4)	369 (2) ^b	38.05
P_TM29 (plasmodione 39e)	57.4 ± 12,3 (4) ^c	29 ± 2 (3) ^d	> 32 ^d
CQ	69.9 (1)	110 ± 20 (4) ^d	51.5 ^d

Table 12. IC₅₀ values of 3-benzylmenadione derivatives as antimalarial and cytotoxic agents against human cells (lung fibroblasts MRC-5) *in vitro*.^a In vitro growth inhibition of malarial parasites (Dd2) by 3-benzylmenadione derivatives for a selected number of 3-benzyl representatives. The IC₅₀ values were determined using the multidrug resistant *P. falciparum* clone Dd2 in the SYBR green I assay as described before.³⁷ Values are the mean ± SD of (n) independent determinations. The mean ± SD of at least three independent determinations is shown. The IC₅₀ value of the antimalarial drug chloroquine against Dd2 strain is indicated as a reference; it is in the range of the reported value, *i.e.* 82.4 ± 1.6 (3).^{46 b} The IC₅₀ values were determined using the multidrug resistant *P. falciparum* clone Dd2 in the ³H-hypoxanthine incorporation based assay as described before.^{47 c} The IC₅₀ value of the antimalarial lead plasmodione against Dd2 strain is indicated as a reference; it is in the range of the reported value, *i.e.* 58 ± 11 (9).^{46 d} IC₅₀ values from Ref. 47. The IC₅₀ values in *P. falciparum* assays (SYBR green I assay) were measured by Dr. Katharina Ehrhardt in co-tutelle between Strasbourg and Heidelberg.¹²⁰

¹²⁰ Katharina Ehrhardt, PhD thesis, University of Strasbourg, October 5, 2014, Strasbourg.

Part 2: Synthesis a gold(I)-phosphole-thiosugar complex as a thioredoxin reductase inhibitor

Avant-propos

In this chapter I will present the first syntheses that I developed in the team when I arrived as PhD student in October 2013. Some of the ^{13}C -enriched starting materials were ordered for the plasmodione project, but the shipment was delayed by 2 months. During this time, I prepared the known human thioredoxin reductase (TrxR) inhibitor, named “GoPI-sugar”, for a broad evaluation of the biological activity against various parasites, in particular the worm *Schistosoma mansoni*. As for human TrxR the *S. mansoni* TrxR is also seleno-dependent. In the frame of the Labex ParaFrap and established collaborations of the team the GoPI-sugar (LF-028) that I re-synthesized in bulk was considered in screening assays as a potential antiparasitic agent against various parasites (protozoans, worms causing human infectious diseases) and as inhibitor of a set of parasitic NADPH-dependent disulfide reductases.

I. Introduction

Discovery and development of new drugs are expensive and time-consuming, that cost a large amount of social resource and often requires more than 10 years to complete nowadays.¹²¹ However, about 70%-90% of new drugs were failing at the clinical trials stages.¹²² Repurposing “old drug” is one of the best way for new therapeutic exploration and identification, because of the drug availability and credibility. Compared to new drug discovery programs the the research time and cost of drug development, especially at the clinical trial phases, are reduced. Consequently, the patients would benefit from new therapies in a more mature and fast process.

The chrysotherapy had long history in most of major civilizations; however, most of them were administered as spiritual placebo.¹²³ After the alchemists discovered using aqua regia to dissolve gold in the middle ages, gold compounds were started to be used in medicinal treatments.¹²⁴ Robert Koch

¹²¹ Pessetto Z.Y., Weir S.J., Sethi G., Broward M.A., Godwin A.K. Drug repurposing for gastrointestinal stromal tumor. *Mol Cancer Ther.*, **2013**, *12*, 1299-1309.

¹²² Woodcock J., Woosley R. The FDA critical path initiative and its influence on new drug development. *Annu Rev Med*, **2008**, *59*, 1-12.

¹²³ Frank Shaw III C., Gold-based therapeutic agents. *Chem. Rev.*, **1999**, *99*, 2589-2600

¹²⁴ Higby G. J., Gold in medicine, *Gold Bull.* **1982**, *15*, 130-140

first observed the bacteriostatic activity of $K[Au(CN)_2]$ in the 1890s, introducing gold therapies into modern medicine.¹²⁵ Then, Jacques Forestier treated with inorganic gold salts patients affected by rheumatoid arthritis (RA), demonstrating the effectiveness of chrysotherapies for the treatment of partial RA patients.^{126,127} RA is a disease associated with dysfunction of the immune system, persistent inflammation and joint swelling.^{128,129} In the 1940's, the Au(I)-phosphine auranofin (Figure 30) was discovered, considered safer than the injectable inorganic gold salts, approved by FDA for oral administration of RA therapy in 1985 and exploited in the past 40 years.^{123,130} Auranofin was proved to be safely used by oral administration and its pharmacokinetic was sufficiently studied. The tetra-acetylated thioglucose moiety of auranofin, the acetylated groups of which are likely to be intracellularly hydrolyzed, was shown to facilitate the permeability of the drug across the plasma membrane.¹³¹ Nowadays, auranofin was rediscovered as potential alternative treatment for other diseases, such as some cancers, bacterial infections, HIV, neurodegenerative disorders and parasitic infections.¹³²

The inhibition of reduction/oxidation enzymes containing sulfur or selenium within the active site such as glutathione reductase (GR), thioredoxin reductase (TrxR), is the principal mechanisms of action of auranofin and most of the gold complex-based drugs.^{121,133,134,135,136,137} These NADPH-dependent flavoenzymes are indispensable enzymes in maintaining low the intracellular reactive oxygen species (ROS) levels. Inhibition of these NADPH-dependending disulfide reductases can disturb the intracellular redox balance, leading to increased concentration levels of ROS and intracellular

¹²⁵ Koch R., Über bakteriologische Forschung. *Dtsch. Med. Wochenstr.* **1890**, *16*, 756-757

¹²⁶ Forestier J., Rheumatoid arthritis and its treatment by gold salts. *The Lancet*, **1934**, *224*, 646-648.; B: 20, 827-840.

¹²⁷ Forestier J., Rheumatoid arthritis and its treatment by gold salts: The results of six years' experience. *J. Lab. Clin. Med.* **1935**, *20*, 827-840

¹²⁸ Messori L., Marcon G., Gold complexes in the treatment of rheumatoid arthritis. *Met Ions Biol Syst.* **2004**, *41*, 279-304

¹²⁹ Croke S.T., Mirabelli C.K., Molecular mechanisms of action of auranofin and other gold complexes as related to their biologic activities, *Am J Med.*, **1983**, *75*, 109-113.

¹³⁰ Tejman-Yarden N., Miyamoto Y., Leitsch D., Santini J., Debnath A., Gut J., McKerrow J.H., Reed S.L., Eckmann L., A reprofiled drug, auranofin, is effective against metronidazole-resistant *Giardia lamblia*., *Antimicrob. Agents Chemother.*, **2013**, *57*, 2029-2035

¹³¹ Tepperman K., Finer R., Donovan S., Elder R.C., Doi J., Ratliff D., Ng K., Intestinal uptake and metabolism of auranofin, a new oral gold-based antiarthritis drug. *Science*, **1984**, *225*, 430-432.

¹³² Andrade R.M., Reed S.L., New drug target in protozoan parasites: the role of thioredoxin reductase, *Front Microbiol.*, **2015**, *6*, 975.

¹³³ Fan C., Zheng W., Fu X., Li X., Wong Y.S., Chen T., Enhancement of auranofin-induced lung cancer cell apoptosis by selenocystine, a natural inhibitor of TrxR1 in vitro and in vivo, *Cell Death Dis.* **2014**, *5*, 1191.

¹³⁴ Fiskus W., Saba N., Shen M., Ghias M., Liu J., Gupta S.D., *et al.* Auranofin induces lethal oxidative and endoplasmic reticulum stress and exerts potent preclinical activity against chronic lymphocytic leukemia, *Cancer Res.* **2014**, *74*, 2520-2532

¹³⁵ Marzano C., Gandin V., Folda A., Scutari G., Bindoli A., Rigobello M.P., Inhibition of thioredoxin reductase by auranofin induces apoptosis in cisplatin-resistant human ovarian cancer cells, *Free Radic Biol Med.* **2007**, *42*, 872-881

¹³⁶ Jortzik E., Farhadi M., Ahmadi R., Toth K., Lohr J., Helmke B.M., Kehr S., Unterberg A., Ott I., Gust R., Deborde V., Davioud-Charvet E., Réau R., Becher K., Herold-Mende C., Antiglioma activity of GoPi-sugar, a novel gold(I)-phosphole inhibitor: Chemical synthesis, mechanistic studies, and effectiveness in vivo, *Biochim. Biophys. Acta*, **2014**, *1844*, 1415-1426.

¹³⁷ Gromer S., Arscott L.D., Williams C.H., Jr., Schirmer R.H., Becker K., Human placenta thioredoxin reductase Isolation of the selenoenzyme, steady state kinetics, and inhibition by therapeutic gold compounds, *J. Biol. Chem.*, **1998**, *273*, 20096-20101.

oxidative stress and cause the cellular apoptosis. This behavior promises to increase the drug cytotoxicity particularly in rapidly-dividing cells because they over-express disulfide reductases, such as cancer cells, memory T cells that harbor proviral HIV DNA and many parasites¹³⁸. Due to its central role in cell metabolism, the thioredoxin system is involved in many pathological conditions and provides potential targets for therapeutic approaches.

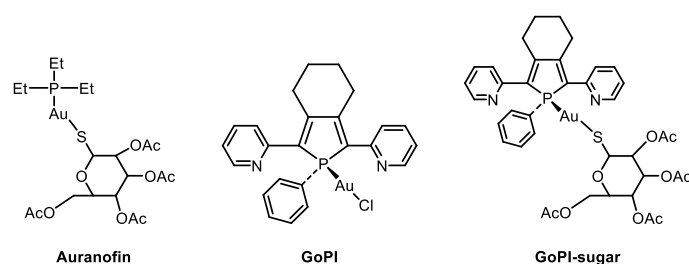


Figure 30. Structures of gold(I) phosphine complexes identified as inhibitors of human glutathione reductase and thioredoxin reductase and *Schistosoma mansoni* thioredoxin-glutathione *in vitro* or *in vivo*.

II. Preliminary Results from the team

Due to its central role in cell metabolism, the thioredoxin system is involved in many pathological conditions and provides potential targets for therapeutic approaches. The organic gold compounds auranofin and aurothioglucose which are widely used in the treatment of RA, inhibit the NADPH-reduced form of human thioredoxin reductase (hTrxR) specifically with a K_i of 4 nM. Liquid and solid tumors, as in the cases of RA and psoriasis disorders, are associated with an expression of several fold increased TrxR. Some potent antineoplastic agents such as carmustine, cisplatin and auranofin are effective inhibitors of mammalian TrxRs.

Phospholes are phosphacyclopentadienes that have very limited aromatic character^{139,140,141,142} (for an example, see the central unit of both compounds, GoPI and GoPI-sugar, shown in Figure 30)

¹³⁸ Roder C., Thomson M.J., Auranofin: repurposing an old drug for a golden new age. *Drugs R. D.*, **2015**, *15*, 13-20

¹³⁹ Hay C., Hissler M., Fischmeister C., Rault-Berthelot J., Toupet L., Nyulászi L., Réau R., Phosphole-containing pi-conjugated systems: from model molecules to polymer films on electrodes, *Chemistry*, **2001**, *7*, 4222-4236.

¹⁴⁰ Hay C., Fave C., Hissler M., Rault-Berthelot J., Réau R., Synthesis and electronic properties of alternating alpha,alpha'-thiophene-phosphole oligomers, *Org. Lett.*, **2003**, *5*, 3467-3470.

¹⁴¹ Fave C., Cho T.Y., Hissler M., Chen C.W., Luh T.Y., Wu C.C., Réau R., First examples of organophosphorus-containing materials for light-emitting diodes. *J Am Chem Soc.*, **2003**, *125*, 9254-9255.

¹⁴² Su H.C., Fadhel O., Yang C.J., Cho T.Y., Fave C., Hissler M., Wu C.C., Réau R., Toward functional pi-conjugated organophosphorus materials: design of phosphole-based oligomers for electroluminescent devices. *J Am Chem Soc.*, **2006**, *128*, 983-995.

and a nucleophilic phosphorus atom, which makes them good reagents for chemical modification, for example, with thiols or selenols. The work with gold(I) phosphole complexes, initially started on a collaboration between my supervisor, Elisabeth Davioud-Charvet and Régis Réau, Rennes University. The free electro-active phospholes ligands and their Palladium complexes were designed in Rennes for applications for optical and electrochemical devices and as catalysts for asymmetric synthesis, respectively. For therapeutic applications, the platinum and gold complexes were prepared in Rennes. Former studies in our team showed that palladium complexes, the novel platinum and gold phosphole complexes were potent inhibitors of TrxRs, with improved solubility, stability and bioavailability compared to auranofin.¹⁴³ In addition, gold complexes such as the most potent TrxR named GoPi (1-phenyl-2,5-di(2-pyridyl) phosphole}AuCl) and its 2,5-dipyridyl- and 2,5-dithienylphosphole derivatives)^{136,144} were found to bind with high affinity to DNA - as auranofin does it^{134,137} - limiting the aggressively cancer cell growth. However, the stability of GoPi was not satisfactory, this gold complex is highly sensitive to the light and oxygen in the solution state.¹⁴¹ Consequently, in order to increase the molecular hydrophilicity and bioavailability of GoPi, a novel gold complex GoPi-sugar, hybrid with auranofin, was designed from the structure of GoPi and auranofin (Figure 30).¹⁴⁴

Detailed enzymic studies strongly indicate that the selenocysteine residue of human TrxR is the site of action of the platinum-complexes tested. The hypothesis of the penultimate selenocysteine of human TrxR being the main target of the inhibitor attack was supported when comparing the inhibition of human TrxR and its mutant human TrxR-Sec498Cys.

The results from the team and German collaborators, have shown that i) the gold(I) complex GoPI (with -Cl as leaving atom) acts as an inhibitor of both human GR and TrxR and, ii) the more stable analogue, the gold(I) phosphole complex named “GoPI-thiosugar” (with a thiosugar instead of -Cl as leaving group) possesses potent growth-inhibitory properties on human tumor cells and antiglioblastoma activity in rats *in vivo*.¹³⁶

The organic gold complexes *per se* are not thought to interact with the flavoenzymes directly but to behave as pro-drugs *in vivo*, providing a source of biological available gold.^{123,142,145,146} The organic

¹⁴³ Irmeler A., Bechthold A., Davioud-Charvet E., Hofmann V., Réau R., Gromer S., Schirmer R. H., Becker K. Disulfide reductases – current developments, **2002**, 803-815. In *Flavins and Flavoproteins 2002*. Chapman, S.K., Perham, R.N., Scrutton N.S., Eds. Agency for Scientific Publications, Berlin, 2002.

¹⁴⁴ Urig S., Fritz-Wolf K., Réau R., Herold-Mende C., Tóth K., Davioud-Charvet E., Becker K., Undressing of phosphine gold(I) complexes as irreversible inhibitors of human disulfide reductases, *Angew. Chem. Int. Ed.*, **2006**, *45*, 1881-1886.

¹⁴⁵ Angelucci F., Sayed A.A., Williams D.L., Boumis G., Brunori M., Dimastrogiovanni D., Miele A.E., Pauly F., Bellelli A., Inhibition of *Schistosoma mansoni* Thioredoxin-glutathione Reductase by Auranofin, *J. Biol. Chem.*, **2009**, *284*, 28977-28985

¹⁴⁶ Saccoccia F., Angelucci F., Boumis G., Brunori M., Miele A.E., Williams D.L., Bellelli A., On the mechanism and rate of gold incorporation into thiol-dependent flavoreductases, *J. Inorg. Biochem.*, **2012**, *108*, 105–111

ligands confer to the gold complexes better hydrophilicity, lipophilicity and bioavailability.^{134,137,138} As previously reported, auranofin undergoes sequential ligand exchange reactions with cellular thiols through a prodrug effect.¹⁴⁷ The improvement of the chemical properties allows the gold drug to satisfy water solubility, oral administration and adequate stability for storage.¹²⁹ The triethylphosphine ligand of auranofin, which is lipophilic, provides to the gold complex membrane solubility and protein affinity.¹²³ According to the recent study, the acetylthioglucose ligand of auranofin was lost soon after administration to the patient, substituted by albumin cysteine 34 residue to form albumin-S-Au-PEt₃ complex, leading cell membrane transition of gold compound.^{123,148}

A long time ago it has been suggested for auranofin that this thiol exchange terminates when both thioglucose and triethylphosphine ligands have been displaced by the final dithiol target, causing the therapeutic effects similar to those observed with inorganic gold salts.¹⁴⁹ While it was not demonstrated by these authors, the thiol shift effect was finally proved when the 3D structure of the human GR:GoPI complex was solved (Figure 31).¹⁴⁴

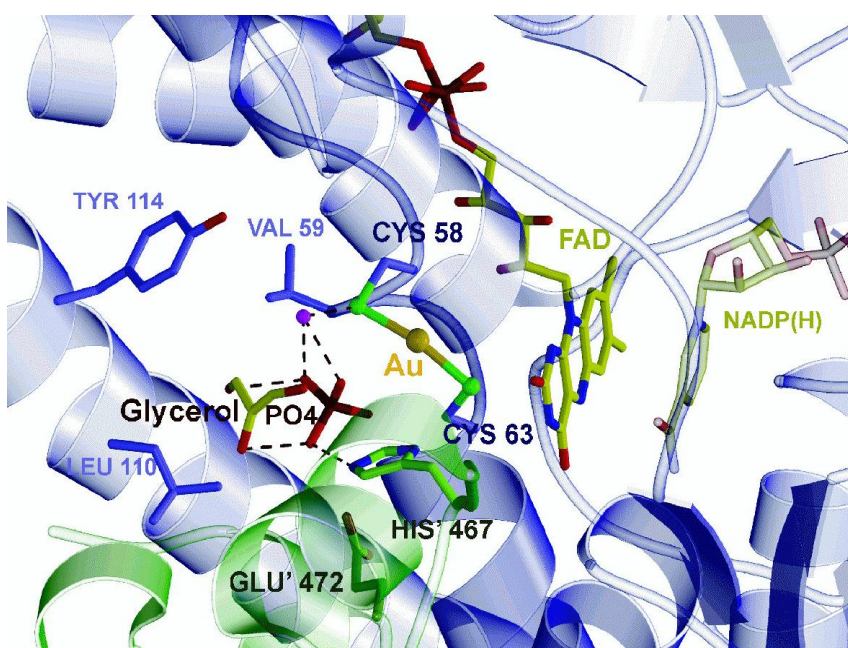


Figure 31. Refined structure of human GR modified by GoPI. The crystal structure of the alkylated human GR revealed a S-Au(I)-S geometry at the catalytic cysteine pair (image copied from Ref. 144).

¹⁴⁷ Snyder R.M., Mirabelli C.K., Crooke S.T., The cellular pharmacology of auranofin. *Semin. Arthritis Rheum.* **1987**, *17*, 71–80.

¹⁴⁸ Jones C.J., Thornback J.R. Medicinal Applications of Coordination Chemistry, *Royal Society of Chemistry*, **2007**, chapter 4 (4.4.3), 285-291, ISBN: 978-0-85404-596-9.

¹⁴⁹ Abrams M.J., Murrer B.A., Metal compounds in therapy and diagnosis. *Science*, **1993**, *261*, 725–730.

III. Personal results

III.1. The synthesis of GoPi-sugar

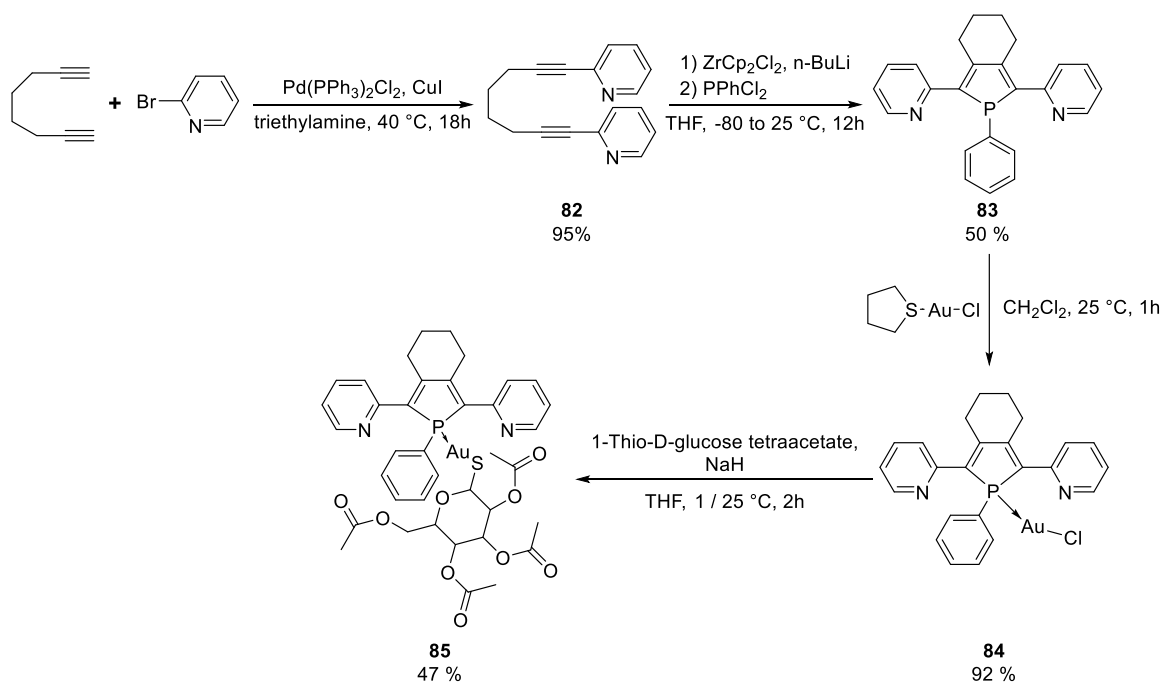
The strategy of GoPi-sugar synthesis was designed by a reported 3 steps route: the synthesis of bis(2-pyridyl)phosphole ligand, gold complexes formation and nucleophilic acetylthioglucose substitution (Scheme 45).^{136,139} The diyne **82** was obtained in excellent yield by Sonogashira coupling reaction of octa-1,7-diyne with 2-bromopyridine under classical condition.¹⁵⁰ The diyne **82** was first oxidative cyclized with zirconocene to give corresponding zirconacyclopentadiene, followed by the electrophilic [ZrCp2]/PPhCl₂ substitution reaction.¹⁵¹ This Fagan-Nugent route, which afforded a classical and efficient method for heterocycles synthesis, provided phosphole ligand **83** in moderate yields.^{139,152} However, the resulting phosphole ligand **83** was extremely air and moisture sensitive, the resulting crude product had to turn in next step of reaction without purification. Subsequently, the phosphole ligand was coordinated to the central metal gold with flash prepared AuCl(tetrahydrothiophene) to yield GoPi **84**.¹⁵³ Finally, a classical nucleophilic substitution reaction was performed by deprotonated acetylthioglucose, leading to the air stable GoPi-sugar **85** with high purity and moderate yield.¹³⁶ Several batches were produced in 300 mg scale.

¹⁵⁰ Sonogashira K., Development of Pd–Cu catalyzed cross-coupling of terminal acetylenes with sp²-carbon halides, *J. Organomet. Chem.*, **2002**, 53, 46–49

¹⁵¹ Aranda Perez A.I., Biet T., Graule S., Agou T., Lescop C., Branda N.R., Crassous J., Réau R., Chiral and extended π -conjugated bis(2-pyridyl)phospholes as assembling N,P,N pincers for coordination-driven synthesis of supramolecular [2,2]paracyclophane analogues, *Chem. Eur. J.*, **2011**, 17, 1337–1351

¹⁵² Yan X., Xi C., Conversion of zirconacyclopentadienes into metalloles: Fagan-Nugent reaction and beyond, *Acc Chem Res.*, **2015**, 48, 935-946

¹⁵³ Deponte M., Urig S., Arscott L.D., Fritz-Wolf K., Réau R., Herold-Mende C., Koncarevic S., Meyer M., Davioud-Charvet E., Ballou D.P., Williams C.H. Jr., Becker K., Mechanistic studies on a novel, highly potent gold-phosphole inhibitor of human glutathione reductase, *J Biol Chem.*, **2005**, 280, 20628-20637



Scheme 45. The synthesis of GoPi-sugar **85**.

IV. Inhibition of parasitic TrxRs and GR/TR by GoPi-sugar

Recently, several laboratories considered gold complexes acting as inhibitors of TrxRs from parasites to develop new antiparasitic drugs.^{14,144,153,154} Former studies showed that GoPi-sugar acted as a potent irreversible inhibitors of human TrxRs, *Schistosoma mansoni* TGR and *Brugia pahangi* TrxR with IC₅₀ in low nanomolar concentration (Table 13).^{128,134,135,137,146,155} Comparing auranofin and GoPi, the acetylthioglucose ligand reduced inhibitory activity of the gold complexes to human GR, which does not contain selenium in the active site. Due to the S atom in auranofin the acetylthioglucose ligand is more tightly bound to Au than the Cl atom in GoPI, and the human GR was more difficult to be inhibited by auranofin *versus* GoPi. In addition, GoPi-sugar have almost the same inhibitory capability as auranofin.

¹⁵⁴ Viry, E., Battaglia, E., Deborde, V., Müller, T., Réau, R., Davioud-Charvet, E., Bagrel, D. A sugar-modified phosphole gold complex with antiproliferative properties acting as a thioredoxin reductase inhibitor in MCF-7 cells. *ChemMedChem*. **2008**, 3, 1667-1670.

¹⁵⁵ Kuntz N.A., Davioud-Charvet E., Sayed A.A., Califf L.L., Dessolin J., Arnér E.S.J., Williams D.V., Thioredoxin Glutathione Reductase from *Schistosoma mansoni*: An Essential Parasite Enzyme and a Key Drug Target, *PLoS. Med.*, **2007**, 4, e206

Gold-complexes	Human	Human	Human	Human	<i>S. mansoni</i> TGR ^e			<i>L. infantum</i>	<i>S. mansoni</i>	<i>B. pahangi</i>
	TrxR ^{a,b}	TrxR ^{a,b}	TrxR ^{c,d}	GR ^{a,b,c}				TR ^f	TGR ^g	TrxR ^h
	hTRX ^{C72S}	DTNB	DTNB/Trx	GSSG	DTNB	GSSG	HED	DTNB	DTNB	DTNB
GoPi-sugar	4.3±1.6	0.49±0.04		88.5±28					12.5	5.5
GoPi	6.9	0.8		1						
auranofin			20	40000	7	9	6	155±35	1.1	0.5
aurothioglucose			65	>>100000	70	3000	400			
Aurothiomalate			280	ND	90	50	50			

Table 13. IC₅₀ Values (nM) for human TrxR and GR, for parasite TGR, TR and TrxR inhibition from the literature. Conditions of enzyme inhibition assays can be found in the following references: ^{a,b}: The enzyme activity was measured by adding GSSG (100 μM), DTNB (3 mM), or hTrx (20 μM) to the mixtures;^{136,144} ^{c,d}: The enzyme activity was measured by adding TrxS₂ (50 μM and 75 μM), NADPH (100 μM) and TrxR (1.7 nM); or DTNB (3 mM) and NADPH (250 μM);^{137,156} ^e: Comparison of the activity of auranofin and related gold complexes against recombinant *Schistosoma mansoni* TGR The enzyme activity was measured by adding DTNB (3 mM) and NADPH (100-200 μM);¹⁵⁵ ^f: The enzyme activity was measured by adding NADPH (100 μM), TR and TS₂ (50-400 μM);¹⁷⁷ ^{g,h}: unpublished data; ^h: *Brugia pahangi* TrxR was measured by adding DTNB (6 mM) and NADPH (200 μM).¹⁶⁹

¹⁵⁶ Rigobello M.P., Messori L., Marcon G., Agostina Cinellu M., Bragadin M., Folda A., Scutari G., Bindoli A., Gold complexes inhibit mitochondrial thioredoxin reductase: consequences on mitochondrial functions, *J. Inorg. Biochem.*, **2004**, 98, 1634-41

V. Anti-parasitic activity of GoPi-sugar

In order to determine the therapeutic index of GoPI-sugar, the gold(I) complexes auranofin and GoPI-sugar (LF-028) were tested for cytotoxicity on RAW 264.7 macrophages (Table 14). The results showed that GoPi-sugar had almost the same cytotoxicity as the clinically used auranofin in humans. These interesting data lead us to further investigate GoPi-sugar for its anti-parasitic activity and screen a large panel of pathogens for humans to identify the most sensitive parasites to GoPi-sugar compared to auranofin.

Compounds	Cytotoxicity on RAW 264.7 macrophages CC ₅₀ (μM) ± SD
LF-028	4.35 ± 0.04
Auranofine	4.43 ± 0.08

Table 14. CC₅₀ Value (μM) of cytotoxicity on RAW 264.7 macrophages.

V.1. Anti-*Schistosoma mansoni* worms activity of gold complexes

Schistosomiasis, or named as bilharzia, is a parasitic disease infected over than 230 million people and cause 280,000 deaths per year in many tropical areas, such as Africa.^{157,158,159} The pathogen of schistosomiasis is caused by the *Schistosoma spp.* parasites.¹⁵⁴ Praziquantel have been discovered to cure schistosomiasis since 1980s, which is the only one most efficiency drug.^{160,161} Artemether has been investigated as a new drug for schistosomiasis, which is also an antimalarial drug.¹⁶² However, in order to protect artemisinin-based drugs far from development of drug resistance in the malaria parasite, artemether was limited to treat schistosomiasis.¹⁵⁵ Nevertheless, these current

¹⁵⁷ King C.H., Dickman K., Tisch D.J., Reassessment of the cost of chronic helminthic infection: a meta-analysis of disability-related outcomes in endemic schistosomiasis, *Lancet.*, **2005**, 365, 1561-1569

¹⁵⁸ Hotez P.J., Molyneux D.H., Fenwick A., Ottesen E., Sachs S.E., Sachs J.D., Incorporating a Rapid-Impact Package for Neglected Tropical Diseases with Programs for HIV/AIDS, Tuberculosis, and Malaria, *PLoS Med.*, **2006**, 3, e102.

¹⁵⁹ Colley D.G., Bustinduy A.L., Secor W.E., King C.H., Human schistosomiasis, *Lancet.*, **2014**, 383, 2253-2264

¹⁶⁰ The American Society of Health-System Pharmacists, **2016**

¹⁶¹ da Silva V.B.R., Campos B.R.K.L., de Oliveira J.F., Decout J.L., do Carmo Alves de Lima M., Medicinal chemistry of antischistosomal drugs: Praziquantel and oxamniquine, *Bioorg. Med. Chem.*, **2017**, 25, 3259-3277

¹⁶² Utzinger J., Keiser J., Shuhua X., Tanner M., Singer B.H., Combination chemotherapy of schistosomiasis in laboratory studies and clinical trials, *Antimicrob. Agents Chemother.*, **2003**, 47, 1487-1495.

result inspired us to seek alternative antimalarial compounds which might be possible to have high anti-*Schistosoma* activity. Auranofin and its gold complexes derivatives were currently identified as potential antimalarial lead drug, targeting disulfide reductase.¹⁶³ Therefore, it was rational to test both gold complexes as potential anti-*Schistosoma* agents.

Both TrxR and GR enzymes are absent in *Schistosoma mansoni*, and are substituted by thioredoxin-glutathione reductase (TGR).¹⁶⁴ TGR is a unique multifunctional selenoenzyme reducing both GSSG and Trx, which has been validated as an essential parasite protein.¹⁵⁹ Gold (I) complexes, represented by auranofin, are known as highly specific inhibitors of several eukaryotic selenoenzymes. GoPi-sugar and auranofin share similar structural features and inhibitory capabilities.¹⁵⁵

Both auranofin and GoPi-sugar were highly effective *S. mansoni* TGR inhibitors with IC₅₀ values in the nanomolar range, and able to kill *ex vivo* *S. mansoni* worms (Table 15). It was found that both compounds displayed similar in vitro anti-parasitic activity, with auranofin being slightly more active.

Compound	Conc. (μM)	Dead (%) Day 1	Dead (%) Day 2	Dead (%) Day 3	Dead (%) Day 4	Dead (%) Day 5
Auranofin	10	100				
LF-028	10	100				
Auranofin	5	100				
LF-028	5	100				
Auranofin	2.5	50	100			
LF-028	2.5	0	0	0	50	100
Auranofin	1	0	0	0	0	0
LF-028	1	0	0	0	0	0

Table 15. Comparison of the worm killing activity of auranofin and GoPi-sugar against *Schistosoma mansoni* worms using the RUMC adult *ex vivo* *S. mansoni* worm assay.

These assays were evaluated in Prof. David L. Williams's laboratory (Rush University, Illinois, USA).

¹⁶³ Sannella A.R., Casini A., Gabbiani C., Messori L., Bilia A.R., Vincieri F.F., Majori G., Severini C., New uses for old drugs. Auranofin, a clinically established antiarthritic metallodrug, exhibits potent antimalarial effects in vitro: Mechanistic and pharmacological implications, *FEBS. Lett.*, **2008**, 582, 844-847

¹⁶⁴ Alger H.M., Williams D.L., The disulfide redox system of *Schistosoma mansoni* and the importance of a multifunctional enzyme, thioredoxin glutathione reductase, *Mol. Biochem. Parasitol.*, **2002**, 121, 129-139

V.2. Anti-*Brugia pahangi* worms activity of gold complexes

River blindness (Onchocerciasis) and lymphatic filariasis, which cause elephantiasis, are two neglected tropical diseases infecting millions of people in developing countries.^{165,166} Both diseases are caused by filariid nematodes. While existing drugs mainly kill the first-stage larvae (microfilariae) there is no drug available that would be highly effective to kill adult filarial worms.¹⁶⁷ The agents used in clinics can reduce the transmission of infections^{149,168} but, as they have limited activity against the adult worms these drugs cannot inhibit the reproduction of the adult worms, which can continue to produce microfilariae and perpetuate disease transmission. Finding a drug that could kill the adult worms would be an important strategy in eliminating filarial infections. Recently, auranofin was found to kill adult filarial worms and reduce the worm infection in a *Brugia pahangi*-infected gerbil model *in vivo*, likely through inhibition of filarial TrxR activity.¹⁶⁹ Here, we compared the *in vitro* anti-*B. pahangi* activity of auranofin and GoPi-sugar finding that both compounds have similar anti-parasitic activity, with auranofin being slightly more active (Table 16). Both gold complexes were active to kill *B. pahangi* worms at 5 μ M, at which concentration can be obtained from the plasma after oral administration.

¹⁶⁵ USAID's NTD Program Onchocerciasis or River Blindness, **2014**

¹⁶⁶ **World Health Organization**, 2014, Lymphatic Filariasis Fact Sheet

¹⁶⁷ Hoerauf A., Pfarr K., Mand S., Debrah A.Y., Specht S., Filariasis in Africa--treatment challenges and prospects, *Clin. Microbiol. Infect.*, **2011**, *17*, 977-985

¹⁶⁸ Taylor M.J., Hoerauf A., Bockarie M., Lymphatic filariasis and onchocerciasis, *Lancet.*, **2010**, *376*, 1175-1185

¹⁶⁹ Bulman C.A., Bidlow C.M., Lustigman S., Cho-Ngwa F., Williams D., Rascón A.A. Jr., Tricoche N., Samje M., Bell A., Suzuki B., Lim K.C., Supakorndej N., Supakorndej P., Wolfe A.R., Knudsen G.M., Chen S., Wilson C., Ang K.H., Arkin M., Gut J., Franklin C., Marcellino C., McKerrow J.H., Debnath A., Sakanari J.A., Repurposing auranofin as a lead candidate for treatment of lymphatic filariasis and onchocerciasis, *PLoS Negl. Trop. Dis.*, **2015**, *9*, e0003534

Compound	Conc. (μM)	Average Day 1	Average Day 2	Average Day 3	Average Day 6
Auranofin	10	99	100	99	98
LF-028	10	91	98	100	99
Auranofin	3	98	100	99	98
LF-028	3	24	41	40	96
Auranofin	1	25	45	48	98
LF-028	1	20	16	22	48

Table 16. Comparison of the worm killing activity of auranofin and GoPi-sugar against *Brugia pahangi* worms using the UCSF *B. pahangi* female in vitro assay. Results from a single concentration screen.

These assays were evaluated in Dr. Judy Sakanari's lab (UCSF's laboratory, California, USA).

V.3. Anti-*Trypanosoma brucei gambiense* activity of gold complexes

The human African trypanosomiasis (HAT), also known as sleeping sickness, is a parasitic disease threatening over than 70 million people in Africa.¹⁷⁰ *Trypanosoma brucei gambiense*, which is the pathogenic parasite of HAT, relies on the unique trypanothione reductase (TR) to prevent an intracellular rise of reactive oxygen species (ROS) and protect from oxidative damage.¹³⁸ Gold(I) complexes, such as auranofin, were discovered to be potent TR inhibitors with very low IC₅₀ values.^{138,171} However, no study on its antitrypanosomal action has been reported.

Based on previous pharmacokinetic studies with oral dosing of auranofin, 15%~25% of the drug can remain in the plasma 1-2 hours after administration and the plasma concentration was found to be 10 $\mu\text{g}/\text{mL}$, much higher than the concentrations resulting in *in vitro* parasite death.^{128,138,172,173} Here, we compared the anti-*T. brucei gambiense* activity of miltefosine, pentamidine, auranofin and GoPi-sugar (Table 17). Both IC₅₀ values showed that gold complexes kill the parasites efficiently, albeit less

¹⁷⁰ World Health Organization. 2013. New phase in fight against neglected tropical diseases heralds universal access to health interventions for world's poorest.

¹⁷¹ Lobanov A.V., Gromer S., Salinas G., Gladyshev V.N., Selenium metabolism in *Trypanosoma*: characterization of selenoproteomes and identification of a Kinetoplastida-specific selenoprotein, *Nucleic Acids Res.*, **2006**, *34*, 4012-4024

¹⁷² Kean W.F., Kean I.R., Clinical pharmacology of gold, *Inflammopharmacology*, **2008**, *16*, 112-125

¹⁷³ Kean W.F., Hart L., Buchanan W.W., Auranofin, *Br. J. Rheumatol.*, **1997**, *36*, 560-572

actively than pentamidine, which is the currently recommended anti-*T. brucei* drug, suggesting that both gold compounds may be promising alternatives against drug-resistant parasites.

Compounds	<i>Trypanosoma brucei gambiense</i> IC ₅₀ (μM) ± SD
GoPi-sugar	1.11 ± 0.12
Auranofine	0.21 ± 0.01
Miltefosine	ND
Pentamidine	0.0011 ± 0.0001

Table 17. Comparison of IC₅₀ value (μM) of miltefosine, pentamidine, auranofin and GoPi-sugar anti-*Trypanosoma brucei gambiense* activity on bloodstream forms.

These assays were evaluated in Prof. Philippe Loiseau's laboratory (University of Paris-Sud).

V.4. Anti-*Leishmania donovani* activity of gold complexes

Leishmaniasis is one of the most common parasitic disease in the world, which has been considered as one of six main neglected tropical diseases by WHO.¹⁷⁴ *Leishmania spp.* belong to the kinetoplastid parasites and are responsible for the infection of leishmaniasis.¹⁷⁵ Trypanothione synthetase and trypanothione reductase (TR) are essential proteins for *Leishmania* parasite survival.^{176,177} Auranofin has been previously described to be an apoptosis-stimulating agent in *Leishmania major* and *Leishmania amazonensis* with promising *in vitro* and *in vivo* antileishmanial

¹⁷⁴ Shirian S., Oryan A., Hatam G.R., Panahi S., Daneshbod Y., Comparison of conventional, molecular, and immunohistochemical methods in diagnosis of typical and atypical cutaneous leishmaniasis, *Arch. Pathol. Lab. Med.*, **2014**, *138*, 235-240.

¹⁷⁵ Bauer S., Morris M.T., Glycosome biogenesis in trypanosomes and the de novo dilemma, *PLoS Negl. Trop. Dis.*, **2017**, *11*, e0005333.

¹⁷⁶ Van Assche T., Deschacht M., da Luz R.A., Maes L., Cos P., Leishmania-macrophage interactions: insights into the redox biology, *Free Radic. Biol. Med.*, **2011**, *51*, 337-351

¹⁷⁷ A. Ilari, P. Baiocco, L. Messori, A. Fiorillo, A. Boffi, M. Gramiccia, T. Di Muccio, G. Colotti, A gold-containing drug against parasitic polyamine metabolism: The X-ray structure of trypanothione reductase from *Leishmania infantum* in complex with auranofin reveals a dual mechanism of enzyme inhibition. *Amino. Acids*, **2012**, *42*, 803-811.

activities.¹⁷⁸ Moreover, previous studies showed that this drug is an effective TR inhibitor of trypanothione reductase in *L. infantum*.¹⁷⁷

Comparing the anti-*Leishmania donovani* LV9 amastigotes activity of miltefosine, pentamidine, auranofin and GoPi-sugar, both auranofin and GoPi-sugar were shown to be potent TR inhibitors and exerted anti-*Leishmania* activity (Table 18). The IC₅₀ value on *Leishmania donovani* LV9 shown below suggest that both gold-containing compounds are very effective to inhibit parasite growth, in the same range as miltefosine. The IC₅₀ value of these two gold compounds ranged in the very low micromolar concentration, within the expected plasma concentration of auranofin after oral administration.

Compounds	<i>Leishmania donovani</i> LV9 axenic	<i>Leishmania donovani</i> LV9 intramacrophagic
	amastigotes IC ₅₀ (μM) ± SD	amastigotes IC ₅₀ (μM) ± SD
GoPi-sugar	1.45 ± 0.07	0.42 ± 0.15
Auranofine	0.56 ± 0.03	0.70 ± 0.24
Miltefosine	1,28 ± 0.12	4.49 ± 1.08
Pentamidine	ND	ND

Table 18. Comparison of IC₅₀ value (μM) of miltefosine, pentamidine, auranofin and GoPi-sugar anti- *Leishmania donovani* LV9 amastigotes activity.

These assays were evaluated in Prof. Philippe Loiseau's laboratory (University of Paris-Sud).

V.5. Anti-*Acanthamoeba castellanii* activity of gold complexes

Entamoeba histolytica, a protozoan parasite infecting human and cause amoebiasis, which is an intestinal disease leading about 40,000 to 100,000 death per year.^{179,180} Due to deficiency of both glutathione reductase (GR) and glutathione synthetic enzymes (GS) from *E. histolytica*, the role of its

¹⁷⁸ Sharlow E.R., Leimgruber S., Murray S., Lira A., Sciotti R.J., Hickman M., Hudson T., Leed S., Caridha T., Barrios A.M., Close D., Grögl M. and Lazo J.S. Auranofin is an apoptosis-stimulating agent with *in vitro* and *in vivo* anti-leishmanial activity. *ACS Chem. Biol.*, **2014**, 9, 663-672.

¹⁷⁹ World Health Organization; 1998. The World Health Report 1998: life in the 21st century.

¹⁸⁰ Wertheim H.F.L., Horby P., Woodall J.P., Atlas of Human Infectious Diseases, *Blackwell Publishing Ltd.*, **2012**, First Edition, 127

thioredoxin reductase (TrxR) becomes more important than in other organisms, in prevention and repair of oxidative damage.^{181,182,183} With an effective TrxR inhibition, which was profiled by transcription and direct assays, auranofin has been discovered for its anti-amebicidal activity and repurposed as anti-amoebiasis drug.¹⁸¹ Compared to *E. histolytica*, *Acanthamoeba* is a free living amoeba, which possess mitochondria and live in aerobic environment: thus, *Acanthamoeba* can synthesize glutathione and have authentic glutathione reductase in addition to TrxR.^{184,185}

Here, evaluation of the activity against *Acanthamoeba castellanii* showed that auranofin and GoPi-sugar have noticeable anti-acanthamoebal activities, but less active than pentamidine (Table 19). Nevertheless, their cytotoxicity at around 4 μM against macrophages resulted in a low therapeutic index.

Compounds	<i>Acanthamoeba castellanii</i> ATCC 30010 IC ₅₀ (μM) \pm SD
GoPi-sugar	13.04 \pm 1.53
Auranofine	5.79 \pm 1.02
Miltefosine	9.21 \pm 2.04
Pentamidine	1.39 \pm 0.37

Table 19. Comparison of IC₅₀ value (μM) of miltefosine, pentamidine, auranofin and GoPi-sugar anti-*Acanthamoeba castellanii* activity.

These assays were evaluated in Prof. Philippe Loiseau's laboratory (University of Paris-Sud).

¹⁸¹ Arias D.G., Gutierrez C.E., Iglesias A.A., Guerrero S.A., Thioredoxin-linked metabolism in *Entamoeba histolytica*, *Free Radic. Biol. Med.*, **2007**, *42*, 1496–1505

¹⁸² Hirt R.P., Muller S., Embley T.M., Coombs G.H., The diversity and evolution of thioredoxin reductase: new perspectives, *Trends Parasitol.*, **2002**, *18*, 302–308

¹⁸³ Debnath A., Parsonage D., Andrade R.M., He C., Cobo E.R., Hirata K., Chen S., García-Rivera G., Orozco E., Martínez M.B., Gunatilleke S.S., Barrios A.M., Arkin M.R., Poole L.B., McKerrow J.H., Reed SL., A high-throughput drug screen for *Entamoeba histolytica* identifies a new lead and target. *Nat Med.*, **2012**, *18*, 956-960.

¹⁸⁴ Ondarza R.N., Iturbe A., Hernández E., Hurtado G., Thiol compounds from a free-living pathogenic opportunistic amoeba, *Acanthamoeba polyphaga*. *Biotechnol. Appl. Biochem.*, **2002**, *36*, 195-204.

¹⁸⁵ Ondarza R.N., Iturbe A., Hernández E., The effects by neuroleptics, antimycotics and antibiotics on disulfide reducing enzymes from the human pathogens *Acanthamoeba polyphaga* and *Naegleria fowleri*, *Exp. Parasitol.*, **2007**, *115*, 41-47

Part 3: General conclusion and perspectives

This PhD work focused on the antimalarial drug metabolism investigation and development of plasmodione. In order to identify the structural information of active drug metabolites, the fully $^{13}\text{C}_{18}$ -enriched plasmodione was obtained by total synthesis and applied in the drug metabolism study with drug-treated parasitized red blood cells (pRBCs). Furthermore, for improving the solubility of plasmodione, both oxetane and *N*-alkyl-aryl derivatives of plasmodione, previously identified as antiparasitic hits in the team, were re-synthesized in 1 g-scale through efficient aromatic nucleophilic substitution ($\text{S}_{\text{N}}\text{Ar}$) and palladium-catalyzed Buchwald-Hartwig coupling reaction, respectively. Finally, a gold(I) phosphole complex known to act as an irreversible and potent inhibitor of the human seleno-dependent thioredoxin reductase, has been synthesized in several 300 mg scale, and investigated for its broad anti-parasitic activity profile against various pathogen parasites.

In chapter I, the $^{13}\text{C}_{18}$ -plasmodione (LF129) was synthesized by a 10 steps-long sequence via an optimized “tetralone express route” with an overall yield of 5 %. Besides, 2 mono- $^{13}\text{C}_1$ -labeled plasmodiones were produced. In the course of this work, we could observe that some reactions to produce the ^{13}C -enriched compounds and unlabeled compounds have different yields. Essentially, ^{13}C atoms have the same number of electrons as ^{12}C but different number of neutrons. The ^{13}C -labeled compounds keep the same chemical properties as ^{13}C -unenriched compounds. However, higher number of neutrons means increasing the weight of the molecule and decreasing the kinetic energy. Consequently, we cannot predict if this can have an impact on the reactivity of the ^{13}C -enriched compounds compared to that of unlabeled compounds. Therefore, it was difficult to predict the kinetics of the ^{13}C -enriched reaction *versus* the same reaction with unlabeled starting materials in the synthetic process. At least, we could check that plasmodione from two distinct routes and all isotopically-heavier plasmodiones display the same antimalarial activities against *ex vivo P. berghei*.

Besides, we also observed that the presence of 100% abundance of ^{13}C atom causes huge differences of signal patterns in ^1H and ^{13}C NMR spectra of ^{13}C -labeled *versus* unlabeled compounds. The most significant effect is generating $^2J_{^{13}\text{C}-^1\text{H}}$ coupling constants of the ^1H NMR signals, which are ranged from 120 Hz to 170 Hz. By analyzing the NMR chemical shifts, the ^{13}C -labeled compounds could be correctly profiled by NMR spectra.

In chapter II, 6 putative drug metabolites were freshly re-prepared and employed in the drug metabolism investigation. The extraction method had been well established with different conditions and used in experiments to track the drug metabolites. With the help of SPE, better acquisition of the HPLC/MS-MS system was obtained from pRBC lysate. The perspective of this investigation is to repeat the experiments at various time of drug incubation under the same conditions. Repeating the last experiment by using 5 hours incubation will allow us to confirm the mass of drug metabolites adducts. Subsequently, the objectives will be aimed at fully characterizing the fragmentation of all drug metabolites-adducts by varying the collision energy of the mass spectrometry and anticipating the structure of the adducts. Finally, depending on the mass and fragmentation of the drug metabolites-adducts, the synthesis of these adducts would allow to confirm the hypothesis and identification of the mode of action of plasmodione metabolism.

In chapter III, from a previous preliminary investigation to study the locus where to introduce an oxetane group in plasmodione a strategy was built on a 4 high yielding steps synthetic route to produce 3'-(oxetane-3-yloxy)plasmodione. After optimization of this synthetic route, we have obtained 1 g of the desired 3'-(oxetane-3-yloxy)plasmodione (batch LF148) for a detailed chemical pharmacokinetic and biological characterization. Furthermore, during the optimization, a new 3'-fluoro-[4'-(tri-oxetane-3-yloxy)-methyl-benzyl] derivative was discovered. The perspectives of this project will focus on the investigation of synthetic methodologies for the synthesis of new oxetane derivatives of plasmodione for drug development by moving the oxetane in the plasmodione skeleton. In addition, a specific attention will be concentrated on the 3'-fluoro-[4'-(tri-oxetane-3-yloxy)-methyl-benzyl] derivative after a new batch has been re-synthesized for characterizing its antiparasitic properties.

In chapter IV, an optimized synthetic route of piperazine-based benzylmenadione derivative was investigated and developed in gramme scale. With this 4 steps synthesis, the piperazine-based benzylmenadione derivative was re-prepared in 1 g with 40% total, for a detailed chemical, pharmacokinetic and biological characterization. Furthermore, a half of piperazine-based benzylmenadione derivative was salinized by HCl to produce piperazine-based benzylmenadione derivative salt (batch LF166), which might have better hydrophilicity and better pharmacokinetic properties. This batch of compound will allow to study the detailed anti-Chagas activity profile using different strains of *Trypanosoma cruzi* from the field, and to attempt to select resistant parasites under drug pressure.

In part 2, the Au(I)-phosphole complex named GoPi-sugar was synthesized (batch LF028). By comparing to auranofin used as reference, GoPi-sugar has been shown to inhibit the growth of various parasites in parasite screening assays: the bloodstream stages of *Trypanosoma brucei gambiense* and the intramacrophagic amastigote stage of *Leishmania donovani* LV9, the free living amoeba living in our rivers in Europe *Acanthamoeba castellanii*, the adult filarial worms *Brugia pahangi* (nematodes) and the flatworms *Schistosoma mansoni*. New perspectives are open to develop nanoformulations of GoPI-sugar using nanoparticles to vectorize the TrxR inhibitor in specific organisms like *Schistosoma mansoni* or *Brugia pahangi* worms and express a multivalent antiparasitic effect against the most sensitive parasites to GoPI-sugar *versus* auranofin, *Leishmania* spp.

Part 4: Materials and methods

1. General information for organic synthesis

Solvents and reagents: Commercially available starting materials were purchased from Sigma-Aldrich, ABCR GmbH & Co. KG, Alfa Aesar, and Apollo Scientific and were used without further purification. Solvents were obtained from Sigma-Aldrich and Carlos Erba. Unless noticed, reagent grade was used for reactions and column chromatography and analytical grade was used for recrystallizations. When specified, anhydrous solvents were required; tetrahydrofuran (THF) was distilled over sodium/benzophenone under argon or dried by passage through an activated alumina column under argon. All reactions were performed in standard glassware. Thin Layer Chromatography (TLC) was used to monitor reactions (*vide infra*). Crude mixtures were purified either by recrystallization or by flash column chromatography. Monitoring and primary characterization of products were achieved by Thin Layer Chromatography on plastic sheets coated with silica gel 60 F254 purchased from E. Merck. Eluted TLC's were revealed under UV (325 nm and 254 nm) and with detection reagents. Analytical TLC was carried out on pre-coated Sil G-25 UV₂₅₄ plates from Macherey Nagel. Flash chromatography was performed using silica gel G60 (230–400 mesh) from Macherey Nagel. All ¹³C-enriched available chemical products were purchased by commercial sources without further purification.

Chromatography: Generally, column chromatography was performed using silica gel 60 (230-400 mesh, 0.040-0.063 mm) or Aluminum oxide activated, basic, Brockmann Grade I (60 mesh, 58 Å) purchased from E. Merck. Analytical TLC was carried out on pre-coated Silica gel 60 F₂₅₄ aluminum plates from Merck.

Nuclear Magnetic Resonance (NMR): The Nuclear Magnetic Resonance (NMR) spectra were registered either with a *Bruker avance 400* apparatus (¹H NMR 400 MHz, ¹³C NMR 100 MHz, ¹⁹F

NMR 375 MHz, ^{31}P NMR 81 MHz) or with a *Bruker avance 300* apparatus (^1H NMR 300 MHz, ^{13}C NMR 75 MHz, ^{19}F NMR 281 MHz, ^{31}P NMR 60 MHz) at ECPM. All chemical shifts (δ) are quoted in parts per million (ppm). The chemical shifts are referred to the used partial deuterated NMR solvent (for CDCl_3 : ^1H NMR, 7.26 ppm and ^{13}C NMR, 77.36 ppm; for DMSO ^1H NMR, 2.54 ppm and ^{13}C NMR, 40.45 ppm). The coupling constants (J) is given in Hertz (Hz). Resonance patterns are reported with the following notations: br (broad), s (singlet), d (doublet), t (triplet), q (quartet), m (multiplet), dd (doublet of doublets). In addition, the following acronyms will be used: C=O carbonyl group; C_q : quaternary carbon; CH_2 : secondary carbon; CH_3 : methyl group; ArH: aromatic proton of the menadione core; PhenylH: aromatic proton of the phenyl moiety; PyH: aromatic proton of the pyridine moiety.

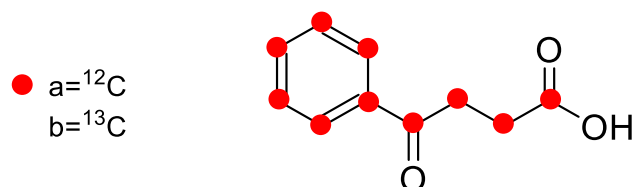
Elemental analysis: Elemental analyses were performed by “*Service de Microanalyses*” at the *Institut de Chimie de Strasbourg*.

Mass spectrometry: Mass spectrometry was performed at Service de Spectrométrie de Mass-Université de Strasbourg. Mass spectra (ESI-MS) was obtained on a microTOF LC spectrometer (Bruker Daltonics, Bremen). High Resolution Mass (HRMS) spectra were measured and fitted with calculated data.

Melting point: Melting points were determined on a Büchi melting point apparatus and were not corrected.

2. Synthesis of the multi $^{13}\text{C}_{18}$ - and mono $^{13}\text{C}_1$ -labeled plasmodiones

Synthesis of 4-oxo-4-phenylbutanoic acid (40):



4-oxo-4-(phenyl- $^{13}\text{C}_6$)butanoic-1,2,3,4- $^{13}\text{C}_4$ acid

Dihydrofuran-2,5-dione-2,3,4,5- $^{13}\text{C}_4$ (1 equiv., 500 mg, 4.81 mmol) was refluxed in sulfuryl chloride (24.2 mL) for 3 hours under argon atmosphere. Excess of sulfuryl chloride was removed under vacuum and the residue suspended in tetrachloroethane (20 mL) in an ice-water bath. Addition of benzene-1,2,3,4,5,6- $^{13}\text{C}_6$ (1 equiv., 404 mg, 0.43 mL, 6.71 mmol) was followed by portion-wise addition of fresh aluminium chloride (4.71 equiv., 3015 mg, 22.6 mmol) with stirring. The resulting mixture was stirred overnight at room temperature under argon atmosphere, gradually deepening in color. The reaction was poured into the mixture of ice (50 g) and concentrated HCl (5 ml, 37%), the solvent was removed under reduced pressure. The remaining mixture was extracted with ether (5×25 ml). The combined organic layers were washed with water (2×25 ml), brine, dried over MgSO_4 and concentrated under reduced pressure to give a yellowish solid (887 mg, 98%).

4-oxo-4-phenylbutanoic acid (40a):

^1H NMR (400 MHz, CDCl_3): δ 7.99 (d, 2H, $J=7.2$ Hz, phenylH), 7.58 (t, 1H, $J=7.6$ Hz, phenylH), 7.47 (t, 2H, $J=7.6$ Hz, phenylH), 3.32 (t, 2H, $J=6.6$ Hz, CH_2), 2.82 (t, 2H, $J=6.6$ Hz, CH_2) ppm.

^{13}C NMR (100 MHz, CDCl_3): δ 197.9, 178.4, 136.5, 133.5, 128.8, 128.2, 33.3, 28.1 ppm.

HRMS (ESI) m/z : $[\text{M}+\text{H}]^+$ calcd for $\text{C}_{10}\text{H}_{11}\text{O}_3$: 179.0703; found 179.0702.

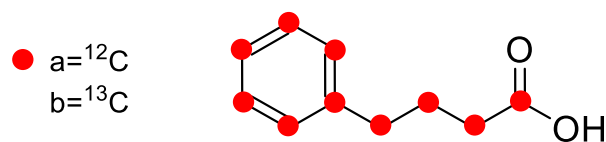
4-oxo-4-(phenyl-¹³C₆)butanoic-1,2,3,4-¹³C₄ acid (40b):

¹H NMR (400 MHz, CDCl₃): δ 7.98 (dm, 2H, *J*=164.0 Hz, phenylH), 7.56 (dt, 1H, *J*=150.2 Hz, *J*=7.7Hz, phenylH), 7.47 (dt, 2H, *J*=161.3 Hz, *J*=7.9 Hz phenylH), 3.32 (dm, 2H, *J*=126.8 Hz, *J*=5.6 Hz, CH₂), 2.82 (ddm, 2H, *J*=129.3 Hz, *J*=7.5 Hz, *J*= 3.5 Hz, CH₂) ppm.

¹³C NMR (100 MHz, CDCl₃): δ 198.0 (dd, *J*=52.5 Hz, *J*=39.8 Hz), 177.7 (d, *J*=56.3 Hz), 136.5 (qm, *J*=49.5 Hz), 133.5 (tm, *J*=50.3 Hz), 128.5 (td, *J*=39.1 Hz, *J*=3.5 Hz), 128.5 (dt, *J*= 76.7 Hz, *J*=53.3 Hz, *J*=3.5 Hz), 33.4 (td, *J*=40.0 Hz, *J*=13.1 Hz), 28.0 (dd, *J*=56.8 Hz, *J*=38.3 Hz) ppm.

ESI-MS m/z: [M+H]⁺ calcd for ¹³C₁₀H₁₁O₃: 189.15; found 189.10.

Synthesis of 4-phenylbutanoic acid (41):



4-(phenyl-¹³C₆)butanoic-1,2,3,4-¹³C₄ acid

To a solution of 4-oxo-4-(phenyl-¹³C₆)butanoic-1,2,3,4-¹³C₄ acid (1 equiv., 800 mg, 4.25 mmol) in diethylene glycol (12.9 mL) was added hydrazine monohydrate (5.2 equiv., 1108 mg, 1.08 mL, 22.1 mmol). After stirring at room temperature for 30 min, KOH (4.57 equiv., 1282 mg, 19.4 mmol) was added and the reaction mixture was heated at 120°C for 1.5 hours. Then the reaction mixture was heated (T= 215°C) to distilled low boiling material; when diethylene glycol started to be distilled, the heating was stopped. The reaction mixture was then refluxed for 3 hours. After cooling down, the reaction mixture was poured into ice (25 g), acidified to pH=2 and extracted with Et₂O (5×20 mL). The combined organic layers were washed with water (2×25 mL) and brine, dried over MgSO₄ and concentrated under reduce pressure to give a brownish visqueous oil (699.2 mg, 94%).

4-phenylbutanoic acid (41a):

¹H NMR (400 MHz, CDCl₃): δ 7.28 (m, 2H, phenylH), 7.19 (m, 3H, phenylH), 2.67 (t, 2H, *J*=7.5 Hz, CH₂), 2.37 (t, 2H, *J*=7.5 Hz, CH₂), 1.97 (p, 2H, *J*=7.5 Hz, CH₂) ppm.

¹³C NMR (100 MHz, CDCl₃): δ 179.6, 141.5, 128.8, 128.7, 126.4, 35.3, 33.6, 26.6 ppm.

HRMS (ESI) m/z: [M+H]⁺ calcd for C₁₀H₁₃O₂ 165.0910; found 165.0908.

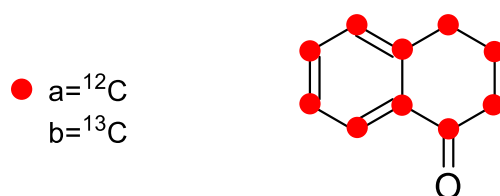
4-(phenyl-¹³C₆)butanoic-1,2,3,4-¹³C₄ acid (41b):

¹H NMR (400 MHz, CDCl₃): δ 7.45 (m, 2H, phenylH), 7.07 (m, 3H, phenylH), 2.68 (dm, 2H, *J*=121.3 Hz, CH₂), 2.37 (dm, 2H, *J*=122.1 Hz, CH₂), 1.98 (dm, 2H, *J*=131.2 Hz, CH₂) ppm.

¹³C NMR (100 MHz, CDCl₃): δ 180.23(d, *J*=54.1 Hz), 142.4-140.61(m), 129.0(t, *J*=39.3 Hz), 128.5 (t, *J*=39.3 Hz), 127.3-125.5(m), 35.3(t, *J*=38.6 Hz), 33.7(dd, *J*=55.2 Hz, *J*=34.5 Hz), 26.5(t, *J*=34.4 Hz) ppm.

ESI-MS m/z: [M+H]⁺ calcd for ¹³C₁₀H₁₃O₂: 175.13; found 175.09

Synthesis of 3,4-dihydronaphthalen-1(2H)-one (42):



3,4-dihydronaphthalen-1(2H)-one-¹³C₁₀

4-(phenyl-¹³C₆)butanoic-1,2,3,4-¹³C₄ acid (1 equiv., 660 mg, 3.79 mmol) was added to methanesulfonic acid (41.3 equiv., 15036 mg, 10.15 mL, 156.5 mmol) and the mixture was heated at 90 °C for 30 min under argon atmosphere. The reaction mixture was then poured into ice-water and extracted with ether (3×40 mL). The combined organic layers were washed with diluted sodium bicarbonate (20 mL), water (2×15 mL) and brine, dried over MgSO₄ and concentrated under reduce pressure to give a yellowish liquid (554.7 mg, 94%).

3,4-dihydronaphthalen-1(2H)-one (42a):

$^1\text{H NMR}$ (400 MHz, CDCl_3): δ 8.03 (d, 1H, $J=7.9\text{Hz}$, ArH), 7.47 (td, 1H, $J=7.6\text{Hz}$, $J=1.1\text{Hz}$, ArH), 7.31 (t, 1H, $J=7.7\text{Hz}$, ArH), 7.25 (m, 1H, ArH), 2.97 (t, 2H, $J=5.9\text{ Hz}$, CH_2), 2.66 (t, 2H, $J=6.6\text{ Hz}$, CH_2), 2.14 (tt, 2H, $J=5.9\text{ Hz}$, $J=6.6\text{ Hz}$, CH_2) ppm

$^{13}\text{C NMR}$ (100 MHz, CDCl_3): δ 198.7, 144.8, 133.7, 132.9, 129.1, 127.5, 126.9, 39.5, 30.1, 23.6 ppm.

HRMS (ESI) m/z : $[\text{M}+\text{H}]^+$ calcd for $\text{C}_{10}\text{H}_{11}\text{O}_1$: 147.0804; found 147.0812.

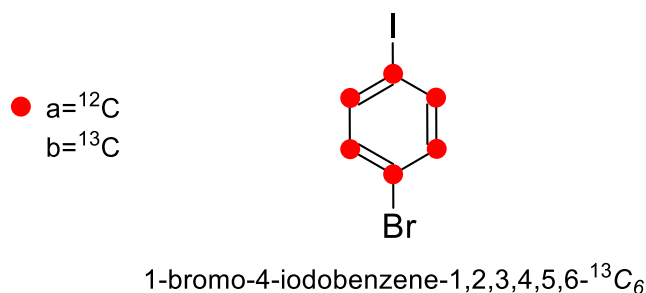
3,4-dihydronaphthalen-1(2H)-one- $^{13}\text{C}_{10}$ (42b):

$^1\text{H NMR}$ (400 MHz, CDCl_3): δ 8.03 (d, 1H, $J=106.1\text{Hz}$, ArH), 7.47 (m, 1H, $J=157.4\text{Hz}$, ArH), 7.31 (m, 1H, $J=162.4\text{Hz}$, ArH), 7.25 (m, 1H, $J=158.3\text{Hz}$, ArH), 2.96 (d, 2H, $J=132.3\text{ Hz}$, CH_2), 2.66 (dm, 2H, $J=127.7\text{Hz}$, $J=5.7\text{Hz}$, CH_2), 2.14 (d, 2H, $J=131.3$, CH_2) ppm

$^{13}\text{C NMR}$ (100 MHz, CDCl_3): δ 198.5(dd, $J=50.1\text{Hz}$, $J=41.0\text{Hz}$), 144.6(dd, $J=102.7\text{Hz}$, $J=50.4\text{Hz}$), 133.3(q, $J=51.9\text{Hz}$), 132.9(dd, $J=140.3\text{Hz}$, $J=57.8\text{Hz}$), 128.9(tq, $J=56.3\text{Hz}$, $J=3.0\text{Hz}$), 127.5(m), 126.9(m), 39.5(ddd, $J=42.1\text{Hz}$, $J=31.8\text{Hz}$, $J=12.2\text{Hz}$), 30.1(dd, $J=39.8\text{Hz}$, $J=34.5\text{Hz}$), 23.6(t, $J=33.2$) ppm.

ESI-MS m/z : $[\text{M}+\text{H}]^+$ calcd for $^{13}\text{C}_{10}\text{H}_{11}\text{O}_1$: 157.16; found 157.12.

Synthesis of 1-bromo-4-iodobenzene (43):



To a solution of 1,4-dibromobenzene-1,2,3,4,5,6- $^{13}\text{C}_6$ (1 equiv., 1000 mg, 4.13 mmol) in tetrahydrofuran (62.4 mL) at -78°C was added dropwise over 15 min a solution of *n*-butyllithium (1.03 equiv., 1.6 M in hexane, 2.66 mL, 4.26 mmol) under argon atmosphere. The reaction mixture was

added dropwise over 15 min to a solution of iodine (1.2 equiv., 1259 mg, 1.23 mL, 4.96 mmol) in 10 mL of tetrahydrofuran and stirred for 15 min at -78°C , and then for an additional 1 hour at room temperature. Saturated $\text{Na}_2\text{S}_2\text{O}_3$ was added and stirred for 15 min and the resulting mixture became colorless. The reaction mixture was partitioned in 20 mL of water and 30 mL of diethylether. The resulting aqueous layer was extracted with diethylether (4 \times 25 mL). The combined organic layers were dried over MgSO_4 and concentrated under reduced pressure. The crude product was purified by silica chromatography (100%, cyclohexane Rf: 0.89), white solid product was obtained (1355 mg, 76%).

1-bromo-4-iodobenzene (43a):

^1H NMR (400 MHz, CDCl_3): δ 7.55 (d, 2H, $J=8.5$ Hz, phenylH), 7.23 (d, 2H, $J=8.5$ Hz, phenylH) ppm.

^{13}C NMR (100 MHz, CDCl_3): δ 139.2, 133.5, 122.3, 92.1 ppm.

1-bromo-4-iodobenzene-1,2,3,4,5,6- $^{13}\text{C}_6$ (43b):

^1H NMR (400 MHz, CDCl_3): δ 7.54 (dq, 2H, $J=167.7$ Hz, $J=8.5$ Hz, phenylH), 7.22 (dq, 2H, $J=167.2$ Hz, $J=8.5$ Hz, phenylH) ppm.

^{13}C NMR (100 MHz, CDCl_3): δ 139.2 (ddd, $J=61.8\text{Hz}$, $J=54.1\text{Hz}$, $J=7.7\text{Hz}$), 133.5 (ddd, $J=62.4\text{Hz}$, $J=55.3\text{Hz}$, $J=7.7\text{Hz}$), 122.3 (td, $J=64.1\text{Hz}$, $J=11.1\text{Hz}$), 92.1 (td, $J=61.8\text{Hz}$, $J=11.1\text{Hz}$, $J=2.3\text{Hz}$) ppm.

Synthesis of 1-bromo-4-(trifluoromethyl)benzene (44):



1-bromo-4-(trifluoromethyl)benzene-1,2,3,4,5,6- $^{13}\text{C}_6$

N-Methyl-2-pyrrolidone (NMP) (50 mL) was added to 1-bromo-4-iodobenzene-1,2,3,4,5,6-¹³C₆ (1 equiv., 1278 mg, 4.42 mmol), copper(I) iodide (1.5 equiv., 1263 mg, 6.63 mmol) and methyl 2,2-difluoro-2-(fluorosulfonyl)acetate (5 equiv., 4249 mg, 2.82 mL, 22.12 mmol). The brown reacting mixture was heated and stirred at 80 °C under argon atmosphere for 16 hours. The reacting mixture was diluted by diethylether (25 mL) and filtered over celite. To the filtrate was added water and the aqueous layer was extracted with diethylether (4×25 mL). The organic layer was washed with water (2×25 mL) and brine, dried over MgSO₄ and concentrated under reduced pressure. The light-yellow oil crude was used in the next step.

1-bromo-4-(trifluoromethyl)benzene (44a):

¹H NMR (400 MHz, CDCl₃): δ 7.63 (d, 2H, *J*=8.3 Hz, phenylH), 7.49 (d, 2H, *J*=8.3 Hz, phenylH) ppm.

¹³C NMR (100 MHz, CDCl₃): δ 132.2, 129.7 (q, *J*=33.5 Hz), 127.0, 126.6, 124.0 (q, *J*=275.9 Hz, CF₃) ppm.

¹⁹F NMR (375 MHz, CDCl₃): δ -62.79 ppm.

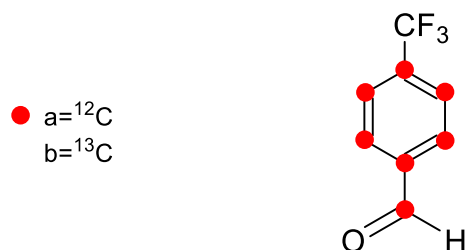
1-bromo-4-(trifluoromethyl)benzene-1,2,3,4,5,6-¹³C₆ (44b):

¹H NMR (400 MHz, CDCl₃): δ 7.63 (dq, 2H, *J*=167.1 Hz, *J*=7.3 Hz, phenylH), 7.49 (dq, 2H, *J*=161.0 Hz, *J*=9.1 Hz, phenylH) ppm.

¹³C NMR (100 MHz, CDCl₃): δ 132.2 (tt, *J*=59.9 Hz, *J*=6.5 Hz), 129.7 (dm, *J*=30.6 Hz, *J*=8.3 Hz), 127.0 (tt, *J*=56.3 Hz, *J*=4.9 Hz), 126.4 (td, *J*=56.2 Hz, *J*=9.6 Hz), 124.0 (q, *J*=275.9 Hz, CF₃) ppm.

¹⁹F NMR (375 MHz, CDCl₃): δ -62.78 (dtd, *J*=32.0 Hz, *J*=4.2 Hz, *J*=1.5 Hz) ppm.

Synthesis of 4-(trifluoromethyl)benzaldehyde (45):



4-(trifluoromethyl)benzaldehyde-1,2,3,4,5,6-¹³C₆

To a solution of 1-bromo-4-(trifluoromethyl)benzene-1,2,3,4,5,6-¹³C₆ (1 equiv., 1021 mg, 4.42 mmol) in tetrahydrofuran (4.42 mL) with Na₂SO₄ anhydrous (0.4 g), isopropylmagnesium bromide (0.53 equiv., 2.9 M in 2-methyltetrahydrofuran, 0.81 mL, 2.34 mmol) was added dropwise for 30 min under argon atmosphere at 0 °C. After 10 min stirring, *n*-butyllithium (1.06 equiv., 1.6 M in hexane, 2.93 mL, 4.69 mmol) was added dropwise for 30 min, and the reaction mixture was stirred for 1 hour at -10 °C. A solution of *N,N*-dimethylformamide-¹³C (1.3 equiv., 426 mg, 0.45 mL, 5.75 mmol) in tetrahydrofuran (4.42 mL) was added dropwise for 30 min to the mixture at -10 °C and the reaction mixture was stirred for 1 hour at room temperature. 1M citric acid solution (10 mL) was added to the mixture and the aqueous layer was extracted with diethylether (3×25 mL) and dried over MgSO₄ and concentrated under reduced pressure. The crude product was purified by silica chromatography (Pentane/Et₂O, 9/1 Rf: 0.63), the colorless oil was obtained (249 mg, 31%).

4-(trifluoromethyl)benzaldehyde (45a):

¹H NMR (400 MHz, CDCl₃): δ 10.1 (s, 1H, CHO), 8.01 (d, 2H, *J*=8.0 Hz, phenylH), 7.82 (d, 2H, *J*=8.0 Hz, phenylH) ppm.

¹³C NMR (400 MHz, CDCl₃): δ 191.2, 138.8, 135.8 (q, *J*=34.3 Hz), 130.1, 126.3, 124.9 ppm.

¹⁹F NMR (375 MHz, CDCl₃): δ -63.22 ppm.

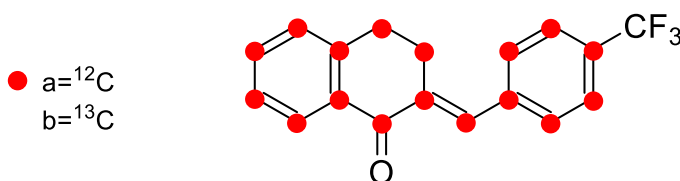
4-(trifluoromethyl)benzaldehyde-1,2,3,4,5,6-¹³C₆ (45b):

¹H NMR (400 MHz, CDCl₃): δ 10.1 (dd, 1H, *J*=177.0 Hz, *J*=24.1 Hz, CHO), 8.01 (dt, 2H, *J*=163.2 Hz, *J*=5.8 Hz, phenylH), 7.82 (dq, 2H, *J*=164.0 Hz, *J*=7.4 Hz, phenylH) ppm.

¹³C NMR (100 MHz, CDCl₃): δ 191.2 (dt, *J*=52.4Hz, *J*=4.0Hz), 138.8 (dtd, *J*=51.4Hz, *J*=58.7Hz, *J*=9.3Hz), 135.8 (m, *J*=31.1Hz), 130.1 (tt, *J*=58.0Hz, *J*=5.3Hz), 126.2 (tq, *J*=58.4Hz, *J*=3.7Hz), 124.9 ppm.

¹⁹F NMR (375 MHz, CDCl₃): δ -63.22 (dt, *J*=32.7 Hz, *J*=3.7 Hz,) ppm.

Synthesis of 2-(4-(trifluoromethyl)benzylidene)-3,4-dihydronaphthalen-1(2H)-one (46):



2-((4-(trifluoromethyl)phenyl-1,2,3,4,5,6-¹³C₆)methylene-¹³C)-3,4-dihydronaphthalen-1(2H)-one-¹³C₁₀

A mixture of 3,4-dihydronaphthalen-1(2H)-one-¹³C₁₀ (1 equiv., 159.5 mg, 1.02 mmol) and 4-(trifluoromethyl)benzaldehyde-1,2,3,4,5,6-¹³C₆ (1 equiv., 185 mg, 1.02 mmol) was stirred at room temperature. Then, KOH (1.2 equiv., 68.8 mg, 1.23 mmol) in ethanol (4 mL) was added dropwise to the mixture. The mixture was poured in 30 mL ice cold water and the white pure product precipitated. The product was filtrated, washed with ice cold water (2×5 mL) and dried under vacuum to yield a beige solid (248 mg, 76%). (TLC: cyclohexane/EtOAc, 8/2, R_f = 0.51).

2-(4-(trifluoromethyl)benzylidene)-3,4-dihydronaphthalen-1(2H)-one (46a):

¹H NMR (400 MHz, CDCl₃): δ 8.14 (1H, m, ArH), 7.85 (1H, s, olefineH), 7.68 (2H, d, *J*=8.1 Hz, phenylH), 7.53 (2H, d, *J*=8.1 Hz, phenylH), 7.52 (1H, m, ArH), 7.38 (1H, m, ArH), 7.27 (1H, m, ArH), 3.10 (2H, t, *J*=6.5 Hz, CH₂), 2.97 (2H, t, *J*=6.3 Hz, CH₂) ppm.

¹³C NMR (100 MHz, CDCl₃): δ 187.9, 143.5, 139.8, 137.7, 135.0, 133.9, 133.6, 130.3, 128.7, 128.6, 127.5, 125.7, 29.2, 27.5 ppm.

^{19}F NMR (375 MHz, CDCl_3): δ -62.70 ppm.

HRMS (ESI) m/z : $[\text{M}+\text{H}]^+$ calcd for $\text{C}_{18}\text{H}_{14}\text{F}_3\text{O}_1$: 303.0991; found 303.0971.

2-((4-(trifluoromethyl)phenyl-1,2,3,4,5,6- $^{13}\text{C}_6$)methylene- ^{13}C)-3,4-dihydronaphthalen-1(2H)-one- $^{13}\text{C}_{10}$ (46b):

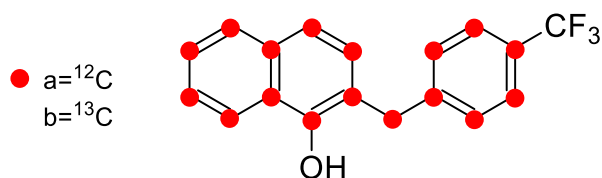
^1H NMR (400 MHz, CDCl_3): δ 8.14 (d, 1H, $J=157.7\text{Hz}$, ArH), 7.85 (d, 1H, $J=156.4\text{Hz}$, olefineH), 7.68 (d, 2H, $J=161.6\text{Hz}$, phenylH), 7.53 (d, 2H, $J=159.0\text{Hz}$, phenylH), 7.52 (1H, m, ArH), 7.38 (d, 1H, $J=155.1\text{Hz}$, ArH), 7.27 (d, 1H, $J=162.8\text{Hz}$, ArH), 3.19 (d, 2H, $J=56.8\text{Hz}$, CH_2), 2.88 (d, 2H, $J=56.8\text{Hz}$, CH_2) ppm.

^{13}C NMR (100 MHz, CDCl_3): δ 187.9(t, $J=52.0\text{Hz}$), 143.5(q, $J=51.3\text{Hz}$), 139.8(q, $J=57.1\text{Hz}$), 138.6-136.9(m), 134.7(q, $J=61.7\text{Hz}$), 134.0(q, $J=55.4\text{Hz}$), 133.7(t, $J=52.1\text{Hz}$), 130.3(t, $J=57.9\text{Hz}$), 128.7(m), 128.6(m), 127.5(m), 125.7(t, $J=60.8\text{Hz}$), 29.2(t, $J=37.0\text{Hz}$), 27.5(t, $J=37.0\text{Hz}$) ppm.

^{19}F NMR (375 MHz, CDCl_3): δ -62.70(td, $J=31.3\text{Hz}$, $J=3.2\text{Hz}$) ppm.

ESI-MS m/z : $[\text{M}+\text{H}]^+$ calcd for $^{13}\text{C}_{17}^{12}\text{C}_1\text{H}_{14}\text{F}_3\text{O}_1$: 320.20; found 320.16.

Synthesis of 2-(4-(trifluoromethyl)benzyl)naphthalen-1-ol (47):



2-((4-(trifluoromethyl)phenyl-1,2,3,4,5,6- $^{13}\text{C}_6$)methyl- ^{13}C)naphthalen-1-ol- $^{13}\text{C}_{10}$

2-((4-(trifluoromethyl)phenyl-1,2,3,4,5,6- $^{13}\text{C}_6$)methylene- ^{13}C)-3,4-dihydronaphthalen-1(2H)-one- $^{13}\text{C}_{10}$ (1 equiv., 223 mg, 0.699 mmol) was solubilized in well degassed ethanol (15 mL). Trichlororhodium trihydrate (0.15 equiv., 27.6 mg, 0.105 mmol) was added. The mixture was reflux under argon atmosphere and stirred for 5 hours. The mixture was evaporated and the resulting mixture was dissolved in ethyl acetate and extracted with water. The aqueous layer was washed with ethyl

acetate (3×25 mL). The organic layer was combined and washed with brine, dried over MgSO₄ and concentrated under reduced pressure. The crude product was purified by silica chromatography (cyclohexane/EtOAc, 9/1, R_f = 0.50) to give the light-yellow solids (175 mg, 78%).

2-(4-(trifluoromethyl)benzyl)naphthalen-1-ol (47a):

¹H NMR (400 MHz, CDCl₃): δ 8.05 (d, 1H, *J*=8.0 Hz, ArH), 7.83 (d, 1H, *J*=7.83 Hz, ArH), 7.54 (d, 2H, *J*=7.7 Hz, phenylH), 7.51-7.45 (m, 3H, ArH), 7.36 (d, 2H, *J*=7.9 Hz, phenylH), 7.28-7.23 (m, 1H, ArH), 5.26 (s, 1H, OH), 4.23 (s, 2H, CH₂) ppm.

¹³C NMR (100 MHz, CDCl₃): δ 149.0, 144.4, 134.2, 129.2, 129.1 (q, *J*=33.0 Hz), 129.0, 128.3, 126.3, 126.0, 125.9 (q, *J*=3.0 Hz), 125.0, 124.4 (q, *J*=265.0 Hz), 121.3, 120.8, 120.0, 36.5 ppm.

¹⁹F NMR (375 MHz, CDCl₃): δ -62.43 ppm.

HRMS (ESI) m/z: [M+H]⁺ calcd for C₁₈H₁₄F₃O₁: 303.0991; found 303.0996.

2-((4-(trifluoromethyl)phenyl-1,2,3,4,5,6-¹³C₆)methyl-¹³C)naphthalen-1-ol-¹³C₁₀ (47b):

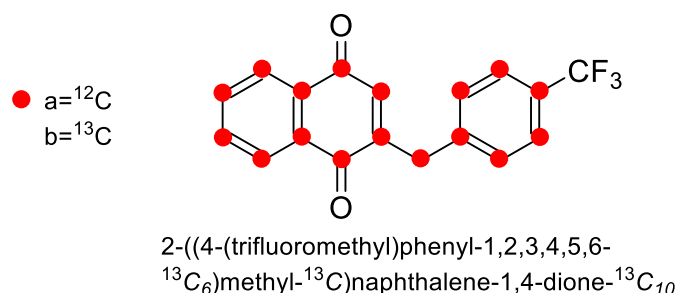
¹H NMR (400 MHz, CDCl₃): δ 8.04 (dm, 1H, *J*=154.5 Hz, ArH), 7.83 (dm, 1H, *J*=154.0 Hz, ArH), 7.54 (dm, 2H, *J*=156.1 Hz, phenylH), 7.46 (dm, 3H, *J*= 154.5 Hz, ArH), 7.35 (dm, 2H, *J*=156.1 Hz, phenylH), 7.25 (dm, 1H, *J*= 154.5 Hz, ArH), 5.14 (q, 1H, *J*=3.7 Hz, OH), 4.23 (d, 2H, *J*=129.1 Hz, CH₂) ppm.

¹³C NMR (100 MHz, CDCl₃): δ 149.0 (t, *J*=68.4 Hz), 144.3 (ddm, *J*=99.6 Hz, *J*=53.0 Hz), 134.1 (q, *J*=54.3 Hz), 129.4 (tm, *J*=58.3 Hz), 129.1 (q, *J*=33.0 Hz), 129.0 (tm, *J*=59.7 Hz), 128.3 (tm, *J*=56.1 Hz), 126.4 (tm, *J*=54.1 Hz), 125.7 (tm, *J*=53.6 Hz), 125.9 (qm, *J*=31.7 Hz), 124.9 (qm, *J*=61.1 Hz), 124.4 (q, *J*=265.0 Hz), 121.3 (tm, *J*=59.8 Hz), 120.7 (tm, *J*=56.5 Hz), 119.9 (qm, *J*=61.3 Hz), 36.5 (t, *J*=44.3 Hz) ppm.

¹⁹F NMR (375 MHz, CDCl₃): δ -62.44 (dt, *J*=32.1 Hz, *J*=3.1 Hz) ppm.

ESI-MS m/z: [M+H]⁺ calcd for ¹³C₁₇¹²C₁H₁₄F₃O₁: 320.23; found 320.16.

Synthesis of 2-(4-(trifluoromethyl)benzyl)naphthalene-1,4-dione (48):



2-((4-(trifluoromethyl)phenyl-1,2,3,4,5,6-¹³C₆)methyl-¹³C)naphthalen-1-ol-¹³C₁₀ (1 equiv., 160 mg, 0.501 mmol) was solubilized in 8.7 mL of a solution of acetonitrile-water (3:1). Phenyliodonium Diacetate (2 equiv., 323 mg, 1.00 mmol) was added in 10 min at -5°C. The reaction mixture was stirred at -5°C for 30 min and warm to room temperature for 1 hour. The reaction mixture was concentrated using a rotavap to evaporate acetonitrile and 10 mL of saturated NaHCO₃ was added. The resulting mixture was extracted with diethylether, the aqueous layer was washed with diethylether (3×10 mL) and the organic layer was washed with brine (2×10 mL), dried over MgSO₄ and concentrated under reduced pressure. The crude product was purified by silica chromatography (cyclohexane/EtOAc 8.5/1.5, R_f = 0.39) to yield a yellow solid (127 mg, 76%).

2-(4-(trifluoromethyl)benzyl)naphthalene-1,4-dione (48a):

¹H NMR (400 MHz, CDCl₃): δ 8.13-8.04 (m, 2H, ArH), 7.76-7.72 (m, 2H, ArH), 7.59 (d, 2H, *J*=8.0 Hz, phenylH), 7.39 (d, 2H, *J*=8.1 Hz, phenylH), 6.63 (s, 1H, ArH), 3.95 (s, 2H, CH₂) ppm.

¹³C NMR (100 MHz, CDCl₃): δ 185.2, 185.1, 150.1, 141.3, 136.2, 134.3, 134.2, 132.4, 130.1, 129.7 (q, *J*=32.5 Hz), 127.1, 126.6, 126.1 (q, *J*=3.83 Hz), 124.4 (q, *J*=274.9 Hz) 36.0 ppm.

¹⁹F NMR (375 MHz, CDCl₃): δ -62.55 ppm.

HRMS (ESI) m/z: [M+H]⁺ calcd for C₁₈H₁₂F₃O₂: 317.0784; found 317.0791.

2-((4-(trifluoromethyl)phenyl-1,2,3,4,5,6-¹³C₆)methyl-¹³C)naphthalene-1,4-dione-¹³C₁₀ (48b):

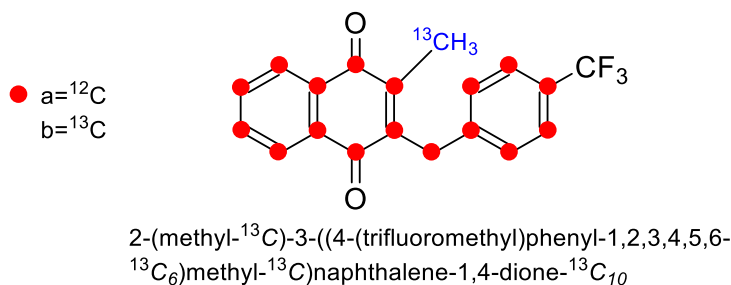
¹H NMR (400 MHz, CDCl₃): δ 8.08 (dm, 2H, *J*=157.4 Hz, ArH), 7.74 (dm, 2H, *J*=157.3 Hz, ArH), 7.59 (dm, 2H, *J*=157.3 Hz, phenylH), 7.39 (d, 2H, *J*=157.5 Hz, phenylH), 6.63 (dm, 1H, *J*=159.0 Hz ArH), 3.96 (d, 2H, *J*=130.4 Hz, CH₂) ppm.

¹³C NMR (100 MHz, CDCl₃): δ 185.2 (t, *J*=49.0 Hz), 185.1 (t, *J*=49.0 Hz), 150.1 (qm, *J*=52.7 Hz), 141.3 (qm, *J*=51.6 Hz), 136.9-135.4 (m), 135.0-133.4 (m), 132.4 (tm, *J*=41.3 Hz), 130.1 (tm, *J*=53.9 Hz), 129.2 (qd, *J*=29.2 Hz, *J*=8.6 Hz), 126.9 (tm, *J*=59.1 Hz), 126.3 (tm, *J*=53.8 Hz), 126.1 (tm, *J*=55.7 Hz), 36.0 (t, *J*=44.3 Hz) ppm.

¹⁹F NMR (375 MHz, CDCl₃): δ -62.56 (dt, *J*=31.8 Hz, *J*=3.5 Hz) ppm.

ESI-MS m/z: [M+H]⁺ calcd for ³C₁₇¹²C₁H₁₂F₃O₂: 334.21; found 334.14 m/z.

Synthesis of 2-(methyl-¹³C)-3-(4-(trifluoromethyl)phenyl)naphthalene-1,4-dione (49):



2-((4-(trifluoromethyl)phenyl)-1,2,3,4,5,6-¹³C₆)methyl-¹³C)naphthalene-1,4-dione-¹³C₁₀ (1 equiv., 108.3 mg, 0.325 mmol) and acetic-2-¹³C acid (5 equiv., 99.2 mg, 0.095 mL, 1.63 mmol) were solubilized in 14 mL of a solution acetonitrile-water (3:1). The reaction mixture was heated at 85°C and silver nitrate (0.35 equiv., 19.3 mg, 0.114 mmol) was added. Ammonium persulfate (1.3 equiv., 96.4 mg, 0.423 mmol) in a solution of acetonitrile-water (3:1) was added dropwise. The reaction mixture was stirred for 90 min. The resulting mixture was evaporated and 10 mL of dichloromethane was added. The aqueous layer was extracted with dichloromethane (3×10 mL) and the organic layers were combined and extracted with brine, dried over MgSO₄ and concentrated under reduced pressure. The crude product was purified by silica chromatography (toluene, R_f=0.51) and recrystallization (n-hexane, 50 mL) to give a pure yellow solid (52.1 mg, 46%).

2-(methyl-¹³C)-3-(4-(trifluoromethyl)benzyl)naphthalene-1,4-dione (49a):

¹H NMR (400 MHz, CDCl₃): δ 8.10-8.06 (m, 2H, ArH), 7.72-7.70 (m, 2H, ArH), 7.52 (d, 2H, *J*=8.2 Hz, phenylH), 7.34 (d, 2H, *J*=8.1 Hz, phenylH), 4.08 (s, 2H, CH₂), 2.25 (s, 3H, CH₃) ppm.

¹³C NMR (100 MHz, CDCl₃): δ 185.2, 184.6 (d, *J*=3.6 Hz), 145.0 (d, *J*=45 Hz), 144.5, 142.3, 133.8, 132.2, 132.0, 129.0, 129.0 (q, *J*=32.3 Hz, C-CF₃), 126.6, 126.5, 125.7, 125.7, 124.3 (q, *J*=273.0 Hz, CF₃), 32.5 (d, *J*=2.2 Hz), 13.5 (t, *J*=21.5 Hz) ppm.

¹⁹F NMR (375 MHz, CDCl₃): -62.49 ppm.

ESI-MS m/z: [M+H]⁺ calcd for ¹³C¹²C₁₈H₁₄F₃O₂: 332.10; found 332.09.

2-(methyl-¹³C)-3-((4-(trifluoromethyl)phenyl-1,2,3,4,5,6-¹³C₆)methyl-¹³C)-naphthalene-1,4-dione-¹³C₁₀ (49b):

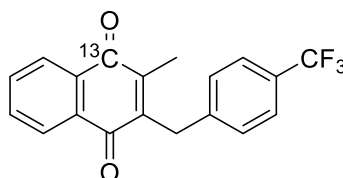
¹H NMR (400 MHz, CDCl₃): δ 8.09 (dm, 2H, *J*=167.0 Hz, ArH), 7.721 (dm, 2H, *J*=148.5 Hz, ArH), 7.52 (dm, 2H, *J*=160.8 Hz, phenylH), 7.35 (dm, 2H, *J*=151.6 Hz, phenylH), 4.09 (d, 2H, *J*=129.5 Hz, CH₂), 2.25 (d, 3H, *J*=131.6 Hz, CH₃) ppm.

¹³C NMR (100 MHz, CDCl₃): δ 185.2 (t, *J*=48.8 Hz), 184.7 (t, *J*=49.9 Hz), 146.1-143.4 (m), 143.3-141.3 (m), 134.6-132.8 (m), 132.8-130.9 (m), 129.9-128.1 (tm, *J*=58.0 Hz), 127.4-125.8 (m), 125.6 (t, *J*=56.1 Hz), 32.5 (t, *J*=42.6 Hz), 13.9-13.1 (m) ppm.

¹⁹F NMR (375 MHz, CDCl₃): -62.51 ppm (dt, *J*=31.6 Hz, *J*=3.0 Hz).

ESI-MS (Q-TOF) m/z: [M+H]⁺ calcd for ¹³C₁₈¹²C₁H₁₄F₃O₂: 349.15; found 349.1546.

Synthesis of 2-methyl-3-(4-(trifluoromethyl)benzyl)naphthalene-1,4-dione-1-¹³C (49c):



2-methyl-3-(4-(trifluoromethyl)benzyl)naphthalene-1,4-dione-1-¹³C

2-methylnaphthalene-1,4-dione-1-¹³C (1 equiv., 108.3 mg, 0.325 mmol) and 2-(4-(trifluoromethyl)phenyl)acetic acid (5 equiv., 99.2 mg, 0.095 mL, 1.63 mmol) were solubilized in 14 mL of a solution acetonitrile-water (3:1). The reaction mixture was heated at 85°C and silver nitrate (0.35 equiv., 19.3 mg, 0.114 mmol) was added. Ammonium persulfate (1.3 equiv., 96.4 mg, 0.423 mmol), in a solution of acetonitrile-water (3:1), was added dropwise. The reaction mixture was stirred for 3 hours. The resulting mixture was evaporated and 10 mL of dichloromethane was added. The aqueous layer was extracted with dichloromethane (3×10 mL) and the organic layer were combined and extracted with brine, dried over MgSO₄ and concentrated under reduced pressure. The crude product was purified by silica chromatography (toluene, R_f=0.51) and recrystallization (*n*-hexane, 50 mL) to give a pure yellow solid (52.1 mg, 46%).

2-methyl-3-(4-(trifluoromethyl)benzyl)naphthalene-1,4-dione-1-¹³C (49c):

¹H NMR (400 MHz, CDCl₃): δ 8.13-8.06 (m, 2H, ArH), 7.75-7.68 (m, 2H, ArH), 7.52 (d, 2H, *J*=8.2 Hz, phenylH), 7.35 (d, 2H, *J*=8.1 Hz, phenylH), 4.08 (s, 2H, CH₂), 2.25 (d, 3H, *J*=3.7 Hz, CH₃) ppm.

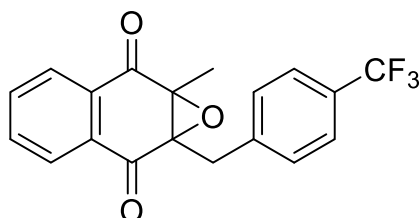
¹³C NMR (100 MHz, CDCl₃): δ 185.3 (t, *J*=50.7 Hz), 185.1-184.7 (m), 145.0 (d, *J*=50.1 Hz), 144.7, 142.5, 134.0, 132.2 (d, *J*=54.0 Hz), 132.1, 129.2, 129.1 (q, *J*=33.0 Hz, C-CF₃), 126.7 (d, *J*=2.7 Hz), 126.7, 125.9, 125.9, 124.4 (q, *J*=269.6 Hz, CF₃), 32.7 (d, *J*=3.4 Hz), 13.7 ppm.

¹⁹F NMR (375 MHz, CDCl₃): -62.32 ppm.

EI-MS m/z: [M]⁺ calcd for ¹³C¹²C₁₈H₁₃F₃O₂: 331.10; found 331.10.

3. Synthesis of putative drug metabolites

Synthesis of 1a-methyl-7a-(4-(trifluoromethyl)benzyl)-1a,7a-dihydronaphtho[2,3-*b*]oxirene-2,7-dione (50):



1a-methyl-7a-(4-(trifluoromethyl)benzyl)-
1a,7a-dihydronaphtho[2,3-*b*]oxirene-2,7-dione

2-methyl-3-{{[4-(trifluoromethyl)phenyl]methyl}}-1,4-dihydronaphthalene-1,4-dione (1 equiv., 300 mg, 0.908 mmol) was dissolved in a mixture of solvent: distilled water (1 mL) and methanol (4 mL) (MeOH/H₂O 4:1). Then sodium hydroxide (0.5 equiv., 3 M, 0.151 mL, 0.454 mmol) was added to the mixture at 0°C. The resulting mixture was stirred for 10 min and subsequently H₂O₂ (1.5 eq., 132 mg, 0.13 mL, 1.36 mmol) was added. The reaction mixture was stirred at 0°C for 3 hours. The reaction was quenched by 10 mL of distilled water. The resulting mixture was extracted by diethyl ether (3×10 mL), the organic phase was extracted with brine, dried over MgSO₄ and concentrated under reduced pressure. The crude product was purified by recrystallization (Et₂O/*n*-hexane, 1/3, 20 mL) to give a pure white crystal. (185 mg, 59%).

1a-methyl-7a-(4-(trifluoromethyl)benzyl)-1a,7a-dihydronaphtho[2,3-*b*]oxirene-2,7-dione (50):

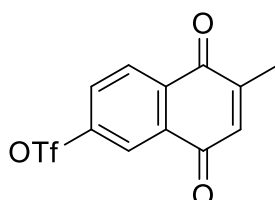
¹H NMR (400 MHz, CDCl₃): δ 8.02-7.91 (m, 2H, ArH), 7.78-7.69 (m, 2H, ArH), 7.55 (d, *J*=8.1 Hz, 2H, phenylH), 7.46 (d, *J*=8.1 Hz, 2H, phenylH), 3.67 (d, *J*=15.0 Hz, 1H, CH₂), 3.40 (d, *J*=15.0 Hz, 1H, CH₂), 1.84 (s, 3H, CH₃) ppm.

¹³C NMR (100 MHz, CDCl₃): δ 192.5, 192.2, 140.0, 134.6, 134.5, 132.1, 132.0, 129.8, 129.3 (q, *J*=32.3 Hz, C-CF₃), 127.4, 127.3, 125.6, 125.5, 124.2 (q, *J*=254.6 Hz, CF₃), 67.3, 65.9, 31.9, 12.7 ppm.

¹⁹F NMR (375 MHz, CDCl₃): -62.56 ppm.

ESI-MS (Q-TOF) m/z: $[M+H]^+$ calcd for $C_{19}H_{15}F_3O_3$: 347.08; found 347.0894.

Synthesis of 6-methyl-5,8-dioxo-5,8-dihydronaphthalen-2-yl trifluoromethane-sulfonate (53a):



6-methyl-5,8-dioxo-5,8-dihydronaphthalen-2-yl
trifluoromethane-sulfonate

To a solution of 6-hydroxy-2-methyl-1,4-dihydronaphthalene-1,4-dione (1 equiv., 100 mg, 0.531 mmol) in dry CH_2Cl_2 (17.5 mL) was added dropwise pyridine (2 equiv., 84.1 mg, 0.086 mL, 1.06 mmol) at 0 °C under an argon atmosphere. After 10 min, trifluoromethanesulfonic anhydride (1.5 equiv., 224 mg, 0.132 mL, 0.797 mmol) was added to the resulting mixture. The mixture was warmed to room temperature and stirred for 2 hours. The reaction mixture was treated with a solution of 5% $NaHCO_3$ (1 mol/L). The mixture extracted with CH_2Cl_2 . The organic phases were dried with $MgSO_4$ and concentrated in vacuo to afford menadione triflate as a yellow solid (161.7 mg, 95%).

6-methyl-5,8-dioxo-5,8-dihydronaphthalen-2-yl trifluoromethane-sulfonate (53a):

1H NMR (400 MHz, $CDCl_3$): δ = 8.19 (d, 1H, $J=8.4$ Hz, ArH), 7.98 (d, 1H, $J=2.4$ Hz, ArH), 7.62 (dd, 1H, $J=8.4$ Hz, $J=2.4$ Hz, ArH), 6.91 (q, 1H, $J=1.6$ Hz, ArH), 2.23 (d, 3H, $J=1.6$ Hz, CH_3) ppm.

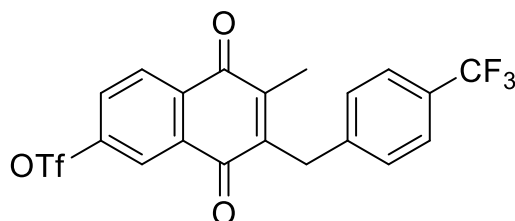
^{13}C NMR (100 MHz, $CDCl_3$): δ = 183.70 (C=O), 183.10 (C=O), 152.91 (C_q), 148.71 (C_q), 135.84 (CH), 134.30 (C_q), 131.65 (C_q), 129.13 (CH), 126.41 (CH), 119.37 (CH), 118.69 (q, $J_{C-F} = 318.9$ Hz, CF_3), 16.51 (CH_3) ppm.

^{19}F NMR (375 MHz, $CDCl_3$): δ = 72.65 ppm.

HRMS-ESI (m/z): $[M+H]^+$ calcd for $C_{12}H_8F_3O_5S$: 321.0039, found 321.0085.

m.p. 82-84 °C (from petroleum ether/ethyl acetate)

Synthesis of 6-methyl-5,8-dioxo-7-[[4-(trifluoromethyl)phenyl]methyl]-5,8-dihydronaphthalen-2-yl trifluoromethanesulfonate (54a):



6-methyl-5,8-dioxo-7-[[4-(trifluoromethyl)phenyl]methyl]-5,8-dihydronaphthalen-2-yl trifluoromethanesulfonate

6-methyl-5,8-dioxo-5,8-dihydronaphthalen-2-yl trifluoromethanesulfonate (1 equiv., 177 mg, 0.555 mmol) and 4-(trifluoromethyl)phenylacetic acid (2 equiv., 226 mg, 1.11 mmol) were solubilized in 11.5 mL of a solution acetonitrile-water (3:1). The mixture was heated at 85°C and silver nitrate (0.35 equiv., 33 mg, 0.194 mmol) was added. Then, ammonium persulfate (1.3 equiv., 164 mg, 0.0832 mmol), in 3.8 mL of a solution acetonitrile-water (3:1), was added dropwise. The reaction was stirred for 4.5 hours. The resulting mixture was evaporated, and then 20 mL of dichloromethane was added and the two phases were separated. The aqueous layer was extracted with dichloromethane (3×10 mL) and the organic layer were combined and extracted with brine, dried over MgSO₄ and concentrated under reduced pressure. The crude product was purified by silica chromatography (toluene, R_f=0.51) to give a pure yellow solid (193 mg, 73%).

6-methyl-5,8-dioxo-7-[[4-(trifluoromethyl)phenyl]methyl]-5,8-dihydronaphthalen-2-yl trifluoromethanesulfonate (54a):

¹H NMR (300 MHz, CDCl₃): δ = 8.23 (d, 1H, *J* = 8.4 Hz, ArH), 7.97 (d, 1H, *J* = 2.7 Hz, ArH), 7.60 (dd, 1H, *J* = 8.4 Hz, *J* = 8.4 Hz, ArH), 7.46 (d, 2H, *J* = 8.3 Hz, phenylH), 7.27 (d, 2H, *J* = 8.3 Hz, phenylH), 4.10 (s, 2H, CH₂), 2.28 (s, 3H, CH₃) ppm.

¹³C NMR (75 MHz, CDCl₃): δ = 183.41 (C=O), 182.64 (C=O), 152.93 (C_q), 145.38 (C_q), 144.97 (C_q), 141.62 (C_q), 134.03 (C_q), 131.45 (C_q), 129.36 (CH), 129.18 (q, *J* = 34.35 Hz, C_q), 128.90 (2xCH),

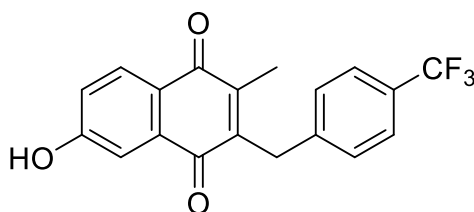
126.41 (CH), 125.71 (q, $J=3.3$ Hz, 2xCH), 124.17 (q, $J=264.53$ Hz, CF₃), 119.33 (CH), 118.39 (q, $J=317.7$ Hz, S-CF₃), 32.46 (CH₂), 13.46 (CH₃) ppm.

¹⁹F NMR (375 MHz, CDCl₃): $\delta = -62.55, -72.67$ ppm.

elemental analysis calcd (%) for C₂₀H₁₂F₆O₅S: C, 50.22; H, 2.83; found C 50.14, H 2.82

m.p. 127-129 °C (from hexane/EtOAc).

Synthesis of 6-hydroxy-2-methyl-3-[[4-(trifluoromethyl)phenyl]methyl]-1,4-dihydronaphthalene-1,4-dione (55a):



6-hydroxy-2-methyl-3-(4-(trifluoromethyl)benzyl)naphthalene-1,4-dione

To a solution of 6-methyl-5,8-dioxo-7-[[4-(trifluoromethyl)phenyl]methyl]-5,8-dihydronaphthalen-2-yl trifluoromethanesulfonate (1 equiv., 190 mg, 0.397 mmol) in THF (1.9 mL), tetrabutylammonium fluoride trihydrate (3 equiv., 375 mg, 1.19 mmol) was added and stirred for 3 hours. The resulting mixture was diluted with EtOAc (10 mL) and THF was evaporated. The mixture was neutralized with a solution of HCl (1M). The organic layer was separated and dried over anhydrous MgSO₄, concentrated in vacuo and purified by column of silica chromatography EtOAc /Cyclohexane 4:1 (Rf: 0.16) to give the yellow solid (127.9 mg, 93%).

6-hydroxy-2-methyl-3-[[4-(trifluoromethyl)phenyl]methyl]-1,4-dihydronaphthalene-1,4-dione (55a):

¹H NMR (400 MHz, CDCl₃): $\delta = 8.04$ (d, 1H, $J=8.5$ Hz, ArH), 7.52 (d, 2H, $J=8.2$ Hz, phenylH), 7.46 (d, 1H, $J=2.5$, ArH), 7.33 (d, 2H, $J=7.9$ Hz, phenylH), 7.13 (dd, 1H, $J=8.5$ Hz, $J=2.7$ Hz, ArH), 5.70 (s, 1H, OH), 4.06 (s, 2H, CH₂), 2.23 (s, 3H, CH₃) ppm.

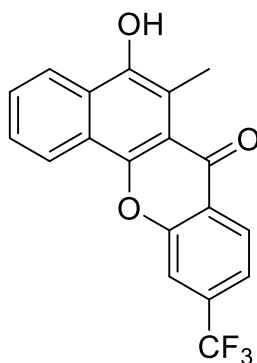
¹³C NMR (100 MHz, DMSO-*D*₆): δ = 184.69 (C=O), 183.85 (C=O), 163.11 (C_q), 145.50 (C_q), 143.56 (C_q), 143.09 (C_q), 134.09 (C_q), 129.55 (2xCH), 129.44 (CH), 127.39 (q, *J* = 30.9 Hz, C_q), 125.80 (q, *J* = 3.3 Hz, 2xCH), 125.75 (C_q), 124.77 (q, *J* = 270.6 Hz, CF₃), 121.18 (CH), 112.25 (CH), 32.13 (CH₂), 13.52 (CH₃) ppm.

¹⁹F NMR (375 MHz, CDCl₃): δ = 62.49 ppm.

HRMS (ESI) m/z: [M+Na]⁺ calcd for C₁₉H₁₃F₃O₃Na 369.0709; found 369.0672.

m.p. >200 °C (from hexane/EtOAc).

Synthesis of 5-hydroxy-6-methyl-10-(trifluoromethyl)-7H-benzo[*c*]xanthen-7-one (60):



5-hydroxy-6-methyl-10-(trifluoromethyl)-7H-benzo[*c*]xanthen-7-one

To a solution of 10-(methoxymethoxy)-11-methyl-3-(trifluoromethyl)-12H-5-oxatetraphen-12-one (1 equiv., 73 mg, 0.188 mmol) in isopropanol (11.4 mL), HCl (1.2 equiv., 1.25 M, 0.18 mL, 0.226 mmol) was added dropwise. The mixture was stirred for 24 hours, evaporated in vacuum. The resulting crude product was recrystallized in cyclohexane and ethyl acetate (5 mL) to give a yellow solid (60.7 mg, 94%).

5-hydroxy-6-methyl-10-(trifluoromethyl)-7H-benzo[*c*]xanthen-7-one (60):

¹H NMR (400 MHz, DMSO-*D*₆): δ = 9.37 (s, 1H, OH), 8.79 (d, 1H, *J*=8.2 Hz, ArH), 8.42 (d, 2H, *J*=8.1 Hz, ArH), 8.38 (d, 1H, *J*=8.1 Hz, ArH), 7.91-7.77 (m, 3H, ArH), 2.88 (s, 3H, CH₃) ppm.

¹³C NMR (75 MHz, DMSO-D₆): δ = 176.87 (C=O), 153.74 (C_q), 148.96 (C_q), 146.30 (C_q), 133.43 (d, J = 32 Hz, C-CF₃), 129.66 (CH), 128.97 (C_q), 127.57 (CH), 126.60 (CH), 124.73 (C_q), 123.37 (q, J = 273 Hz, CF₃), 122.72 (CH), 122.37 (C_q), 122.30 (CH), 120.10 (CH), 116.92 (C_q), 115.92 (C_q), 115.88 (d, J = 3.9 Hz, CH), 14.01 (CH₃) ppm.

¹⁹F NMR (375 MHz, DMSO-D₆): δ = 61.43 ppm.

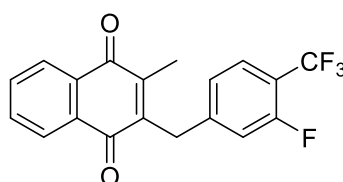
Elemental analysis %: calcd for C₁₉H₁₁O₃F₃ C 66.28, H 3.22; found C 66.28 H 3.58.

HRMS (ESI) m/z: [M+H]⁺ calcd for C₁₉H₁₂F₃O₃ 345.0739; found 345.0733.

m.p. 229-231 °C (from cyclohexane/EtOAc).

4 Synthesis of 3'-(oxetane-3-yloxy)plasmodione

Synthesis of 2-(3-fluoro-4-(trifluoromethyl)benzyl)-3-methylnaphthalene-1,4-dione (71)



2-(3-fluoro-4-(trifluoromethyl)benzyl)-3-methylnaphthalene-1,4-dione

Menadione (1 equiv., 1937 mg, 11.3 mmol) and 2-[3-fluoro-4-(trifluoromethyl)-phenyl]acetic acid (2 equiv., 5000 mg, 22.5 mmol) were solubilized in a solution of acetonitrile-water (3:1, 231 mL). The mixture was heated at 85°C and silver nitrate (0.35 equiv., 669 mg, 3.94 mmol) was added. Then, the ammonium persulfate (1.3 equiv., 3338 mg, 14.6 mmol), dissolved in a solution of acetonitrile-water (3:1, 77 mL), was added dropwise to the resulting mixture. The reaction mixture was stirred for 4.5 hours. The resulting mixture was evaporated and 50 mL of dichloromethane was added. The aqueous layer was extracted with dichloromethane (4×50 mL) and the organic layer were combined and extracted with brine, dried over MgSO₄ and concentrated under reduced pressure.

The crude product was purified by silica chromatography (toluene, R_f=0.50) and recrystallization (*n*-hexane, 800 mL) gave a pure yellow solid (3214 mg, 82%).

2-(3-fluoro-4-(trifluoromethyl)benzyl)-3-methylnaphthalene-1,4-dione (71):

¹H NMR (400 MHz, CDCl₃): δ = 8.15-8.06 (m, 2H, ArH), 7.76-7.69 (m, 2H, ArH), 7.50 (t, 1H, *J*=7.7 Hz, phenylH), 7.12 (d, 1H, *J*=8.0 Hz, phenylH), 7.07 (d, 1H, *J*=11.2 Hz, phenylH), 4.07 (s, 2H, CH₂), 2.25 (s, 3H, CH₃) ppm.

¹³C NMR (100 MHz, CDCl₃): δ = 185.3 (CO), 184.7 (CO), 160.2 (d, *J*=255.1 Hz, C-F), 145.6 (Cq), 145.5 (Cq), 144.0 (Cq), 134.1 (CH), 134.1 (CH), 132.4 (Cq), 132.1 (Cq), 127.6 (q, *J*=3.1 Hz, CH), 126.9 (CH), 126.8 (CH), 124.5 (d, *J*=3.0 Hz, CH), 122.9 (q, *J*=268.8 Hz, CF₃), 117.3 (d, *J*=21.0 Hz, CH), 116.9 (dd, *J*=32.9 Hz, *J*=12.3 Hz, C-CF₃), 32.6 (CH₂), 13.8 (CH₃) ppm.

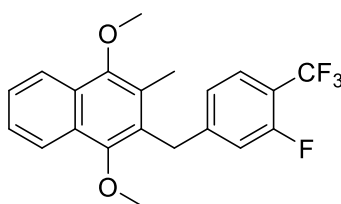
¹⁹F NMR (375 MHz, CDCl₃): δ = -61.23 (d, 3F, *J*=12.3 Hz, CF₃), -114.12 (q, 1F, *J*=12.4 Hz, phenylF) ppm.

HRMS (ESI) m/z: [M+H]⁺ calcd for C₁₉H₁₃F₄O₂ 349.0846; found 349.0811.

Elemental analysis %: calcd for C₁₉H₁₂F₄O₂ C 65.52, H 3.47; found C 65.35, H 3.49.

m.p. 92°C-93 °C (from *n*-hexane).

Synthesis of 2-(3-fluoro-4-(trifluoromethyl)benzyl)-1,4-dimethoxy-3-methyl-naphthalene (72):



2-(3-fluoro-4-(trifluoromethyl)benzyl)-1,4-dimethoxy-3-methylnaphthalene

2-(3-fluoro-4-(trifluoromethyl)benzyl)-3-methylnaphthalene-1,4-dione (1 equiv., 2600 mg, 7.47 mmol) was suspended in ethanol (29.1 mL) under argon atmosphere. Then, stannous chloride (3 equiv.,

4242 mg, 1.07 mL, 22.4 mmol) was dissolved in conc. HCl (8.01 equiv., 6056 mg, 5.05 mL, 59.8 mmol) and added dropwise to the resulting solution and the reaction mixture was stirred for 2 hours at room temperature until a white solid appeared. The solvent of the mixture was removed in vacuum. The resulting white solid was washed with distilled water and filtrated. Then, the resulting crude product was redissolved in acetone (36.4 mL) under argon atmosphere and dimethylsulfate (3 equiv., 2824 mg, 2.12 mL, 22.4 mmol) was added. Subsequently, a solution of KOH (5 equiv., 2094 mg, 37.3 mmol) in methanol (16.6 mL) was added dropwise for 1 hour to the previous mixture at 60°C and the mixture was stirred for 4 hours. The reaction was quenched by adding KOH solution (3.5 M, 17 mL), the colour of the mixture was changed obviously to dark brown. The resulting mixture was extracted with dichloromethane (5×35 mL), dried over MgSO₄ and concentrated under reduced pressure. The crude product was purified by silica chromatography (cyclohexane/dichloromethane, 7/3, R_f=0.48) to give a pure light yellow oil (2686 mg, 95%).

2-(3-fluoro-4-(trifluoromethyl)benzyl)-1,4-dimethoxy-3-methyl-naphthalene (72):

¹H NMR (400 MHz, CDCl₃): δ = 8.14-8.05 (m, 2H, ArH), 7.56-7.49 (m, 2H, ArH), 7.46 (t, 1H, *J*=7.8 Hz, phenylH), 7.01 (d, 1H, *J*=8.2 Hz, phenylH), 6.94 (d, 1H, *J*=11.5 Hz, phenylH), 4.30 (s, 2H, CH₂), 3.87 (s, 3H, OCH₃), 3.85 (s, 3H, OCH₃), 2.25 (s, 3H, CH₃) ppm.

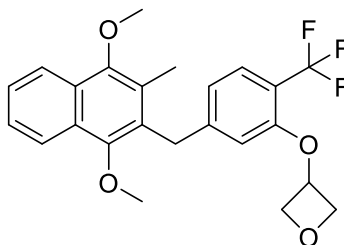
¹³C NMR (100 MHz, CDCl₃): δ = 159.9 (d, *J*=256.3 Hz, C-F), 151.0 (d, *J*=6.5 Hz, Cq), 148.4 (Cq), 148.3 (Cq), 128.7 (Cq), 127.8 (Cq), 127.5 (Cq), 127.3 (q, *J*=3.1 Hz, CH), 126.7 Hz (Cq), 126.5 (CH), 126.0 (CH), 124.0 (d, *J*=2.6 Hz, CH), 123.1 (q, *J*=272.4 Hz, CF₃), 122.9 (CH), 122.7 (CH), 116.7 (d, *J*=20.6 Hz, CH), 116.3 (dd, *J*=32.9 Hz, *J*=13.0 Hz, C-CF₃), 62.6 (CH₃), 61.8 (CH₃), 32.9 (CH₂), 13.0 (CH₃) ppm.

¹⁹F NMR (375 MHz, CDCl₃): δ = -61.08 (d, 3F, *J*=12.3 Hz), -114.9 (q, 1F, *J*=12.4 Hz) ppm.

HRMS (ESI) m/z: [M⁺] calcd for C₂₁H₁₈F₄O₂ 378.1257, found 378.1237.

Elemental analysis %: calcd for C₂₁H₁₈F₄O₂ C 66.87, H 5.03, found C 66.66, H 4.80.

Synthesis of 3-(5-((1,4-dimethoxy-3-methylnaphthalen-2-yl)methyl)-2-(trifluoromethyl)-phenoxy)oxetane (73):



3-(5-((1,4-dimethoxy-3-methylnaphthalen-2-yl)methyl)-2-(trifluoromethyl)phenoxy)oxetane

To a solution of oxetan-3-ol (3 equiv., 338 mg, 0.29 mL, 4.57 mmol) in DMSO (17.3 mL), NaH (3 equiv., 182 mg, 4.57 mmol) was added portion-wise under argon atmosphere. The yellow mixture was stirred until homogenous (for about 40 min). The resulting mixture was added dropwise to a solution of 2-(3-fluoro-4-(trifluoromethyl)benzyl)-1,4-dimethoxy-3-methylnaphthalene (1 equiv., 576 mg, 1.52 mmol) in DMSO (8.6 mL) and the reaction mixture turned to dark brown. The resulting mixture was stirred at room temperature for 2.5 hours under argon atmosphere and controlled by TLC. The reaction was quenched with 1M HCl solution and diluted with dichloromethane, the layers were separated and the aqueous layer was extracted with dichloromethane (2×25 mL), the resulting organic layers were collected and washed with H₂O (5×25 mL) and brine, dried over MgSO₄ and concentrated under reduced pressure. The crude product was purified by silica chromatography (Cyclohexane/EtOAc, from 9/1 to 7/3, R_f=0.59) and the light-yellow oil (488 mg, 74 %) was obtained.

3-(5-((1,4-dimethoxy-3-methylnaphthalen-2-yl)methyl)-2-(trifluoromethyl)-phenoxy)oxetane (73):

¹H NMR (CDCl₃): δ = 8.13-8.05 (m, 2H, ArH), 7.56-7.49 (m, 2H, ArH), 7.46 (d, *J*=8.0 Hz, 1H, phenylH), 6.83 (d, 1H, *J*=7.9 Hz, phenylH), 6.25 (s, 1H, phenylH), 5.08 (m, 1H, *J*=5.7 Hz, CH), 4.75 (dd, 2H, *J*=7.0 Hz, *J*=6.5 Hz, CH₂), 4.68 (dd, 2H, *J*=7.2 Hz, *J*=5.7 Hz, CH₂), 4.24 (s, 2H, CH₂), 3.86 (s, 3H, OCH₃), 3.84 (s, 3H, OCH₃), 2.23 (s, 3H, CH₃) ppm.

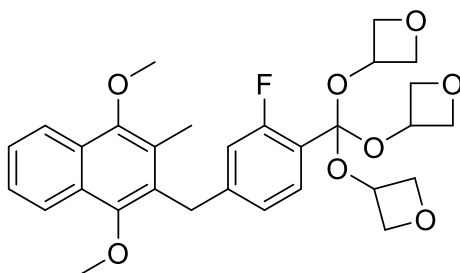
¹³C NMR (CDCl₃): δ = 154.9 (Cq), 150.9 (Cq), 147.1 (Cq×2), 128.5 (Cq), 128.1 (Cq), 127.9 (q, *J*=5.4 Hz, CH), 127.5 (Cq), 126.8 (Cq), 126.5 (CH), 126.1 (CH), 123.9 (q, *J*=274.5 Hz, CF₃), 122.8 (CH), 122.7 (CH), 120.9 (Cq), 116.9 (q, *J*=32.1 Hz, C-CF₃), 112.7 (Cq), 77.8 (CH₂), 62.6 (CH₃), 61.8 (CH₃), 33.1 (CH₂), 13.0 (CH₃) ppm.

¹⁹F NMR (CDCl₃): δ = -61.94 ppm.

HRMS (ESI) m/z: [M⁺] calcd for C₂₄H₂₃F₃O₄ 432.1543, found 432.1579.

Elemental analysis %: calcd for C₂₄H₂₃F₃O₄ C 66.60, H 5.43; found C 66.66, H 5.36.

Synthesis of 3,3',3''-(((4-((1,4-dimethoxy-3-methylnaphthalen-2-yl)methyl)-2-fluorophenyl)methanetriyl)tris(oxy))tris(oxetane) (75)



3,3',3''-(((4-((1,4-dimethoxy-3-methylnaphthalen-2-yl)methyl)-2-fluorophenyl)methanetriyl)tris(oxy))tris(oxetane)

To a solution of oxetan-3-ol (3 equiv., 117.5 mg, 0.10 mL, 1.58 mmol) in DMSO (4.6 mL), NaH (3 equiv., 63.4 mg, 1.58 mmol) was added portion-wise under argon atmosphere. The yellow mixture was stirred until homogenous (for about 40 min). The resulting mixture was added dropwise to a solution of 2-(3-fluoro-4-(trifluoromethyl)benzyl)-1,4-dimethoxy-3-methylnaphthalene (1 equiv., 200 mg, 0.528 mmol) in DMSO (4.6 mL) at 100 °C and the reaction mixture turned to dark brown. The resulting mixture was stirred at 100 °C for 2.5 hours under argon atmosphere. The reaction was quenched with 1M HCl solution and diluted with dichloromethane, the layers were separated and the aqueous layer was extracted with dichloromethane (2×25 mL), the resulting organic layers were collected and washed with H₂O (5×25 mL) and brine, dried over MgSO₄ and concentrated under

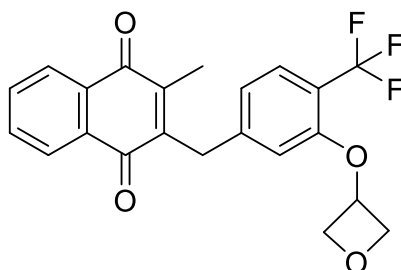
reduced pressure. The crude product was purified by silica chromatography (Cyclohexane/EtOAc, from 9/1 to 7/3, Rf=0.21) and the white solid (208 mg, 73 %) was obtained.

¹H NMR (CDCl₃): δ = 8.09 (m, 2H, ArH), 7.51 (m, 3H, 2 ArH + 1 phenylH), 6.97 (d, 1H, J = 8.1 Hz, phenylH), 6.8 (d, 1H, J = 11.8 Hz, phenylH), 4.78 (m, 3H, CH), 4.58 (t, 6H, J = 6.5 Hz, CH₂), 4.48 (t, 6H, J = 6.5 Hz, CH₂), 4.26 (s, 2H, CH₂), 3.86 (s, 3H, OCH₃), 3.84 (s, 3H, OCH₃), 2.22 (s, 3H, CH₃) ppm.

¹⁹F NMR (CDCl₃): δ = -112.78 ppm.

HRMS (ESI) m/z: [M⁺] calcd for C₃₀H₃₃F₁O₈ 540.2154, found 540.2105.

Synthesis of 2-methyl-3-(3-(oxetan-3-yloxy)-4-(trifluoromethyl)benzyl)naphthalene-1,4-dione (74):



2-methyl-3-(3-(oxetan-3-yloxy)-4-(trifluoromethyl)benzyl)naphthalene-1,4-dione

3-(5-((1,4-dimethoxy-3-methylnaphthalen-2-yl)methyl)-2-(trifluoromethyl)phenoxy)oxetane (1 equiv., 1096 mg, 2.53 mmol) was dissolved in a solution of acetonitrile-water (3:178 mL), cerium ammonium nitrate (2.1 equiv., 2917 mg, 5.32 mmol) was added portion-wise to give a yellow solution, the reaction mixture was stirred at room temperature for 6 hours. The resulting mixture was evaporated and 50 mL of dichloromethane was added. The aqueous layer was extracted with dichloromethane (3×50 mL) and the organic layers were combined and extracted with brine, dried over MgSO₄ and concentrated under reduced pressure. The crude product was purified by silica chromatography

(Cyclohexane/EtOAc, from 9/1 to 7/3, Rf=0.48) and recrystallization (*n*-hexane, 600 mL) to give a pure yellow solid (800 mg, 78%).

2-methyl-3-(3-(oxetan-3-yloxy)-4-(trifluoromethyl)benzyl)naphthalene-1,4-dione (74):

¹H NMR (CDCl₃): δ = 8.13-8.05 (m, 2H, ArH), 7.76-7.68 (m, 2H, ArH), 7.48 (d, 1H, *J*=8.0 Hz, phenylH), 6.88 (d, 1H, *J*=8.0 Hz, phenylH), 6.48 (s, 1H, phenylH), 5.25 (m, 1H, *J*=5.8 Hz, CH), 4.94 (t, 2H, *J*=6.9 Hz, CH₂), 4.76 (dd, 2H, *J*=7.5 Hz, *J*=5.7 Hz, CH₂), 4.00 (s, 2H, CH₂), 2.26 (s, 3H, CH₃) ppm.

¹³C NMR (CDCl₃): δ = 185.3 (CO), 184.9 (CO), 154.9 (Cq), 145.1 (Cq), 144.4 (Cq), 144.3 (Cq), 134.1 (CH), 134.1 (CH), 132.3 (Cq), 132.1 (Cq), 128.14 (q, *J*=5.1 Hz, CH), 126.8 (CH×2), 123.7 (q, *J*=271.5 Hz, CF₃), 121.2 (CH), 117.9 (q, *J*=31.3 Hz, C-CF₃), 113.6 (CH), 77.9 (CH₂), 70.9 (CH), 32.9 (CH₂), 13.7 (CH₃) ppm.

¹⁹F NMR (CDCl₃): δ = -62.14 ppm.

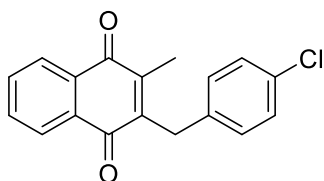
HRMS (ESI) m/z: [M+H]⁺ calcd for C₂₂H₁₈F₃O₄ 403.1152; found 403.1169.

Elemental analysis %: calcd for C₂₂H₁₇F₃O₄ C 65.83, H 4.40; found C 65.67, H 4.26.

m.p. 130°C-131°C (from *n*-hexane).

5. Synthesis of a 3-benzylmenadione derivative with potential antimalarial properties

Synthesis of 2-(4-chlorobenzyl)-3-methylnaphthalene-1,4-dione (76):



2-(4-chlorobenzyl)-3-methylnaphthalene-1,4-dione

Menadione (1 equiv., 450 mg, 2.61 mmol) and 2-(4-chlorophenyl)acetic acid (2 equiv., 891 mg, 5.23 mmol) were solubilized in a solution of 3:1 acetonitrile and water (54 mL). The mixture was stirred at 85°C and silver nitrate (0.35 equiv., 155 mg, 0.915 mmol) was added. Then, the ammonium persulfate (1.3 equiv., 775 mg, 0.392 mL, 3.4 mmol), dissolved in a solution of 3:1 acetonitrile and water, was added dropwise to the resulting mixture. The reaction mixture was stirred for 3.5 hours. The resulting mixture was evaporated and 50 mL of dichloromethane was added. The aqueous layer was extracted with dichloromethane (4×50 mL) and the organic layer were combined and extracted with brine, dried over MgSO₄ and concentrated under reduced pressure. The crude product was purified by silica gel column chromatography (toluene R_f=0.58) and recrystallized (*n*-hexane, 200 mL) to give a pure yellow solid (662 mg, 85%).

2-(4-chlorobenzyl)-3-methylnaphthalene-1,4-dione (76):

¹H NMR (300 MHz, CDCl₃): δ 8.11-8.04 (m, 2H, ArH), 7.72-7.67 (m, 2H, ArH), 7.22 (dt, 2H, *J* = 8.4 Hz, *J* = 2.1 Hz, phenylH), 7.16 (dt, 2H, *J* = 8.6 Hz, *J* = 2.1 Hz, phenylH), 3.99 (s, 2H, CH₂), 2.23 (s, 3H, CH₃) ppm.

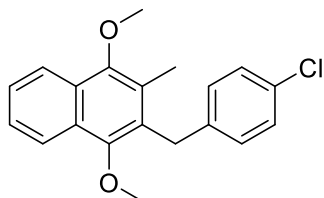
¹³C NMR (75 MHz, CDCl₃): δ 185.3 (C_q), 184.6 (C_q), 144.9 (C_q), 144.7 (C_q), 136.6 (C_q), 133.7 (CH), 132.4 (C_q), 132.2 (C_q), 132.0 (C_q), 130.0 (CH), 128.9 (CH), 126.6 (CH), 126.4 (CH), 31.99 (CH₂), 13.45 (CH₃) ppm.

MS (EI): (m/z (%)): 296.1 ([M]⁺, 25), 281.0 (100).

Elemental analysis %: calcd for C₁₈H₁₃ClO₂ C 72.85 H 4.42; found C 72.89 H 4.38

m.p. 134–136 °C (from *n*-hexane)

Synthesis of 2-(4-chlorobenzyl)-1,4-dimethoxy-3-methylnaphthalene (77):



2-(4-chlorobenzyl)-1,4-dimethoxy-3-methylnaphthalene

2-(4-chlorobenzyl)-3-methylnaphthalene-1,4-dione (1 equiv., 1150 mg, 3.88 mmol) was suspended in ethanol (15.1 mL) under argon atmosphere. Then, stannous chloride (3 equiv., 2202 mg, 0.558 mL, 11.6 mmol) was dissolved in conc. HCl (8.01 equiv., 3143 mg, 2.62 mL, 31 mmol) and added dropwise to the resulting solution and the reaction mixture was stirred for 2 hours at room temperature until a white solid appeared. The solvent of the mixture was removed in vacuum. The resulting white solid was washed with distilled water and filtrated. Then immediately after, the resulting crude product was redissolved in acetone (18.9 mL) under argon atmosphere and dimethylsulfate (3 equiv., 1466 mg, 1.1 mL, 11.6 mmol) was added. Subsequently, a solution of KOH

(5 eq., 1087 mg, 19.4 mmol) in methanol (8.6 mL) was added dropwise for 1 hour (*CAUTION*: exothermic) to the previous solution at 60 °C and the mixture was stirred for 4 hours. The reaction was quenched by adding KOH solution (3.5 M, 8.7 mL), the colour of the mixture was obviously changed to dark brown. The resulting mixture was extracted with dichloromethane (5×35 mL). The organic layers were combined, dried over MgSO₄ and concentrated under reduced pressure. The crude product was purified by silica chromatography (cyclohexane/dichloromethane, 7/3, R_f=0.60) to give a white solid (1153 mg, 91%).

2-(4-chlorobenzyl)-1,4-dimethoxy-3-methylnaphthalene (77):

¹H NMR (300 MHz, CDCl₃): δ 8.13-8.06 (m, 2H, ArH), 7.54-7.47 (m, 2H, ArH), 7.20 (dt, 2H, *J* = 8.5 Hz, *J* = 2.0 Hz, phenylH), 7.05 (dt, 2H, *J* = 8.4 Hz, *J* = 2.0, phenylH), 4.23 (s, 2H, CH₂), 3.86 (s, 3H, OCH₃), 3.83 (s, 3H, OCH₃), 2.24 (s, 3H, CH₃) ppm.

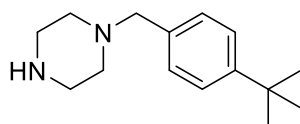
¹³C NMR (75 MHz, CDCl₃): δ 150.7 (C_q), 150.6 (C_q), 139.1 (C_q), 131.7 (C_q), 129.6 (CH), 128.8 (C_q), 128.6 (CH), 128.2 (C_q), 127.3 (C_q), 127.0 (C_q), 126.0 (CH), 125.7 (CH), 122.6 (CH), 122.4 (CH), 62.5 (CH₃), 61.6 (CH₃), 32.3 (CH₂), 12.8 (CH₃) ppm.

MS (EI): (m/z (%)): 326.12 ([M]⁺, 100), 311.10 (43), 296.08 (8), 279.07 (10), 261.11 (5), 244.10 (10), 215.10 (8).

Elemental analysis %: calcd for C₂₀H₁₉ClO₂ C 73.50 H 5.86; found C 73.30 H 5.90.

m.p. 100–102 °C (from cyclohexane/CH₂Cl₂).

Synthesis of 1-(4-(tert-butyl)benzyl)piperazine (78c):



1-(4-(*tert*-butyl)benzyl)piperazine

Anhydrous piperazine (6 equiv., 14000 mg, 162 mmol) was suspended in distilled THF (60.2 mL) under argon atmosphere. The mixture was heated to reflux until piperazine completely dissolved.

Then, 4-*tert*-butylbenzyl bromide (1 equiv., 6153 mg, 4.98 mL, 27.1 mmol) was added dropwise to the resulting mixture at 70 °C and white solid appeared. The reaction was stirred under refluxing for 2.5 hours. The solid was filtered and washed with THF and ethyl acetate. The filtrates were combined and concentrated to 10% of the original volume. The resulting mixture was basified with 5% KOH/brine solution (pH>12). The aqueous layer was extracted with dichloromethane (2×25 mL) and ethyl acetate (2×25 mL), the organic layers were combined, dried over MgSO₄, concentrated under reduced pressure. The crude product was purified by silica chromatography (ethyl acetate/methanol/triethylamine, 80/19/1, R_f=0.35) to give a white solid (5454 mg, 87%).

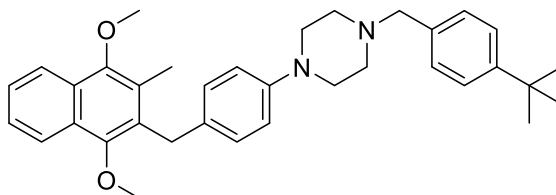
1-(4-(*tert*-butyl)benzyl)piperazine (78c):

¹H NMR (300 MHz, CDCl₃): δ = 7.33 (d, 2H, *J* = 8.1 Hz, phenylH), 7.24 (d, 2H, *J* = 7.9 Hz, phenylH), 3.47 (s, 2H, CH₂), 2.89 (t, 4H, *J* = 4.8 Hz, CH₂), 2.42 (s, 4H, CH₂), 1.31 (s, 9H, C(CH₃)₃) ppm.

¹³C NMR (75 MHz, CDCl₃): δ = 150.1 (C_q), 135.0 (C_q), 129.1 (CH), 125.2 (CH), 63.5 (CH₂), 54.5 (CH₂), 46.2 (CH₂), 34.6 (C_q), 31.5 ((CH₃)₃) ppm.

Mp: 54-55 °C (from EtOAc/MeOH/NEt₃)

Synthesis of 1-(4-(*tert*-butyl)benzyl)-4-(4-((1,4-dimethoxy-3-methylnaphthalen-2-yl)methyl)phenyl)piperazine (79c):



1-(4-(*tert*-butyl)benzyl)-4-(4-((1,4-dimethoxy-3-methylnaphthalen-2-yl)methyl)phenyl)piperazine

2-[(4-chlorophenyl)methyl]-1,4-dimethoxy-3-methylnaphthalene (1 equiv., 1200 mg, 3.67 mmol), 1-(4-(*tert*-butyl)benzyl)piperazine (4 equiv., 3412 mg, 14.7 mmol), Bis(dibenzylideneacetone)-palladium(0) (0.1 equiv., 211 mg, 0.367 mmol), 1,3-bis(2,6-

diisopropylphenyl)imidazolium chloride (0.05 equiv., 84 mg, 0.198 mmol) and sodium *tert*-butoxide (2.01 eq., 709 mg, 7.38 mmol) were dissolved in dry dimethoxyethane (36 mL). The reaction mixture was stirred at 80 °C for 24 hours under argon atmosphere. Then, the solvent was removed under reduced pressure. The crude product was purified by silica gel column chromatography to give grey solid (1900 mg, 99%).

1-(4-(*tert*-butyl)benzyl)-4-(4-((1,4-dimethoxy-3-methylnaphthalen-2-yl)methyl)-phenyl)-piperazine (79c)

¹H NMR (300 MHz, CDCl₃): δ = 8.09 – 8.07 (m, 2H, ArH), 7.49 – 7.47 (m, 2H, ArH), 7.34 (d, 2H, J = 8.2 Hz, phenylH), 7.26 (d, 2H, J = 8.1 Hz, phenylH), 6.99 (d, 2H, J = 8.4 Hz, phenylH), 6.79 (d, 2H, J = 8.6 Hz, phenylH), 4.18 (s, 2H, CH₂), 3.85 (s, 3H, OCH₃), 3.81 (s, 3H, OCH₃), 3.53 (s, 2H, CH₂), 3.13 (t, 4H, J = 4.8 Hz, CH₂), 2.59 (t, 4H, J = 4.6 Hz, CH₂), 2.26 (s, 3H, CH₃), 1.32 (s, 9H, C(CH₃)₃) ppm.

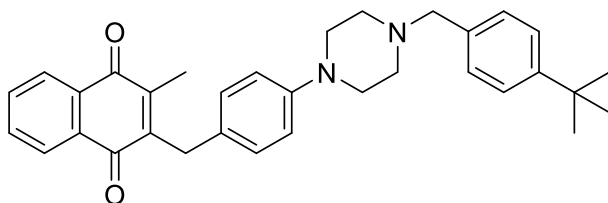
¹³C NMR (75 MHz, CDCl₃): δ = 150.6 (C_q), 150.4 (C_q), 150.2 (C_q), 149.6 (C_q), 135.0 (C_q), 131.6 (C_q), 129.8 (C_q), 129.1 (CH), 128.8 (CH), 128.0 (C_q), 127.4 (C_q), 125.7 (CH), 125.5 (CH), 125.3 (CH), 122.6 (CH), 122.3 (CH), 116.3 (CH), 62.8 (CH₂), 62.5 (CH₃), 61.5 (CH₃), 53.3 (CH₂), 49.5 (CH₂), 34.6 (C_q), 32.0 (CH₂), 31.5 ((CH₃)₃), 12.8 (CH₃) ppm.

MALDI MS: (m/z): 522.1 [M⁺]

Elemental analysis %: calcd for C₃₅H₄₂N₂O₂: C 80.42, H 8.10, N 5.36; found C 80.19, H 8.01, N 5.35.

m.p. 62 – 65 °C (from CH₂Cl₂/MeOH/NEt₃).

Synthesis of 2-(4-(4-(4-(*tert*-butyl)benzyl)piperazin-1-yl)benzyl)-3-methyl-naphthalene-1,4-dione (80c):



2-(4-(4-(4-(*tert*-butyl)benzyl)piperazin-1-yl)benzyl)-3-methylnaphthalene-1,4-dione

To the solution of 1-(4-(*tert*-butyl)benzyl)-4-(4-((1,4-dimethoxy-3-methylnaphthalen-2-yl)methyl)phenyl)piperazine (1 equiv., 750 mg, 1.43 mmol) in distilled dichloromethane (30 mL), boron tribromide (4.5 equiv., 1 M, 6.46 mL, 6.46 mmol) was added dropwise at -78 °C under argon atmosphere. The reaction mixture was stirred at room temperature for 16 hours. Then, the reaction was quenched by adding dropwise ice cold water (30 mL). The resulting mixture was extracted with dichloromethane (3×30 mL). The organic layers were combined, dried over MgSO₄, concentrated under reduced pressure. The crude product was purified by silica chromatography (dichloromethane/methanol/triethylamine, 98/1/1) to give red solid (308 mg, 44%).

2-(4-(4-(4-(*tert*-butyl)benzyl)piperazin-1-yl)benzyl)-3-methyl-naphthalene-1,4-dione (80c):

¹H NMR (400 MHz, CDCl₃): δ = 8.12 – 8.04 (m, 2H, ArH), 7.72 – 7.65 (m, 2H, ArH), 7.34 (d, 2H, J = 8.4 Hz, phenylH), 7.25 (d, 2H, J = 7.7 Hz, phenylH), 7.11 (d, 2H, J = 8.7 Hz, phenylH), 6.81 (d, 2H, J = 8.7 Hz, phenylH), 3.94 (s, 2H, CH₂), 3.52 (s, 2H, CH₂), 3.13 (t, 4H, J = 4.9 Hz, CH₂), 2.58 (t, 4H, J = 4.7 Hz, CH₂), 2.25 (s, 3H, CH₃), 1.31 (s, 9H, C(CH₃)₃) ppm.

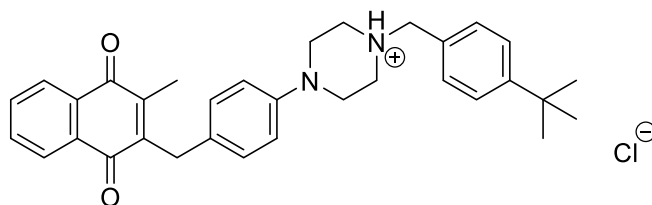
¹³C NMR (101 MHz, CDCl₃): δ = 185.7 (C_q), 184.9 (C_q), 150.2 (C_q), 150.1 (C_q), 145.9 (C_q), 144.0 (C_q), 134.9 (C_q), 133.5 (CH), 133.5 (CH), 132.3 (C_q), 132.2 (C_q), 129.5 (CH), 129.1 (CH), 128.9 (C_q), 126.6 (CH), 126.3 (CH), 125.3 (CH), 116.4 (CH), 62.8 (CH₂), 53.2 (CH₂), 49.3 (CH₂), 34.6 (C_q), 31.6 (CH₂), 31.5 ((CH₃)₃), 13.4 (CH₃) ppm.

FAB MS: (NBA, m/z(%)): 492.2 ([M]⁺, 100)

Elemental analysis %: calcd for C₃₃H₃₆N₂O₂: C 77.19, H 7.12, N 5.41; found C 77.34, H 7.43, N 5.32 (0.3 equiv. CH₂Cl₂).

m.p. 81 – 83 °C (from CH₂Cl₂/MeOH/NEt₃).

Synthesis of 1-(4-(*tert*-butyl)benzyl)-4-(4-((3-methyl-1,4-dioxo-1,4-dihydro-naphthalen-2-yl)methyl)phenyl)piperazin-1-ium (81c)



1-(4-(*tert*-butyl)benzyl)-4-(4-((3-methyl-1,4-dioxo-1,4-dihydro-naphthalen-2-yl)methyl)phenyl)piperazin-1-ium

2-(4-(4-(4-(*tert*-butyl)benzyl)piperazin-1-yl)benzyl)-3-methylnaphthalene-1,4-dione (1 equiv., 270 mg, 0.548 mmol) was dissolved in the minimum volume of methanol (about 50 mL). Then, chlorotrimethylsilane (4 equiv., 238 mg, 0.28 mL, 2.19 mmol) was added and the reaction mixture was stirred for 30 min at room temperature. The resulting solution was evaporated under reduced pressure and the yellow residue was washed with ether (3×10 mL) and dried under vacuum. The resulting crude residue was purified by recrystallization (diffusion liquid/liquid pentane to dichloromethane) and washed by ether (3×50 mL) and pentane (1×50 mL) to give a pure yellowish brown powder (296 mg, 95%).

1-(4-(*tert*-butyl)benzyl)-4-(4-((3-methyl-1,4-dioxo-1,4-dihydro-naphthalen-2-yl)methyl)phenyl)-piperazin-1-ium (81c):

¹H NMR (400 MHz, CDCl₃): δ = 8.09 – 8.01 (m, 2H, ArH), 7.70 – 7.64 (m, 2H, ArH), 7.55 (d, 2H, J = 8,1 Hz, phenylH), 7.43 (d, 2H, J = 8,1 Hz, phenylH) 7.13 (d, 2H, J = 8.4 Hz, phenylH), 6.83 (d, 2H, J = 7.4 Hz, phenylH), 4.17 (s, 2H, CH₂), 3.93 (s, 2H, CH₂), 3.76-3.60 (m, 2H, CH₂), 3.48 (t, 4H, J = 14.0 Hz, CH₂), 3.14-2.90 (m, 2H, CH₂), 2.21 (s, 3H, CH₃), 1.29 (s, 9H, C(CH₃)₃) ppm.

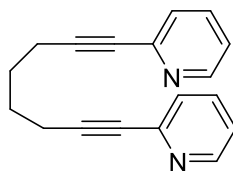
¹³C NMR (100 MHz, CDCl₃): δ = 185.4 (C_q), 184.8 (C_q), 153.7 (C_q), 145.3 (C_q), 144.3 (C_q), 133.6 (CH), 132.2 (C_q), 132.1 (C_q), 131.4 (CH), 128.8 (CH), 126.5 (CH), 126.4 (CH), 126.4 (CH), 124.6 (C_q), 117.9 (CH), 60.6 (CH₂), 50.9 (CH₂), 47.1 (CH₂), 34.9 (C_q), 31.7 (CH₂), 31.4 ((CH₃)₃), 13.4 (CH₃) ppm.

HRMS (ESI) m/z: [M remove Cl⁻]⁺ calcd for C₃₃H₃₇N₂O₂: 493.2850, found 493.2882.

Elemental analysis calcd (%) for C₃₃H₃₇ClN₂O₂: C, 74.19; H, 7.05; N, 5.29; found C, 72.64; H, 6.89; N, 5.22

6. Synthesis of GoPi-sugar

Synthesis of 1,8-di(pyridin-2-yl)octa-1,7-diyne (82):



1,8-di(pyridin-2-yl)octa-1,7-diyne

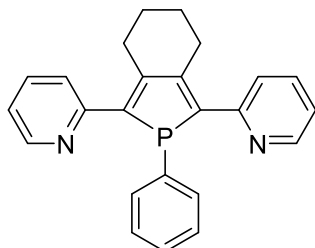
The Pd(PPh₃)₂Cl₂ (5 % equiv., 263 mg, 0.377 mmol) and CuI (5 % equiv., 71.8 mg, 0.377 mmol) were added in the flask for drying under vacuum during 2 hours. Triethylamine (141 mL) was degassed under argon for 1h before adding into the flask. The 2-bromopyridine (2 equiv., 2381 mg, 1.44 mL, 15.1 mmol) and 1,7-octadiyne (1 equiv., 800 mg, 1 mL, 7.54 mmol) were added dropwise into the prepared solution. The reaction was heated at 40 °C and continuously stirred overnight. The solvent was removed in vacuo. Then, 40 mL of water was added and the aqueous layer was extracted with 3x25 mL of Et₂O. The organic layers were combined, dried over Na₂SO₄ and concentrated. The crude product was purified by silica gel column chromatography (Et₂O/Cyclohexane: 1/1 to Et₂O 100%) to give a yellow solid (220.7 mg, 90%).

1,8-di(pyridin-2-yl)octa-1,7-diyne (82):

¹H NMR (400 MHz, CDCl₃): δ = 8.51 (d, 2H, *J* = 4.8 Hz, PyH), 7.58 (td, 2H, *J* = 7.8, *J* = 1.8 Hz, PyH), 7.35 (d, 2H, *J* = 7.8 Hz, PyH), 7.16-7.13 (m, 2H, PyH), 2.49 (m, 4H, CH₂), 1.80 (m, 4H, CH₂) ppm.

¹³C NMR (100 MHz, CDCl₃): δ = 149.7, 143.9, 136.2, 126.8, 122.3, 90.3, 80.5, 27.4, 18.6 ppm.

Synthesis of 2,2'-(2-phenyl-4,5,6,7-tetrahydro-2H-isophosphindole-1,3-diyl)- dipyridine (83):



2,2'-(2-phenyl-4,5,6,7-tetrahydro-2H-isophosphindole-1,3-diyl)dipyridine

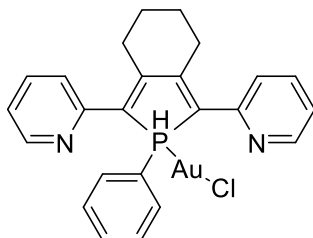
1,8-di(pyridin-2-yl)octa-1,7-diyne (1 equiv., 200 mg, 0.768 mmol) and $ZrCp_2Cl_2$ (1 equiv., 224 mg, 0.768 mmol) were treated under vacuum during 2h. Then the freshly distilled THF (12 mL) was added into the mixture. The n-BuLi (2.1 equiv., 1.6 M, 1.01 mL, 1.61 mmol) was added into the colorless solution at $-78^\circ C$ and the solution was stirred for 1 hour. Then, the cool bath was removed and the solution was stirred at room temperature under argon for 12 hours. The mixture was filtrated by prepared alumina basic column (under vacuum for 1 hour). Freshly distilled $PPhCl_2$ (1.1 equiv., 151 mg, 0.115 mL, 0.845 mmol) was added into the filtrate at $-78^\circ C$ under argon. Then, the mixture was stirred at RT for 4 hours. The crude product (364 mg) was evaporated under vacuum and used directly in the next step.

2,2'-(2-phenyl-4,5,6,7-tetrahydro-2H-isophosphindole-1,3-diyl)- dipyridine (83):

1H NMR (400 MHz, $CDCl_3$): δ = 8.51 (ddd, 2H, J = 4.6 Hz, J = 1.9 Hz, J = 1.1 Hz, PyH), 7.69 (ddd, 2H, J = 8.0 Hz, J = 1.5 Hz, J = 15.9 Hz, phenylH), 7.42 (dd, 2H, J = 7.7 Hz, J = 1.1 Hz, PyH), 6.97 (ddd, 2H, J = 7.5 Hz, J = 7.7 Hz, J = 1.9 Hz, PyH), 6.74-6.90 (m, 3H, phenylH), 6.45 (ddd, 2H, J = 4.6, J = 7.5 Hz, J = 1.0 Hz, PyH), 3.50 (m, 2H, CH_2), 2.85 (m, 2H, CH_2), 1.61 (m, 2H, CH_2), 1.46 (m, 2H, CH_2) ppm.

^{31}P NMR (81 MHz, $CDCl_3$): δ = 11.7 ppm.

Synthesis of (2-phenyl-1,3-di(pyridin-2-yl)-4,5,6,7-tetrahydro-2H-2λ⁵-isophosphindol-2-yl)gold(II) chloride (84):

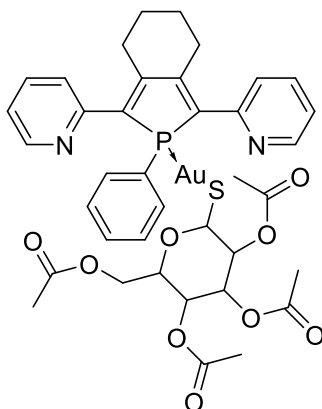


(2-phenyl-1,3-di(pyridin-2-yl)-4,5,6,7-tetrahydro-2H-2λ⁵-isophosphindol-2-yl)gold(II) chloride

The 2-[2-phenyl-3-(pyridin-2-yl)-4,5,6,7-tetrahydro-2H-isophosphindol-1-yl] pyridine (1 equiv., 364 mg, 0.988 mmol) was dried under vacuum during 1 hour in the flask and then CH₂Cl₂ (123 mL) was added into the flask. The fresh tetrahydrothiophene-AuCl (1 equiv., 316 mg, 0.988 mmol) was added into the solution of the phosphore compound by a syringe under argon. Then, the mixture was stirred at room temperature for 1 hour. The solvent was removed by evaporation. The crude product was washed with 2 x 10ml of diethylether and 10ml of freshly distilled pentane. The yellow powder (545 mg, 92%) was collected under vacuum and stored under argon without light.

³¹P NMR (81 MHz, CDCl₃): δ = 39.7 ppm.

Synthesis of GoPi-sugar (85):



GoPi-sugar

NaH (2.21 equiv., 79.4 mg, 1.99 mmol), [3,4,5-tris(acetyloxy)-6-sulfanyloxan-2-yl] methyl acetate (1.1 equiv., 360 mg, 0.988 mmol) and distilled THF (59.6 mL) were added in the flask. The

heterogeneous mixture was stirred for 1h at room temperature. The solution was filtered and added into the THF (59.6 mL) solution of (2-phenyl-1,3-di(pyridin-2-yl)-4,5,6,7-tetrahydro-2H-2λ⁵-isophosphindol-2-yl)gold(II) chloride (1 equiv., 540 mg, 0.899 mmol). The mixture was stirred for 1.5 hours at room temperature and evaporated under vacuum. After purification by silica gel column chromatography (Et₂O/AcOEt: 7/3), GoPi-sugar (388 mg, 47 %) was obtained as a yellow powder.

GoPi-sugar (85):

¹H NMR (CDCl₃, 400 MHz): δ = 8.58 (dd, 2H, *J* = 25.1 Hz, *J* = 4.7 Hz, PyH), 7.79 (d, 3H, *J* = 7.9 Hz, PyH), 7.77 (d, 1H, *J* = 7.9 Hz, PyH), 7.65 (qd, 2H, *J* = 7.9 Hz, *J* = 1.2 Hz, phenylH), 7.35-7.24 (m, 3H, phenylH), 7.11 (ddd, 2H, *J* = 12.4 Hz, *J* = 7.5 Hz, *J* = 4.9 Hz, PyH), 5.18-5.02 (m, 3H), 4.95 (t, 1H, *J* = 9.8 Hz, CH), 4.11 (dd, 1H, *J* = 3.3 Hz, *J* = 13.4 Hz, CH), 4.01 (dd, 1H, *J* = 2.3 Hz, *J* = 12.3 Hz, CH), 3.73-3.64 (m, 1H, CH), 3.39-3.25 (m, 2H, CH₂), 3.08-2.95 (m, 2H, CH₂), 2.06 (s, 3H, CH₃), 1.99 (s, 3H, CH₃), 1.97 (s, 3H, CH₃), 1.82 (m, 4H, CH₂), 1.76 (s, 3H, CH₃) ppm.

¹³C NMR (100 MHz, CDCl₃): δ = 171.2, 170, 169.7, 169.5, 153.4, 152.8, 152.5, 152.3, 149.4, 149.3, 136.1, 135.3, 134.5, 134.2, 131.6, 128.8, 126.5, 124.4, 123.9, 122.5, 122.3, 83.5, 77.9, 75.6, 74.5, 68.9, 63.1, 29.7, 29.6, 22.5, 21.9, 20.9, 20.6, 20.4 ppm.

³¹P NMR (81 MHz, CDCl₃): δ = 46.6 ppm.

HRMS (ESI) m/z: [M+Na]⁺ calcd for C₃₈H₄₀AuN₂NaO₉PS: 951.1755; found 951.1762.

7. General information for drug metabolism study

Cultivation of *Plasmodium falciparum*

All experiments with *P. falciparum* cultures and drug treated parasites were performed at the Institut de Biologie Moléculaire et Cellulaire (IBMC, anopheles group, director Dr. Stéphanie Blandin, Strasbourg). The chloroquine-sensitive 3D7 strain of *P. falciparum* (common laboratory strains or

culture-adapted strains obtained from patient isolates and grown in culture for an extended period) were used in this study. Parasites were maintained at 1 to 10% parasitaemia and 4% haematocrit in an RPMI 1640 culture medium supplemented with A+ erythrocytes, 0.5% lipid-rich bovine serum albumin (Albumax), 9 mM (0.16%) glucose, 0.2 mM hypoxanthine, 2.1 mM L-glutamine, and 22 mg/ml gentamicin. All incubations were carried out at 37°C in 3% O₂, 3% CO₂, and 94% N₂.

Synchronization of cultures over a large time window (0 to 20 h postinvasion [p.i.]) was established by 5% (w/v) sorbitol treatment. Synchronization over a short time window (0 to 4 h p.i.) was achieved using successive treatments with sorbitol. The synchronized ring stage parasites were used in the drug-treated experiment.

The synchronized ring stage parasite cultures were treated with 5 mM plasmodione (in DMSO) and incubated for 5 hours. The drug treated parasite cultures were centrifuged (873 g, 5 min, 25 °C) and the supernatants were collected (stored at -80 °C). The resulting pRBCs pellet was washed in buffer (1x PBS, 10 mL) twice and prepared for the next experiment.

MS data acquisition of drug metabolites

The experiment was performed by using an Ultimate 3000 LC system ((Thermo Fisher Scientific, Les Ulis, France) coupled to a Maxis Impact HD QqTOF instrument (Bruker Daltonics, Bremen, Germany) equipped with an electrospray ionization interface (ESI) operating in the positive ion mode at Laboratoire d'Etudes du Métabolisme des Médicaments (LEMM, director François Fenaille, CEA Saclay). The instrument was controlled via Compass ver.1.3 (Bruker Daltonik) software package.

The pRBCs samples were loaded and separated on a C18 Hypersil GOLD column (1.9 µm, 2.1 mm × 150 mm, Thermo Scientific) maintained at 30°C, with a flow rate set at 500 µL/min. The gradient condition was described as follows: Mobile phases were water containing 0.1% formic acid (mobile phase A) and acetonitrile (ACN) containing 0.1% formic acid (mobile phase B). The gradient conditions implied first a 2-min equilibration at 5% B, then the proportion of B was raised to 100% in

11 min. The column was then washed with 100% B during 12.5 min before a 4.5-min re-equilibration at 5% B (total runtime: 30 min).

The column eluent was directly introduced into the electrospray source of the mass spectrometer, and analyses were performed in the positive ion mode. The source conditions were as follows: The mass spectrometer settings were as follows: capillary voltage of 3800 V, end plate offset of 500 V, nebulizer pressure of 2.8 Bar, drying gas of 9 L/min, and drying temperature of 200 °C. The instrument was set up to automatically acquire full scan over the 50-1000 m/z range followed by MS/MS spectra (scan mode MRM, spectra rate = 3 Hz) of the three ions (331.0942 ± 0.02 m/z, 345.0767 ± 0.02 m/z, 347.0907 ± 0.02 m/z, collision energy 23 eV, 35 eV, 23 eV, respectively). Data analysis was performed manually in the Compass DataAnalysis (version 4.2).

The fully $^{13}\text{C}_{18}$ -enriched plasmodione **49b** treated pRBCs samples were analyzed under the same LC-MS condition as before. In addition, these samples were also analyzed by another the MS/MS spectra with scan mode Auto MS/MS (preference SILE, delta mass = 18.0612 ± 0.20 m/z, charge = 1 or 2, cross correlation 0.60, intensity ratio = 0.05 - 20, mass range = 50 - 1000 m/z, spectra rate = 1.00 Hz).

8. Extraction yields of putative drug metabolites investigation

Evaluation of extraction yields of putative drug metabolites from plasmodione treated culture medium using 3 different conditions

Extraction of culture medium with MeOH.

The experiment followed the conditions below and was repeated for each of them three times:

- A. 1200 μL of MeOH was added to 300 μL of culture medium at 4°C, then the mixture was incubated at -20°C for 1 hour. The resulting mixture was centrifuged (2000 g with 5 min, 4°C) and the supernatant was collected. The supernatant was evaporated under nitrogen flow (at 40°C).
- B. Following the condition A above, and 3 μL of the mixture solution (500 mM of plasmodione or one of the six putative drug metabolites in MeOH) was added.

C. Before the extraction experiment under condition A, 3 μL of the mixture solution (500 mM of plasmodione or one of the six putative drug metabolites in MeOH) was added.

Resuspended all the resulting pellet in 50 μL of MeOH, then centrifuged (2000 g with 5 min, 4°C). Finally, the supernatant was collected and loaded for MS acquisition experiment. The concentration of plasmodione and of the 6 putative drug metabolites was estimated by the intensity of each peak of compounds from the MS data. The extraction yields were calculated by formula $[\text{intensity observed under condition B}] - [\text{intensity observed under condition A}] / [\text{intensity observed under condition C}] - [\text{intensity observed under condition A}]$.

Extraction of culture medium with solvent mixture ($\text{CHCl}_3/\text{MeOH}/\text{H}_2\text{O}$, 1/3/1, v/v/v).

The experiment followed the conditions below and was repeated for each of them three times:

- A. 1200 μL of solvent mixture ($\text{CHCl}_3/\text{MeOH}/\text{H}_2\text{O}$, 1/3/1, v/v/v) was added to 300 μL of culture medium at 4°C, then the mixture was incubated at -20°C for 1 hour. The resulting mixture was centrifuged (2000 g with 5 min, 4°C) and the supernatant was collected. The supernatant was evaporated under nitrogen flow (at 40°C).
- B. Following the condition A above, and 3 μL of the mixture solution (500 mM of plasmodione or one of the six putative drug metabolites in MeOH) was added.
- C. Before the extraction experiment under condition A, 3 μL of the mixture solution (500 mM of plasmodione or one of the six putative drug metabolites in MeOH) was added.

Resuspended all the resulting pellet in 50 μL of MeOH, then centrifuged (2000 g with 5 min, 4°C). Finally, the supernatant was collected and loaded for MS acquisition experiment. The concentration of plasmodione and of the 6 putative drug metabolites was estimated by the intensity of each peak of compounds from the MS data. The extraction yields were calculated by formula $[\text{intensity observed under condition B}] - [\text{intensity observed under condition A}] / [\text{intensity observed under condition C}] - [\text{intensity observed under condition A}]$.

Extraction of culture medium with acidified MeOH (5% volume of formic acid).

The experiment followed the conditions below and was repeated for each of them three times:

- A. 15 μL of formic acid was added to 300 μL of culture medium at 4°C, following 1200 μL of MeOH

was added, then the mixture was incubated at -20°C for 1 hour. The resulting mixture was centrifuged (2000 g with 5 min, 4°C) and the supernatant was collected. The supernatant was evaporated under nitrogen flow (at 40°C).

- B. Following the condition A above, and $3\ \mu\text{L}$ of the mixture solution (500 mM of plasmodione or one of the six putative drug metabolites in MeOH) was added.
- C. Before the extraction experiment under condition A, $3\ \mu\text{L}$ of the mixture solution (500 mM of plasmodione or one of the six putative drug metabolites in MeOH) was added.

Resuspended all the resulting pellet in $50\ \mu\text{L}$ of MeOH, then centrifuged (2000 g with 5 min, 4°C). Finally, the supernatant was collected and loaded for MS acquisition experiment. The concentration of plasmodione and of the 6 putative drug metabolites was estimated by the intensity of each peak of compounds from the MS data. The extraction yields were calculated by formula $[\text{intensity observed under condition B}] - [\text{intensity observed under condition A}] / [\text{intensity observed under condition C}] - [\text{intensity observed under condition A}]$.

Evaluation of extraction yields of putative drug metabolites from plasmodione treated parasitized RBC with 3 different SPE

Extraction of drug treated pRBC lysate with MeOH (with or without 5% volume of formic acid).

The 5 mM plasmodione treated pRBC (parasitemia 5%, haematocrit 4%, 2.8×10^7 of pRBC) was harvested and lysed by 15 mg of glass beads (425-600 μm , Sigma Aldrich) and $100\ \mu\text{L}$ of H_2O .

The extraction followed the conditions below:

- A. $800\ \mu\text{L}$ of MeOH was added to the lysate solution and incubated -20°C for 1 hour. The resulting mixture was centrifuged (2000 g with 5 min, 4°C), the supernatant was collected and evaporated by SpeedVac at room temperature. Resuspended the resulting pellet in $50\ \mu\text{L}$ of MeOH, and then centrifuged (2000 g with 5 min, 4°C). The supernatant was collected and evaporated again by SpeedVac at room temperature.
- B. Following the condition A above, and $2\ \mu\text{L}$ of the mixture solution (500 mM of plasmodione or one of the six putative drug metabolites in MeOH) was added.
- C. Before the extraction experiment under condition A, $2\ \mu\text{L}$ of the mixture solution (500 mM of plasmodione or one of the six putative drug metabolites in MeOH) was added.
- D. $10\ \mu\text{L}$ of HCOOH was added to the lysate solution and then follow the extraction under condition A.
- E. $10\ \mu\text{L}$ of HCOOH was added to the lysate solution and then follow the extraction under condition

B.

- F. 10 μL of HCOOH was added to the lysate solution and then follow the extraction under condition C.

Resuspended all the resulting pellet in 50 μL of MeOH , then centrifuged (2000 g with 5 min, 4°C). Finally, the supernatant was collected and loaded for MS acquisition experiment. The concentration of plasmodione and of the 6 putative drug metabolites was estimated by the intensity of each peak of compounds from the MS data. The extraction yields were calculated by formula $[\text{intensity observed under condition B}] - [\text{intensity observed under condition A}] / [\text{intensity observed under condition C}] - [\text{intensity observed under condition A}]$ (without acidification) and $[\text{intensity observed under condition E}] - [\text{intensity observed under condition D}] / [\text{intensity observed under condition F}] - [\text{intensity observed under condition D}]$ (with acidification).

Extraction of drug treated pRBC lysate with SPE (Phenomenex: C18-E (55 μm , 70Å), 50 mg/ 1 mL).

The 5 mM plasmodione treated pRBC (parasitemia 5%, haematocrit 4%, 2.8×10^7 of pRBC) was harvested and lysed by 15 mg of glass beads (425-600 μm , Sigma Aldrich) and 100 μL of H_2O .

The extraction followed the conditions below:

- A. 800 μL of MeOH was added to the lysate solution and incubated -20°C for 1 hour. The resulting mixture was centrifuged (2000 g with 5 min, 4°C), the supernatant was diluted with 1600 μL of H_2O and loaded to the SPE column (calibration condition described below). The resulting eluent was evaporated by SpeedVac at room temperature. Resuspended the resulting pellet in 50 μL of MeOH , then centrifuged (2000 g with 5 min, 4°C). The supernatant was collected and evaporated again by SpeedVac at room temperature.
- B. Following the condition A above, and 2 μL of the mixture solution (500 mM of plasmodione or one of the six putative drug metabolites in MeOH) was added.
- C. Before the extraction experiment under condition A, 2 μL of the mixture solution (500 mM of plasmodione or one of the six putative drug metabolites in MeOH) was added.
- D. 10 μL of HCOOH was added to the lysate solution and then follow the extraction under condition A.
- E. 10 μL of HCOOH was added to the lysate solution and then follow the extraction under condition B.
- F. 10 μL of HCOOH was added to the lysate solution and then follow the extraction under condition C.

Calibration of SPE column.

The SPE column was activated with 1 mL of MeOH, and then equilibrated with 1 mL of H₂O. The supernatant extracted from pRBC pellet was loaded to the SPE column. Following the SPE column was washed with 1 mL of H₂O and finally eluted with 1 mL of MeOH.

Resuspended all the resulting pellet in 50 μ L of MeOH, then centrifuged (2000 g with 5 min, 4°C). Finally, the supernatant was collected and loaded for MS acquisition experiment. The concentration of plasmodione and of the 6 putative drug metabolites was estimated by the intensity of each peak of compounds from the MS data. The extraction yields were calculated by formula $[\text{intensity observed under condition B}] - [\text{intensity observed under condition A}] / [\text{intensity observed under condition C}] - [\text{intensity observed under condition A}]$ (without acidification) and $[\text{intensity observed under condition E}] - [\text{intensity observed under condition D}] / [\text{intensity observed under condition F}] - [\text{intensity observed under condition D}]$ (with acidification).

Extraction of drug treated pRBC lysate with SPE (Phenomenex: C18-E (55 μ m, 70Å), 100 mg/ 3 mL).

The 5 mM plasmodione treated pRBC (parasitemia 5%, haematocrit 4%, 2.8×10^7 of pRBC) was harvested and lysed by 15 mg of glass beads and 100 μ L of H₂O. The extraction followed the conditions below:

- A. 800 μ L of MeOH was added to the lysate solution and incubated -20°C for 1 hour. The resulting mixture was centrifuged (2000 g with 5 min, 4°C), the supernatant was diluted with 1600 μ L of H₂O and loaded to the SPE column (calibration condition described below). The resulting eluent was evaporated by SpeedVac at room temperature. Resuspended the resulting pellet in 50 μ L of MeOH, then centrifuged (2000 g with 5 min, 4°C). The supernatant was collected and evaporated again by SpeedVac at room temperature.
- B. Following the condition A above, and 2 μ L of the mixture solution (500 mM of plasmodione or one of these six putative drug metabolites in MeOH) was added.
- C. Before the extraction experiment under condition A, 2 μ L of the mixture solution (500 mM of plasmodione or one of these six putative drug metabolites in MeOH) was added.
- D. 10 μ L of HCOOH was added to the lysate solution and then follow the extraction under condition

- A.
- E. 10 μL of HCOOH was added to the lysate solution and then follow the extraction under condition B.
- F. 10 μL of HCOOH was added to the lysate solution and then follow the extraction under condition C.

Calibration of SPE column.

The SPE column was activated with 1.5 mL of MeOH, and then equilibrated with 1.5 mL of H_2O . The supernatant extracted from pRBC pellet was loaded to the SPE column. Following the SPE column was washed with 1.5 mL of H_2O and finally eluted with 1.5 mL of MeOH.

Resuspended all the resulting pellet in 50 μL of MeOH, then centrifuged (2000 g with 5 min, 4°C). Finally, the supernatant was collected and loaded for MS acquisition experiment. The concentration of plasmodione and of the 6 putative drug metabolites was estimated by the intensity of each peak of compounds from the MS data. The extraction yields were calculated by formula $[\text{intensity observed under condition B}] - [\text{intensity observed under condition A}] / [\text{intensity observed under condition C}] - [\text{intensity observed under condition A}]$ (without acidification) and $[\text{intensity observed under condition E}] - [\text{intensity observed under condition D}] / [\text{intensity observed under condition F}] - [\text{intensity observed under condition D}]$ (with acidification).

Extraction of drug treated pRBC lysate with SPE (Phenomenex: Strata-X. 33 μm polymeric Reversed Phase, 60 mg/ 3 mL).

The 5 mM plasmodione treated pRBC (parasitemia 5%, haematocrit 4%, 2.8×10^7 of pRBC) was harvested and lysed by 15 mg of glass beads and 100 μL of H_2O . The extraction followed the conditions below:

- A. 800 μL of MeOH was added to the lysate solution and incubated -20°C for 1 hour. The resulting mixture was centrifuged (2000 g with 5 min, 4°C), the supernatant was diluted with 1600 μL of H_2O and loaded to the SPE column (calibration condition described below). The resulting eluent was evaporated by SpeedVac at room temperature. Resuspended the resulting pellet in 50 μL of MeOH, and then centrifuged (2000 g with 5 min, 4°C). The supernatant was collected and evaporated again by SpeedVac at room temperature.

- B. Following the condition A above, and 2 μL of the mixture solution (500 mM of plasmodione or one of the six putative drug metabolites in MeOH) was added.
- C. Before the extraction experiment under condition A, 2 μL of the mixture solution (500 mM of plasmodione or one of the six putative drug metabolites in MeOH) was added.

Calibration of SPE column.

The SPE column was activated with 1.5 mL of MeOH, and then equilibrated with 1.5 mL of H₂O. The supernatant extracted from pRBC pellet was loaded to the SPE column. Following the SPE column was washed with 1.5 mL of H₂O and finally eluted with 1.5 mL of a solution of 2% formic acid MeOH (v/v).

Resuspended all the resulting pellet in 50 μL of MeOH, then centrifuged (2000 g with 5 min, 4°C). Finally, the supernatant was collected and loaded for MS acquisition experiment. The concentration of plasmodione and of the 6 putative drug metabolites was estimated by the intensity of each peak of compounds from the MS data. The extraction yields were calculated by formula $[\text{intensity observed under condition B}] - [\text{intensity observed under condition A}] / [\text{intensity observed under condition C}] - [\text{intensity observed under condition A}]$ (without acidification).

9. Preliminary drug metabolism study with fully ¹³C-enriched plasmodione treated pRBCs preparation

The 5 mM plasmodione mixture (2.5 mM unlabeled plasmodione and 2.5 mM ¹³C-enriched plasmodione) treated pRBC (parasitemia 9%, haematocrit 4%, 1.2×10^8 of pRBC) was harvested and lysed by 15 mg of glass beads and 200 μL of H₂O under violent vortex. The resulting lysate was extracted under following the condition and repeated three times:

- A. 8000 μL of MeOH was added to the lysate solution and incubated -20°C for 1 hour. The resulting mixture was centrifuged (2000 g with 5 min, 4°C), the supernatant was evaporated by SpeedVac at room temperature. Resuspended the resulting pellet in 300 μL of MeOH, then centrifuged (2000 g with 5 min, 4°C). The supernatant was collected and evaporated again by SpeedVac at room

temperature.

- B. 8000 μL of MeOH was added to the lysate solution and incubated -20°C for 1 hour. The resulting mixture was centrifuged (2000 g with 5 min, 4°C), the supernatant was evaporated by SpeedVac at room temperature. Resuspended the resulting pellet in 800 μL of MeOH and diluted with 1600 μL of H_2O and loaded to the SPE column (Phenomenex: C18-E (55 μm , 70 \AA), 100 mg/ 3 mL, calibration condition described above). The resulting eluent was evaporated by SpeedVac at room temperature then centrifuged (2000 g with 5 min, 4°C). Resuspended the resulting pellet in 300 μL of MeOH, then centrifuged (2000 g with 5 min, 4°C). The supernatant was collected and evaporated again by SpeedVac at room temperature.
- C. Followed condition B but changed the SPE column (Vac tC18 (37-55 μm , 125 \AA , 100 mg/ 1 mL), Waters Sep-Pak)
- D. 10 μL of HCOOH was added to the lysate solution and then followed the extraction under condition A.
- E. 10 μL of HCOOH was added to the lysate solution and then followed the extraction under condition B.
- F. 10 μL of HCOOH was added to the lysate solution and then followed the extraction under condition C.

All resulting pellets were resuspended in 50 μL of MeOH, and then centrifuged (2000 g with 5 min, 4°C). Finally, the supernatant was collected and loaded for MS acquisition experiment (Scan mode Auto MS/MS, preference SILE, delta mass = 18.0612 ± 0.20 m/z, charge = 1 or 2, cross correlation 0.60, intensity ratio = 0.05 - 20, mass range = 50 to 1000 m/z, spectra rate 1.00 Hz).

LISTE DES PUBLICATIONS

1) publiées

Cesar Rodo E., [Feng L.](#), Jida M, Ehrhardt K., Bielitz M., Boilevin J., Lanzer M., Williams D.L., Lanfranchi D.A., Davioud-Charvet E., A Platform of Regioselective Methodologies to Access Polysubstituted 2-Methyl-1,4-naphthoquinone Derivatives: Scope et Limitations, *Eur. J. Org. Chem.* **2016**, 1982–1993.

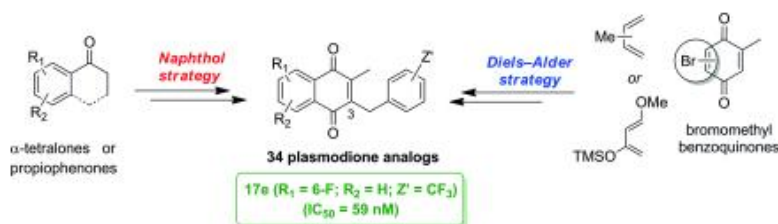
1,4-Naphthoquinone Synthesis



A Platform of Regioselective Methodologies to Access Polysubstituted 2-Methyl-1,4-naphthoquinone Derivatives: Scope and Limitations (pages 1982–1993)

Elena Cesar Rodo, Liwen Feng, Mouhamad Jida, Katharina Ehrhardt, Max Bielitz, Jérémy Boilevin, Michael Lanzer, David Lee Williams, Don Antoine Lanfranchi and Elisabeth Davioud-Charvet

Version of Record online: 21 MAR 2016 | DOI: 10.1002/ejoc.201600144



A platform of synthetic methodologies to prepare regioselectively potent antimalarial polysubstituted 3-benzylmenadione derivatives has been established involving 1) the naphthol route, starting from either a α -tetralone or a propiophenone, or 2) regioselective Diels–Alder reactions.

2) En préparation

[Feng L.](#), Ehrhardt K., Davioud-Charvet E. Synthesis of ^{13}C -enriched plasmodione for drug metabolism/uptake investigations.

Goetz A. A., [Feng L.](#), Franke Fayard B., Deregnacourt C., Ehrhardt K., Janse C., Davioud-Charvet E., Blandin S. An improved analogue of antimalarial Plasmodione has dual activity against asexual and sexual parasite stages with potent transmission blocking activity.

[Feng L.](#), Huerta Navarro, J. A., Maes L., P., Yardley, V., Croft, S., Kelly J.M., Davioud-Charvet E. Synthesis and anti-Chagas activity profile of a novel redox-active benzylmenadione revealed by highly sensitive in vivo imaging.

Feng L., Pomel S., Loiseau, P., Williams D. L. Davioud-Charvet E. Repurposing an old anti-arthritis golden drug and its anticancer GoPI-sugar surrogate for the treatment of human parasitic diseases : from Leishmania to helminth infections.

1,4-Naphthoquinone Synthesis

A Platform of Regioselective Methodologies to Access Polysubstituted 2-Methyl-1,4-naphthoquinone Derivatives: Scope and Limitations

Elena Cesar Rodo,^[a] Liwen Feng,^[a] Mouhamad Jida,^[a] Katharina Ehrhardt,^{[a,b][‡]}
Max Bielitz,^[a] Jérémy Boilevin,^[a] Michael Lanzer,^[c] David Lee Williams,^[d]
Don Antoine Lanfranchi,^{*[a]} and Elisabeth Davioud-Charvet^{*[a]}

Abstract: A platform of synthetic methodologies has been established to access a focused library of polysubstituted 3-benzylmenadione derivatives functionalized on the aromatic ring of the naphthoquinone core. Two main routes were explored: 1) The naphthol route, starting from either an α -tetralone or a propiophenone, and 2) the regioselective Diels–Alder reaction, starting from various dienes and two 2-bromo-5(or 6)-methyl-1,4-benzoquinones. 6-Substituted 2-methylnaphthols were synthesized by using a xanthate-mediated free-radical addition/cyclization sequence for the construction of the 6-substituted

menadione subunit. Furthermore, an efficient and simple new pathway that allows the formation of 6- or 7-substituted 3-(substituted-benzyl)menadione regioisomers from a common commercial scaffold has also been developed by the naphthol route, advantageous with regard to step economy. Our synthetic methodologies exemplified by 34 compounds have allowed structure–activity relationships to be deduced for use as the basis for the development of new antimalarial redox-active polysubstituted benzylmenadione derivatives.

Introduction

1,4-Naphthoquinones are ubiquitously distributed throughout all kingdoms of life, including eubacteria, archaeobacteria, fungi, protists, plants, and animals.^[1] They have been used for centuries in folk medicine, cosmetics, and industrial dye applications.^[2] Well-known examples^[3] of 1,4-naphthoquinones are the menadione (2-methyl-1,4-naphthoquinone, also called vitamin K3) and plumbagin (2-methyl-5-hydroxy-1,4-naphthoquinone) derivatives, exemplified by the bio-inspired representatives in Figure 1. Owing to the broad occurrence of the 1,4-naphthoquinone motif in compounds of natural origin and their peculiar redox properties,^[4] there is a growing interest in the chemistry of polysubstituted 1,4-naphthoquinones as final products or key synthetic intermediates. Numerous 1,4-naphthoquinones^[5]

do not contain the 2-methyl substituent, rendering their synthesis easy and straightforward from substituted benzenes.^[5a] Also, among the menadione derivatives, the substitution pattern has to be considered (Figure 1). Functionalization of the eastern part of the molecule affords the vitamin K series upon isoprenylation of vitamin K3 (menadione).^[6] By using solid- and solution-phase synthesis, a library of synthetic menadione, juglone, and plumbagin derivatives has been prepared allowing the introduction of broad structural diversity into the eastern part of the quinone core.^[7] Functionalization of the western part of menadione is also commonly found in plants, as exemplified by chimaphilin derivatives^[8] (Figure 1). Larger ring systems (e.g., biaryls, macrocycles), although less common, appear in natural products, as exemplified by bivitamin K,^[9] gossypol-

[a] UMR 7509 Centre National de la Recherche Scientifique and Strasbourg University, Bioorganic and Medicinal Chemistry, European School of Chemistry, Polymers and Materials (ECPM), 25 Rue Becquerel, 67087 Strasbourg, France
E-mail: lanfranchi@unistra.fr
elisabeth.davioud@unistra.fr
http://www-ecpm.u-strasbg.fr/umr7509/labo_davioudcharvet/

[b] Center of Infectious Diseases, Parasitology, Heidelberg University, Im Neuenheimer Feld 324, 69120 Heidelberg, Germany

[c] German Centre for Infection Research (DZIF), Partner Site Heidelberg, Heidelberg, Germany

[d] Department of Immunology/Microbiology, Rush University Medical Center, 1735 West Harrison Street, Chicago, IL 60612, USA

[‡] Present address: Institut de Biologie Moléculaire et Cellulaire, Strasbourg, France.

Supporting information and ORCID(s) for this article are available on the WWW under <http://dx.doi.org/10.1002/ejoc.201600144>.

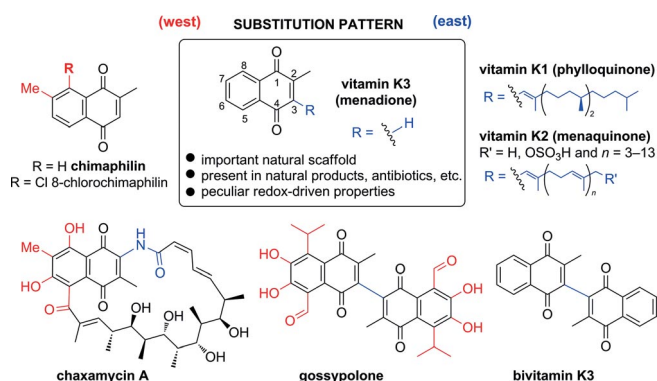
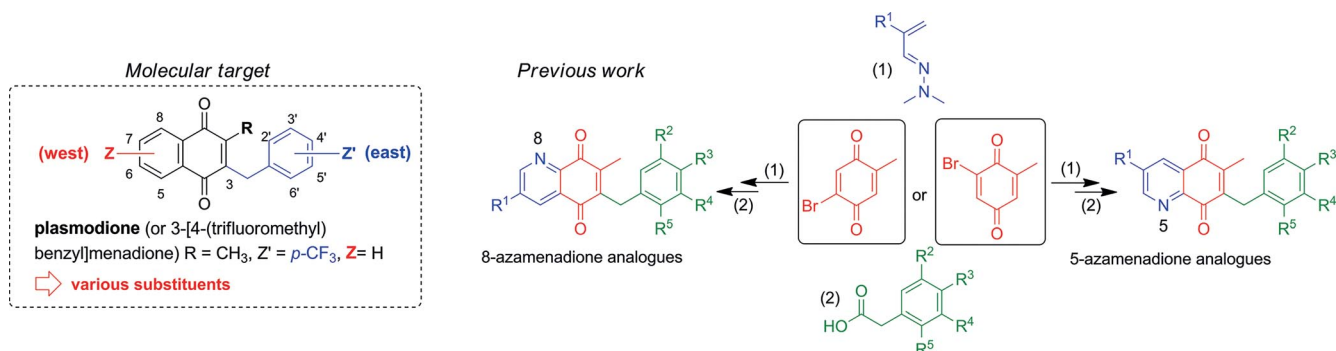


Figure 1. Natural and synthetic polysubstituted menadione derivatives.



Scheme 1. Synthesis of synthetic 3-benzylmenadione derivatives and aza analogues.

one,^[10] and the antibiotic chaxamycin A,^[11] which result from biotransformations of low-weight menadione-, plumbagin-, and chimaphilin-based scaffolds upon dimerization, isoprenylation of mevalonate, and macrocyclization, etc. (Figure 1). Therefore, the synthetic methodologies have to be highly regioselective for the preparation of menadione derivatives.

In contrast to the previous eastern-substituted series, general methods for regioselective transformations to prepare synthetic menadione derivatives substituted at both the phenyl ring ("western" part) and quinone moiety ("eastern" part) of the 1,4-naphthoquinone core are rare. Although numerous reports have described synthetic routes to various menadione derivatives, large collections with a diversity of substitutions in the western ring are not commercially available in bulk. Although regioselective annulations of quinones by the Diels–Alder strategy are commonly used to build the 1,4-naphthoquinone nucleus in the total synthesis of natural products,^[12] it remains a challenge to control the regioselectivity of the reaction when moderately reactive dienes with unsymmetrical 2-methylquinones are used in the cycloaddition reaction.^[13] Many factors increasing the regioselectivity of [4+2] cycloaddition reactions have been reported: 1) The presence of Lewis^[14] and Brønsted^[15] acid catalysts, 2) the presence of a halogen atom such as a bromine at the quinone dienophilic double bond, which also facilitates HBr elimination and the recovery of the quinone moiety following the cycloaddition.^[16] Various combinations of factors governing the regioselectivity of cycloaddition reactions can produce highly selective results, but these approaches depend on structural features of the substrates, which results in unpredictable reaction outcomes.

The recent discovery of the antimalarial lead 3-[4-(trifluoromethyl)benzyl]menadione (Scheme 1), henceforth called plasmodione (compound **1c** in refs.^[17–19]), has led to reassessment of the synthetic methodologies used to prepare large numbers of diverse analogues and potential metabolites functionalized on both the eastern and western parts of the molecule (Scheme 1). As a first step to access the target molecules, we reported a methodology for the preparation of polysubstituted 6-methylquinoline-5,8-dione scaffolds (5- and 8-azamenadione analogues).^[20] The methodology consisted of a two-step sequence involving a regioselective (hetero) Diels–Alder reaction followed by radical alkylation of the 1,4-naphthoquinone core with a carboxylic acid in the presence of Ag^I nitrate and

ammonium peroxydisulfate^[21] to afford the corresponding alkylated product in good yields (Scheme 1).

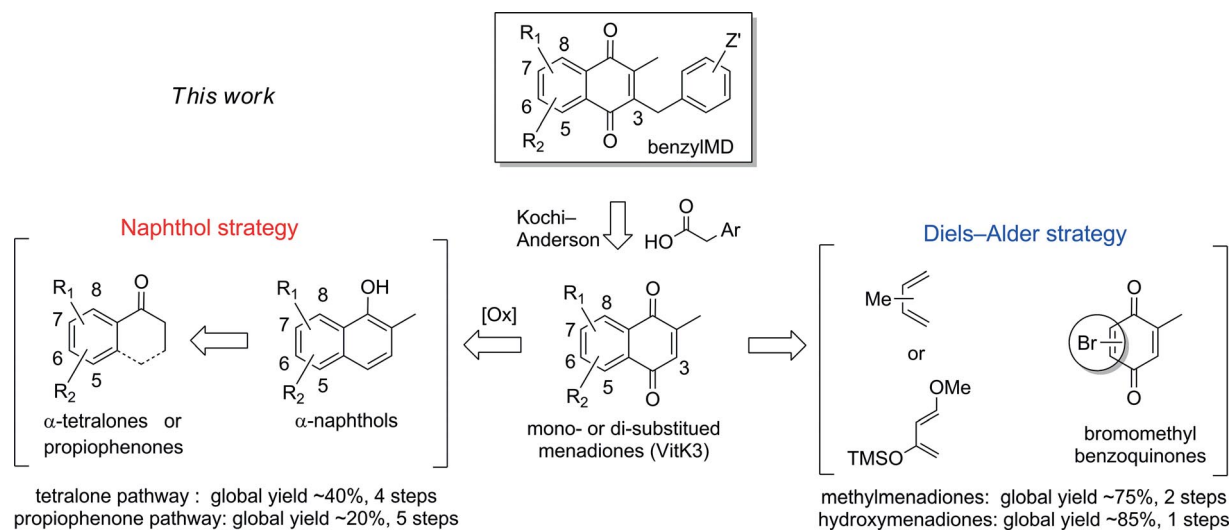
Thus, identification of plasmodione, currently a first antimalarial lead/early hit, highlights the potential of redox-active 3-benzylmenadiones (benzylMDs) with the following properties: A large chemical space for derivatization and a wide range of redox potentials. The generation of more effective analogues can only be approached by the total synthesis of 2-methyl-1,4-naphthoquinones substituted on the phenyl ring, which necessitates the total regiocontrol of the synthetic reactions. Owing to the lack of versatile and general methodologies to prepare polysubstituted 3-benzyl-2-methyl-1,4-naphthoquinone derivatives, the study described herein focused on the development and application of efficient methods to overcome these shortcomings (see Scheme 2).

Results and Discussion

Chemistry

Many methodologies for the preparation of synthetic and natural 1,4-naphthoquinone derivatives have been reported in the literature. In general, these synthetic routes utilize a naphthol intermediate, which, upon oxidation, affords the related 1,4-naphthoquinone. A more direct and regioselective approach is based on the Diels–Alder reactions of 1,4-benzoquinones and dienes.^[13,14,16] However, in the case of menadione, the 2-methyl group presents two major difficulties that need to be overcome: 1) It leads to dissymmetry of the molecule and 2) its acidic hydrogen atoms are responsible for the instability of the menadione core in basic media. For these reasons, and aside from a few examples,^[22] there are no general methodologies to prepare polysubstituted menadiones with various substituents introduced regioselectively at any locus of the aromatic ring, in particular, at C-6 or C-7 of the menadione core.

As a continuation of our studies into antiplasmodial drug development, we envisaged that polysubstituted 2-methyl-1,4-naphthoquinones could also be synthesized through two key strategies (Scheme 2): the Diels–Alder and naphthol routes. Toward this end, it was decided to prepare these scaffolds starting from various commercially available 4-substituted propiophenones **5a** and **5b**, 6- and/or 7-substituted tetralones **1a–d**, or dienes in the presence of the corresponding 2-bromo-5-methyl-



Scheme 2. Platform of synthetic methodologies to prepare a large number of diverse polysubstituted menadiones and analogues of the redox-active antimalarial lead 3-[4-(trifluoromethyl)benzyl]menadione, called plasmodione (Scheme 1).

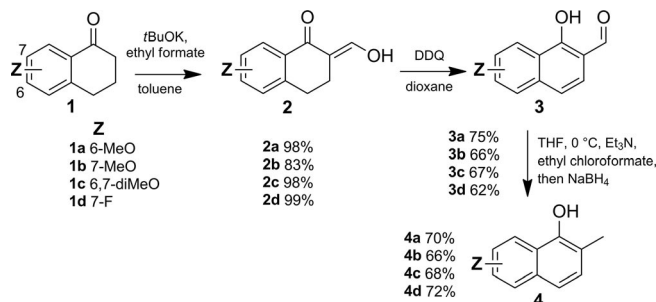
1,4-benzoquinone (**12a**) or 2-bromo-6-methyl-1,4-benzoquinone (**12b**). In this study, a small library of menadione analogues was built as key intermediates for the preparation of benzylMD derivatives that might be useful as templates both in drug discovery and medicinal chemistry. Thus, we report herein new regioselective synthetic methods to obtain polysubstituted menadiones by both the naphthol and Diels–Alder strategies (Scheme 2).

Naphthol Route – Synthesis of Methylnaphthols **4** and **9**

Two methods were employed to synthesize the polysubstituted methylnaphthols using commercially available tetralones or propiophenones.

Synthesis of Methylnaphthols **4** From Tetralones

The commercially available 1-tetralones **1** were quantitatively transformed in the presence of ethyl formate and *t*BuOK into the corresponding 2-hydroxymethylene derivatives **2** (Scheme 3).^[23] These compounds were aromatized with dichloro-5,6-dicyano-1,4-benzoquinone (DDQ) in dioxane^[24] to afford the intermediates **3** in good yields. Then the formyl group was reduced under mild conditions using a known protocol.^[25] 1-Hydroxy-2-naphthaldehydes **3** were treated with ClCO₂Et in the presence of Et₃N to give quantitatively the carb-



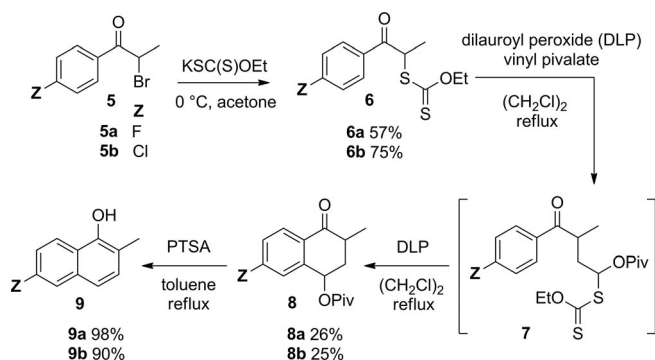
Scheme 3. Preparation of 2-methylnaphthols **4** starting from tetralones.

onate derivative, the treatment of which with NaBH₄ in aqueous THF at 0 °C directly afforded the desired 2-methylnaphthols **4** in good yields.

Synthesis of Methylnaphthols **9** from Propiophenones

Since the pioneering work of Quiclet-Sire and Zard, extensive research efforts have focused on the construction of diverse polysubstituted naphthols as starting blocks for the synthesis of complex natural products.^[26] Few examples of naphthoquinones have been reported; the synthesis of (±)-10-norparvulone and (±)-*O*-methylasparvenone were developed starting from commercially available *m*-methoxyphenol, hinging on a xanthate-mediated addition/cyclization sequence for the construction of the α -tetralone subunit, but lacking the methyl group.^[27] Furthermore, the synthesis of 6,7-substituted 2-methyltetralones was also developed by using a xanthate-mediated free-radical addition/cyclization sequence for the construction of the α -methyltetralone subunit starting from 4-substituted propiophenones, first by us,^[28a–c] and then by others.^[28d] Thus, bromopropiophenones **5** were easily synthesized from commercial propiophenones by bromination with Br₂ in AcOH.^[29] The treatment of propiophenones **5** with potassium ethyl xanthate in acetone at 0 °C afforded the desired radical precursors **6** in good yields (Scheme 4). Zard's procedure was used for the preparation of the key bicyclic intermediates **8**, starting with the radical addition of the xanthates **6** to vinyl pivalate using dilauroyl peroxide (DLP) as initiator in 1,2-dichloroethane (DCE) to yield the protected xanthates **7**, which can be used as a starting point for another radical sequence. When the xanthate **7** solutions were heated at reflux in DCE and treated with 1.2 equiv. of DLP (added portionwise), tetralones **8** were obtained in yields of 25 and 26 %.

The selection of vinyl pivalate as the radical trap was not arbitrary. It was anticipated that the OPiv group could serve as a leaving group for the aromatization in acidic media to facilitate the last step of the route. Next, tetralones **8** were treated with *p*-toluenesulfonic acid (PTSA)^[27b] in toluene at reflux to



Scheme 4. Preparation of 2-methylnaphthols via xanthates.

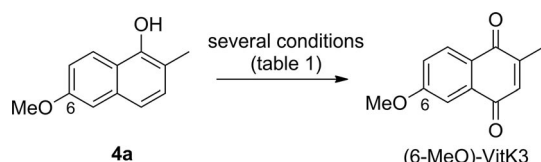
give the corresponding naphthols **9** in excellent yields (Scheme 4).

Synthesis of Polysubstituted Menadiones **10** and **11**

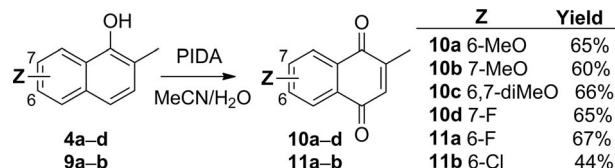
To find the best reaction conditions for the synthesis of the prototype menadione derivatives, 6-methoxy-2-methylnaphthol (**4a**) was chosen as the model substrate to optimize the reaction conditions. In the literature, many oxidizing agents have been employed for this purpose, including copper or copper(II) chloride (CuCl_2),^[22a] hypervalent iodine derivatives (phenyliodonium diacetate, PIDA),^[30] Fremy's salt,^[31] manganese dioxide (MnO_2),^[32] chromium trioxide (CrO_3),^[33] and radical oxidation [cerium(IV) ammonium nitrate, CAN],^[34] to cite but a few. We tested several conditions for the oxidation of 6-methoxy-2-methylnaphthol to 6-methoxymenadione (Table 1). The reaction did not proceed when performed with MnO_2 or Ag_2O ^[35] for 48 h. Oxidation by CAN, NBS (*N*-bromosuccinimide),^[36] and CuCl_2 gave the desired menadione after 1–2 h in poor yields. Using Fremy's salt as the oxidizing reagent gave the 6-methoxymenadione in quantitative yield when the reaction was performed on a small scale. However, Fremy's salt is unstable and expensive. For this reason, we selected PIDA, which gave a yield of 60 %, as the most appropriate oxidizing agent and pragmatic choice for the large-scale preparation of the 6-methoxymenadione.

Table 1. Optimization of the oxidation of 2-methylnaphthols **4a**.

Conditions	Yield [%]
MnO_2 (5 equiv.), CH_2Cl_2 , 48 h, r.t.	(starting material)
Ag_2O (5 equiv.), CH_2Cl_2 , 48 h, r.t.	(starting material)
CuCl (3 equiv.), air, r.t., 2 h	40
NBS (4 equiv.), $\text{AcOH}/\text{H}_2\text{O}$, 1 h, 65 °C	40
CAN (3 equiv.), $\text{MeCN}/\text{H}_2\text{O}$, 1 h, r.t.	24
Fremy's salt (2.8 equiv.), KH_2PO_4 (0.8 equiv.), acetone/ H_2O , 2 h, 0 °C	99
PIDA, (2.5 equiv.), $\text{MeCN}/\text{H}_2\text{O}$, 2 h, –5 to 10 °C	60



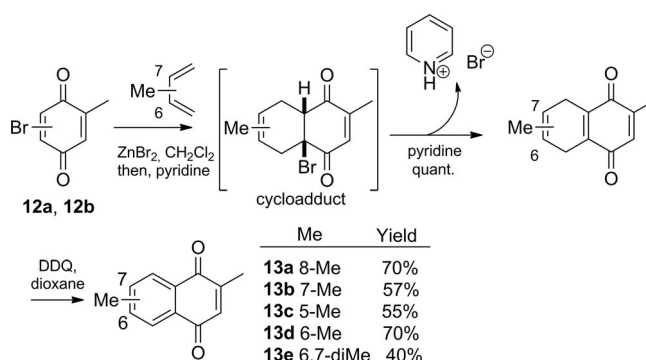
The oxidation reactions of naphthols **4** and **9** with PIDA were successfully performed, and moderate-to-good yields of **10a–d** and **11a,b** were obtained when the reactions were conducted on a multigram scale. Thus, a large variety of menadione analogues can be prepared by this approach (Scheme 5).



Scheme 5. Oxidation of the corresponding α -naphthols **4** and **9** to menadione analogues **10** and **11**.

Diels–Alder Route – Synthesis of Methylmenadiones **14a–e**

Regioselective annulations of quinones by Diels–Alder reactions can be achieved when haloquinones react with dienes bearing electron-donating groups in the presence of Lewis acids.^[37] In this work, 5-, 6-, 7-, 8-methyl or 6,7-dimethylmenadione derivatives **13a–e** were obtained by ZnBr_2 -catalyzed Diels–Alder reactions with piperylene, isoprene, or 2,3-dimethylbuta-1,3-diene as the diene and 2-bromo-5-methylbenzoquinone (**12a**) or 2-bromo-6-methylbenzoquinone (**12b**) as the dienophile. The oxidation of the Diels–Alder adducts was not anticipated to be difficult: Treatment of the reaction mixture under basic conditions is a common method for generating oxidized naphthoquinones. Disappointingly, in contrast to the examples reported in the literature, elimination of HBr did not occur in situ and several conditions had to be tested to find a convenient method to synthesize the methylmenadione scaffolds. Heating the cycloadduct intermediate in toluene at reflux for 24 h or treating it with oxidizing agents such as CAN or DDQ^[38] afforded the starting material. Furthermore, the addition of bases such as Et_3N or *i* Pr_2NEt did not promote the desired elimination, but degradation of the intermediate. In fact, the cycloaddition product displayed an unusual sensitivity to basic conditions. Finally, the reaction was optimized by the addition of 1 equivalent of pyridine as base. Note that the addition of pyridine following the cycloaddition favors HBr elimination and prevents product degradation. In this way, treatment of the cycloadduct with pyridine and dehydrogenation with DDQ in dioxane af-

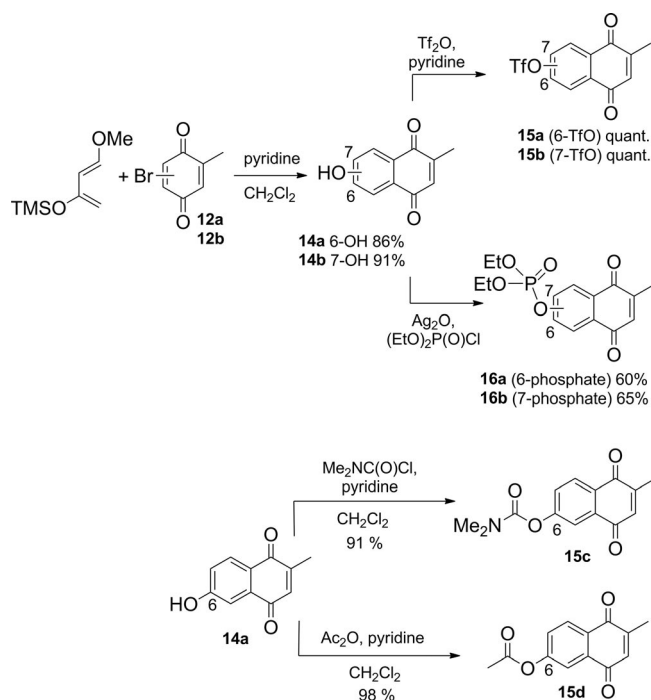


Scheme 6. Synthesis of methylated menadiones by Diels–Alder reactions.

forded the corresponding methylmenadiones **13a–e** in satisfactory yields (Scheme 6).

Synthesis and Functionalization of 6- and 7-Hydroxymenadiones

6- and 7-Hydroxymenadiones **14a** and **14b** were synthesized by Diels–Alder reactions using Danishefsky's diene^[39] and bromo-1,4-benzoquinones **12a** and **12b** as substrates, respectively (Scheme 7).



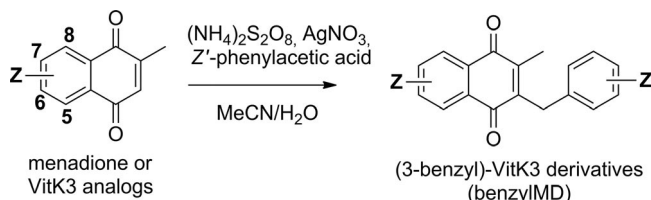
Scheme 7. Synthesis and functionalization of hydroxymenadione derivatives by Diels–Alder reactions.

The cycloadducts of 1,3-dioxybutadienes and bromoquinones underwent aromatization with the loss of 1 equivalent of MeOH. The reactions were carried out in CH_2Cl_2 by using pyridine as a base to promote the elimination of HBr. Indeed, deprotonation of the hydroxy group with pyridine and subsequent reaction with triflic anhydride, carbamoyl chloride, or acetic anhydride in CH_2Cl_2 afforded the desired menadione derivatives **15a–d**, respectively, in excellent yields (Scheme 7). However, the reaction did not proceed when pyridine was used in the reaction with diethyl chlorophosphate.^[40] Finally, after further optimization using Ag_2O in CH_2Cl_2 , 6- and 7-phosphate diethyl esters **16a** and **16b** were obtained in yields of 60 and 65 %, respectively (Scheme 7). Thus, diversely functionalized menadiones can be easily synthesized in excellent yields starting from readily prepared hydroxymenadiones, as exemplified by 6-hydroxymenadione **14a** (Scheme 7).

Synthesis of 3-(Substituted-benzyl)menadione Derivatives

3-(Substituted-benzyl)MD derivatives were synthesized by Jacobsen–Torrshell reactions^[41] (better known as the Kochi–Anderson

reaction^[21]) between commercial phenylacetic acids and the synthesized menadione analogues (2-methyl-1,4-naphthoquinones), as shown in Scheme 8.



Scheme 8. Synthesis of 3-benzylmenadione derivatives.

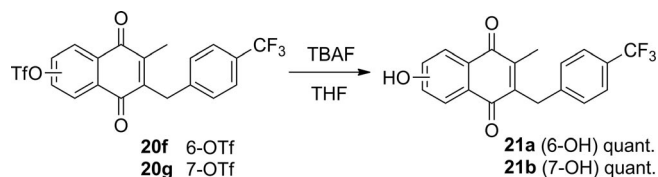
This synthetic methodology is the most useful pathway for the preparation of alkylated menadiones in bulk. The scope of this versatile reaction is illustrated by the successful use of 4'-Br, 4'-CF₃, 2',5'-diMeO, and 3',5'-diMeO-functionalized phenylacetic acids and a wide array of substituted menadiones in the reaction. Only alcohols and amino groups have been reported to stop the Ag^{II} catalysis under Kochi–Anderson reaction conditions.^[17] The overall yields of this reaction are presented in Table 2. It is noteworthy that this procedure offers an efficient synthesis of 3-(substituted-benzyl)menadione derivatives. Furthermore, Z and Z' could be electron-donating or -withdrawing functionalities at different positions of the substrate; they were well tolerated and gave the desired compounds in good-to-excellent yields. As expected, the reaction was compatible with a wide range of substituents, such as halogens, methyl, meth-

Table 2. Synthesis of 3-(substituted-benzyl)menadione derivatives **17–20** by the Kochi–Anderson reaction.

BenzylMD ^[a]	Z	Z'	Yield [%]
17a	6-MeO	4'-CF ₃	80
17b	7-MeO	4'-CF ₃	70
17c	6,7-diMeO	4'-CF ₃	80
17d	7-F	4'-CF ₃	65
17e	6-F	4'-CF ₃	55
17f	6-Cl	4'-CF ₃	71
18a	6-MeO	4'-Br	78
18b	7-MeO	4'-Br	63
18c	6,7-diMeO	4'-Br	75
18d	7-F	4'-Br	86
18e	6-F	4'-Br	85
19a	8-Me	4'-CF ₃	75
19b	7-Me	4'-CF ₃	68
19c	5-Me	4'-CF ₃	76
19d	6-Me	4'-CF ₃	65
19e	6,7-diMe	4'-CF ₃	87
20a	8-Me	4'-Br	67
20b	7-Me	4'-Br	70
20c	5-Me	4'-Br	76
20d	6-Me	4'-Br	50
20e	6,7-diMe	4'-Br	82
20f	6-TfO	4'-CF ₃	80
20g	7-TfO	4'-CF ₃	70
20h	7-MeO	3',5'-diMeO	77
20i	7-MeO	2',5'-diMeO	65
20j	6,7-diMeO	3',5'-diMeO	55
20k	6,7-diMeO	2',5'-diMeO	72
20l	6-MeO	3',5'-diMeO	71
20m	6-MeO	2',5'-diMeO	65
20n	6-P(O) ₂ (EtO) ₂	4'-CF ₃	77
20o	7-P(O) ₂ (EtO) ₂	4'-CF ₃	70

oxy, and protected hydroxy groups, providing the corresponding products with good purity. In all cases, the results show excellent efficiency of the Ag(II)-mediated radical decarboxylation reaction between menadiones and commercial phenylacetic acids, affording 31 targeted products (**17a–f**, **18a–e**, **19a–e**, and **20a–o**) in good-to-excellent yields (50–87 %). In general, the reactions were clean, rapid, and efficient.

Pursuing our ongoing interest to increase the diversity of available 3-benzylMD derivatives, we decided to regenerate the hydroxy substituent group by deprotection of the triflate group in the menadione substrates **20f** and **20g**. TBAF-promoted triflate removal (in THF at room temperature)^[42] was used for this reaction to yield the expected compounds **21a** and **21b** quantitatively (Scheme 9).



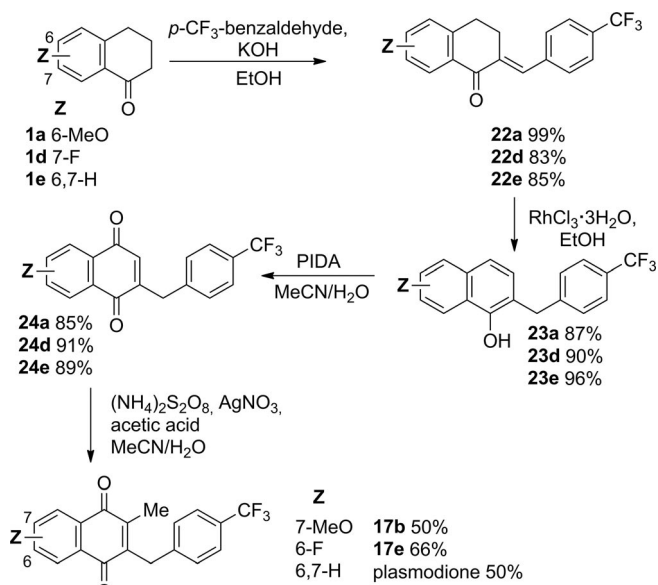
Scheme 9. Synthesis of 6- or 7-hydroxy-3-benzylmenadiones.

Expeditious and High-Yielding Route to 3-(Substituted-benzyl)menadione Derivatives

An elegant pathway that allows the formation of two 3-(substituted-benzyl)menadione regioisomers at C-6 or C-7 from the same starting material has also been envisioned. In this new process, the final benzylic chain is proposed to be introduced in the first step through the coupling of benzaldehydes to various commercial tetralones.

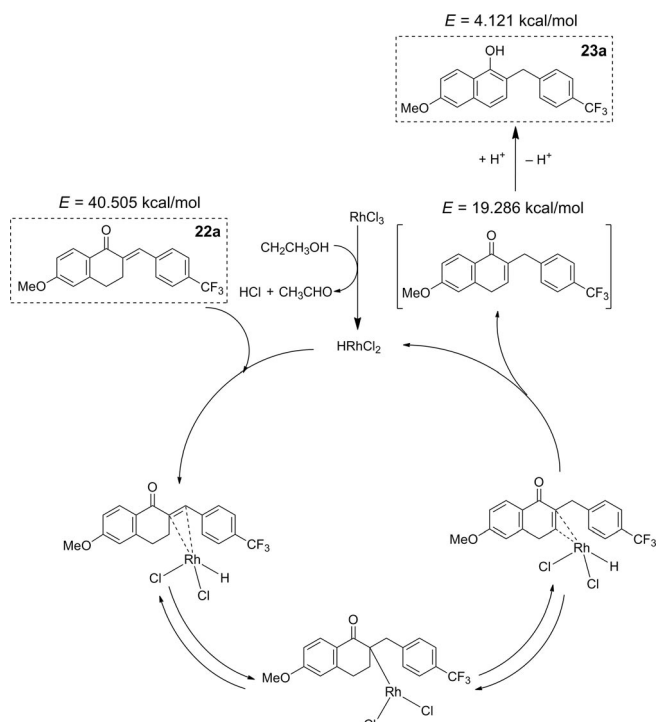
In this alternative scenario, the naphthol route is advantageous with regard to step economy, because 6- or 7-substituted 3-benzylMD regioisomers can be prepared in high yields by two pathways from the same tetralones **1a**, **1d**, or **1e**, that is, in five steps for the 6-regioisomers **17a** and **17e** (Schemes 3, 5, and 8), or only in four steps in the following expeditious route to plasmodione and the regioisomers **17b** and **17e**, respectively (Scheme 10). The conditions screened for aromatization included treatment of the starting α -methylene ketone **22a** with various oxidation catalysts. These conditions were 1) PIDA, MeCN, 12 h, room temperature, 2) TFA, CH₂Cl₂, 12 h, room temperature, 3) tBuOK, DMSO, 12 h, room temperature,^[43] 4) RuCl₃, EtOH, 24 h, reflux, 5) DDQ, dioxane, 24 h, reflux,^[44] 6) trimethylphenol, TFA, 90 °C, 24 h,^[44] 7) MnO₂ (5 equiv.), CH₂Cl₂, 48 h, room temperature, 8) Ag₂O (5 equiv.), CH₂Cl₂, 48 h, room temperature, 9) CrO₃, H₂O, AcOH, 90 °C, 12 h, 10) Ag₂O (16 equiv.), 6 M HNO₃, dioxane, room temperature, 11) CuCl₂, THF, H₂O, 24 h, room temperature, or 12) RhCl₃, (10 mol-%) EtOH, reflux, 6 h.^[45] Only RhCl₃ efficiently catalyzed the aromatization of the α -methylene tetralone **22a** to the desired naphthol **23a** to give a very satisfactory yield (87 %); all the other reactions led to recovery of the starting material.

However, the reactivity of the Rh catalyst was highly dependent on the stability of the Rh^I species. According to the mechanistic study described by Paiaro et al.,^[45a] Rh^{III}Cl₃ is first reduced by ethanol to form HRhCl₂ and then coordinates to the olefin



Scheme 10. Express synthesis of 3-(substituted-benzyl)menadione derivatives starting from tetralones.

functional group (Scheme 11). Subsequently, oxidative addition and β -elimination forces a shift of the double bond (Scheme 11) and finally aromatization to the most thermodynamically stable naphthol **23a** (the calculated free energies were estimated by ChemBioOffice 2012^[53]). Indeed, the active Rh^I intermediate was found to be sensitive to oxygen in open air and lost efficiency; however, the use of well-degassed dry solvents and strict anaerobic conditions, both the yield (increased to 95 %) and reproducibility of this reaction were optimized.



Scheme 11. Proposed mechanism for the rhodium-catalyzed olefin isomerization.

Compounds **23a**, **23d**, and **23e** were then successfully oxidized with PIDA followed by the Kochi–Anderson reaction to give the three benzylIMDs, namely plasmodione, **17b**, and **17e** in moderate-to-good yields.

In the final step, methylation with acetic acid was thought to be feasible; however, the yields of the preliminary reactions were not satisfactory. By using a phenylacetic acid as partner in the coupling reactions with menadiones, the yields of the radical alkylation products ranged from 50 to 87 %. However, when using acetic acid instead of phenylacetic acid, the methylation yield was limited to 30 %, because the stability of the methyl radical is much lower^[46] than that of the benzyl radical, and the more reactive methyl radical may destroy the desired product. To increase the yield of this reaction, the relative amounts of acetic acid, silver nitrate, and ammonium persulfate were varied without impacting the outcome of the reaction.

To follow the reaction kinetics and track the reaction products by NMR spectroscopy, we used 2-[4-(trifluoromethyl)benzyl]naphthalene-1,4-dione (**24e**) as the starting material for the reaction model. After stirring for 30 min, the reaction conversion reached over 50 % and we observed the rapid generation of 2-benzylIMD. After 1 hour, the starting material had been almost completely consumed and the benzylIMD was almost exclusively the final product, as shown by the complete disappearance of the proton ($\delta = 6.70$ ppm) at C-2 present in the starting material (see the kinetics of the reaction by the change in the NMR spectra over time, Figure 2, a). However, after 1 h,

the formation of side-products was observed and the yield of the reaction decreased (Figure 2, b). Based on the kinetic profile determined by ¹⁹F NMR analysis in a mixture of CD₃CN/D₂O, the protocol of this reaction was optimized to give a yield of 50–60 % after two purification steps (chromatography followed by precipitation). The preparation of plasmodione and the analogues **17b** and **17e** (Scheme 10) reflects the optimized process.

Antimalarial Activities of 3-(Substituted-benzyl)menadione Derivatives

1,4-Naphthoquinones are widely distributed in naturally occurring quinones. Their role in biochemistry has often been highlighted because of their electron-transfer properties in numerous important pathways from the respiratory chain of living cells to maintaining the redox equilibrium in cytosol. In the first part of our investigation of menadione properties, we evaluated the oxidant character of newly synthesized 2-methyl-1,4-naphthoquinones by cyclic voltammetry to evaluate and establish a predictive structure–redox potential model (QSPR: quantitative structure–property relationship) based on the electro- and physicochemical properties of various redox-active compounds.^[4b] With these new tools in hand, we made available an on-line evaluation (through the Web interface) of the oxidant character of redox agents to help chemists targeting such desired redox properties. Also, seminal studies on several synthetic naphthoquinones found that these compounds possess antiprotozoal activities.^[47] These include potent antimalarial properties, which have been reported for synthetic atovaquone (as the main active principle of Malarone[®]),^[48] and by us, for synthetic 2-methyl-1,4-naphthoquinone (or menadione) derivatives like plasmodione.^[17–19] In the present study, we explored the consequences of the incorporation of halogen, methyl, methoxy, and hydroxy groups into the phenyl ring of the menadione core on the antimalarial activity of the privileged benzylIMD structure. Therefore, the structure–activity relationships of the polysubstituted benzylIMD series were assessed through a study of the effect of the functionalization of both the phenyl ring of the menadione core (Z) and benzyl chain (Z') on the antimalarial activities in comparison with the lead plasmodione, which has been reported previously.^[17] The 50 % inhibitory concentration (IC₅₀) was determined for each compound by using the SYBR green assay in the presence of *P. falciparum* strain Dd2 parasitized red blood cells in culture (Table 3). In parallel, the IC₅₀ values of positive controls, chloroquine (82.4 nM) and Methylene Blue (3.6 nM), were determined to be of the same order of magnitude as the values reported elsewhere.^[18] In the data presented in Table 3, the IC₅₀ values of the lead plasmodione (Z = H, Z' = 4'-CF₃) and its 4-bromobenzyl derivative (Z = H, Z' = 4'-Br), called benzylIMD **1a** in the previous report,^[17] are lower than the value of the antimalarial drug chloroquine, attesting to a slightly superior antiplasmodial activity (58 and 82 vs. 99 nM) against the multidrug-resistant *P. falciparum* strain Dd2. Interestingly, among the newly synthesized benzylIMD derivatives (Z, Z'), the most potent antimalarial compounds are the 6- and 7-fluoro analogues of plasmodione,

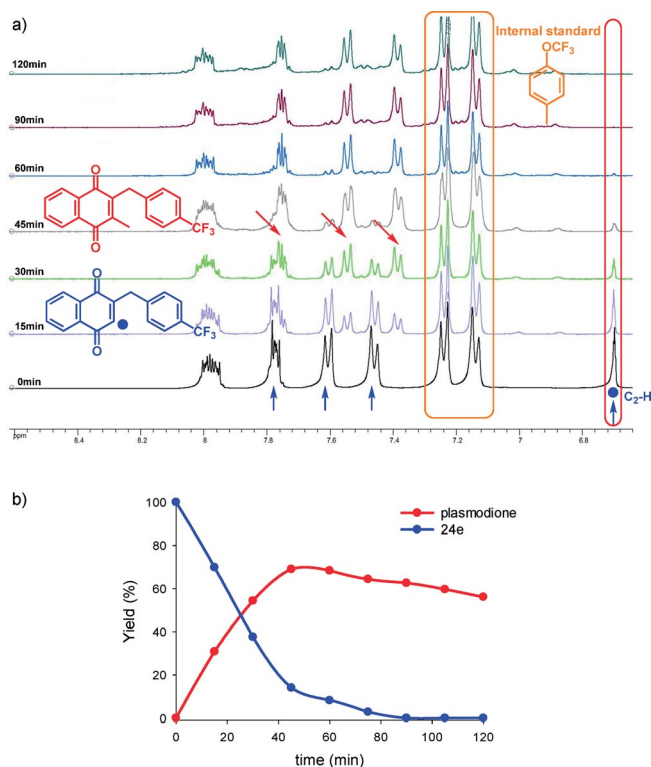
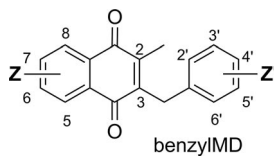


Figure 2. a) Kinetic ¹H NMR spectroscopy study of the Kochi–Anderson reaction between demethylmenadione **24e** and acetic acid. b) Kinetic profile for the Kochi–Anderson reaction of **24e** to plasmodione, determined by ¹⁹F NMR analysis experiments. The two NMR studies were performed in a mixture of CD₃CN/D₂O using 1-methyl-4-(trifluoromethoxy)benzene as internal standard.

Table 3. Averaged IC₅₀ values for polysubstituted 3-benzylmenadiione derivatives determined from growth inhibition assays with *Plasmodium falciparum* strain Dd2.


BenzylMD	Z	Z'	IC ₅₀ [nM] (n) ^[a]	BenzylMD	Z	Z'	IC ₅₀ [nM] (n) ^[a]
17a	6-MeO	4'-CF ₃	186 ± 58 (3)	20b	7-Me	4'-Br	992 ± 107 (3)
17b	7-MeO	4'-CF ₃	3187 (1)	20c	5-Me	4'-Br	1820 ± 71 (3)
17c	6,7-diMeO	4'-CF ₃	3685 (1)	20d	6-Me	4'-Br	171 ± 66 (3)
17d	7-F	4'-CF ₃	83 ± 12 (4)	20e	6,7-Me	4'-Br	2706 ± 26 (2)
17e	6-F	4'-CF ₃	59 ± 11 (3)	20f	6-OTf	4'-CF ₃	236 ± 37 (4)
17f	6-Cl	4'-CF ₃	242 ± 60 (4)	20g	7-OTf	4'-CF ₃	3546 ± 902 (3)
18a	6-MeO	4'-Br	171 ± 69 (3)	20h	7-MeO	3',5'-diMeO	778 ± 89 (4)
18b	7-MeO	4'-Br	3230 (1)	20i	7-MeO	2',5'-diMeO	2187 (1)
18c	6,7-diMeO	4'-Br	881 ± 129 (4)	20j	6,7-diMeO	3',5'-diMeO	2704 (1)
18d	7-F	4'-Br	74 ± 32 (4)	20k	6,7-diMeO	2',5'-diMeO	1365 ± 521 (4)
18e	6-F	4'-Br	83 ± 23 (3)	20m	6-MeO	2',5'-diMeO	104 ± 58 (4)
19a	8-Me	4'-CF ₃	3004 ± 941 (2)	20n	6-P(O) ₄ (Et) ₂	4'-CF ₃	157 ± 49 (2)
19b	7-Me	4'-CF ₃	439 ± 205 (5)	20o	7-P(O) ₄ (Et) ₂	4'-CF ₃	518 ± 231 (3)
19c	5-Me	4'-CF ₃	3638 ± 193 (2)	BenzylMD 1a ^[b]	H	4'-Br	82 ± 20 (7)
19d	6-Me	4'-CF ₃	215 ± 68 (3)	Plasmodione ^[c]	H	4'-CF ₃	58 ± 11 (9)
19e	6,7-diMe	4'-CF ₃	3243 ± 260 (3)	2-Demethylplasmodione 24e	H	4'-CF ₃	3698 ± 191 (2)
20a	8-Me	4'-Br	3761 ± 972 (3)	CQ ^[d]	–	–	82.4 ± 1.6 (3)

[a] Activity against cultured parasites of the *P. falciparum* Dd2 strain is presented as mean IC₅₀ values ± standard deviation (SD) determined from *n* independent growth inhibition assays in triplicate using the SYBR® green technique. [b] From ref.^[17] [c] Plasmodione, named benzylMD **1c**, in ref.^[17–19] and its 4-bromo analogue, named benzylMD **1a** in ref.^[17], were used as internal references. The lower nanomolar IC₅₀ values previously reported for plasmodione and its 4-bromo analogue against the drug-multiresistant *P. falciparum* Dd2 strain were evaluated in a distinct assay based on tritiated hypoxanthine incorporation (ref.^[17]). [d] Methylene Blue [MB, IC₅₀ = 3.6 ± 0.4 (4)] and chloroquine (CQ) were used as standard drugs.

17e (6-F, 4'-CF₃), **18e** (6-F, 4'-Br), **17d** (7-F, 4'-CF₃), and **18d** (7-F, 4'-Br), respectively (**17e**: 59 nM, **18e**: 83 nM, **17d**: 83 nM, and **18d**: 74 nM vs. 58 nM with plasmodione), which suggests that the introduction of fluorine at C-6 or C-7 might be a favorable/tolerant substitution to maintaining antimalarial activity. In contrast to the substitution by halogens, the antimalarial activities of the methylated and methoxylated Z analogues of the lead plasmodione are significantly reduced, regardless of the substitution position on the phenyl ring, but with substitution at C-6 always being the most favorable when Z' is an electron-withdrawing group (4'-CF₃, 4'-Br). For instance, the IC₅₀ values range from 171 nM (for the 6-MeO- and 6-Me-substituted benzylMDs **18a** and **20d** with a 4'-Br-benzyl chain, respectively) to 186 nM and 215 nM (for the 6-MeO- and 6-Me-substituted benzylMDs **17a** and **19d** with a 4'-CF₃-benzyl chain, respectively). Furthermore, methylation at C-5 or C-8 dramatically reduces the activity, with the IC₅₀ values increasing to 3638 nM for the 5-Me-substituted benzylMD **19c** (4'-CF₃) and to 3004 nM and 3761 nM for the 8-Me-substituted benzylMDs **19a** and **20a** (4'-CF₃ and 4'-Br). Finally, 2-demethylplasmodione **24e**, with a hydrogen atom instead of a methyl group at C-2, displays a very weak antimalarial activity, attesting to the essential requirement of the 2-methyl group in the menadiione core.

Conclusions

This study has provided new insights into the synthetic methodologies that can be used to prepare various biologically ac-

tive polysubstituted 2-methyl-3-benzyl-1,4-naphthoquinones by efficient and versatile strategies, namely the naphthol route, starting from either a tetralone or a propiophenone, or regio-selective Diels–Alder reactions. These original procedures were found to be useful for the synthesis of focused chemical libraries of benzylMD analogues with broad structural diversity. The structural complexity, ease of synthesis, and variation in substitution patterns present in these molecules will allow quantitative structure–activity relationship studies, useful for various biological applications. In this work we have found compounds displaying a wide variation of activity against *P. falciparum* parasites. These synthetic templates may be employed as an important class of “privileged scaffolds” in redox medicinal chemistry.

Experimental Section

Detailed descriptions of experimental procedures are given in the Supporting Information.

General Procedure 1 for the α -Formylation of Tetralone: A mixture of tetralone in toluene (1 equiv., 0.45 mmol mL⁻¹) and ethyl formate (2.0 equiv.) was prepared. The solution was cooled to –78 °C under argon and mechanically stirred while potassium *tert*-butoxide (2.0 equiv.) was added in portions: The solution became milky and pinky in color. The solution was warmed to –5 °C until TLC monitoring (petroleum ether/Et₂O, 3:1) indicated the completion of the reaction. The solution was quenched with 10 % HCl (the pink color disappeared) and the mixture extracted with Et₂O. The organic phases were dried (brine, MgSO₄) and concentrated in vacuo to yield α -formyl tetralone (usually as a solid).

Typical Procedure for the Synthesis of 2-(Hydroxymethylene)-6-methoxy-3,4-dihydronaphthalen-1(2H)-one (2a): Commercially available 6-methoxytetralone (12.0 g, 68.14 mmol, 1 equiv.) was used as the starting material and treated according to the general procedure 1 to give **2a** (13.62 g, 66.8 mmol), yield 98 %; light-brown solid; m.p. 66–67 °C (ref.^[24] 68–69 °C). ¹H NMR (200 MHz, CDCl₃): δ = 7.91 (d, *J* = 8.6 Hz, 1 H), 6.82 (dd, *J* = 8.6, 2.4 Hz, 1 H), 6.68 (d, *J* = 2.4 Hz, 1 H), 3.82 (s, 3 H), 2.82 (t, *J* = 7.3 Hz, 2 H), 2.51 (t, *J* = 7.3 Hz, 2 H) ppm. ¹³C NMR (75 MHz, CDCl₃): δ = 208.1 (C=O), 175.1 (CH), 163.5 (C_q), 144.5 (C_q), 128.8 (CH), 126.2 (CH), 113.1 (CH), 112.6 (C_q), 108.21 (CH), 55.5 (OCH₃), 29.4 (CH₂), 23.3 (CH₂) ppm.

General Procedure 2 for the Aromatization of α-Formyltetralone to α-Formylnaphthol: 2,3-Dichloro-5,6-dicyano-1,4-benzoquinone (DDQ; 1.0 equiv.) was added to a solution of α-formyltetralone in dioxane (1.0 equiv., 0.2 M) at room temperature. A white precipitate appeared rapidly. After completion of the reaction (TLC monitoring), the white precipitate was removed by filtration. The filtrate was concentrated under reduced pressure. The crude was purified by column chromatography (silica gel, cyclohexane/Et₂O, 3:1) to give the desired compound.

Typical Procedure for the Synthesis of 1-Hydroxy-6-methoxy-2-naphthaldehyde (3a): Compound **2a** was used as the starting material (4.08 g, 19.69 mmol) and treated according to the general procedure 2 to give **3a** (2.86 g, 14.2 mmol), yield 75 %; white powder; m.p. 128–129 °C (ref.^[24] 133 °C). ¹H NMR (200 MHz, CDCl₃): δ = 12.70 (s, 1 H), 9.90 (s, 1 H), 8.35 (d, *J* = 9.2 Hz, 1 H), 7.45 (d, *J* = 8.8 Hz, 1 H), 7.26 (d, *J* = 8.8 Hz, 1 H), 7.18 (dd, *J* = 9.2, 2.6 Hz, 1 H), 7.09 (d, *J* = 2.6 Hz, 1 H), 3.96 (s, 3 H) ppm. ¹³C NMR (75 MHz, CDCl₃): δ = 195.6 (C=O), 162.0 (C_q), 161.5 (C_q), 139.6 (C_q), 127.5 (CH), 126.1 (C_q), 119.0 (CH), 116.4 (CH), 116.2 (CH), 113.2 (C_q), 106.3 (CH), 55.5 (OCH₃) ppm.

General Procedure 3 for the Reduction of 2-Formyl-1-naphthols: Triethylamine (1.2 equiv.) was added to a solution of 2-formyl-1-naphthol in tetrahydrofuran (1.0 equiv., 1 mmol mL⁻¹). The solution was cooled to 0 °C and then ethyl chloroformate (1.2 equiv.) was added over a period of 30 min. The solution was stirred during 30–60 min (white precipitate formed). The precipitate (triethylamine hydrochloride) was removed by filtration and washed with tetrahydrofuran (twice less than the amount used for the reaction). An aqueous solution of NaBH₄ (4.0 equiv., 2.6 M) was added to the combined filtrates at 5–15 °C. When the addition was complete, the reaction mixture was stirred at room temperature for 1–2 h and then diluted with water. The solution was cooled to 0 °C and made acidic by the slow addition of aqueous HCl (10 %). The aqueous solution was extracted with Et₂O. The organic phases were washed with a dilute solution of NaOH (10 %), dried (brine, MgSO₄), and concentrated in vacuo to yield methyl-naphthol (usually as a solid or oil that crystallized on standing).

Typical Procedure for the Synthesis of 6-Methoxy-2-methylnaphthalen-1-ol (4a): Compound **3a** was used as the starting material (1.32 g, 6.47 mmol) and treated according to the general procedure 3 to give **4a** (0.85 g, 4.53 mmol), yield 70 %; deliquescent white powder. ¹H NMR (300 MHz, CD₂Cl₂): δ = 8.03 (d, *J* = 9.8 Hz, 1 H), 7.24 (AB system, *J* = 8.1 Hz, 2 H), 7.11 (m, 2 H), 5.19 (s, 1 OH), 3.90 (s, 3 H), 2.37 (s, 3 H) ppm. ¹³C NMR (75 MHz, CD₂Cl₂): δ = 158.1 (C_q), 15.7 (CH₃), 55.8 (OCH₃), 149.4 (C_q), 135.3 (C_q), 130.3 (CH), 123.2 (CH), 120.1 (C_q), 119.5 (CH), 118.3 (CH), 114.8 (C_q), 106.2 (CH) ppm. MS (EI): *m/z* (%) = 188.1 (100) [M]⁺, 145.0 (83), 115.0 (62), 189.1 (15) [M + H]⁺.

General Procedure 8 for the Oxidation of Methyl-naphthols to Menadiones: (Diacetoxyiodo)benzene (PIDA) (12.1 mmol, 2.1 equiv.) was added portionwise to a stirred solution of the methyl-naphthol (5.8 mmol, 1 equiv.) in acetonitrile (70 mL) and water (30 mL) at –5 °C over 20–30 min. After stirring for 30 min at –5 °C, the reaction mixture was stirred at room temperature for 1 h. A saturated NaHCO₃ solution was added to the orange reaction mixture and the reaction mixture extracted with Et₂O (3 × 120 mL). The combined organic extracts were washed with brine and dried with anhydrous MgSO₄. The crude was purified by flash chromatography on silica gel (hexane/Et₂O, 2:3) to give the desired compound.

Typical Procedure for the Synthesis of 6-Methoxy-2-methylnaphthalene-1,4-dione (10a): Compound **4a** was used as the starting material (2.0 g, 10.63 mmol) and treated according to the general procedure 8 to give **10a** (1.40 g, 6.91 mmol), yield 65 %; yellow powder; m.p. 146–148 °C (Et₂O). ¹H NMR (200 MHz, CDCl₃): δ = 8.04 (d, *J* = 8.6 Hz, 1 H), 7.49 (d, *J* = 2.8 Hz, 1 H), 7.18 (dd, *J* = 8.6, *J* = 2.8 Hz, 1 H), 6.79 (q, *J* = 1.8 Hz, 1 H), 3.94 (s, 3 H), 2.18 (d, *J* = 1.8 Hz, 3 H) ppm. ¹³C NMR (75 MHz, CDCl₃): δ = 185.06 (C=O), 184.56 (C=O), 163.96 (C_q), 148.52 (C_q), 135.25 (CH), 134.33 (C_q), 129.02 (CH), 125.77 (C_q), 120.21 (CH), 109.29 (CH), 55.91 (OCH₃), 16.52 (CH₃) ppm. HRMS (ESI): calcd. for C₁₂H₁₀O₃Na 225.0522 [M + Na]⁺; found 225.0522.

General Procedure 9 for the Preparation of Menadiones by the Diels–Alder Reaction: A solution of 2-bromo-5-methyl-1,4-benzoquinone (**12a**) or 2-bromo-6-methyl-1,4-benzoquinone (**12b**; 1.0 equiv.) in dry CH₂Cl₂ (0.15 mmol mL⁻¹) was added to a suspension of ZnBr₂ (1.2 equiv.) in dry CH₂Cl₂ (1.5 mmol mL⁻¹). The mixture was stirred for 5 min and the appropriate diene was added (10 equiv.). After stirring overnight the reaction mixture was quenched with a solution of saturated NH₄Cl. The reaction mixture was extracted with CH₂Cl₂ and the combined CH₂Cl₂ layers were washed with brine and dried with MgSO₄. Pyridine (2 equiv.) was added and the mixture was stirred at room temperature for 4 h. CH₂Cl₂ was evaporated to yield the quinone as a yellow oil. The quinone (1.0 equiv.) was dissolved in dioxane (0.3 M) and DDQ (1.0 equiv.) was added at room temperature. After completion of the reaction (TLC monitoring), the white precipitate was removed by filtration. The filtrate was concentrated under reduced pressure. The crude was purified by column chromatography (silica gel, cyclohexane/EtOAc, 4:1) to give the desired compound.

Typical Procedure for the Synthesis of 2,8-Dimethylnaphthalene-1,4-dione (13a): 2-Bromo-6-methyl-1,4-benzoquinone (**12b**; 2.50 g, 13.55 mmol) and piperylene (10 mL, 135.5 mmol) were used as the starting materials and treated according to the general procedure 9 to give **13a** (1.76 g, 9.48 mmol), yield 70 %; yellow needles; m.p. 132 °C (hexane/EtOAc). ¹H NMR (300 MHz, CDCl₃): δ = 7.99 (dd, *J* = 10.5, *J* = 2.4 Hz, 1 H), 7.61–7.49 (m, 2 H), 6.81 (q, *J* = 2.1 Hz, 1 H), 2.75 (s, 3 H), 2.18 (d, *J* = 2.1 Hz, 3 H) ppm. ¹³C NMR (75 MHz, CDCl₃): δ = 187.51 (C=O), 185.34 (C=O), 149.45 (C_q), 141.28 (C_q), 137.65 (CH), 134.27 (CH), 133.76 (C_q), 132.79 (CH), 129.84 (C_q), 124.99 (CH), 22.89 (CH₃), 16.86 (CH₃) ppm. HRMS (ESI): calcd. for C₁₂H₁₁O₂ 187.0754 [M + H]⁺; found 187.0761.

General Procedure 10 for the Diels–Alder Reaction with Danishefsky's Diene: 1-Methoxy-3-(trimethylsilyloxy)-1,3-butadiene (2.0 equiv.) was added dropwise to 2-bromo-5-methyl-1,4-benzoquinone (**12a**) or 2-bromo-6-methyl-1,4-benzoquinone (**12b**; 1.0 equiv.) in CH₂Cl₂ (0.2 M) at 0 °C. The solution was stirred at room temperature for 2 h, then pyridine (1.5 equiv.) was added, and the suspension stirred under air at room temperature for 6 h. Concentration and flash column chromatography (ethyl acetate/toluene, 1:2) gave hydroxy-2-methylnaphthalene-1,4-dione.

Typical Procedure for the Synthesis of 6-Hydroxy-2-methylnaphthalene-1,4-dione (14a): 2-Bromo-6-methyl-1,4-benzoquinone (**12b**; 2.00 g, 9.90 mmol, 1 equiv.) and Danishefsky's diene (2.9 mL, 14.85 mmol, 1.5 equiv.) were used as the starting materials and treated according to the general procedure 10 to give **14a** (1.60 g, 8.50 mmol), yield 86 %; orange solid; m.p. 175 °C (hexane/EtOAc). ¹H NMR (400 MHz, [D₆]DMSO): δ = 10.96 (s, 1 H), 7.92 (d, *J* = 8.4 Hz, 1 H), 7.29 (d, *J* = 2.8 Hz, 1 H), 7.19 (dd, *J* = 8.4, *J* = 2.8 Hz, 1 H), 6.93 (q, *J* = 1.6 Hz, 1 H), 2.15 (d, *J* = 1.6 Hz, 3 H) ppm. ¹³C NMR (100 MHz, [D₆]DMSO): δ = 185.18 (C=O), 184.31 (C=O), 163.07 (C_q), 148.75 (C_q), 135.27 (CH), 134.49 (C_q), 129.56 (CH), 124.44 (C_q), 121.03 (CH), 111.82 (CH), 16.45 (CH₃) ppm. HRM (ESI): calcd. for C₁₁H₉O₃ 189.0546 [M + H]⁺; found 189.0557.

General Procedure 13 for the Synthesis of Benzyl Menadione Derivatives: The corresponding menadione derivative (1 equiv., 0.05 mmol mL⁻¹) and phenylacetic acid derivative (2 equiv.) were added to a stirred solution of MeCN/H₂O (3:1) and heated at 85 °C (70 °C in the flask). AgNO₃ (0.35 equiv.) was first added and then (NH₄)₂S₂O₈ (1.3 equiv., 0.36 mmol mL⁻¹) in MeCN/H₂O (3:1) was added dropwise. The reaction mixture was then heated for 2–3 h at 85 °C. MeCN was evaporated and the mixture extracted with DCM. The crude mixture was purified by flash chromatography on silica gel using a mixture of diethyl ether and cyclohexane as eluent. When necessary, the benzylmenadione was recrystallized from hexane or a mixture of EtOAc/hexane to give the desired analytically pure benzylMD derivatives in good-to-excellent yields.

Typical Procedure for the Synthesis of 2,6-Dimethyl-3-[4-(trifluoromethyl)benzyl]naphthalene-1,4-dione (19d): Yield 65 %; yellow needles; m.p. 93–94 °C (hexane/EtOAc). ¹H NMR (300 MHz, CDCl₃): δ = 7.98 (d, *J* = 7.4 Hz, 1 H), 7.87 (s, 1 H), 7.53–7.48 (m, 3 H), 7.17 (d, *J* = 7.4 Hz, 2 H), 4.07 (s, 2 H), 2.48 (s, 3 H), 2.23 (s, 3 H) ppm. ¹³C NMR (75 MHz, CDCl₃): δ = 184.98 (C=O), 184.81 (C=O), 144.82 (C_q), 144.74 (C_q), 144.17 (C_q), 142.31 (C_q), 134.38 (CH), 131.81 (C_q), 129.87 (C_q), 128.87 (2 × CH), 128.58 (q, *J* = 28.9 Hz, C_q), 126.88 (CH), 126.62 (CH), 125.6 (q, *J* = 3.8 Hz, 2 CH), 124.18 (q, *J* = 269.7 Hz, CF₃), 32.34 (CH₂), 21.85 (CH₃), 13.33 (CH₃) ppm. HRM (ESI): calcd. for C₂₀H₁₅F₃O₂Na 367.0916 [M + Na]⁺; found 367.0911.

General Procedure for the Condensation of 4-Trifluorobenzaldehyde and Commercial Tetralones: A solution of KOH (41.04 mmol, 1.2 equiv.) in EtOH (105.5 mL) was added to a mixture of α-tetralone (4.562 mL, 34.2 mmol, 1 equiv.) and 4-CF₃-benzaldehyde (37.62 mmol, 1.1 equiv.). The solution was stirred at room temperature for 4 h. The reaction mixture was poured into water and a white solid precipitated. The solid was filtered, washed with water (2 × 50 mL), and dried under vacuum to give the desired alkenes in excellent yields.

Typical Procedure for the Synthesis of (E)-2-[4-(trifluoromethyl)benzylidene]-3,4-dihydronaphthalen-1(2H)-one (22e): Yield 85 %; white solid; m.p. 170–172 °C (from EtOH). ¹H NMR (300 MHz, CDCl₃): δ = 8.05 (dd, *J* = 7.8, *J* = 1.5 Hz, 1 H), 7.75 (s, 1 H), 7.52 [(AB)₂ system, *J* = 8.1 Hz, 4 H], 7.40 (dd, *J* = 7.8, 1.5 Hz, 1 H), 7.31–7.28 (m, 1 H), 7.26–7.16 (m, 1 H), 3.01–2.97 (m, 2 H), 2.91–2.85 (m, 2 H) ppm. ¹³C NMR (75 MHz, CDCl₃): δ = 187.49 (C=O), 143.19 (C_q), 139.47 (C_q), 137.41 (C_q), 134.66 (CH), 133.56 (CH), 133.23 (C_q), 130.02 (q, *J* = 31.57 Hz, C_q), 129.91 (2 CH), 129.42 (CH), 128.31 (CH), 127.18 (CH), 125.60 (q, *J* = 3.3 Hz, 2 CH), 124.07 (q, *J* = 270.3 Hz, CF₃), 28.81 (CH₂), 27.20 (CH₂) ppm. ¹⁹F NMR (376 MHz, CDCl₃): δ = –62.69 ppm. HRM (ESI): calcd. for C₁₈H₁₄F₃O 303.0991 [M + H]⁺; found 303.0971.

General Procedure for the Isomerization to the Corresponding Benzyl naphthol Derivatives: A solution of the corresponding

alkene (3.31 mmol, 1 equiv.) and RhCl₃ (0.331 mmol, 0.1 equiv.) was heated at reflux in ethanol (70 mL) for 6 h. During this process, when the reaction was carried out in open air, oxygen was observed to interfere in the catalytic cycle by oxidizing Rh(I) to Rh(III)* species, accounting for the arrest of the isomerization reaction. Thus, well-degassed solvent and strict anaerobic conditions were necessary for this reaction to occur. After concentration, the residue was partitioned between water and ethyl acetate, and the organic phase was dried with MgSO₄ and concentrated. Chromatography (cyclohexane/EtOAc, 5:1) gave the pure products in excellent yields.

Typical Procedure for the Synthesis of 2-[4 (trifluoromethyl)benzyl]naphthalen-1-ol (23e): Yield 96 %; white solid; m.p. 83.5–84 °C (cyclohexane). ¹H NMR (300 MHz, CDCl₃): δ = 7.87–7.84 (m, 1 H), 7.65–7.61 (m, 1 H), 7.37–7.26 (m, 5 H), 7.20–7.14 (m, 2 H), 7.10–7.05 (m, 1 H), 4.99 (s, 1 H, OH), 4.03 (s, 2 H) ppm. ¹³C NMR (75 MHz, CDCl₃): δ = 148.63 (C_q), 144.05 (C_q), 133.82 (C_q), 128.90 (2 CH), 128.81 (q, *J* = 33.42 Hz, C_q), 128.63 (CH), 128.00 (CH), 126.79 (CH), 125.71 (CH), 125.63 (q, *J* = 3.83 Hz, 2 CH), 124.59 (C_q), 124.2 (q, *J* = 264.23 Hz, CF₃), 120.98 (CH), 120.72 (CH), 119.57 (C_q), 36.2 (CH₂) ppm. ¹⁹F NMR (376 MHz, CDCl₃): δ = –62.39 ppm. MS (E): *m/z* (%) = 302.1 (100) [M]⁺. HRMS (ESI): calcd. for C₁₈H₁₄F₃O 303.0991 [M + H]⁺; found 303.0996.

General Procedure for the Oxidation of the Benzyl naphthol Derivatives to 2-Benzyl-1,4-naphthoquinones: (Diacetoxyiodo)benzene (PIDA) (5.29 mmol, 2.1 equiv.) was added portionwise to a stirred solution of naphthol (2.65 mmol, 1 equiv.) in acetonitrile (35 mL) and water (12 mL) at –5 °C over 20–30 min. After stirring for 30 min at –5 °C, the reaction mixture was stirred at room temperature for 1 h. A saturated NaHCO₃ (15 mL) solution was added to the orange reaction mixture and the mixture was extracted with Et₂O (3 × 50 mL). The combined organic extracts were washed with brine and dried with anhydrous MgSO₄. The crude product was purified by flash chromatography on silica gel (cyclohexane/EtOAc, 1:10 to 1:5) to give the corresponding desired benzylMDs in excellent yields.

Typical Procedure for the Synthesis of 2-[4-(Trifluoromethyl)benzyl]naphthalene-1,4-dione (24e): Yield 89 %; yellow needles; m.p. 98–100 °C (hexane/EtOAc). ¹H NMR (300 MHz, CDCl₃): δ = 8.13–8.02 (m, 2 H), 7.76–7.71 (m, 2 H), 7.49 [(AB)₂ system, *J* = 8.1 Hz, Δ*ν* = 61.8 Hz, 4 H], 6.63 (t, *J* = 1.5 Hz, 1 H), 3.96 (s, 2 H) ppm. ¹³C NMR (75 MHz, CDCl₃): δ = 184.87 (C=O), 184.72 (C=O), 149.78 (CH), 141.00 (C_q), 135.90 (CH), 133.96 (CH), 133.87 (C_q), 132.05 (C_q), 129.74 (2 CH), 129.41 (q, *J* = 32.48 Hz, C_q), 126.75 (CH), 126.22 (CH), 125.78 (q, *J* = 3.83 Hz, 2 CH), 125.77 (C_q), 124.12 (q, *J* = 269.18 Hz, CF₃), 35.67 (CH₂) ppm. ¹⁹F NMR (376 MHz, CDCl₃): δ = –62.54 ppm. HRMS (ESI): calcd. for C₁₈H₁₂F₃O₂ 317.0784 [M + H]⁺; found 317.0791.

General Procedure for the Kochi–Anderson Reaction of 2-Benzyl-1,4-naphthoquinone Derivatives to the Corresponding 3-Benzylmenadiones: The 2-benzyl-1,4-naphthoquinone (0.316 mmol, 1 equiv.) and acetic acid (1.58 mmol, 5 equiv.) were added to a stirred solution of MeCN/H₂O (3:1, 9.19 mL) and heated at 85 °C. AgNO₃ (0.11 mmol, 0.35 equiv.) was first added, and then (NH₄)₂S₂O₈ (0.411 mmol, 1.3 equiv.) in MeCN/H₂O (3:1, 3.94 mL) was added dropwise in 5 min. The reaction mixture was then heated for 60 min at 85 °C. MeCN was evaporated and the mixture was extracted with DCM. The crude mixture was purified by flash chromatography on silica gel using toluene as eluent. When necessary, the compound was recrystallized from hexane or a mixture of EtOAc/hexane to give the analytically pure benzylMD derivatives.

Biological Assays

Inhibitors: The chloroquine diphosphate salt and Methylene Blue trihydrate were purchased from Sigma–Aldrich. The lead plasmodione was prepared as described previously (as benzylMD **1c** in ref.^[17]). Stock solutions of Methylene Blue and chloroquine were prepared in pure water. Stock solutions of the benzylMD derivatives (6 mM) were prepared in DMSO and stored in aliquots at –20 °C.

Growth Inhibition Assays: *P. falciparum* wild-type strain Dd2 was cultured at 37 °C according to standard protocols^[49] in RPMI medium containing 9 % human serum and type A erythrocytes at a hematocrit level of 3.3 % under a low-oxygen atmosphere (3 % CO₂, 5 % O₂, 92 % N₂, and 95 % humidity). The cultures were synchronized by using the sorbitol method.^[50] Growth inhibition was determined in a SYBR green assay as described previously.^[51,52] Inhibitors were added to synchronized ring stage parasite cultures in microtiter plates (0.5 % parasitemia, 1.25 % hematocrit) and incubated for 72 h. The final inhibitor concentrations in each assay ranged from 22 μM to 5 μM.

In Vitro Anti-Plasmodium Activity Assays: The inhibition of intra-erythrocytic parasite development by benzylMD derivatives and control agents (CQ, MB) was determined in microtiter tests according to standard protocols. The in vitro antimalarial activity is expressed as 50 % inhibitory concentration (IC₅₀). The activities of the lead plasmodione, Methylene Blue, and chloroquine against the *P. falciparum* Dd2 strain (as presented in Table 3) were determined by using the SYBR® green I assay as described before.^[51,52] Briefly, synchronous ring stage parasites were incubated for 72 h in the presence of decreasing drug concentrations in microtiter plates (0.5 % parasitemia, 1.5 % hematocrit final). Each inhibitor was analyzed in three-fold serial dilution in duplicates and with at least three independent repetitions.

Supporting Information (see footnote on the first page of this article): General Procedures 4–7, 11, and 12; detailed descriptions of experimental procedures, spectroscopic data, and ¹H and ¹³C NMR spectra of all new compounds.

Acknowledgments

E. D.-C. thanks Don Antoine Lanfranchi, in recognition of his fundamental contribution to the development of the platform of organic chemistry of the described 2-methyl-1,4-naphthoquinones. The authors wish to thank the National Institutes of Health (NIH), USA (project entitled “Redox balance and drug development in *Schistosoma mansoni*”, grant 1R01AI065622-01A2 to D. L. W.) for creating an effective framework to allow the set-up of the platform of synthetic methodologies (salary to D. A. L.). This work was also made possible by grants of the Agence Nationale de la Recherche (ANR) (ANR_{emergence2010} program, grant SCHISMAL to E.D.-C.), and of the Laboratoire d'Excellence ParaFrap (grant LabEx ParaFrap ANR-11-LABX-0024 to E. D.-C.). The French Centre National de la Recherche Scientifique (CNRS) (grant UMR 7509 to E. D.-C.), the University of Strasbourg, France, and the International Center for Frontier Research in Chemistry, Strasbourg, France (project entitled “Redox-active 1,4-naphthoquinones to kill malarial parasites”, grant ic-FRC-Trinational to E.D.-C.) partly supported this work. K. E. is grateful to the CNRS and to Alain van Dorsselaer for her co-funded CNRS doctoral fellowship (BDI). The authors are indebted to Michel Schmitt for recording a part of the NMR spectra.

Keywords: Synthetic methods · Cycloaddition · Regioselectivity · Redox chemistry · Biological activity · Quinones

- [1] a) T. J. Schmidt, S. A. Khalid, A. J. Romanha, T. M. Alves, M. W. Biavatti, R. Brun, F. B. Da Costa, S. L. de Castro, V. F. Ferreira, M. V. de Lacerda, J. H. Lago, L. L. Leon, N. P. Lopes, R. C. das Neves Amorim, M. Niehues, I. V. Ogungbe, A. M. Pohlit, M. T. Scotti, W. N. Setzer, M. de N. C. Soeiro, M. Steindel, A. G. Tempone, *Curr. Med. Chem.* **2012**, *19*, 2176–2228; b) H. Eilenberg, S. Pnini-Cohen, Y. Rahamim, E. Sionov, E. Segal, S. Carmeli, A. Zilberstein, *J. Exp. Bot.* **2010**, *61*, 911–922; c) C. M. Holsclaw, K. M. Sogi, S. A. Gilmore, M. W. Schelle, M. D. Leavell, C. R. Bertozzi, J. A. Leary, *ACS Chem. Biol.* **2008**, *3*, 619–624.
- [2] a) A. Fournet, A. Angelo, V. Muñoz, F. Roblot, R. Hocquemiller, A. Cavé, *J. Ethnopharmacol.* **1992**, *37*, 159–164; b) V. P. Papageorgiou, A. N. Assimopoulou, E. A. Couladouros, D. Hepworth, K. C. Nicolaou, *Angew. Chem. Int. Ed.* **1999**, *38*, 270–301; *Angew. Chem.* **1999**, *111*, 280.
- [3] S. Padhye, P. Dandawate, M. Yusufi, A. Ahmad, F. H. Sarkar, *Med. Res. Rev.* **2012**, *32*, 1131–1158.
- [4] a) E. A. Hillard, F. Caxico de Abreu, D. C. Melo Ferreira, G. Jaouen, M. Oliveira Fonseca Goulart, C. Amatore, *Chem. Commun.* **2008**, 2612–2628; b) M. Elhabiri, P. Sidorov, E. Cesar-Rodo, G. Marcou, D. A. Lanfranchi, E. Davioud-Charvet, D. Horvath, A. Varnek, *Chem. Eur. J.* **2015**, *21*, 3415–3424; c) K. W. Wellington, *RSC Adv.* **2015**, *5*, 20309–20338.
- [5] a) A. Mahapatra, S. P. Mativandela, B. Binneman, P. B. Fourie, C. J. Hamilton, J. J. Meyer, F. van der Kooy, P. Houghton, N. Lall, *Bioorg. Med. Chem.* **2007**, *15*, 7638–7646; b) J.-S. Yu, *Synlett* **2014**, *25*, 2377–2378.
- [6] a) M. J. Shearer, P. Newman, *J. Lipid Res.* **2014**, *55*, 345–362.
- [7] a) L. Salmon-Chemin, A. Lemaire, S. De Freitas, B. Deprez, C. Sergheraert, E. Davioud-Charvet, *Bioorg. Med. Chem. Lett.* **2000**, *10*, 631–635; b) L. Salmon-Chemin, E. Buisine, V. Yardley, S. Kohler, M.-A. Debreu, V. Landry, C. Sergheraert, S. L. Croft, R. L. Krauth-Siegel, E. Davioud-Charvet, *J. Med. Chem.* **2001**, *44*, 548–565.
- [8] G. Saxena, S. W. Farmer, R. E. Hancock, G. H. Towers, *J. Nat. Prod.* **1996**, *59*, 62–65.
- [9] a) R. B. Gupta, R. N. Khanna, N. N. Sharma, *Indian J. Chem., Sect. B* **1977**, *15*, 394–395; b) R. B. Gupta, R. N. Khanna, V. P. Manchanda, *Indian J. Chem., Sect. B* **1979**, *18*, 217–218.
- [10] Y. Gu, P. K. Li, Y. C. Lin, Y. Rikihisa, R. W. Brueggemeier, *J. Steroid Biochem. Mol. Biol.* **1991**, *38*, 709–715.
- [11] M. E. Rateb, W. E. Houssen, M. Arnold, M. H. Abdelrahman, H. Deng, W. T. Harrison, C. K. Okoro, J. A. Asenjo, B. A. Andrews, G. Ferguson, A. T. Bull, M. Goodfellow, R. Ebel, M. Jaspars, *J. Nat. Prod.* **2011**, *74*, 1491–1499.
- [12] C. C. Nawrat, C. J. Moody, *Angew. Chem. Int. Ed.* **2014**, *53*, 2056–2077; *Angew. Chem.* **2014**, *126*, 2086.
- [13] a) L. Boisvert, P. Brassard, *J. Org. Chem.* **1988**, *53*, 4052–4059; b) M. Miyashita, T. Yamasaki, T. Shiratani, S. Hatakeyama, M. Miyazawaa, H. Irie, *Chem. Commun.* **1997**, 1787–1788.
- [14] a) J. Tou, W. Reusch, *J. Org. Chem.* **1980**, *45*, 5012–5014; b) R. L. Nunes, L. W. Bieber, *Tetrahedron Lett.* **2001**, *42*, 219–221.
- [15] a) Y.-F. Ji, Z.-M. Zong, X.-Y. Wei, G.-Z. Tu, L. Xu, L.-T. He, *Synth. Commun.* **2003**, *33*, 763–772; b) J. N. Payette, H. Yamamoto, *J. Am. Chem. Soc.* **2007**, *129*, 9536–9537.
- [16] a) J. G. Bauman, R. Hawley, H. Rapoport, *J. Org. Chem.* **1985**, *50*, 1573–1577; b) B. Kesteleyn, N. De Kimpe, *J. Org. Chem.* **2000**, *65*, 640–644.
- [17] T. Müller, L. Johann, B. Jannack, M. Bruckner, D. A. Lanfranchi, H. Bauer, C. Sanchez, V. Yardley, C. Deregnaucourt, J. Schrevel, M. Lanzer, R. H. Schirmer, E. Davioud-Charvet, *J. Am. Chem. Soc.* **2011**, *133*, 11557–11571.
- [18] K. Ehrhardt, E. Davioud-Charvet, H. Ke, A. Vaidya, M. Lanzer, M. Deponte, *Antimicrob. Agents Chemother.* **2013**, *57*, 2114–2120.
- [19] M. Bielitz, D. Belorgey, K. Ehrhardt, L. Johann, D. A. Lanfranchi, V. Gallo, E. Schwarzer, F. Mohring, E. Jortzik, D. L. Williams, K. Becker, P. Arese, M. Elhabiri, E. Davioud-Charvet, *Antioxid. Redox Signaling* **2015**, *22*, 1337–1351.
- [20] D. A. Lanfranchi, E. Cesar-Rodo, B. Bertrand, H.-H. Huang, L. Day, L. Johann, M. Elhabiri, K. Becker, D. L. Williams, E. Davioud-Charvet, *Org. Biomol. Chem.* **2012**, *10*, 6375–6387.
- [21] J. M. Anderson, J. K. Kochi, *J. Am. Chem. Soc.* **1970**, *92*, 1651–1659.

- [22] a) G. Bringmann, G. Zhang, A. Hager, M. Moos, A. Irmer, R. Bargou, M. Chatterjee, *Eur. J. Med. Chem.* **2011**, *46*, 5778–5789; b) D. Mal, K. Ghosh, S. Jana, *Org. Lett.* **2015**, *17*, 5800–5803.
- [23] B. C. Pearce, R. A. Parker, M. E. Deason, D. D. Dischino, E. Gillespie, A. A. Qureshi, K. Volk, J. J. Wright, *J. Med. Chem.* **1994**, *37*, 526–541.
- [24] S. H. Kim, J. R. Gunther, J. A. Katzenellenbogen, *Org. Lett.* **2008**, *10*, 4931–4934.
- [25] N. Minanmi, S. Kikima, *Chem. Pharm. Bull.* **1979**, *6*, 1490–1494.
- [26] B. Quiclet-Sire, S. Z. Zard, *Top. Curr. Chem.* **2006**, *264*, 201–236.
- [27] a) A. Cordero-Vargas, B. Quiclet-Sire, S. Z. Zard, *Org. Lett.* **2003**, *5*, 3717–3719; b) A. Cordero-Vargas, I. Pérez-Martín, B. Quiclet-Sire, S. Z. Zard, *Org. Biomol. Chem.* **2004**, *2*, 3018–3025.
- [28] a) D. A. Lanfranchi, L. Johann, D. L. Williams, E. Davioud-Charvet, Eur. Pat. Appl., EP 11305346, **2011**; b) D. A. Lanfranchi, L. Johann, D. L. Williams, E. Davioud-Charvet, E. Cesar-Rodo, PCT Int. Appl. WO 2012131010 A1 20121004, **2012**; c) R. Guignard, *Synlett* **2013**, *24*, 157–160.
- [29] M. Van der Mey, K. M. Bommelé, H. Boss, A. Hatzelmann, M. Van Slingerland, G. J. Sterk, H. Timmerman, *J. Med. Chem.* **2003**, *46*, 2008–2016.
- [30] a) A. Pelter, S. M. A. Elgendy, *J. Chem. Soc. Perkin Trans. 1* **1993**, *16*, 1891–1896; b) P. Bachu, J. Sperry, M. A. Brimble, *Tetrahedron* **2008**, *64*, 3343–3350.
- [31] H.-J. Teuber, W. Rau, *Chem. Ber.* **1953**, *86*, 1036–1047.
- [32] a) L. Krishna Kumari, M. Pardhasaradhi, *Indian J. Chem., Sect. B* **1982**, *21*, 1067–1070; b) N. Kakusawa, K. Inui, J. Kurita, T. Tsuchiya, *Heterocycles* **1996**, *43*, 1601–1604.
- [33] a) G. Fawaz, L. F. Fieser, *J. Am. Chem. Soc.* **1950**, *72*, 996–1000; b) R. Schmid, F. Goebel, A. Warnecke, A. Labahn, *J. Chem. Soc. Perkin Trans. 2* **1999**, 1199–1202; c) A. Bohle, A. Schubert, Y. Sun, W. R. Thiel, *Adv. Synth. Catal.* **2006**, *348*, 1011–1015.
- [34] V. Nair, A. Deepthi, *Chem. Rev.* **2007**, *107*, 1862–1891.
- [35] Y. Tanoue, K. Sakata, M. Hashimoto, S. Morishita, M. Hamada, N. Kai, T. Nagai, *Tetrahedron* **2002**, *58*, 99–104.
- [36] J. R. Grunwell, A. Karipides, C. T. Wigal, S. W. Heinzman, J. Parlow, J. A. Surso, L. Clayton, F. J. Fleitz, M. Daffner, J. E. Stevens, *J. Org. Chem.* **1991**, *56*, 91–95.
- [37] a) B. M. Trost, W. H. Pearson, *Tetrahedron Lett.* **1983**, *24*, 269–272; b) D. A. Lanfranchi, G. Hanquet, *J. Org. Chem.* **2006**, *71*, 4854–4861.
- [38] M. C. Venuti, B. E. Loe, G. H. Jones, J. M. Young, *J. Med. Chem.* **1988**, *31*, 2132–2136.
- [39] S. Danishefsky, T. Kitahara, *J. Am. Chem. Soc.* **1974**, *96*, 7807–7808.
- [40] K. P. Mandal, F. Gao, Z. Lu, Z. Ren, Z. Ramesh, J. S. Birtwistle, K. Kaluarachchi, X. Chen, R. C. Bast, W. Liao, J. S. McMurray, *J. Med. Chem.* **2011**, *54*, 3549–3563.
- [41] a) N. Jacobsen, K. Torssell, *Justus Liebigs Ann. Chem.* **1972**, *763*, 135–147; b) N. Jacobsen, K. Torssell, *Acta Chem. Scand.* **1973**, *27*, 3211–3216.
- [42] T. Ohgiya, S. Nishiyama, *Tetrahedron Lett.* **2004**, *45*, 6317–6320.
- [43] A. Martínez, J. C. Barcia, A. M. Estévez, F. Fernández, L. González, J. C. Estévez, R. J. Estévez, *Tetrahedron Lett.* **2007**, *48*, 2147–2149.
- [44] K. F. Eidman, P. J. Nichols, in: *e-EROS Encyclopedia of Reagents for Organic Synthesis*, Wiley, **2001**, DOI: 10.1002/047084289X.rt236.pub2.
- [45] a) G. Paiaro, A. Musco, G. Diana, *J. Organomet. Chem.* **1965**, *4*, 466–474; b) J. Andrieux, D. H. R. Barton, H. Patin, *J. Chem. Soc. Perkin Trans. 1* **1977**, 359–363; c) D. G. Batt, G. D. Maynard, J. J. Petraitis, J. E. Shaw, W. Galbraith, R. R. Harris, *J. Med. Chem.* **1990**, *33*, 360–370; d) M. Taniura, Y. Tamai, “Process for Producing 2-Methyl-1-naphthol by Isomerization of 2-Methylene-1-tetralone”, Eur. Pat. Appl. EP 558069 A1 19930901, **1993**.
- [46] G. Leroy, D. Peeters, C. Wilante, *THEOCHEM* **1982**, *88*, 217–233.
- [47] a) L. F. Fieser, E. Berliner, F. J. Bondhus, F. C. Chang, W. G. Dauben, M. G. Ettlinger, G. Fawaz, M. Fields, M. Fieser, C. Heidelberger, H. Heymann, A. M. Seligman, W. R. Vaughan, A. G. Wilson, E. Wilson, M. Wu, M. T. Leffler, K. E. Hamlin, R. J. Hathaway, E. J. Matson, E. E. Moore, M. B. Moore, R. T. Rapala, H. E. Zaugg, *J. Am. Chem. Soc.* **1948**, *70*, 3151–3155; b) L. F. Fieser, A. P. Richardson, *J. Am. Chem. Soc.* **1948**, *70*, 3156–3165; c) L. Salmon-Chemin, A. Lemaire, S. De Freitas, B. Deprez, C. Sergheraert, E. Davioud-Charvet, *Bioorg. Med. Chem. Lett.* **2000**, *10*, 631–635; d) L. Salmon-Chemin, E. Buisine, V. Yardley, S. Kohler, M.-A. Debrey, V. Landry, C. Sergheraert, S. L. Croft, R. L. Krauth-Siegel, E. Davioud-Charvet, *J. Med. Chem.* **2001**, *44*, 548–565.
- [48] a) K. Lopez-Shirley, F. Zhang, D. Gosser, M. Scott, S. R. Meshnick, *J. Lab. Clin. Med.* **1994**, *123*, 126–130; b) J. J. Kessl, B. B. Lange, T. Merbitz-Zahradnik, K. Zwicker, P. Hill, B. Meunier, H. Pálsdóttir, C. Hunte, S. Meshnick, B. L. Trumpower, *J. Biol. Chem.* **2003**, *278*, 31312–31318.
- [49] W. Trager, J. B. Jensen, *Science* **1976**, *193*, 673–675.
- [50] C. Lambros, J. P. Vanderberg, *J. Parasitol.* **1979**, *65*, 418–420.
- [51] M. Smilkstein, N. Sriwilaijaroen, J. X. Kelly, P. Wilairat, M. Riscoe, *Antimicrob. Agents Chemother.* **2004**, *48*, 1803–1806.
- [52] D. Beez, C. P. Sanchez, W. D. Stein, M. Lanzer, *Antimicrob. Agents Chemother.* **2011**, *55*, 50–55.
- [53] *ChemBioOffice 2012*, PerkinElmer, Inc., **2012**.

Received: February 9, 2016

Published Online: March 21, 2016

Chemical tools for antimalarial drug development: synthesis of plasmodione analogues et ^{13}C -enriched plasmodione for drug metabolomics investigations

Résumé

Le paludisme est une maladie parasitaire tropicale menaçant les populations dans les zones tropicales et subtropicales, en particulier les jeunes enfants en Afrique. En raison des résistances aux médicaments antipaludiques qui se sont propagées dans le monde entier au cours des 50 dernières années, de nouveaux médicaments sont vraiment nécessaires. La plasmodione (série benzylmenadione) a été identifiée comme un médicament-candidat antipaludique puissant, agissant selon une bioactivation rédox sur les stades sanguins asexués et sexués jeunes, mais son métabolisme est inconnu. Par conséquent, afin d'identifier les structures des métabolites actifs générés par la plasmodione antipaludique, la synthèse complète de la plasmodione $^{13}\text{C}_{18}$ -enrichie a été conçue et réalisée en 10 étapes. En outre, le procédé d'extraction pour l'étude du métabolisme de la molécule a été établi à partir de globules rouges parasités traités par la plasmodione $^{13}\text{C}_{18}$ -enrichie. D'autre part, la préparation de dérivés oxétane et *N*-alkylaryl de plasmodione avec une solubilité potentielle améliorée a également été réalisée par substitution nucléophile aromatique ($\text{S}_{\text{N}}\text{Ar}$) et réaction de couplage Buchwald-Hartwig catalysée par le palladium, respectivement. Enfin, un complexe d'or (I) phosphole, connu comme un inhibiteur irréversible et puissant de la thiorédoxine réductase séléno-dépendante humaine, a été synthétisé et son profil antiparasitaire a été étudié sur de nombreux parasites pathogènes pour l'homme, protozoaires et helminthes en cultures.

Mots-clés: médicament antipaludique, 1,4-naphtoquinone, redox, molécule ^{13}C -enrichie, métabolisme médicamenteux, complexe Au(I)-phosphine.

Abstract:

Malaria is a tropical parasitic disease threatening populations in tropical and sub-tropical areas, especially young children in Africa. Due to the drug resistance spread all over the world in the past 50 years, new drugs are urgently needed. Plasmodione (benzylmenadione series) had been identified as a potent anti-malarial early lead drug, acting through a redox bioactivation on asexual and young sexual blood stages, but its drug metabolism is unknown. Therefore, in order to identify the structures of the active drug metabolites generated from the antimalarial plasmodione, fully $^{13}\text{C}_{18}$ -enriched-plasmodione synthesis was designed and performed in 10 steps. Furthermore, the extraction method for the drug metabolism study was established from $^{13}\text{C}_{18}$ -enriched plasmodione-treated parasitized red blood cells. On the other hand, the preparation of oxetane and *N*-alkylaryl derivatives of plasmodione with potential improved solubility was also investigated through aromatic nucleophilic substitution ($\text{S}_{\text{N}}\text{Ar}$) and palladium-catalyzed Buchwald-Hartwig coupling reaction, respectively. Finally, a gold(I) phosphole complex, known as an irreversible and potent inhibitor of the human seleno-dependent thioredoxin reductase, was synthesized and its antiparasitic profile investigated against a panel of parasites, protozoans and helminthes in cultures.

Keywords: antimalarial drug, 1,4-naphthoquinone, redox, ^{13}C -enriched compound, drug metabolism, Au(I)-phosphine complex